

Sculpting a plant

TCP transcription factors as key regulators
of plant growth and development

Sam W. van Es

Thesis committee

Promotors

Prof. Dr Gerco C. Angenent
Personal chair at the Laboratory of Molecular Biology
Wageningen University & Research

Prof. Dr Richard G.H. Immink
Special Professor Physiology of Flower Bulbs
Wageningen University & Research

Other members

Prof. Dr Mark G.M. Aarts, Wageningen University & Research
Prof. Dr Paula R. Elomaa, University of Helsinki, Finland
Prof. Dr Ronald E. Koes, University of Amsterdam
Dr Ivo Rieu, Radboud University, Nijmegen

This research was conducted under the auspices of the Graduate School
Experimental Plant Sciences

Sculpting a plant

TCP transcription factors as key regulators
of plant growth and development

Sam W. van Es

Thesis

submitted in fulfilment of the requirements for the degree of doctor
at Wageningen University
by the authority of the Rector Magnificus,
Prof. Dr A.P.J. Mol,
in the presence of the
Thesis Committee appointed by the Academic Board
to be defended in public
on Tuesday 18 September 2018
at 1:30 p.m. in the Aula.

Sam W. van Es

Sculpting a plant, TCP transcription factors as key regulators of plant growth and development,

174 pages.

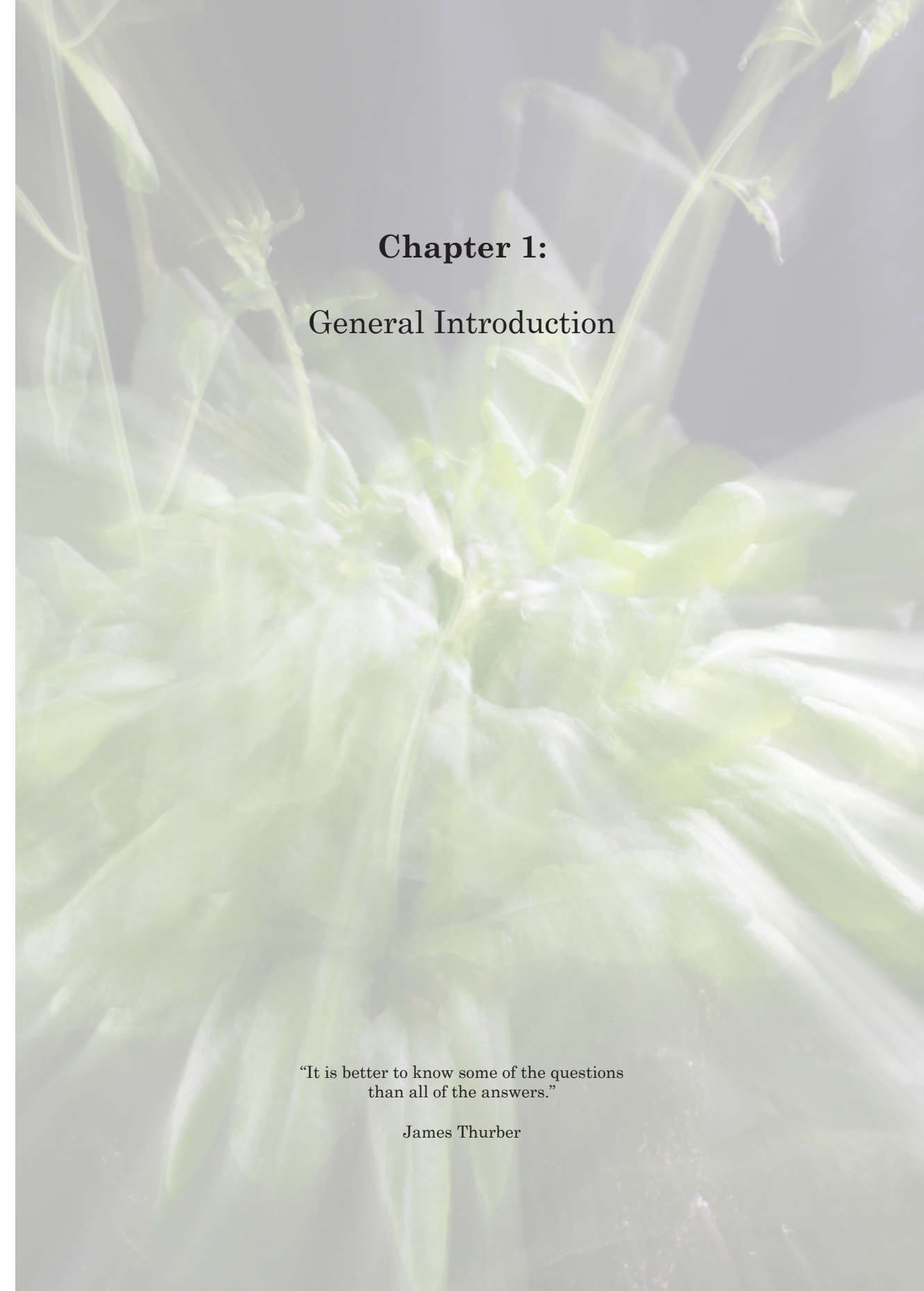
PhD thesis, Wageningen University, Wageningen, the Netherlands (2018)

With references, with summaries in English and Dutch

ISBN 978-94-6343-489-8

DOI <https://doi.org/10.18174/457117>

Chapter 1.....	7
General Introduction	
Chapter 2.....	21
A spatio-temporal analysis of plant growth and development coupled to yield characteristics in several <i>Arabidopsis thaliana</i> TCP mutant backgrounds	
Chapter 3.....	55
Novel functions of the Arabidopsis transcription factor <i>TCP5</i> in petal development and ethylene biosynthesis	
Chapter 4.....	83
The regulatory role of BRC1 in bud dormancy through various downstream signalling pathways	
Chapter 5.....	105
Interactions between the organ identity specifying MADS domain proteins and growth regulatory TCP proteins in Arabidopsis flowers	
Chapter 6.....	125
General Discussion and Future Perspectives	
References	140
Summary	157
Samenvatting	161
Acknowledgements	165
About the author.....	171
EPS Education statement.....	172



Chapter 1:

General Introduction

“It is better to know some of the questions
than all of the answers.”

James Thurber

A huge variation in appearance exists within the plant kingdom, even between plants of the same species. More extreme, simultaneously growing two plants with identical genotypes under identical conditions will yield two different plants, much more different in appearance than identical twins, even if the only variable is that they stand next to each other and therefore not on the exact same spot. An underlying reason of this polymorphism is that plants are sessile organisms and need a huge degree of plasticity in order to survive less favourable conditions. Plants therefore respond to subtle differences in environment.

In contrast to this flexibility, the developmental program that directs the formation to a full-grown adult appears to be extremely tightly controlled. There are countless genetic, hormonal and structural factors determining the final appearance of a plant. Take for example genes that determine the fate of a group of cells, whether they become a sepal or a petal; or the hormone auxin, that is able to regulate gene expression, initiates meristems, and stimulates growth. At cellular level, specific gene sets are responsible for the maintenance of meristematic potential and others for the differentiation of cells into specific types, for example leaf mesophyll cells. The genes and their protein products that regulate all these processes are part of extensive and complex genetic networks in which genes communicate with each other in a specific order.

The regulation of these genetic networks is performed by a group of proteins called transcription factors. Transcription factors (TFs) generally bind cis-regulatory elements in the promoter of a gene and by doing so, they can steer the expression of those genes by allowing transcription, recruitment of co-factors or blocking transcription.

TFs are able to bind many genes and regulate expression of each gene differently at a spatial and temporal level. Furthermore, some master TFs can regulate genes from different networks and hence are pleiotropic and involved in multiple pathways.

A main aspect of plant development is cell division and growth. TFs can regulate genes that are directly involved in cell division and proliferation, such as cell cycle genes, or can control genes that are more indirectly involved in growth. An example of the latter class of target genes are genes coding for proteins involved in hormone biosynthesis or signalling.

One family of TFs involved in the regulation of growth is the TCP family. TCP TFs are plant specific and named after their founding members, *Tb1* in maize, *CYC* in Snapdragon and *PCF1* and *-2* in rice (Cubas *et al.*, 1999). *THEOSINTE BRANCHED1 (TB1)* in maize (*Zea mays*) has been key for the domestication of this crop from its ancestor teosinte by inhibiting the outgrowth of axillary meristems and as such controlling plant architecture and branching (Doebley *et al.*, 1995; Doebley *et al.*, 1997). *CYCLOIDEA (CYC)* is involved in the control of floral bilateral symmetry in Snapdragon (*Antirrhinum majus*) (Luo *et al.*, 1995) and lastly, *PCF1* and *PCF2* are known to bind the promoter

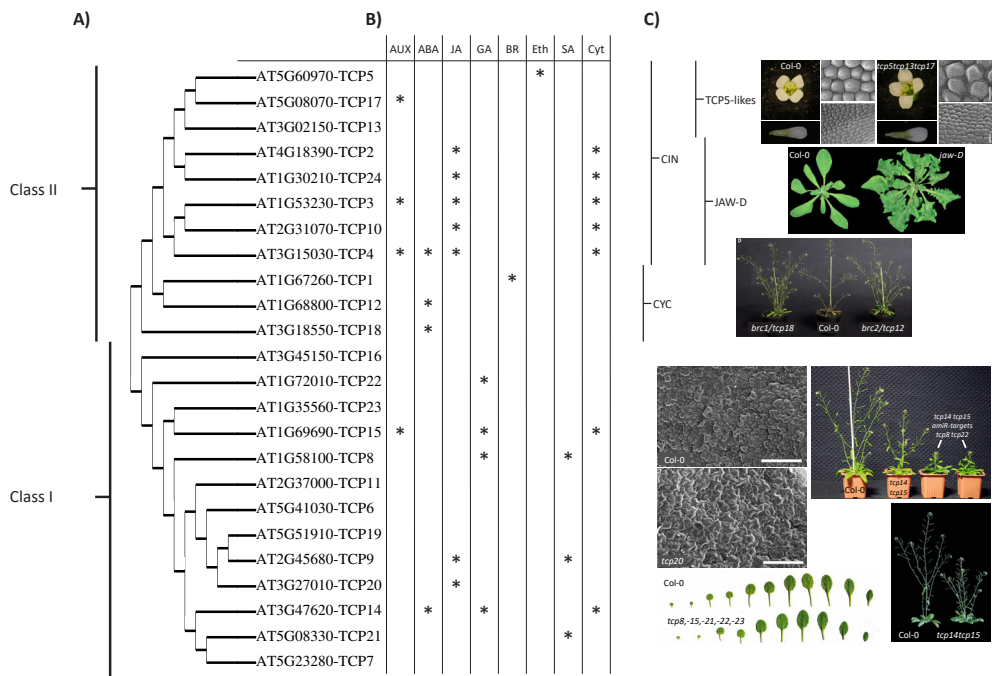


Figure 1. Phylogenetic tree showing all Arabidopsis TCP transcription factors

The phylogenetic tree was based on protein alignment of all 24 Arabidopsis TCP TFs in (A), using phylogeny. fr (Dereeper *et al.*, 2008). Asterisks indicate when an association of a TCP with a certain hormone has been reported (B). Aux: Auxin, ABA: Abscisic Acid, JA: Jasmonic Acid, GA: Gibberilic Acid, BR: Brassinosteroids, Eth: Ethylene, SA: Salicylic Acid, Cyt: Cytokinins. Adapted from S. Danisman (2016). Several examples of the more severe phenotypes are shown in (C). Pictures in (C) taken from: van Es *et al.*, 2018 (*TCP5*-likes); Palatnik *et al.*, 2003 (*jaw-D*); Aguilar-Martínez *et al.*, 2007 (*brc1* and *brc2*); Danisman *et al.*, 2012 (*tcp20*); Davière *et al.*, 2014 (*tcp14*, *tcp15*, *tcp8* and *tcp22*); Kieffer *et al.*, 2011 (*tcp14tcp15*) and Aguilar-Martínez *et al.*, 2013 (*tcp8*, *tcp15*, *tcp21*, *tcp22*, and *tcp23*).

of *PROLIFERATING CELL NUCLEAR ANTIGEN (PCNA)* in rice (*Oryza sativa*), controlling cell cycle in meristems as well as DNA synthesis and repair (Kosugi and Ohashi, 1997). The diversity in function of these three founding members, regulating branching, floral symmetry and cell cycle progression, beautifully illustrates the functional diversity of this class of genes.

The model species *Arabidopsis thaliana* has 24 members belonging to the TCP transcription factor family (Kosugi and Ohashi, 2002), which based on sequence characteristics, can be divided into two classes (Cubas *et al.*, 1999) (Figure 1). Originally thought to act antagonistically, either by promoting cell growth and proliferation (Class I) or through repressing these processes (Class II), more recent views point to far more intricate and extensive regulatory functions for the various class I and II TCPs (Martín-Trillo and Cubas, 2010; Nicolas and Cubas, 2016). TCPs have been extensively studied

for their role in plant development and over the years, several excellent reviews have been published on the functions of TCPs (Martín-Trillo and Cubas, 2010; Uberti Manassero *et al.*, 2013; Nicolas and Cubas, 2015; Nicolas and Cubas, 2016; Danisman, 2016).

Their supposed functions in directly regulating the transcription of cell cycle regulators and as interactors of proteins involved in the control of cell proliferation was reviewed by Uberti Manassero *et al.* (2013) and Nicolas and Cubas (2015). Next to this, members of the TCP family appear to be closely linked to plant hormone signalling (reviewed by Nicolas and Cubas, 2016) (Figure 1B).

The role of TCPs during plant development

The high level of redundancy among members of the TCP family makes *TCPs* challenging genes for biological studies (Danisman *et al.*, 2013). Mutations in a single *TCP* gene rarely yield visible mutant phenotypes and hence, reduced expression or knock-out of multiple closely related TCPs is required to elucidate their function and mode of action. This becomes evident when investigating the function of TCPs during plant development, where a phenotype in a single TCP mutant is highly uncommon (but present in for example *brc1/tcp18*) or only evident after very thorough phenotyping at microscopic level (e.g. bigger conical cells in petals of the *tcp5* mutant). This does not mean that TCPs are highly redundant and therefore not important, the opposite might be the case. Even though the lack of selective pressure makes full genetic redundancy unstable (Thomas, 1993; Hughes, 1994), redundancy might be nature's way of ensuring robustness of vital processes; if one gene fails, another can take its place (Kafri *et al.*, 2006). The expansion of the TCP TF family is partly attributed to genome duplications (Navaud *et al.*, 2007). This allows subfunctionalisation of one of the paralogs while the original gene function is retained by the other paralog (Nowak *et al.*, 1997). In such a case partial redundancy exists between the two genes.

One reason for believing genes to act redundantly due to their lack of a discernible phenotype, is that we're simply not looking at the right place for a phenotype; a biologist studying flower development might completely miss a root phenotype and vice versa. The nature of the phenotypic analysis is determining our view on redundancy to a great extent. A detailed molecular characterization of single mutants has proven to be effective in revealing the function of that gene at the molecular level, paving the way for uncovering visible phenotypes (Simon *et al.*, 2013). Furthermore, other or more stressful conditions could reveal different functions for 'redundant' genes.

Nevertheless, double and higher order TCP mutants do exhibit mutant phenotypes. These phenotypes give a hint to the function and underlying mechanisms in which individual *TCP* genes are involved. I will address this issue in Chapter 2, in which I performed a large-scale phenotyping experiment aiming, in part, to identify developmental effects of several single, double and higher order mutants.

TCP Class II

The family of TCP transcription factors can, as mentioned earlier, be divided into two classes based on differences in their TCP domain (Cubas *et al.*, 1999). The second class of TCPs (Class II) can be sub-divided into CYC/TB1 and CIN genes and all members have been assigned functions based on their mutant phenotypes. In contrast, Class I lacks an obvious subdivision and mutant phenotypes seem more sporadic and less well defined. Figure 1C provides a brief overview of the two classes and their phenotypes.

The CYC/TB1 subclass of Class II TCPs contains *TCP1*, *BRC1* (*TCP12*) and *BRC2* (*TCP18*) in Arabidopsis and the CIN subclass houses *TCP2*, *-3*, *-4*, *-5*, *-10*, *-13*, *-17*, and *-24*. The function of *BRC1* and *-2* in Arabidopsis is highly similar to that of the maize *TB1* gene, namely to inhibit the outgrowth of axillary meristems (Aguilar-Martínez *et al.*, 2007; Finlayson, 2007). *TCP1*, although closely related to *BRC1* and *BRC2*, and expressed at later stages of axillary meristem development (Cubas *et al.*, 2001), seems to have no effect on branching in Arabidopsis.

The CIN-type TCPs are represented in Arabidopsis by the *Jagged and Wavy* (*JAW*) TCPs (*TCP2*, *-3*, *-4*, *-10* and *-24*) and the *TCP5*-like genes (*TCP5*, *-13* and *-17*). All five *JAW*-TCPs are targeted by the same microRNA, *miR319*, which simultaneously downregulates the action of *TCP2*, *-3*, *-4*, *-10* and *-24* upon overexpression of the microRNA in the *jaw-D* mutant (Palatnik *et al.*, 2003). This multiple TCP knock-down gives rise to the crinkled leaf phenotype, characteristic of *jaw-D*, by postponing the arrest of cell proliferation in the leaf margin, resulting in an overproduction of cells at these places (Palatnik *et al.*, 2003; Nath *et al.*, 2003). In petals of the Arabidopsis *jaw-D* mutant, the overproduction of cells is most apparent at the distal end of the petal (Efroni *et al.*, 2008). It has been suggested that the other CIN-genes, *TCP5*, *TCP13* and *TCP17*, although not targeted by *miR319*, are responsible for similar processes in a redundant manner (Efroni *et al.*, 2008). However, mutants in the *TCP5*-like genes show some phenotypic differences, a characteristic I'll elaborate on in Chapter 3 of this thesis.

TCP Class I

Sequence-based sub-division of Class I TCPs is less profound and slightly different parameters in phylogeny studies yield rather different phylogenetic trees (Martín-Trillo and Cubas, 2010; Danisman *et al.*, 2013; Aguilar-Martínez and Sinha, 2013; Danisman, 2016). Therefore, it is difficult to predict potential functional redundancy among Class I TCPs solely based on sequence information. Today, several Arabidopsis class I TCPs have given us a glimpse of their function; for example *TCP14* and *TCP15*, two closely related TCPs that influence plant stature by promoting cell division in young internodes (Kieffer *et al.*, 2011). Approaches in which a VP16 activation domain or an SRDX repression domain were used, have suggested that *TCP20* is involved in the regulation of

cell division, growth and expansion (Hervé *et al.*, 2009). This finding was confirmed by Danisman *et al.*, (2012), who performed mutant analysis and found that *TCP20* inhibits cell elongation in leaves, in a redundant manner with *TCP19*. A similar SRDX approach led to the conclusion that *TCP7* and *TCP23* control cell proliferation in leaves. Furthermore, a single knock-out mutant of *TCP23* was the only one out of five single Class I TCP mutant lines that exhibited a different leaf phenotype. Nevertheless, when stacking these mutations in the quintuple *tcp8 tcp15 tcp21 tcp22 tcp23* mutant, a severe phenotype was apparent, with broader leaf blades in comparison to the leaves of wild type (Aguilar-Martinez and Sinha, 2013). Remarkably, a slightly different quadruple mutant composition, *tcp8 tcp14 tcp15 tcp22*, exhibits severe dwarfism and has a reduced responsiveness to gibberellic acid (GA) (Davière *et al.*, 2014). This observation suggests complex interactions between these particular class I TCP genes and a partial overlap in their functions.

Most phenotypes mentioned above are snapshots and detailed analyses of very specific functions, i.e. a comprehensive and detailed phenotyping of the various *tcp* gene mutants is lacking. Adding a temporal component to the analysis is essential to understand the role and importance of each individual TCP gene during plant development. Next to this, when looking for phenotypic alterations in leaf growth for example, changes in other developmental parameters will inevitably be overlooked. I will address this issue with the large-scale phenotyping experiment in Chapter 2, aiming at the identification of correlations between growth, development and yield parameters and characteristics.

TCPs are involved in more than just growth

Having only 24 members, the family of TCP transcription factors is relatively small, especially compared to for instance the MADS-box TF family (107 members (Parenicova *et al.*, 2003)), bHLH and MYB TF-families (162 and 339, respectively (Feller *et al.*, 2011)). TCPs, as well as for instance NAC, WRKY, AP2/ERF and ARF transcription factors, are plant specific. In contrast, MADS and bHLH transcription factors can be found in various taxa (Riechmann, Heard, Martin, Reuber, C.,-Z., Jiang, *et al.*, 2000). It has long been thought that all TCPs share a function in the direct control of cell proliferation and growth controlling genes (Cubas *et al.*, 1999), which, when looking at the observed mutant phenotypes, seems legitimate. However, a closer look reveals that TCPs often do not directly control growth genes (Efroni *et al.*, 2008; Danisman *et al.*, 2012) and additionally, affect other processes, such as plant defence (Kim *et al.*, 2014b; Wang *et al.*, 2015b) and flowering time. TCP23 seems to be a negative regulator of flowering time (Balsemão-Pires *et al.*, 2013) and the interaction of BRC1 with FLOWERING LOCUS T (FT) and TWIN SISTER OF FT might explain the early flowering phenotype in *brc1* mutants (Niwa *et al.*, 2013). An interesting feature of TCP20, one of the Class I TCPs, is its role in nutrient foraging of Arabidopsis roots (Guan *et al.*, 2014). The *tcp20* knockout mutant lacks the ability to produce lateral roots in medium with a high nitrate

concentration. Furthermore, two TCPs have been implicated in the regulation of pollen development, *TCP16* and *TCP11* (Takeda *et al.*, 2006; Viola *et al.*, 2011). Finally, *TCP21* was found to be a key player in the regulation of the circadian clock (Pruneda-Paz *et al.*, 2009) and in plants mutated for *TCP11* or *TCP15*, the expression of core clock components is also altered (Giraud *et al.*, 2010).

Linking TCPs with hormones

Over the years, several studies, describing a link between TCPs and hormones, have been published (reviewed by Nicolas and Cubas, 2016). The majority of plant hormones is represented: auxin (*TCP15*, Uberti-Manassero *et al.*, 2012; *TCP17*, Zhou *et al.*, 2017), jasmonic acid (*TCP4*, Schommer *et al.*, 2008; *TCP4* and *TCP20*, Danisman *et al.*, 2012), gibberellic acid (*CIN*, Das Gupta *et al.*, 2014, *TCP14* and *TCP15*, Davière *et al.*, 2014), brassinosteroids (*TCP1*, Guo *et al.*, 2010), abscisic acid (*TCP14*, Tatematsu *et al.*, 2008; *TCP15*, Uberti-Manassero *et al.*, 2012; *BRC1*, González-Grandío *et al.*, 2017), cytokinin (*TCP4*, Efroni *et al.*, 2013), salicylic acid (*TCP8*, Wang *et al.*, 2015), and in Pea, strigolactones (*PsBRC1*, Dun *et al.*, 2012). The latest addition to this list, and at the same time adding the last missing plant hormone, is ethylene, which appears to be under control of *TCP5* (Chapter 3). Figure 1 presents a phylogenetic tree of all *Arabidopsis* TCPs and the hormones they have been connected to (Figure 1A and 1B respectively). The involvement of TCPs in biosynthesis and signalling of particular hormones provides an alternative and indirect molecular mode-of-action how these TFs regulate cell cycle genes as opposed to the original hypothesis that TCPs were directly regulating these genes (Kosugi and Ohashi, 1997; Li *et al.*, 2005).

An interesting finding is that Class I and Class II TCPs can regulate hormone production antagonistically. In leaves, Jasmonic acid (JA) biosynthesis is e.g. inhibited by *TCP20*, a Class I protein that binds and thereby downregulates the JA biosynthesis gene *LIPOXYGENASE2* (*LOX2*). *TCP4*, a Class II TCP, on the other hand, promotes JA biosynthesis by inducing *LOX2* expression (Danisman *et al.*, 2012). Interestingly, *LOX2* is suppressed by *TCP4* in floral tissue (Rubio-Somoza and Weigel, 2013), showing a completely opposite and context dependent regulatory mechanism.

Molecular mode of action

The members of the TCP gene family all share a 60 amino acid long conserved sequence, the TCP domain (Cubas *et al.*, 1999 and Figure 2A). This TCP domain shares little sequence similarity with any of the previously known transcription factor families. Secondary structure prediction revealed that the TCP domain forms a basic region followed by two helices separated by a loop (Kosugi and Ohashi, 1997; Cubas, *et al.*, 1999), even though their primary amino acid sequences are unrelated to that of all other members of the bHLH family (Heim *et al.*, 2003). Characteristics of this TCP domain have led to the identification of the two classes (Class I and Class II). Comparing amino

acid similarities between members of Class I and Class II clearly shows their difference (Figure 2B). Class II genes contain a 4-amino-acid insertion in the TCP domain and have an R-domain, which is predicted to form a coiled coil that may mediate protein-protein interactions (Lupas *et al.*, 1991). Furthermore the residue composition in the loop and hydrophilic faces of helices I and II and the length of helix II differ between Class I and II TCPs (Kosugi and Ohashi, 1997; Cubas *et al.*, 1999). It is the TCP domain that mediates binding of the TCP proteins to GC-rich DNA sequence motifs *in vitro* (Kosugi and Ohashi, 2002). Based on research with TCP4, it is thought that TCPs form homo and heterodimers in both the presence and absence of DNA (Aggarwal, Gupta, *et al.*, 2010).

The consensus-binding site of class I TCPs can be defined by the sequence GTGGGNCC, whereas class II proteins show a preference for the sequence GTGGNCCC based on *in vitro* experiments (Kosugi and Ohashi, 2002; Schommer *et al.*, 2008; Viola *et al.*, 2011). The reason for this difference in preference is attributed to the residue present at position 11 of the basic region (Gly) of the class I TCP domain or the equivalent residue 15 (Asp) of the class II domain (Viola *et al.*, 2012). Intriguingly, Class I TCPs can bind Class II binding sites and vice versa, and some degree of flexibility for TCP4 (a class II TCP) to bind a Class I motif *in vitro* was reported (Schommer *et al.*, 2008).

However, since studies on target site binding specificities of TCPs have been carried out for only a handful of members of the TCP family and were mainly done by *in vitro* experiments, it is not known whether these rules and sub-division for class I and II apply to all members and under native conditions. The Class II TCP4 TF is perhaps most extensively studied with respect to DNA binding features (Schommer *et al.*, 2008; Aggarwal, Das Gupta, *et al.*, 2010; Viola *et al.*, 2012). Of the Class I clade, *TCP16* and *TCP20* (Viola *et al.*, 2012), and *TCP11* (Viola *et al.*, 2011) received most attention. It is important to note that the differences in binding specificity were found by yeast-one-hybrid (Aggarwal, Das Gupta, *et al.*, 2010) or SELEX studies (Viola *et al.*, 2012). Most likely, these methods will identify the high-affinity binding sites, but will probably overlook the low-affinity binding sites. They also do not take into account the role and possible effect of co-factors and of specific interaction partners, which might change the binding specificity of the TCP under scrutiny. To shed light on the native binding capacity of TCP TFs, I have performed a genome-wide and comprehensive analysis on BRC1 targets by ChIP-seq and aimed to identify the preferred binding sequences and regulatory mechanisms (Chapter 4 of this thesis).

TCPs, they're everywhere!

TCPs are a widespread family of transcription factors, found in basal land plants and multicellular algae (first described by Navaud *et al.*, 2007), monocots and dicots (reviewed by (Danisman, 2016)). Genome duplication and diversification has had a major role in the evolution of the TCP TF family: mosses, ferns and lycophytes possess five to six members (Navaud *et al.*, 2007), whereas *Arabidopsis*



numerous other species such as maize (Doebley *et al.*, 1995), rice (Takeda *et al.*, 2003) and Arabidopsis (Aguilar-Martínez *et al.*, 2007). The same holds for the regulation of the JAW-TCPs by miR319; overexpression of this microRNA leads to a striking crinkled leaf phenotype due to an overproduction of cells in these organs (Palatnik *et al.*, 2003; Nath *et al.*, 2003; Efroni *et al.*, 2008). In tomato miR319 is required for normal leaf development by regulating the TCP homologue *LANCEOLATE* (Ori *et al.*, 2007). In monocots too, the function of miR319 seems to be conserved as the overproliferation phenotype was seen in miR319 overexpression plants in Creeping Bentgrass (*Agrostis stolonifera*) that produced wider and thicker leaves (Zhou *et al.*, 2013). Furthermore, the CIN clade contains five members in Arabidopsis (see JAW-D above), whereas Antirrhinum possesses only one member and its loss of function causes similar phenotypes (Nath *et al.*, 2003).

Linking identity and growth through MADS-TCP interactions

Flowers have been extensively studied throughout history and substantial knowledge has been acquired on the identity specification and development of the different flower organs. In this respect, well-known is the ABC model of flower development (Coen and Meyerowitz, 1991), which explains how different genes and gene combinations specify floral organ identity. Except for the Arabidopsis A-class gene *APETALA2* (*AP2*), all these genes encode members of the MADS domain family of TFs and their specific and unique interactions determine the identities of the four types of floral organs: carpels, stamens, petals and sepals (Immink *et al.*, 2010; Coen and Meyerowitz, 1991). The determination of floral organ identity occurs early after the formation of the flower meristem (Alvarez-Buylla *et al.*, 2010), however, the same MADS TFs continue to be expressed regionally in particular floral tissues during the growth and differentiation stages of the floral organs. This has led to hypothesis that organ identity specification and growth regulation might be linked by interactions between MADS domain and TCP TFs (Dornelas *et al.*, 2011). Even more enticing is the fact that the duplication of the CYCLOIDEA-like TCPs almost corresponded with duplication events of floral identity MADS domain proteins: AGAMOUS, SEPALLATA and APETALA3 (Howarth and Donoghue, 2006), in itself no proof for a shared function, but it does strengthen the hypothesis that MADSes and TCPs are linked. A specific set of TCPs are targeted by APETALA1 and SEPALLATA3 (Wellmer *et al.*, 2006; Kaufmann *et al.*, 2009; Kaufmann *et al.*, 2010b) and ABC-MADS proteins are identified as complex partners of several TCPs in immunoprecipitation assays (I will elaborate on this in Chapter 5 of this thesis). In rice, proof for a functional MADS-TCP interaction was found in the form of an interaction between MADS-domain protein OsMADS57 and TCP protein OsTB1, a complex which is supposed to modulate tillering in this species (Guo *et al.*, 2013).

Recent observations provide evidence that specific TCPs can also act as organ identity genes. A cucumber plant, mutated for a TCP was shown to develop shoots instead of tendrils (Wang *et al.*,

2015a). A similar phenotype was found in melons where a single-nucleotide mutation in *CmTCP1* led to the Chiba tendril-less mutation. Also here, the tendrils were converted to shoot and leaf-like structures (Mizuno *et al.*, 2015). Interestingly, in both cases the TCP in question was of a Cucurbita specific TCP family, containing a highly conserved seven-amino-acid motif unique in Cucurbitaceae, adding another layer to the diversity of the TCP TF family. The causal mutations mentioned above are single amino acid residue changes, suggesting that a very specific interaction is disturbed. This hypothesised perturbation of interaction capacity might have caused the change in identity, a molecular explanation that I believe to be more common and that I elaborate upon in Chapter 5 of this thesis.

This thesis

As shown in the paragraphs above, TCP transcription factors play hugely important roles during plant development and other processes required for normal plant growth. Phenotypes of several members of the family have been characterised and molecular modes of action unravelled. This notwithstanding, our knowledge about this family is still very fragmented. The aim of my research was to contribute to our understanding of the TCP transcription factor family. To achieve this I used several approaches, from sophisticated quantitative phenotyping, TCP function analysis to genome-wide DNA binding sites analysis. In Chapter 2 of this thesis I aimed to explore quantitative effects of TCP mutants on growth and other developmental traits and to unveil novel associations between various phenotypes. Do architectural characteristics such as an increase in branching have a positive effect on other traits such as total seed yield? By using a high-throughput phenotyping robot, plant development was monitored throughout time. I aimed to answer questions on redundancy by growing single mutants next to plants mutated for several related TCPs.

A group of TCPs previously mentioned as possibly redundant to the *JAW-TCPs* are the *TCP5*-likes. I will show in Chapter 3 that their phenotypes are rather different and that they can be explained by an alteration in ethylene biosynthesis. I discovered that *TCP5* directly binds the promoter of *ACS2*, an ethylene biosynthesis gene, and that application of ethylene inhibitors can revert the mutant phenotypes to wild type.

One of the TCPs frequently standing out in the phenotypic analysis mentioned above and previously described with striking phenotypes is *BRC1*, the *TB1* orthologue from Arabidopsis. With a multitude of axillary branches, it is one of the few TCPs that shows a strong phenotype as a single mutant. Despite having been characterised a decade ago in Arabidopsis (Aguilar-Martínez *et al.*, 2007) its exact molecular function remains elusive. Previous research showed its ability to enhance abscisic acid (ABA) accumulation through the regulation of three related Homeodomain leucine zipper protein (HD-ZIP)-encoding genes: *HB21*, *HB40* and *HB53*. The increase of ABA biosynthesis is causal for the

suppression of bud development (González-Grandío *et al.*, 2017). Using a combined transcriptomics and ChIP-seq analysis I will show in Chapter 4 that BRC1 binds to and possibly regulates several ABA biosynthesis genes directly. Next to this, this study presents the first *in vivo* genome-wide TCP binding site analysis.

In Chapter 5 I investigate the function of the interaction between MADS and TCP proteins, which may support the hypothesis that organ identity specification and growth regulation is linked by interactions between members of these two protein families (Dornelas *et al.*, 2011). I will show by Yeast-2-Hybrid assays and immunoprecipitation that TCPs and MADSeS interact.

This thesis ends with a general discussion on the obtained results, expands on their implication for the field, and highlights possible directions for further research in Chapter 6.

Chapter 2:

A spatio-temporal analysis of plant growth and development coupled to yield characteristics in several *Arabidopsis thaliana* *tcp* mutant backgrounds.

Sam W. van Es

Elwin B. van der Auweraert

Sylvia R. Silveira

Gerco C. Angenent

Aalt D.J. van Dijk

Richard G.H. Immink

“When we try to pick out anything by itself,
we find it hitched to everything else in the
universe.”

John Muir

Abstract

Several members of the *Arabidopsis thaliana* TCP transcription factor (TF) family affect plant growth and development at different moments during the plant life cycle. In this study, we investigated possible associations between single or multiple TCP functions and phenotypic characteristics, such as vegetative growth parameters and several yield aspects, including total seed yield, seed number and seed weight. We showed that mutations in particular members of the *TCP* TF family resulted in an altered branching phenotype and that this coincides with a reduction in seed yield under the applied environmental conditions. Previously, it has been proposed that class I and class II TCP TFs fulfil opposite functions in plant growth and development, but here we reveal that this hypothesis needs revision, as mutation in members from both classes showed similar developmental effects. Additionally, the supposed functional redundancy within particular sub-clades of the TCP TF family was analysed, revealing that stacking of mutations in several TCPs led in some cases to less severe phenotypes in comparison with single mutant phenotypes instead of the expected increased phenotypic effects. Furthermore, for some genes supposed to act redundantly, such as *BRANCHED1* (*BRC1*) and *BRC2*, contrasting phenotypes were found for particular traits in the single mutants. Altogether our analyses showed the importance of comprehensive and comparative phenotyping of mutants and of detailed quantitative analyses in order to get a full understanding of the contribution of individual members of the TCP TF family to particular biological functions.

Introduction

The major challenge of modern agriculture is to produce increasing amounts of high quality biomass for food, feed, and bio-based products, with a minimal ecological footprint. Final yield in the form of seeds, fruits, or leaves (e.g. leafy vegetables) depends strongly on plant architecture, organ size, and tissue longevity (Cai *et al.*, 2016; Busov *et al.*, 2008) and these traits have therefore been the subject of breeding since the dawn of agriculture.

Our research aims at identifying genes involved in the control of plant development and architecture, and finding possible correlations between their functioning and yield characteristics. We focus on key regulatory factors belonging to the TCP transcription factor (TF) family in the plant model species *Arabidopsis thaliana*. Genes of this family orchestrate numerous processes during Arabidopsis development; examples include the involvement of *BRANCHED1* (*BRC1*) and *BRC2* in the outgrowth of axillary branches (Aguilar-Martínez *et al.*, 2007), determination of leaf shape and curvature by *JAW-TCPs* (Nath *et al.*, 2003; Palatnik *et al.*, 2003), effects on leaf size by *TCP5-like* genes (Efroni *et al.*, 2008), and leaf senescence orchestrated by the antagonistic action of *JAW-D* and *TCP20* (Schommer *et al.*, 2008; Danisman *et al.*, 2012).

TCP gene functions appear to be broadly conserved and a mutation in the maize *TEOSINTE BRANCHED1* (*TB1*), the orthologue of the Arabidopsis *BRANCHED*-likes, resulted in a high level of branching and tiller outgrowth, which has been instrumental in the domestication of maize from its ancestor teosinte (Doebley *et al.*, 1995, 1997). Similar branching phenotypes have been observed in rice plants with a mutation in the *TB1*-like gene (Takeda *et al.*, 2003). The *JAW-TCPs* (*TCP2*, *-3*, *-4*, *-10* and *-24*) are simultaneously targeted by a microRNA (miR319) in Arabidopsis. Overexpression of miR319 leads to the *jaw-D* mutant, which has a striking crinkled leaf phenotype due to an overproduction of cells in the leaf margins (Palatnik *et al.*, 2003; Nath *et al.*, 2003; Efroni *et al.*, 2008). Similarly, tomato miR319 is required for normal leaf development by regulating the tomato *JAW-TCP* homologue *LANCEOLATE* (Ori *et al.*, 2007).

The above-mentioned examples indicate the importance of the TCP TF family for the regulation of growth and plant architecture in the model species Arabidopsis and various crops. The more detailed our knowledge on the specific function of these TCPs and their potential combined effects on plant development is, the more we will be able to precisely direct breeding for yield optimization by altering leaf growth, senescence, and branching patterns (tillering).

Even though many reports about members of the TCP family of TFs are available (Danisman, 2016), a comprehensive and detailed phenotyping of the various single and combined *tcp* gene mutants is lacking. This analysis is essential to understanding the role and importance of each individual *TCP* gene, the genetic interactions between the different *TCP* genes, and how effects on one trait influence

other traits and/or final yield parameters. Most phenotypes observed so far consist of snapshots at a given time point or specific stage or on specific tissues or organs. This inevitably complicates the documentation of phenotypes that occur and are dynamic through time. Furthermore, it does not allow to investigate how phenotypes, such as leaf size and final seed yield, might be linked.

One of the difficulties of studying genes affecting growth and growth speed is that phenotypes are often only noticeable when careful measurements are performed. For example, a leaf with a five percent increase in surface area is very difficult to identify with the naked eye, while it will give rise to an enormous increase in biomass production. Furthermore, it is evident that mutations resulting in altered developmental progression, such as *tcp* mutants affecting senescence or leaf growth rate, can be recorded only if a temporal component is included in the analysis (Boyes *et al.*, 2001). Plants mutated for *TCP20* for instance, show an increase in leaf pavement cell size in young developing leaves, whereas no difference in final leaf size could be detected (Danisman *et al.*, 2012).

Senescence is a developmental process and an important trait in plants. It has been estimated that 50% of discarded fresh food is largely attributed to their decay (Blanke, 2015). This concerns both breeders and consumers alike. Several *TCP* genes appear to control senescence, such as *TCP4* and *TCP20* (Schommer *et al.*, 2008; Danisman *et al.*, 2012). Other *TCP* genes have been implicated in the regulation of hormonal pathways known to affect senescence (reviewed by Khan *et al.*, (2013)), such as ethylene (*TCP5*, (van Es *et al.*, 2018)), cytokinins (*TCP4*, Efroni *et al.*, (2013)), salicylic acid (*TCP8*, Wang *et al.*, (2015)), and jasmonic acid (*TCP20*, Danisman *et al.*, 2012), which makes senescence an interesting trait to investigate in relation to TCP functioning.

We analysed a well-defined set of single and multiple *tcp* mutants for several growth and yield parameters, as well as their effect on leaf senescence. Functional redundancy has been shown for various members of the *TCP* family (Danisman *et al.*, 2013; Cubas *et al.*, 1999). For example, a single knockout of a gene of the Arabidopsis *CIN-TCP* clade produces only mild phenotypes, whereas knocking out the whole clade shows dramatic changes in leaf development (Schommer *et al.*, 2008; Palatnik *et al.*, 2003). Using a combination of mutants (e.g. single, double and triple) enables further analyses of the proposed functional redundancy within the TCP family and to decipher the contribution of individual TCPs to specific growth and development related functions.

In this study, the thorough and comprehensive temporal analyses were done using the ‘Phenovator’ phenotyping platform (Flood *et al.*, 2016). Using this Phenovator platform, all the above-mentioned traits and characteristics were monitored in various *tcp* mutant lines and compared to wild type plants. The plants were imaged during the vegetative developmental stage at several moments of the day. This allows the measurement of rosette size, growth rate, and photosynthetic efficiency. Phenotyping of the branching traits, and yield and seed characteristics was done on the matured and full-grown plants. Since the main driver of senescence is aging as intrinsic part of development

(reviewed by Khan *et al.*, 2013), we measured the senescence response upon triggering of this process by darkness in relatively young plants. Because the progress of senescence in whole plants differs from that in detached tissue (Weaver and Amasino, 2001), which reflects shelf-life, senescence was monitored as well in rosette leaves of plants detached from their roots immediately prior to dark induction.

Combining all the phenotypic data on growth, development, aging and yield has provided us with novel insights into the function of several members of the TCP TF family, as well as on the presumed redundancy of several TCPs. Furthermore, we show that, under our growing conditions, an alteration in branching pattern (regardless of an increase or decrease in number of branches), leads to a decrease in final yield.

Results

Mutant selection

A well-defined set of *tcp* mutants was selected to be analysed for a number of developmental, architectural and yield parameters. They were chosen based on their described strong developmental phenotypes, which made validation of the approach and critical evaluation of the followed methodology possible. An example is the *jaw-D* mutant, which is known to exhibit slowly developing leaves that eventually grow larger than in wild type plants (Efroni *et al.*, 2008). Obvious candidates to study the relation between branching and yield are the mutants in the *BRANCHED-like* TCPs (Aguilar-Martínez *et al.*, 2007). Additionally, we focussed on the analysis of redundancy within the TCP TF family, and included among others the double mutants *tcp14tcp15* and *tcp8tcp15*, as well as the single *tcp8* and *tcp15* mutants. A full list of selected mutants which have been grown on the Phenovator platform can be found in Table 1.

Experimental set-up and technical constrains of the ‘Phenovator’ platform

The Phenovator platform (Flood *et al.*, 2016) allows to grow 1440 plants simultaneously in a grid of 24 by 60 plants (Supplemental Figure 1A). The grid was divided into 28 plots in which all 24 selected genotypes (Table 1) were randomly positioned to prevent a possible positional bias. All plants were assigned a coordinate based on their position in this grid. Two different parameters were measured by the camera system: PSII operating efficiency (Φ PSII) by Pulse Amplitude Modulated fluorescence measurement (PAM) and near infrared (NIR) reflection at 790nm. The branching phenotypes and seed yield parameters were manually determined on mature, fully-grown plants.

The NIR reflection was used to estimate the projected leaf area (PLA) as it provides a good estimate of above ground biomass (Leister *et al.*, 1999) and can therefore be used to determine plant growth.

The particular wavelength (790 nm) was chosen so that plants could be measured both day and night without disturbing their circadian rhythm. A full description of the measurement scheme can be found in Table 2. To check for a possible effect of the plant's position in the climate chamber, a regression analysis was performed. The average size of all plants over time, as well as the maximum size was plotted on the X- and Y-coordinate corresponding to their position in the climate cell (Supplemental Figure 1A). We found a correlation between the X-coordinate and both maximum and average growth for our plants (Supplemental Figure 1B). No significant correlation between Y-coordinate and PLA was detected (Supplemental Figure 1C). The R-package SpATS (Rodríguez-Álvarez *et al.*, 2016; Velasco *et al.*, 2017) was used to correct for the observed spatial effect in the X-position. Although the climate cell is expected to have near identical conditions regardless of position within the cell, the observed positional effect in the X-direction might be due to small differences in e.g. air flow, humidity or nutrient availability. Another possibility is that the bias is introduced due to the inflow of water with nutrients from one side of the climate cell ($X \approx 0$; Supplemental Figure 1A).

Creation of a formula to describe the progress of growth for all plants

An essential part in analysing plant size in the time series is to convert the data into an equation representing growth over time. Creating a growth-curve equation fitting the observed data enables to turn different sizes and growth speeds into easily distinguishable parameters. This provides insight into growth dynamics of all mutant lines over time and enables making a step beyond investigating average final plant sizes only.

We choose to use the singular spectrum analysis (SSA) tool, implemented in the R package Rssa (Golyandina *et al.*, 2013) to study the PLA data obtained from the time series. We performed the analysis on time series of individual plants. An SSA analysis decomposes a time series into a given number of elementary components [ECs], based on the covariance between different measurements at different time values. For the SSA, a window size must be chosen, which is equal to the number of ECs into which the time series is decomposed. There are 110 measurements for every individual plant per time series and here a window size of ten was chosen to prevent overcomplication of the analysis. The eigenvalues and their relative contribution to the data shows that there is one EC contributing for more than 99% of the observed variation (red square in Supplemental Figure 2A). This implies that it contains almost all of the variability of the time series and therefore would be an excellent component to use in forecasting the progress of plant growth. Furthermore, the first component closely resembles part of an S-curve (Supplemental Figure 2B), which implies that this part of the time series represents actual growth of the plant (Weraduwaage *et al.*, 2015). Next to this, we should take into account the circadian rhythm of a plant, expressing itself as changes in the PLA because of leaf movements (Engelmann *et al.*, 1992). There are two ECs, that show slowly

Loci affected	Mutant	T-DNA identifier	Created/First described by	Number
AT5G60970	<i>tcp5</i>	SM_3_29639	Efroni <i>et al.</i> , 2008	22
AT5G60970	<i>pATML1::TCP5</i>	Overexpression of TCP5 in epidermis	Van Es <i>et al.</i> , 2018	13
AT3G02150	<i>pATML1::TCP13</i>	Overexpression of TCP13 in epidermis	In house	12
AT5G60970 - AT3G02150 - AT5G08070	<i>tcp5 tcp13 tcp17</i>	SM_3_29639 - SM_3_23151 - SALK_147288	Efroni <i>et al.</i> , 2008	11
AT5G60970 - AT3G02150 - AT5G08070	<i>miR-3TCP: tcp5,-13,-17</i>	Artificial miRNA overexpression	Efroni <i>et al.</i> , 2008	5
AT2G31070	<i>tcp10</i>	SALK_137205	Alonso <i>et al.</i> , 2003	23
AT4G18390 - AT1G53230 - AT3G15030 AT2G31070 - AT1G30210	<i>jaw-D: tcp2,-3,-4,-10,-24</i>	Overexpression of miR319	Palatnik <i>et al.</i> , 2003	14
AT3G18550	<i>brc1/tcp18</i>	SALK_091920	Aguilar-Martínez <i>et al.</i> , 2007	21
AT1G68800	<i>brc2/tcp12</i>	SALK_023116	Aguilar-Martínez <i>et al.</i> , 2007	7
AT1G68800 - AT3G18550	<i>brc1brc2</i>	SALK_091920 - SALK_023116	Aguilar-Martínez <i>et al.</i> , 2007	4
AT1G69690	<i>tcp15</i>	SALK_011491	Alonso <i>et al.</i> , 2003	20
AT3G47620 - AT1G69690	<i>tcp14 tcp15</i>	SALK_011491	Kieffer <i>et al.</i> , 2011	19
AT1G58100 - AT1G69690	<i>tcp8 tcp15</i>	SAIL_656_F11 - SALK_011491	In house	6
AT1G58100	<i>tcp8</i>	SAIL-656-F11	Aguilar-Martínez <i>et al.</i> , 2013	10
AT3G27010 - AT1G58100	<i>tcp20 tcp8</i>	SALK_041906 - SAIL_656_F11	Danisman <i>et al.</i> , 2013	3
AT2G45680	<i>tcp9</i>	SALK_035853	Danisman <i>et al.</i> , 2012	2
AT2G45680 - AT3G27010	<i>tcp9 tcp20</i>	SALK_035853 - SALK_041906	Danisman <i>et al.</i> , 2012	1
AT3G27010	<i>tcp20</i>	SALK_041906	Danisman <i>et al.</i> , 2013	24
AT5G51910 - AT3G27010	<i>tcp19 tcp20</i>	SALK_024434 - SALK_041906	Danisman <i>et al.</i> , 2013	17
AT3G27010 - AT1G72010	<i>tcp20 tcp22</i>	SALK_041906 - SALK_045755	In house	18
AT5G51910 - AT1G72010	<i>tcp19 tcp22</i>	SALK_024434 - SALK_045755	In house	16
AT5G51910 - AT3G27010 - AT1G72010	<i>tcp19 tcp20 tcp22</i>	SALK_024434 - SALK_041906 - SALK_045755	In house	15
	Col0 "WUR"	Wild type background for O.E. mutants		8
	Col0 "NASC"	Wild type background for T-DNA mutants		9

Table 1. Mutant lines and wild type controls used in this study. Shown are the affected loci, mutant name, the T-DNA identifier and reference to the paper in which they were first described. The number in the most right column corresponds to the number used in the graphs.

oscillating behaviour with a period of one day, which corresponds to the leaf movement of the plants (blue square in Supplemental Figure 2A). These two ECs are always found to be a combination of the second to fifth EC, and both enable to model the circadian rhythm as shown in Supplemental Figure 2C and are therefore included.

Concluding, the data obtained from the PLA can be considered to contain two parts, an S-curve and the oscillatory function. This can be written as:

$$f(t) = g(t) + h(t) = g(t) + g(t)h^*(t) = g(t)[1 + h^*(t)] \quad (1)$$

In this function $g(t)$ is the real growth and $h(t)$ the day-night rhythm. As the difference in measured

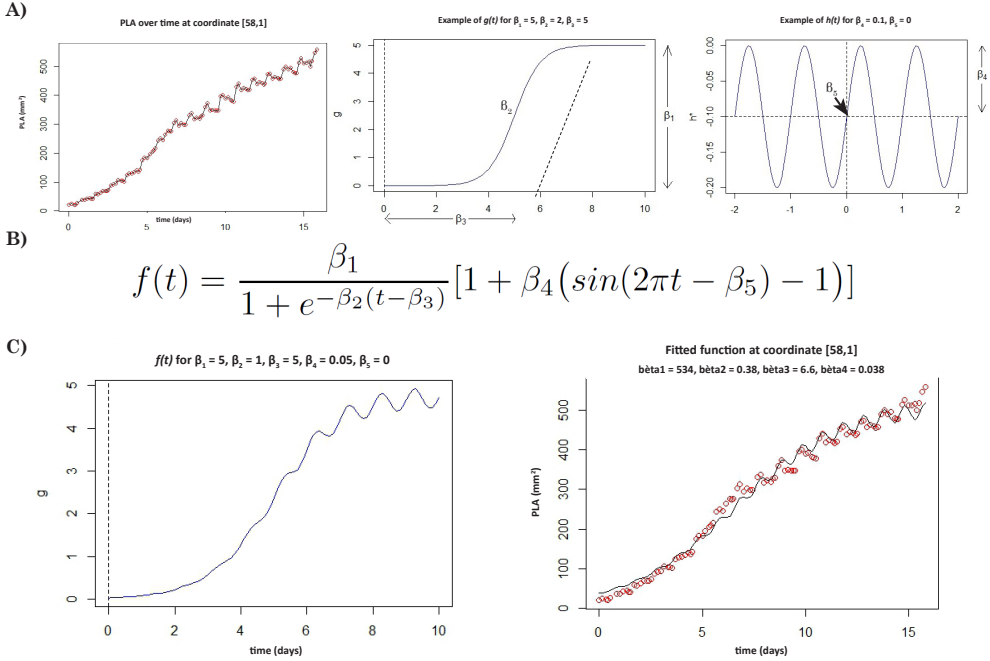


Figure 1. Designing a growth function based on rosette size measurements over time. (A) A fitted curve, showing resemblance to an S-curve (left panel). This was divided into an actual S-curve (middle panel) and an oscillating function to cover for the day/night rhythm (right panel). The equation following the S-curve and oscillation pattern, summed up in the growth function over time, is shown in **(B)**. The combined S-curve and oscillatory function for a set of β values and the final fitted values for this particular example are shown in **(C)**.

leaf surface, due to the day-night rhythm, depends linearly on the actual size of the plant at that time point, the function $h(t)$ is rewritten as $g(t)h^*(t)$. The function of ‘real growth’ $g(t)$ is an S-curve (Figure 1A; middle panel) containing parameters that account for the distance between two asymptotes (β_1), describe the magnitude of the derivative (β_2), and the point at which the derivative of the function reaches its maximum (β_3), all β ’s are ≥ 0 . Taking this into account the S-curve part of the function is obtained as such:

$$g(t) = \frac{\beta_1}{1 + e^{-\beta_2(t-\beta_3)}} \quad (2)$$

Next, the function to describe the day-night rhythm is an oscillatory function with certain amplitude (β_4) and phase transition (β_5) (Figure 1A; right panel). The natural period of this function is one day, and the range of the function should be between -1 and 0, as the measured leaf area can only get smaller by the movement of the plant, but also because the whole function $f(t)$ should be positive:

$$h^*(t) = \beta_4 (\sin(2\pi t - \beta_5) - 1) \quad (3)$$

All this combined allows us to determine the actual growth function. The explicit form is obtained by substituting equations 2 and 3 into equation 1 (see also Figure 1B), resulting in:

$$f(t) = \frac{\beta_1}{1 + e^{-\beta_2(t-\beta_3)}} [1 + \beta_4 (\sin(2\pi t - \beta_5) - 1)] \quad (4)$$

The parameters of function 4 were then estimated by non-linear regression, using the *nls* function in R, for each individual coordinate (i.e. plant). The specific algorithm used was originally introduced as the NL2Sol algorithm (Dennis *et al.*, 1977) and requires lower and upper bounds of the parameters which are implemented in the *port* function. The introduction of bounds can prevent a type of zig-zagging behaviour, and thus increases the chance that the algorithm will converge within a reasonable amount of iterations.

To devise a method to determine a set of starting values for each of the time series, some basic properties of the real-growth function are useful:

$$\beta_1 = \lim_{t \rightarrow \infty} g(t) \quad (5a)$$

$$\beta_2 = \frac{g'(0)}{g(0) - g(0)^2/\beta_1} \quad (5b)$$

$$\beta_3 = \frac{\ln\left(\frac{\beta_1}{g(0)} - 1\right)}{\beta_2} \quad (5c)$$

Thus, if decent estimates can be found for $\lim_{t \rightarrow \infty} g(t)$, $g(0)$ and $g'(0)$, they can then be used to determine starting values of the β 's. A very good approximation of the growth function $g(t)$ can be obtained through the SSA, recalling that the use of the first elementary component contributes to the function for 99%. This component can be computed for each of the time series and is thus the ideal tool for finding the required estimates. For each of the time series this component is a vector of length 110. This vector is denoted as $EC = \{EC_1, EC_2, \dots, EC_{110}\}$, and the vector with the corresponding time values is denoted as $t = \{t_1, t_2, \dots, t_{110}\}$. The required approximations can be written as:

$$\lim_{t \rightarrow \infty} g(t) \approx \max\{EC\} \quad (6)$$

$$g'(0) \approx \frac{EC_5 - EC_1}{t_5 - t_1} \quad (7)$$

$$g(0) \approx EC_1 \quad (8)$$

A biological interpretation of the different β -parameters allows us to look at the growth function in more detail and the use of reasonable bounds for the above-mentioned approximations will be assessed using the available biological information, such as growth stages of Arabidopsis (Boyes *et al.*, 2001). For this, β_1 could represent the maximum possible growth; β_2 a measure for the rate of growth in the exponential phase and β_3 a measure for the time until the rosette of a plant starts its rapid growth phase. β_4 is the change in measured rosette area relative to the real rosette area at that moment and β_5 is the starting point of oscillation related to the circadian rhythm.

The plants were measured until 25 days after sowing, which approaches the time a wild type Arabidopsis plant needs to reach maximum rosette size (Boyes *et al.*, 2001). Therefore, a reasonable guess is that the final size of the plants would be no more than twice the size that it reached during the measurements, which corresponds to $2 * \max\{EC\}$. To ensure that the upper bound for β_1 is not chosen too strictly, it will be set to $\beta_{1,upper} = 3 * \max\{EC\}$. As β_1 represents the maximum possible growth the natural lower bound is $\beta_{1,lower} = 0$. We interpreted β_3 as the time it takes for the plant to reach maximum rosette growth, after the start of the measurements. The measurements started eight days after sowing, so it is unlikely that a plant has already reached the point of most rapid growth at $\beta_{3,lower} = 0$. The duration of the measurement is 17 days, making $\beta_{3,upper} = 30$ a safe upper bound, assuming a plant has reached its maximum growth almost 40 days after sowing. The parameter β_2 is closely related to β_3 and can be inferred by:

$$\beta_2 = \frac{2}{\beta_3 - t_{tang,0}} \quad (9)$$

Here $t_{tang,0}$ is the time coordinate where the this tangent intersects the t -axis. For $t_{tang,0}$ as well, bounds should be derived. As $g(t)$ is a convex function for $t_{tang,0}$, every tangent in that part of the function lies below the function. As we expect that $g(0)$ is very small, this means that $t_{tang,0} \geq 0$ is a reasonable assumption. Most of the growth of the plant happens between $\beta_3 - t_{tang,0}$ and $\beta_3 + (\beta_3 - t_{tang,0})$, that is within a time span of $2(\beta_3 - t_{tang,0})$. It is highly unlikely that most of the growth of the plants happens within 4 days, so $2(\beta_3 - t_{tang,0}) \geq 4$ is a reasonable assumption. This is equivalent to $(\beta_3 - t_{tang,0}) \geq 2$. Combining these bounds with equation (9) yields $\beta_2 \leq 1$ which allows us to formulate the following estimations:

$$0 \leq \beta_1 \leq 3 * \max\{EC\} \quad (10a)$$

$$\frac{1}{15} \leq \beta_2 \leq 1 \quad (10b)$$

$$0 \leq \beta_3 \leq 30 \quad (10c)$$

The second part of the growth function is given by an oscillatory function, see equation (3). Leaf movement is represented by β_4 and should be interpreted as a percentage with a reasonable starting value of $\beta_{4,\text{start}} = 0.05$. As it is unlikely that the day and night movement of the rosette leaves will result in more than 50% change in area, a reasonable upper bound is therefore $\beta_{4,\text{upper}} = 0.5$. The moment the circadian rhythm starts is represented by β_5 , i.e. the phase-shift of the oscillation. The choice of $\beta_{5,\text{start}}$ is not that important, as its range is naturally bound between $0 \leq \beta_5 \leq 2\pi$. The average value of $\beta_{5,\text{start}} = \pi$ will be chosen.

With the prescribed combination of starting values and bounds for the parameters, the algorithm converges for all the time series. Figure 1C (right panel) shows the first of the time series examples, revealing that the growth function nicely fits through the data points and accounts for the oscillatory behaviour. To check whether the bounds are chosen correctly the distribution of the different β 's was checked. As is shown in Supplemental Figure 3, the distribution of $\beta_{2.5}$ lay nicely within the bounds, whereas for β_1 a lot of values cluster close to the upper bound. The underlying reason can be that the time series which have a β_1 close to the upper bound are the ones that have not reached their point of maximum growth. This notwithstanding, the bounds and starting points allow for all series to converge the algorithm. The β -values were corrected for the observed spatial bias (Supplemental Figure 1) and values prior to and after correction are visualised in Supplemental Figure 4.

Growth parameter analyses

The nature of the measurements enables measuring of the rosette surface area, but not distinguishing individual leaves and their shape and size. Still, a careful interpretation is appropriate in order to disassemble the dynamic growth at plant level, although the β -values in the growth equation described above cannot be directly linked to a particular growth parameter. As we did for the estimation of the bounds above, we theorized that β_1 could represent the maximum possible growth; β_2 might be a measure for the rate of growth and β_3 can represent a measure for the time until the rosette of a plant starts its rapid growth phase. The parameters accounting for the oscillatory motion can represent the change in measured rosette area relative to the real rosette area at that moment due to circadian leaf movements (β_4).

Average β -values per plant line were plotted and the parameters β_2 and β_3 were scaled to the lowest value to enhance readability of the graph (Supplemental Figure 5A). Statistical tests show differences

in β -values comparing the mutant lines with wild type control plants. Subsequently, a PCA analysis was done to visualise potential differences for the various *tcp* mutants (Figure 2). A clear example of altered development is the *jaw-D* mutant, shown to have a significantly lower β_2 but higher β_3 . This represents the plants' slow developmental progress through slow growth (β_2) and longer time to reach the rapid growth phase (β_3). Together with the *tcp5tcp13tcp17* triple mutant, *jaw-D* is the only mutant that has a lower β_2 compared to the wild type, as clearly visualized by the PCA plots in Figure 2. In contrast, *tcp10* has a higher β_2 than wild type, i.e. a rapid growth rate.

Another type of developmental progression of plant growth is presented by the *brc1brc2* double mutant. Plants of this mutant reach their maximum growth faster (β_3) and have a significantly smaller final size (β_1) than the wild type control plants. Interestingly, the single mutants *brc1* and *brc2* show opposite behaviour concerning β_1 and deviate from the double in that *brc1* has a higher β_3 value, whereas *brc2* appears to have a higher growth speed (β_2) (Figure 2). Another way to visualise this is by plotting the PLA over time for the raw data versus the model (Figure 3A), showing their resemblance. This was followed by plotting the raw data for the *brc*-mutants and Col-0 control in Figure 3B, revealing the lower β_1 for the *brc1brc2* mutant for example. The single mutants *brc1* and *brc2* show opposite behaviour concerning β_1 (both have a significantly bigger β_1 than Col-0) and deviate from the double *brc1brc2* mutant in that *brc1* has a higher β_3 value, whereas *brc2* appears to have a higher growth speed (β_2). Figure 3B shows that this might have led to the overall bigger *brc2* whereas *brc1* only 'catches up' later.

Photosynthetic capacity of plants

Next to size measurements based on PLA, the 'Phenovator' camera is monitoring photosynthetic efficiency of the plants under study. For this purpose, the system uses Pulse Amplitude Modulated (PAM) chlorophyll fluorescence imaging to measure the light-use efficiency of PSII electron transport (Φ PSII) (Genty *et al.*, 1989; Baker, 2008; Flood *et al.*, 2016). Based on the average output of the Φ PSII measurement for all individual wild type and *tcp* mutant lines, no significant differences were found (Supplemental Figure 6A), revealing that none of the analysed *TCP* transcription factors are having a direct effect on photosynthetic efficiency during plant development.

Characterizing seed yield characteristics

Several aspects of yield were determined, focussing on seeds. Total yield was determined by weighing the total amount of seeds for eight plants per genotype. A closer look at the seed characteristics was done by measuring seed size and seed number per silique on four siliques of five plants per genotype. We found that average seed size was not significantly affected in any of the analysed mutants (Figure 4A), whereas several lines showed a reduction in the average amount of seeds per silique and total

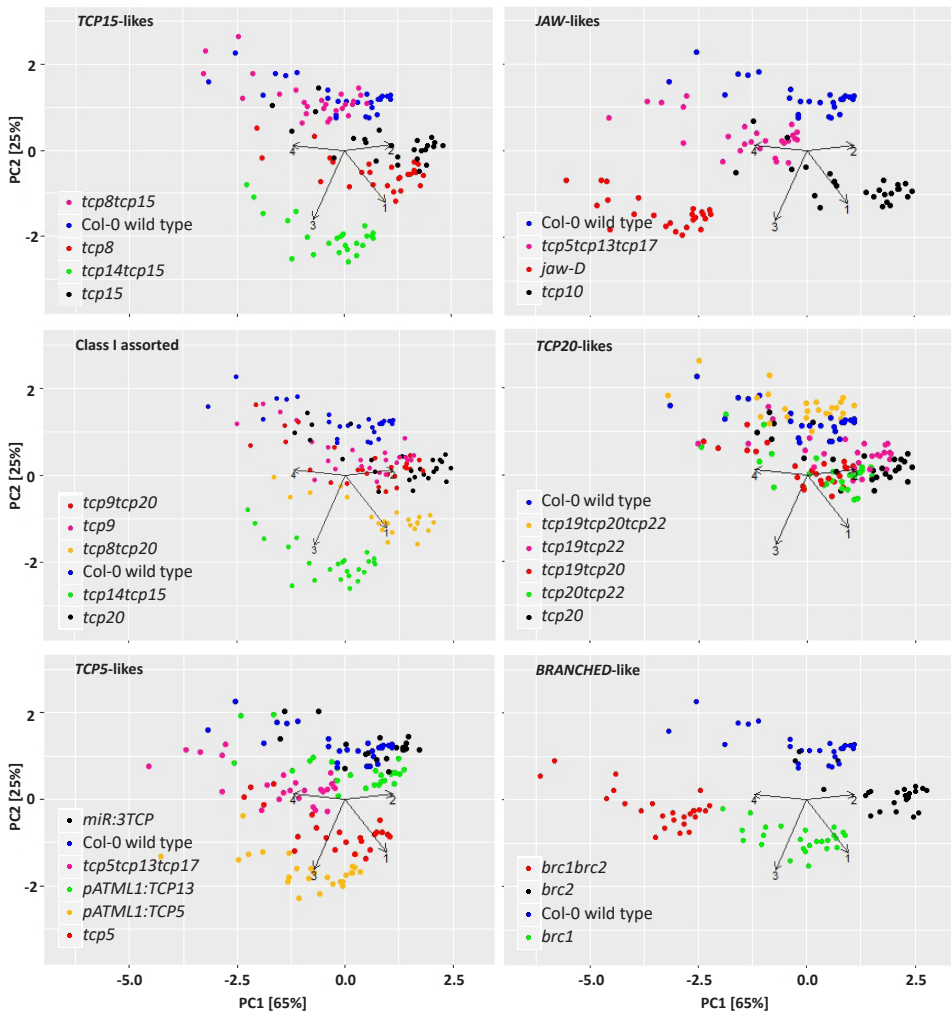


Figure 2. PCA analyses for average β -values of all lines in this study.

Results of a principal component analysis (PCA) for all the β 's to examine a possible difference in mutants versus wild type. The arrows numbered 1, 2, 3 and 4 correspond to β 1, β 2, β 3 and β 4 respectively. Principal component 1 and 2 combined explain 90% of the variance (PC1 explains 65% of the variation, PC2 25%). The plots are made up of groups of related TCPs (e.g. 'Branched-likes') and/or based on sequence homology (e.g. 'Class I assorted').

seed weight (Figure 4B and 4C). Only the seeds of the double mutant *tcp8tcp15* had a significantly lower weight compared to wild type seeds (Figure 4D). Correlation analyses of the different seed characteristics revealed that the number of seeds is negatively correlated to both seed area and seed weight and that seed weight is positively correlated to seed area (Supplemental Figure 7A to 7C). Several lines showed a decrease in total seed weight (i.e. total yield) such as *brc1brc2* double mutant and *jaw-d*, but also two *tcp15*-related double mutants: *tcp8tcp15* and *tcp14tcp15*.

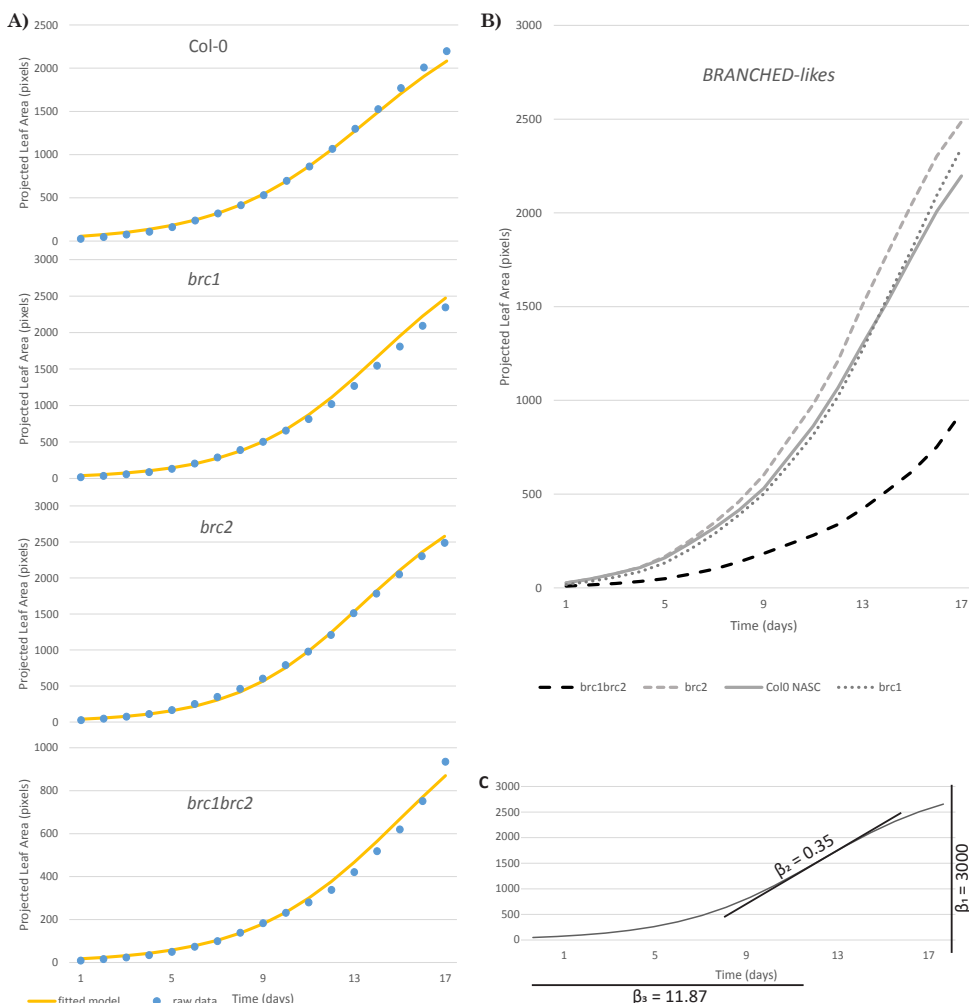


Figure 3. Visualisation of model versus raw data of *BRANCHED* TCPs

(A) shows the fitted model (yellow line) and the raw data (blue data points) for four individual plant lines during the 17 days of measurement. A comparison of the three *branched* mutants and a wild type control (B) showing the different growth curves. An example of a fitted S-curve for three β -values shown in (C). Shown in (A) and (B) is the average PLA per plant for each line, with measurements from one time point during the day, omitting the circadian rhythm for clarity of graph.

TCPs affecting branching parameters; old acquaintances and new friends

When comparing the branching phenotypes (i.e. number and type of branches; Figure 5A) of all lines used in this study, we found that as expected (Aguilar-Martínez *et al.*, 2007), *brc1* and *brc1brc2* double mutants show an increase in secondary branches. Interestingly, the single *brc1* mutant shows a significant effect in number of branches, but the single *brc2* mutant did not, revealing that there is

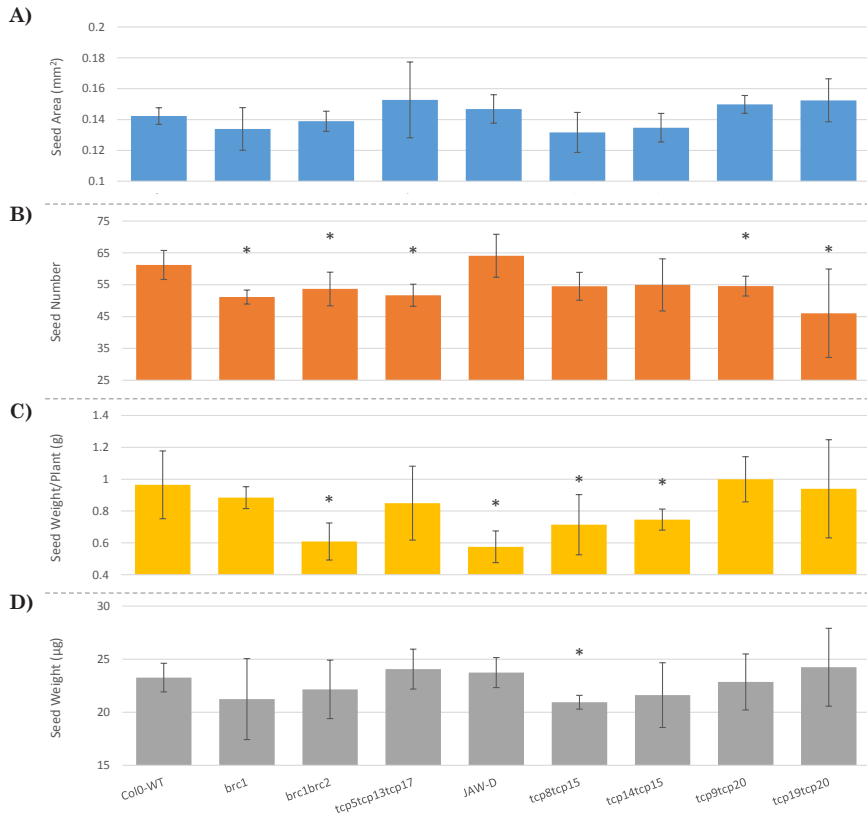


Figure 4. Genotypes showing differences in yield characteristics.

Quantification of yield characteristics such as average seed area (A), average seed number per silique (B), total seed weight per plant and average weight of the individual seed in (C) and (D) respectively. Only genotypes are shown for which statistically significant differences were found compared to wild type control. Average seed number and seed area were determined on four siliques on five plants per genotype. Statistically significant differences ($P < 0.05$) are indicated by an asterisk.

no full redundancy between these genes (Figure 5B). Several other lines showed a reduction in some aspects of branching (Figure 5C), most notably the *jaw-D* (class II TCPs) and *tcp14tcp15* (class I TCPs) mutant lines, that gave a significant reduction in the number of secondary branches. It seems that both an increase as well as a decrease in the number of branches has a negative effect on the amount of seeds harvested from a plant grown under our conditions (*brc1brc2*, *jaw-D* and *tcp14tcp15* in Figure 5D). Alternatively, these genes are independently from the branching function involved in seed characteristics. Interestingly, the number of secondary branches is not correlated to the number of lateral branches (Supplemental Figure 7D) whereas the more secondary branches growing on a plant, the more branched these become.

Growth and photosynthesis during a Dark Induced Senescence assay

Several TCPs have been implicated in the process of senescence, for instance through the regulation of jasmonic acid biosynthesis (Danisman *et al.*, 2012) and therefore, this process was investigated in this study as well. We decided to grow the plants for approximately two weeks under short day conditions (12/12-hour day/night rhythm) before senescence-related measurements started. The experiment can be divided into three phases. The first phase is where plants grew under a 12/12-hour day/night rhythm. The second phase starts on the day when this rhythm changed to a 0/24-hour day/night rhythm, so that the plants did not receive any more light. The third and last phase starts when the rhythm is switched back to a 12/12-hour day/night rhythm. Photosynthetic efficiency (Φ PSII) was determined during the whole experiment and, in combination with measurements on the PLA, used as measure of senescence. A full overview of the experimental setup and the timing of measurements can be found in Table 2B. Furthermore, the timeline is highly important in this experiment as senescence is a time driven process, therefore, a description of the time series is shown in Table 3.

Unfortunately, final and average Φ PSII measurements failed to reveal any significant differences comparing the different genotypes (Supplemental Figure 6B), probably because the plants were still too young and in a developmental stage far prior to the initiation of senescence.

Therefore, we continued by looking at the combined information obtained from both the PLA and the Φ PSII data resulting from this experiment. These data contain valuable information regarding the growth phase and senescence of the plants and should be analysed in close relation to one another. An example of two 'typical' Φ PSII and PLA measurement series is shown in Supplemental Figure 8, which clearly exemplifies the three phases of the experiment, described above. In the first phase the PLA indicates steady growth, then as the second phase starts the PLA suddenly drops off. This is because the leaves point upwards due the initiated dark period, which causes the reduction of the measured leaf surface area, as it is measured from above. As the second phase progresses the PLA recovers to approximately their size at the end of phase one. In phase three the PLA increases again for plants that are still alive. For the Φ PSII time series the first phase is more or less constant, then in the second phase they drop off. In the third phase they recover again for the plants that survived (Supplemental Figure 8A) and stay down, or reach NA values, for plants that died (Supplemental Figure 8B).

Another way of looking at the data is the rate of reduction of photosynthetic efficiency measured by the Φ PSII measurements. Where $t = 7.18$ is the time when the last Φ PSII measurement in phase 1 took place. A few days later, entering into phase 2, $t = 16.03$ was chosen to determine the decline of Φ PSII-values:

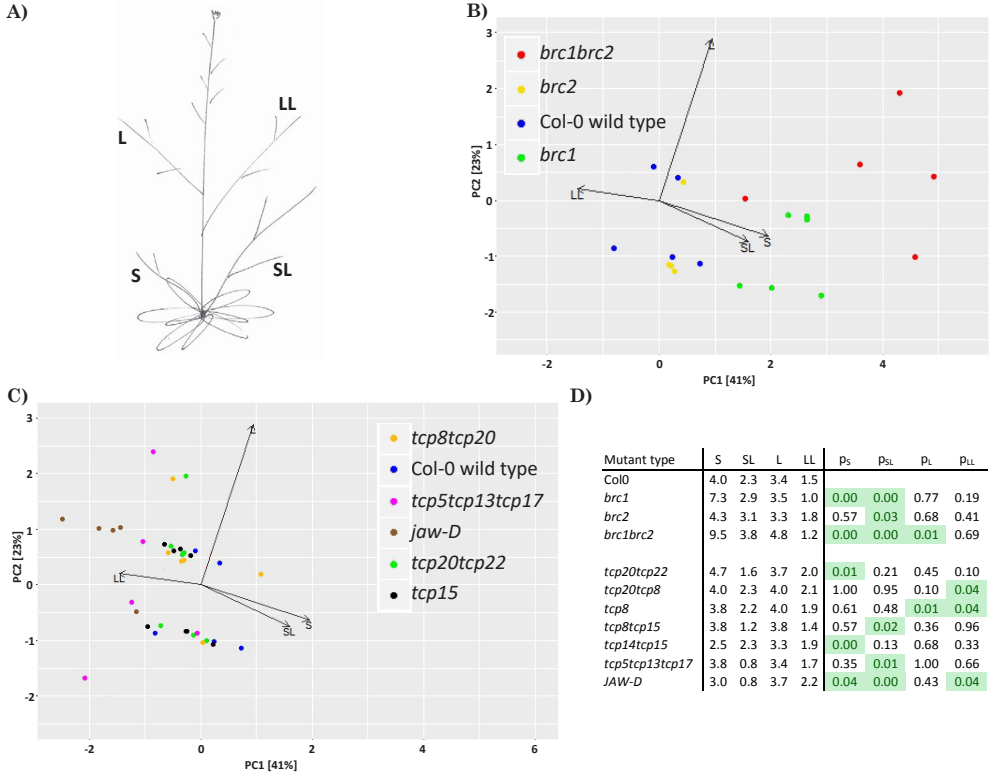


Figure 5. Branching phenotypes

Differences in branching parameters compared to wild type control. Visualization of parameters for secondary branch (S), lateral branch (L), branches on secondary branches (SL) and branches on lateral branches (LL) are shown in (A). (B) shows a principal component analysis (PCA) on mutants that produce more branches, whereas (C) shows the same analysis on mutants that produce fewer branches than wild type. PC1 explains 41% of the variation, PC2 23%. A table with the outcome of t-tests ($p < 0.05$) for the mutants shown in (B) and (C) is shown in (D).

$$\theta_{decay} = \frac{\Phi_{PSII}(16.03) - \Phi_{PSII}(7.18)}{16.03 - 7.18} = \frac{\Phi_{PSII}(16.03) - \Phi_{PSII}(7.18)}{8.85} \quad (11)$$

The resulting θ_{decay} shows a significant difference only for the *tcp20tcp8* double mutant (Supplemental Figure 6D). In addition to these measurements on photosynthetic efficiency, we checked whether plants survived the dark induced senescence or that their photosynthetic efficiency drops below a certain limit preventing recovery of the plant. We used this vitality-parameter as indirect measure for senescence. This resulted in several genotypes that show a difference in their ability to recover from the dark induced senescence trigger (Supplemental Figure 6C).

At the end of the first phase, several plants from each genotype were cut off from their roots and placed

A) Growth				B) Dark induced senescence											
0:00		12:00		0:00	NIR	12:00	NIR	0:00	NIR	12:00	PAM	0:00	NIR	12:00	NIR
0:30		12:30		0:30		12:30	PAM	0:30		12:30		0:30		12:30	PAM
1:00		13:00	NIR	1:00		13:00		1:00		13:00		1:00		13:00	
1:30	NIR	13:30		1:30	NIR	13:30		1:30	NIR	13:30	NIR	1:30	NIR	13:30	
2:00		14:00		2:00		14:00		2:00		14:00		2:00		14:00	
2:30		14:30		2:30		14:30		2:30		14:30		2:30		14:30	
3:00		15:00	PAM	3:00		15:00		3:00		15:00		3:00		15:00	
3:30		15:30		3:30		15:30	PAM	3:30		15:30		3:30		15:30	PAM
4:00		16:00		4:00		16:00		4:00		16:00		4:00		16:00	
4:30	PAM	16:30	NIR	4:30		16:30	NIR	4:30		16:30	NIR	4:30		16:30	NIR
5:00		17:00	PAM	5:00		17:00		5:00		17:00		5:00		17:00	
5:30		17:30		5:30	NIR	17:30		5:30	NIR	17:30		5:30	NIR	17:30	
6:00		18:00		6:00		18:00	PAM	6:00		18:00		6:00		18:00	PAM
6:30		18:30		6:30		18:30		6:30		18:30		6:30		18:30	
7:00		19:00		7:00		19:00		7:00		19:00		7:00		19:00	
7:30		19:30		7:30		19:30	NIR	7:30		19:30	NIR	7:30		19:30	NIR
8:00	PAM	20:00		8:00		20:00		8:00		20:00		8:00		20:00	
8:30		20:30		8:30	NIR	20:30		8:30	NIR	20:30		8:30	NIR	20:30	
9:00		21:00	NIR	9:00		21:00		9:00		21:00		9:00		21:00	
9:30		21:30		9:30	PAM	21:30		9:30		21:30		9:30	PAM	21:30	
10:00		22:00		10:00		22:00		10:00		22:00		10:00		22:00	
10:30		22:30		10:30		22:30	NIR	10:30		22:30	NIR	10:30		22:30	NIR
11:00	PAM	23:00	NIR	11:00		23:00		11:00	NIR	23:00		11:00		23:00	
11:30		23:30		11:30		23:30		11:30		23:30		11:30		23:30	

Table 2. Light and measurement scheme.

(A) shows the scheme of day (yellow), night (grey) and all measurements during the ‘growth’ experiment. (B) shows the schemes during the senescence experiment, from ‘normal’ to ‘dark’ and back. Measurements include near infrared (NIR) reflectance, pulse-amplitude-modulation (PAM) as measure for ΦPSII .

in a petri dish to prevent immediate wilting. This experiment was carried out to study senescence of harvested material (i.e. shelf life). No differences between mutant lines and wild type plants were observed. Interestingly, when analysing all data points regardless of genotype, the θ_{decay} for detached plants was lower than that of normal plants ($p = 1.9 \times 10^{-20}$), indicating that the detached plants maintained their ΦPSII for a longer period of time before it eventually declines.

Significantly more individuals of the normal plants, as we’ve seen above, manage to recover after the dark induced senescence period. An explanation could be that resources are swiftly allocated towards the roots when the plants start senescing, allowing for a comeback (Killingbeck, 1996 and reviewed by Brant and Chen, 2015). Lacking roots, the detached plants maintain their photosynthetic apparatus for as long as possible until they run out of resources.

Discussion

The aim of this research was to provide a comprehensive overview of differences in developmental and seed yield characteristics in a carefully chosen set of *tcp* mutant backgrounds in comparison to wild type plants. We have created an algorithm that describes the growth curve during the vegetative stage of development, using four different biologically meaningful parameters. Variation in these

parameters among different *tcp* mutant lines could be clearly represented by a principal component analysis (PCA; Figure 2). For many of the genotypes studied, a difference in at least one of the growth equation parameters was observed, which is not surprising as TCPs are involved in different aspects of plant development (reviewed by Martín-Trillo and Cubas (2010), Uberti Manassero *et al.*, (2013), Nicolas and Cubas (2015 and 2016), and Danisman (2016)). Next to this, investigation of branching parameters and seed yield characteristics revealed several *tcp* mutant lines to behave differently compared to wild type in number and weight of seeds (Figure 4) in relation to the number of branches (Figure 5).

The role of TCP transcription factors in growth regulation during the vegetative stage of plant development

Even though our study does not venture into the cellular level of development, we can speculate on the underlying mechanism causal for the observed differences in the individual growth equation parameters (β -values). β_3 for example, is supposed to represent the moment a plant enters the rapid growth phase. This moment is typically marked, at the cellular level, by a switch from cell proliferation into cell elongation (Andriankaja *et al.*, 2012). Several class II *tcp* mutants are thought to stay longer in the cell proliferation phase, producing more but often smaller cells, for example *jaw-D* and related *cin* mutants (Nath *et al.*, 2003; Crawford *et al.*, 2004). This is represented in a higher β_3 compared to wild type as it simply takes these mutants longer to reach the phase of rapid and exponential rosette growth. Indeed, *jaw-D* has a significantly higher β_3 value. Several genotypes such as *tcp19tcp20tcp22*, *tcp9* and *tcp20* exhibit a lower β_3 compared to wild type. Interestingly, some of the investigated double mutants, mutated also in *tcp9* or *tcp20* (e.g. *tcp9tcp20* and *tcp19tcp20*) do not show differences in this parameter. Furthermore and surprisingly, several class I mutants show a similar effect on β_3 as the class II *jaw-D* mutant, for example the double mutants *tcp14tcp15* and *tcp8tcp20*.

In addition to an altered β_3 , the *jaw-D* mutant has a lower β_2 than wild type, a characteristic it shares with a line mutated for the closely related *TCP* genes *TCP5*, *TCP13* and *TCP17* (*tcp5tcp13tcp17*; (Efroni *et al.*, 2008)). On a cellular level, β_2 might be explained as the speed of cell elongation, fitting with the observed growth phenotypes of the *jaw-D* and the *tcp5tcp13tcp17* triple mutant.

Focussing on β_1 , which represents the maximum of growth, only *brc1brc2* and *tcp8tcp15* have a lower β_1 than wild type. Several other mutants show a higher β_1 , such as the single *branched* mutants as well as *tcp15* and the *tcp14tcp15* double mutant. Molecularly, β_1 is hard to interpret by our data as the final size is influenced by numerous factors other than altered growth speed and moment of rapid growth. The duration of growth cannot be assumed using our four β 's; however, a plant ending up bigger than wild type (i.e. a higher β_1), but with a lower β_3 , can be classified as a slow grower that

Time [days]	Event
0	First NIR measurement
0.17	First PAM measurement
7.18	Last PAM measurement in phase 1
7.46	Last NIR measurement in phase 1
22.75	First NIR measurement in phase 3
23.05	First PAM measurement in phase 3
24.75	Last NIR measurement for 'detached' plants
24.76	Last PAM measurement for 'detached' plants
26.87	Last NIR measurement for 'normal' plants
26.93	Last PAM measurement for 'normal' plants

Table 3. Schematic overview of the timeline of the dark induced senescence experiment. Time starts at day 0 (zero) when the first measurement is taken.

takes longer to reach its maximum (e.g. *tcp10*). Vice versa, plants with a lower β_1 and a lower β_3 are fast growers that stay smaller than wild type under our experimental conditions (e.g. *brc1brc2*). Next to these growth parameters, we studied mutants affected in their branching pattern. Best studied are the *branched* mutants that grow more branches than wild type, most notably the *brc1brc2* double and the *brc1* single mutants (Aguilar-Martínez *et al.*, 2007). Next to these, we found that the *jaw-D* (class II) and *tcp14tcp15* (class I) mutant lines showed a significant reduction in the number of secondary branches (Figure 5D), whereas *tcp20tcp22* produced slightly more secondary branches. This suggests that more TCPs are involved in the control of axillary bud outgrowth, either directly by acting in the meristem, or indirectly through changes in sink-source relationships, hormone levels or availability of carbon resources.

Two classes of TCPs, showing antagonistic behaviour?

Historically, the TCP family of TFs has been divided into two classes based on sequence characteristics (Cubas *et al.*, 1999). Members of these two classes are believed to act antagonistically, either by promoting cell growth and proliferation (class I) or through the repression of these processes (class II) (Martín-Trillo and Cubas, 2010). Our results question this strict division into two antagonistically functioning classes. Mutants from particular members of class I and class II *TCP* genes show similar changes in specific β -parameters. Important to note is that we have carefully deduced the phenotypic parameters described by the different β 's, therefore phenotypes with the same outcome might behave differently at the cellular/molecular level. An increase in leaf area can be accomplished by an increase in both cell proliferation rate and cell size. More comparative research will be necessary to elude the (lack of) antagonistic behaviour. On the other hand, the results from the branching pattern analyses also lack a strict opposite behaviour for members of the two classes. The increase in branching of *brc1brc2* double mutants would imply that a class I mutant should exhibit fewer branches. This is the case for *tcp14tcp15*, but also the class II mutants *jaw-D* and *tcp5tcp13tcp17* show a decrease in some aspects of branching. This similarity in phenotypes could indicate overlapping functions, or at least final phenotypic effects, for proteins of both classes.

TCPs do not show expected redundant behaviour for phenotypes tested

A group of TCPs that is believed to behave redundantly and that shows striking results regarding their growth phenotypes, is the *BRANCHED* group of TCPs. Looking at the distribution of their β 's in a PCA plot (Figure 2, bottom-right panel), the *brc1* and *brc2* single as well as the *brc1brc2* double mutant are positioned on the same horizontal plane, below Col-0 wild type. The *brc1* single mutant lies straight below wild type, indicating a higher β_1 and β_3 , the double mutant is shifted further to the left, having a much lower β_1 than either Col-0 or *brc1*. Surprisingly, the *brc2* single and *brc1brc2* mutants are oppositely oriented with respect to β_2 . Furthermore, both single mutants have a higher β_1 than the wild type whereas the *brc1brc2* double mutant has a β_1 lower than wild type. Visualising their rosette growth pattern reveals that both the *brc1* and *brc2* single mutants eventually outgrow Col-0 control plants, although *brc1* grows slower in the first few days of measuring. The *brc1brc2* double mutant on the other hand grows slower and remains smaller throughout the duration of the measurements (Figure 3B). This suggests that the *BRC* genes control each other, possibly through a negative feed-back regulation. This could be investigated by analysing expression levels of *BRC1* and *BRC2* in the *brc2* and *brc1* mutant backgrounds, respectively, which could also give a clue on how both single mutations can account for the phenotype observed in the *brc1brc2* double mutant.

A closer look into the 'TCP15-likes' (top-left panel in Figure 2) shows another interesting pattern of single and double mutants. The double mutant *tcp8tcp15* seems almost identical to Col-0 wild type whereas both *tcp8* and *tcp15* look vastly different. In contrast, the double mutant *tcp14tcp15* seems to benefit from an additive effect of a *tcp14* mutation in comparison to the single *tcp15* mutant, as it is positioned furthest away from wild type. In conclusion, this indicates that the combination of *tcp8* and *tcp15* attenuates their individual effects, whereas *tcp14* and *tcp15* enhance each other. Both *tcp8* and *tcp15* single mutants show a higher β_1 , β_2 and β_3 compared to wild type. The double mutant *tcp8tcp15* has even a slightly lower β_1 than wild type, whereas the *tcp14tcp15* double mutant is rather different with a much higher β_1 and β_3 .

Overall, full redundancy would imply that single mutants show behaviour identical to wild type and only double or higher order mutants would exhibit mutant phenotypes. Therefore, the single mutant behaviour we have observed would imply only partial redundancy among the investigated members of the *TCP* family of TFs mentioned above. Based on our data however, there are no examples showing true redundancy among the different groups of related *TCPs* and their growth phenotypes. One example of known partial redundancy is the miR319 regulation of the *JAW-D* *TCPs*. A single knockout of a gene in this clade produces only mild phenotypes, whereas knocking out the whole clade shows dramatic changes in leaf development (Schommer *et al.*, 2008). This effect can be seen in the higher β_1 for the *tcp10* single mutant, this corresponds to an increase in leaf area, something that has been observed previously (Schommer *et al.*, 2008). If the *JAW-D* *TCPs* would have been

fully redundant, then a *tcp10* single knockout would be undistinguishable from Col-0 wild type in the PCA plots.

Previous research ranked pairs of a number of TCP TFs on their likeliness to be functionally redundant, based on protein sequence, gene expression and Y2H analysis (Danisman *et al.*, 2013). Interestingly, this list showed that the closely related TCP19 and TCP20 ranked high in potential functional overlap, which was confirmed by a detached leaf senescence experiment. Although TCP8 is as closely related to TCP20 as is TCP19, no shared function of TCP8 with TCP20 was found (Danisman *et al.*, 2013). Contrastingly, our data shows that during rosette development, TCP19 and TCP20 do not seem to share a function (both *tcp20* and *tcp19tcp20* are similarly different from wild type, independent of the presence or absence of a functional *TCP19* gene), whereas the double mutant *tcp8tcp20* seems to enhance the *tcp20* single mutant phenotype (Figure 2). Further research into the exact molecular function of all individual TCP proteins is necessary to be conclusive on the potential functional redundancy.

The link between plant development and final yield

We have collected data on the architecture of the plants, their developmental progress as well as yield characteristics in terms of total seed production. We have confirmed the link between several seed characteristics by correlation analyses (Supplemental Figure 7A to 7C) and showed that an increase in number of seeds is negatively correlated to both seed area and seed weight. This negative correlation has been found before (Gnan *et al.*, 2014) and is in line with an earlier proposed model describing a fixed amount of resources allocated to reproduction (Paul-Victor and Turnbull, 2009). Strikingly, plants that appear to have several significantly different β 's compared to wild type, such as *jaw-D*, *tcp14tcp15* and *brc1brc2*, also show up in the analysis on altered branching patterns as well as differences in total seed weight. However, a different progression of growth and rosette development (the β parameters) does not necessarily result in differences in yield or branching patterns. Telling examples are the *tcp8* and *tcp15* single mutants, both show a higher β_1 , β_2 and β_3 compared to wild type, but no differences in seed yield characteristics have been observed. It has previously been reported that inflorescence architecture is of great influence on final seed yield characteristics. Pruning in Arabidopsis led to the development of longer and larger siliques that contained fewer, but bigger seeds (Bennett *et al.*, 2012). This was attributed again to a reallocation of resources which could also be applicable in the *brc1* and *brc1brc2* mutants. The production of more branches in these mutants reduces the amount of resources left for seed production, resulting in a reduction in seed yield.

Our study has provided an excellent body of data that takes a closer look at the effect of unique plant developmental alterations on plant yield under our conditions. Note however, that different

conditions, such as higher planting density, altered light intensity or different temperatures, can have profound effects on plant growth and yield and therefore, can provide a complete other view of the functioning and contribution of the individual TCP TFs to final yield characteristics. Hence, growing our selection of mutants under different conditions would be of great interest. This might also shed another light on the possible redundancy of TCP proteins, as different functions may become apparent under defined environmental conditions only. For example, *BRC1* expression is known to be influenced by the red to far-red ratio (R:FR, González-Grandío *et al.*, 2013), something greatly influenced by planting density (Casal *et al.*, 1986). Light intensity is of great effect on plant growth, as recognized since long (Shirley, 1929). Furthermore, with an emerging climate-change, the effect of temperature on plant growth should not be dismissed (Hatfield and Prueger, 2015). In conclusion, different environmental conditions may trigger different responses in our mutants and could provide us with insights into the role of TCPs in adaptation of plant development to changing environmental conditions.

Materials and methods

Plant materials

All lines and genotypes used in this study are shown in table 1. As control line for the T-DNA insertion mutants, we used a newly ordered (NASC) Col-0 wild type. The Col-0 wild type line that was used as background for the *ATML1_{pro}::TCP5/13-GFP* transformations served as control for those particular lines (Col-0 “WUR” in table 1). Both the *ATML1_{pro}::TCP5-GFP* and *ATML1_{pro}::TCP13-GFP* mutant lines were constructed as previously published (van Es *et al.*, 2018).

System setup

The Phenovator allows for 1440 plants to grow simultaneously in a grid of 24 by 60 plants, placed upon an ebb and flood hydroponic system (Flood *et al.*, 2016). The analyses software is unable to distinguish between overlapping plants. To prevent this from happening, we used half the available positions in the growth experiment. The above-mentioned grid was divided into 28 plots in which all 24 genotypes were randomly positioned. This ensures a semi-random orientation of the plants over the grid, preventing possible positional bias. Plants were assigned a coordinate based on their position in the grid. The senescence experiment had different growth conditions (shorter day length, and lack of light after 22 days) which resulted in smaller plants that do not overlap. We therefore used all available positions during this experiment with a similar plant positioning method.

Plant growing conditions

Prior to the experiment all lines mentioned in table 1 were grown under long-day conditions (16/8 light/dark cycle at 21 °C) on Rockwool and received 1 g/l Hyponex plant food solution twice per week. Seeds were harvested simultaneously for use in the large scale phenotyping experiments. Before placement in the climate chamber, the seeds were sown on wet filter paper and stratified for 2 days at 4 °C to ensure uniformed germination. After stratification, the seeds were sown directly on wet Rockwool (www.grodan.com), which had been pre-soaked in a nutrient solution designed for *Arabidopsis* (van Rooijen *et al.*, 2015; Flood *et al.*, 2016). The same nutrient solution was used to irrigate the plants twice per week. One seed was sown per Rockwool block, which was placed in the phenotyping system at day zero.

Two independent experiments were performed, one focussing on growth and development, from now on referred to as the ‘Growth’ experiment. The second experiment was designed to investigate the behaviour of our mutants during dark induced senescence, from now on called ‘Senescence’ experiment.

During the growth experiment the plants were imaged from day 8 until day 25, until overlapping leaves of neighbouring plants made distinguishing between individual plants impossible. Subsequently, the plants were kept until harvesting of dry seeds was possible, i.e. when the plants were fully developed and mature. At this stage the plants were phenotyped on their level of branching, total seed set as well as several yield characteristics such as number of seeds per silique, size of seeds and the seed weight. The plants were grown under constant conditions: a day/night rhythm of 16/8 hour at a constant temperature of 20°C and a relative humidity of 70%. The plants were grown at a constant irradiance of 200µM m-2s-1.

The dark induced senescence experiment deviates on several points described ahead from the above described ‘Growth’ experiment. The seeds were placed in the phenotyping system at day zero after which imaging of the plants took place from day 13 to day 41. The first 22 days contained constant growing conditions: a day/night rhythm of 12/12 hour at 20°C, relative humidity of 70% and an irradiance of 200µM m-2s-1. Starting on the morning of day 23 the room was kept dark to induce senescence, all other setting remained the same. From then on, for 15 days the plants received light only once per every other day for 20 minutes so that the plant gains steady-state photosynthetic capacity, followed by one hour of light to perform the PAM measurement. After the dark period of 15 days, the lights were set at their normal (12/12) schedule for a period of 5 days, in order to check for possible recovery of the photosynthetic activity of the plants. For a detailed overview of the light and measurement regime during both experiments described above, see Table 2.

Measurement schematics

The Phenovator system (Flood *et al.*, 2016) was used to measure two different parameters: PSII operating efficiency (Φ PSII) and near infrared (NIR) reflection at 790nm. Since day length differed between the growth and the dark induced senescence experiment the moments and amount of these measurements differed. Φ PSII was measured daily during the growth experiment, 1, 5, 8, 11 and 13 h into the photoperiod. In the senescence experiment Φ PSII was measured 1, 4, 7 and 10 h into the photoperiod every day during normal light regime. During the period of dark induced senescence Φ PSII was measured every other day, 20 minutes into the photoperiod. Both these setups were considered sufficient to document any variations in the phenotype regarding Φ PSII and allowed time for other measurements such as NIR. A detailed overview of the timing and frequency of the different measurements during both the 'growth' and 'dark induced senescence' experiment can be found in table 2A and 2B respectively.

Phenotyping of branching was done by manually counting the number of lateral shoots and branches on the main inflorescence. Total yield was determined by weighing the total amount of seeds for eight plants per genotype, on dried siliques and seeds. Seeds size and -number per silique was measured for four siliques on five plants per genotype. The seeds were pictured using a setup specially designed for imaging seeds and their germination: the 'germinator' (Joosen *et al.*, 2010). We used this software for seed imaging alone after which the pictures were analysed by the 'Analyse particles' function in ImageJ, obtaining surface area.

Data handling and analysis of growth experiment

Raw data generated by the Phenovator is converted into .csv files with data on the physiological parameters (e.g. Φ PSII or PLA through the NIR images) enabling analysis using data analysis software such as RStudio and Excel. In order to identify non-germinated seeds, we checked for a lack of signal in the PAM dataset of both the growth and senescence experiment on either the 25th or 21st day of the experiment, respectively. Coordinates in which no signal was observed were removed from both NIR and PAM datasets.

Firstly positional effect were assessed by regression analysis in R, version x64 3.4.1, after which the SpATS package (Rodríguez-Álvarez *et al.*, 2016) was used to correct for the observed spatial bias in the PLA dataset. Next the PLA time series was analysed first by performing a singular spectral analysis (SSA) using the R package Rssa (Golyandina *et al.*, 2013). The elementary components (ECs) were retrieved by the command 'residuals()'. The ECs, their eigenvalues and its relative contribution to the variance allowed for the determination of the growth function (4) which consists of two parts. One accounting for the actual growth of the plants and one accounting for the circadian rhythm, in total containing five parameters β_1 - β_5 . Next, an optimal fit of the function given by expression (4) is

computed for all of the time series individually. This is done by the least-squared error criterion in nonlinear regression. In this case the `nls()` function is used with the “port” algorithm in R. Starting values are required, as nonlinear regression algorithms are iterative ones. Note that this has to be done in the order $\beta_{1,start}$, $\beta_{2,start}$ and last $\beta_{3,start}$, as the starting value of β_1 is required to compute that of β_2 and the starting value of β_2 is required to compute that of β_3 . First a nonlinear regression estimation is performed for the function describing solely the β_1 up to β_3 optimal parameter values. These will be used as the starting values for the nonlinear regression to fit the entire function to describe the data, again using the “port” algorithm of the `nls()` function. Identification of differences between average β -values was done by principal component analysis (PCA) using `prcomp()` in R.

Data handling yield characteristics

Yield characteristics were described as mentioned above and several PCA were performed on all measured variables. Again the `prcomp()` command was used to perform this analysis. A single parameter is introduced to capture most of the variance of the four branching parameters, defined as the linear combination given by the first principal component, resulting from the PCA between the four aforementioned branching parameters. Regression analysis using the `lm()` command was done to test whether correlations between the variables number, area and weight exist.

Data handling and analysis of Dark Induced Senescence

The dark-induced-senescence experiment consisted of three phases for which the measurements are shown in Table 3. Analysis started by determining the dead plants. We set a size threshold to exclude coordinates where seeds failed to germinate and to account for plants of extremely small size. The time point $t = 7.33$ was chosen to allow the plant substantial time to establish themselves and develop normally. At this time there were 98 coordinates with zero PLA. That is most probably because these plants did not germinate at all. The average size of the other plants at $t = 7.33$ is 713 mm². Therefore, the threshold will be set to 100 mm², which is approximately ten percent of the average size at that time. There are 43 plants with nonzero PLA at $t = 7.33$, which fall below this threshold.

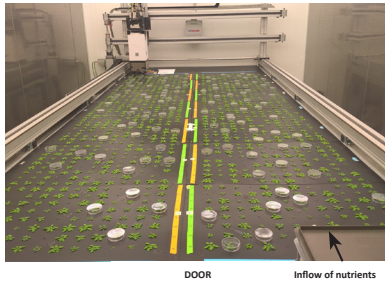
To check for plants that did not survive the dark-induced-senescence we had to choose slightly different characteristics. The Φ_{PSII} and PLA measurements were combined and examined at given moments and two conditions were set. The first condition states that an ‘NA’ has to be observed in the Φ_{PSII} data after the first phase. The first phase is not taken into account, because the plants still receive a normal dose of light in that period and because the plants that failed to germinate or plants of insignificant size are already filtered out. The second condition ensures that the PLA of a plant is lower at the end of the measurements than at the end of phase one. The PLA of a dead plant decreases because the plant withers after its death, leading to shrivelling of the leaves. At the start

of the dark induced senescence experiment 118 plants (± 4 replicates per genotype) of the total 1440 *Arabidopsis* plants were detached from their roots and placed on petridishes. Black filter paper was placed in the petridish and moisturized regularly to prevent wilting of the plants.

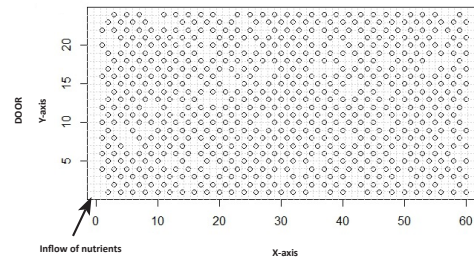
Acknowledgments

We would like to thank Jeremy Harbinson and Aina Prinzenberg for their help in the experimental setup, initial data analyses and fruitful discussions. Our work is supported by grants from the Dutch Scientific Organization (NWO); (NWO-JSTP grant 833.13.008), CAPES/NUFFIC (No 010/07) and CAPES/NUFFIC (No 033/2012). This project was partly financed through an 'Enabling Technologies Hotel' (ZonMw 435002014).

A)

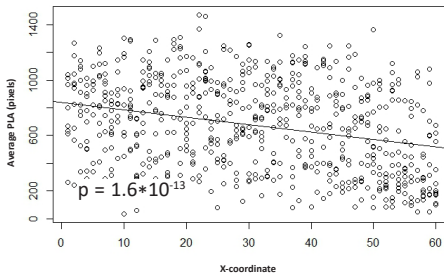


Grid overview

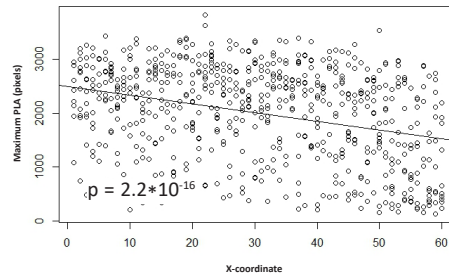


B)

Regression analysis of X-coordinate vs. average PLA

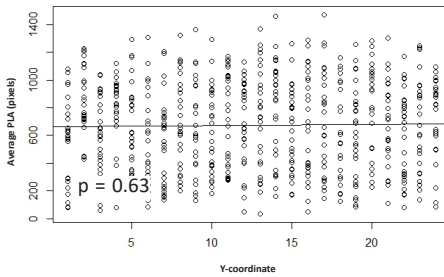


Regression analysis of X-coordinate vs. maximum PLA

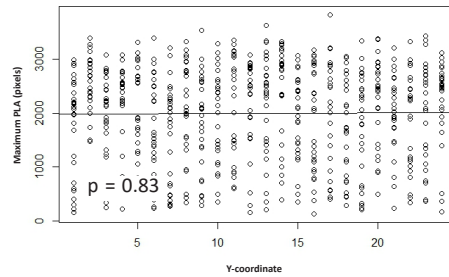


C)

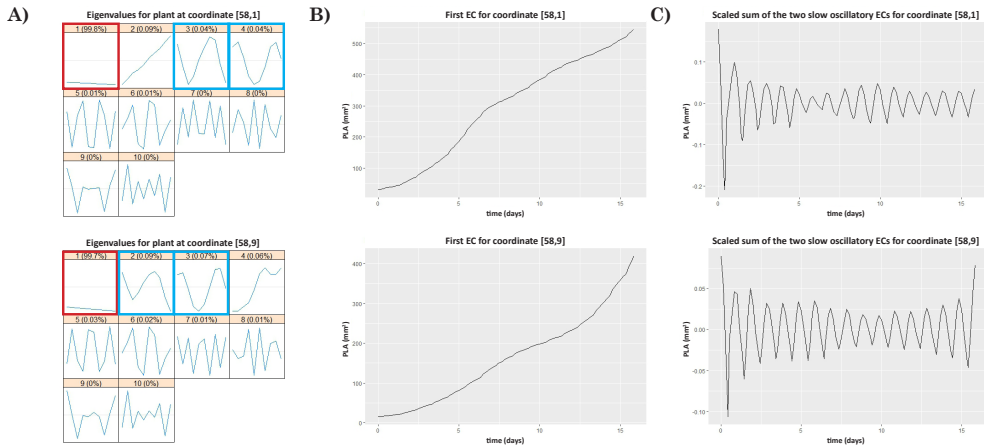
Regression analysis of Y-coordinate vs. average PLA



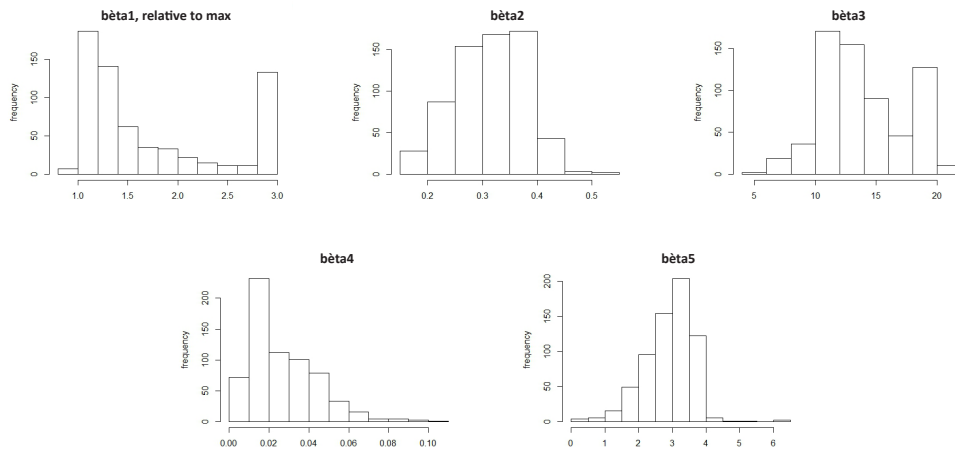
Regression analysis of Y-coordinate vs. maximum PLA



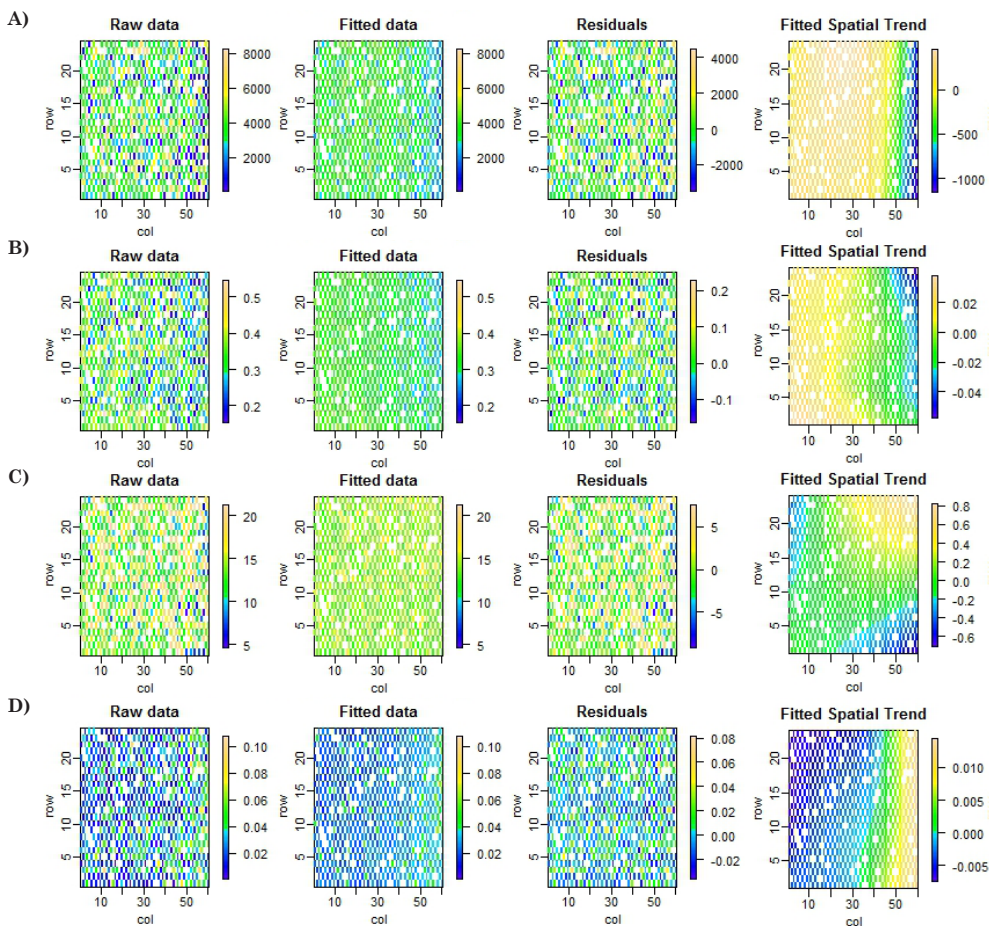
Supplemental Figure 1. Regression analysis of positional effects in the experimental setup. An overview of the system is shown in (A) by a picture, taken from the door, as well as a schematic representation of the grid with the direction of nutrient inflow and position of the door. The two figures in (B) show the regression analysis on the correlation between x-coordinate and average PLA (plant size), and x-coordinate and maximum PLA. In (C) the y-coordinate and average PLA, and y-coordinate and maximum PLA is shown. Correlation analysis was performed with a threshold of $p < 0.05$.



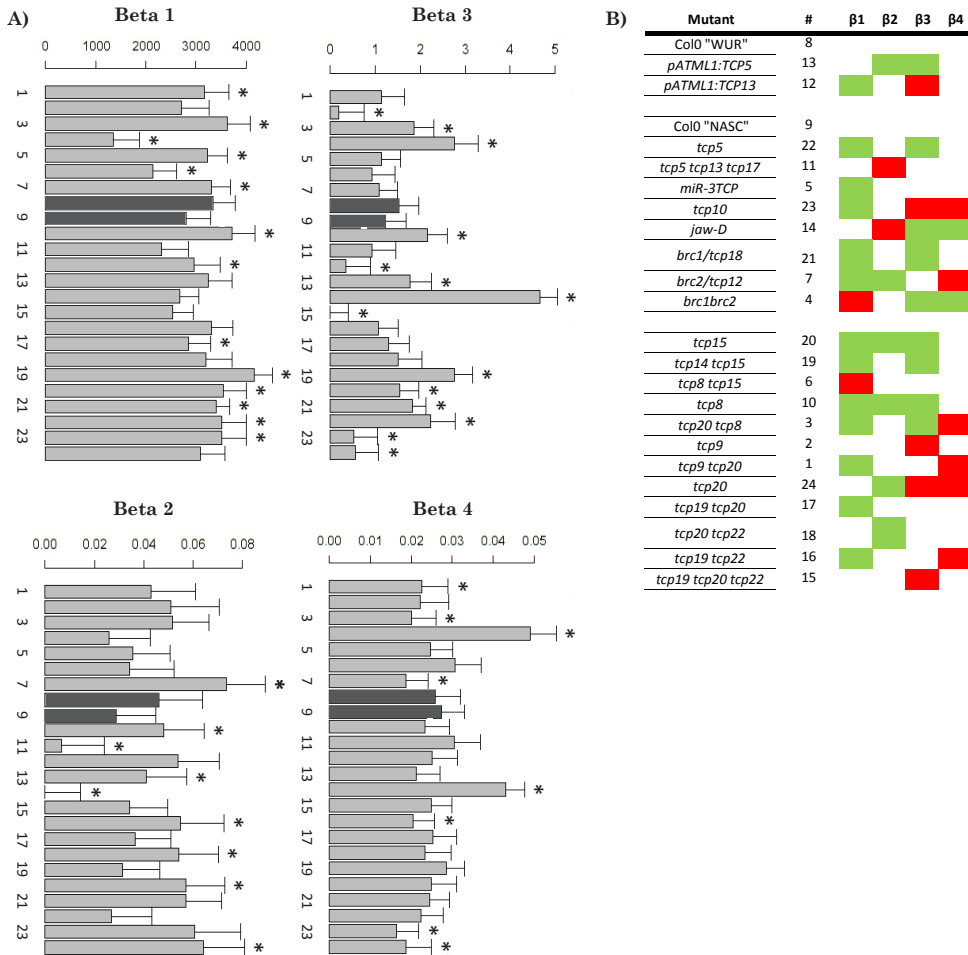
Supplemental Figure 2. ECs and eigenvalues for plant growth curves for two exemplary coordinates. The eigenvalues corresponding to the 10 ECs and their relative contribution to the two given coordinates are shown in **(A)**. The first EC resembling an S-curved function is shown in **(B)** for two coordinates, plotting PLA over time. The oscillatory rhythm, resulting from the circadian movement of the leaves is shown in **(C)**. The S-curve EC is indicated by a red square in **(A)**, the oscillatory ECs are marked in blue.



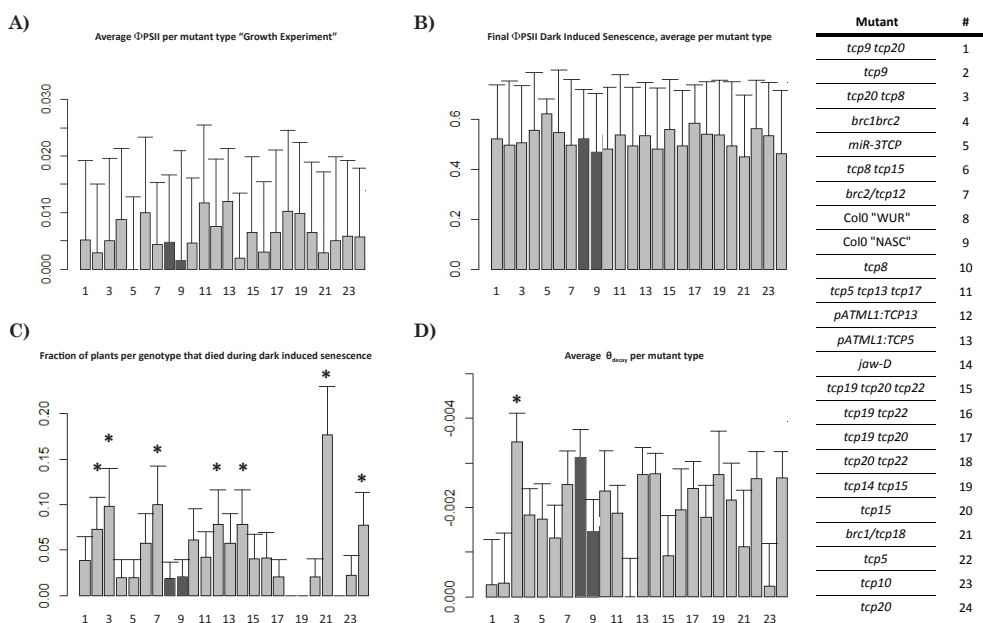
Supplemental Figure 3. Distribution and occurrence of optimal β -values. Shown for β_1 to β_5 are the frequencies at which certain β -values occur between the set upper and lower bounds after the conversion of the algorithm. Visualization by histogram.



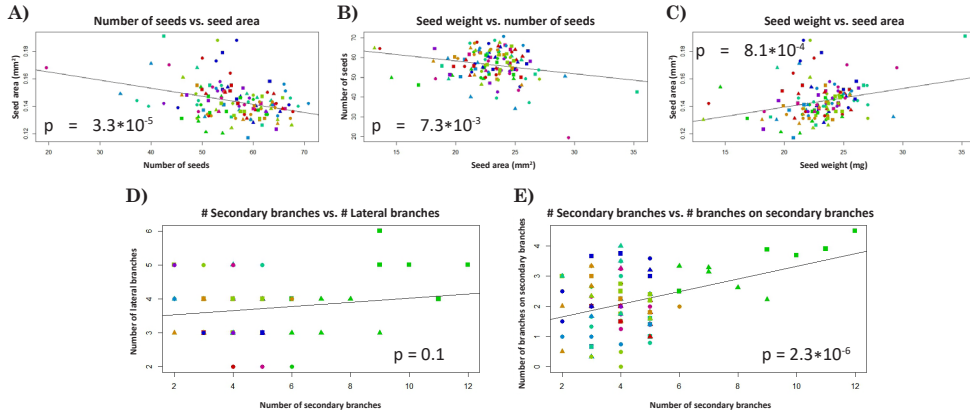
Supplemental Figure 4. Graphical overview of spatial distribution of β -values. Spatial distribution of β -values for β_1 to β_4 are shown in (A) to (D) respectively. The 'Raw data' shows the distribution of the input values of either one of the β 's. The 'Fitted data' show the values corrected for the spatial trend, using the R package SpATS. The 'Residuals' are the data residuals which relate to the raw and fitted data as such: Raw data - Fitted data = Residuals. The 'Fitted Spatial Trend' visualizes the distribution of the respective β -values.



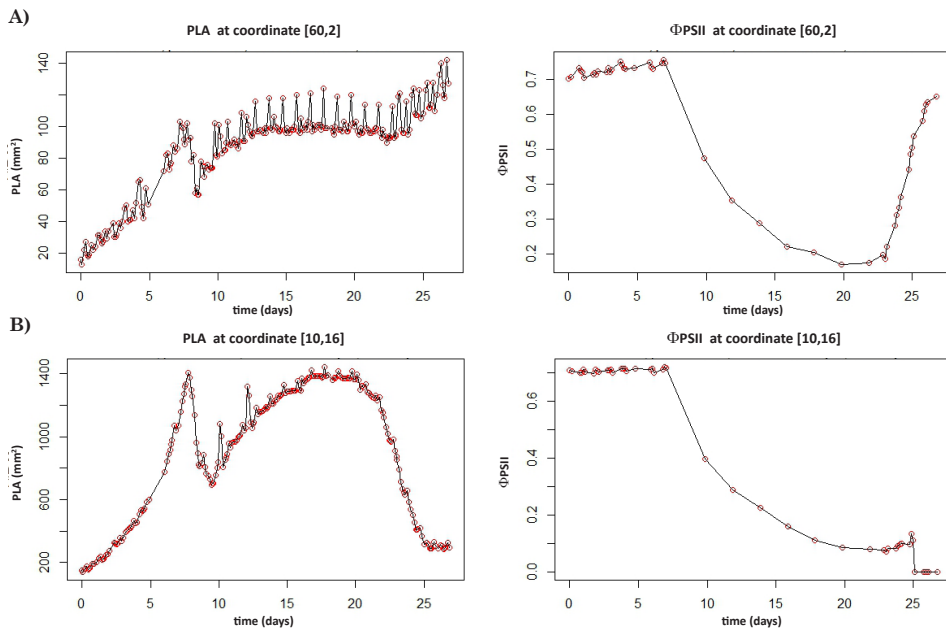
Supplemental Figure 5. Average values for all four Bèta parameters. Overview of the average values of β_1 to β_4 for all lines studied are shown in (A). Both β_2 and β_3 are scaled to the lowest value to enhance readability. Statistical differences are indicated by an asterisk ($p < 0.05$). Dark grey bars show the respective β 's for Col-0. An overview of the statistical difference for all β 's per genotype is shown in (B) with Col-0 "WUR" as background (i.e. control) for the overexpression lines, Col-0 "NASC" serves as control for all other mutants. Red indicates below Col-0 average, green above Col-0 average for that particular genotype.



Supplemental Figure 6. Comparison of photosynthetic efficiency and (dark-induced) senescence for the various *tcp* mutants. The average Φ_{PSII} relative to the lowest value (number 5) in the 'Growth' experiment is shown in (A). The Φ_{PSII} per line on the last moment of measuring in the 'Senescence' experiment (B), the lack of asterisks indicate the absence of statistically significant difference. The percentage of plants dying as a result of the Dark Induced Senescence Assay is shown in (C). The average relative reduction of photosynthetic efficiency for all lines is shown in (D). Genotypes corresponding to the numbers are shown on the right.



Supplemental Figure 7. Correlation analysis of the phenotyped seed and branching parameters. Correlation analysis on the number of seeds versus the seed area in (A), seed weight versus number of seeds in (B) and seed weight versus seed area in (C). In (D) and (E) a correlation analysis is shown on the number of secondary versus lateral branches and the number of branches on the secondary branch. All individual plants were taken into account, regardless of their background and hence, the colour-coding can be ignored. As threshold a significance level of $p < 0.05$ was used.



Supplemental Figure 8. Two typical growth and photosynthesis curves during Dark Induced Senescence. The growth curve (resulting from the NIR measurement) and the 'steady state photosynthetic capacity' (resulting from the PAM measurement) for a typical example of a plant surviving the Dark Induced Senescence Assay in (A) versus one that does not (B).

Chapter 3:

Novel functions of the Arabidopsis transcription factor *TCP5* in petal development and ethylene biosynthesis

Sam W. van Es

Sylvia R. Silveira

Diego I. Rocha

Andrea Bimbo

Adriana P. Martinelli

Marcelo C. Dornelas

Gerco C. Angenent

Richard G.H. Immink

Plant Journal, 2018, doi: 10.1111/tpj.13904

“People from a planet without flowers would think we must be mad with joy the whole time to have such things about us.”

Iris Murdoch

Abstract

Flowers of most dicotyledons have petals that, together with the sepals, initially protect the reproductive organs. Later during development petals are required to open the flower and to attract pollinators. These diverse set of functions demand a tight temporal and spatial regulation of petal development.

We studied the functioning of the *Arabidopsis thaliana* *TCP5*-like transcription factors (TFs) in petals. Overexpression of *TCP5* in petal epidermal cells results in smaller petals, whereas *tcp5 tcp13 tcp17* triple knockout lines have wider petals with an increased surface area. Comprehensive expression studies revealed effects of *TCP5*-like TFs on the expression of genes related to cell cycle, growth regulation, and organ growth. Additionally, the ethylene biosynthesis genes 1-amino-cyclopropane-1-carboxylate (ACC) synthase 2 (*ACS2*) and ACC oxidase 2 (*ACO2*) and several ETHYLENE RESPONSE FACTORS (*ERFs*) are found to be differentially expressed in *TCP5* mutant and overexpression lines. Chromatin immunoprecipitation–quantitative PCR showed direct binding of *TCP5* to the *ACS2* locus *in vivo*. Ethylene is known to influence cell elongation and the petal phenotype of the *tcp5 tcp13 tcp17* mutant could be complemented by treatment of the plants with an ethylene pathway inhibitor. Altogether, this reveals a novel role for *TCP5*-like TFs in the regulation of ethylene-mediated petal development and growth.

Introduction

Flowers have been extensively studied throughout history as they are the most eye-catching and, through fruit and seed production, an economically important part of the plant. Substantial knowledge has been acquired on the identity specification and development of the different flower organs. In this respect, well-known is the ABC model of flower development (Coen and Meyerowitz, 1991) which explains how different genes and gene combinations specify floral organ identity. Except for the Arabidopsis A-class gene *APETALA2* (*AP2*), all these genes encode members of the MADS box family of transcription factors (TFs) and their specific and unique interactions determine the identities of the four types of floral organs: carpels, stamens, petals and sepals (Immink *et al.*, 2010; Coen and Meyerowitz, 1991).

Until recently, little was known about flower organ growth control and the determination of their final size and shape. Nevertheless, over recent years this topic got more attention and insight was gained into the cellular characteristics and underlying genetic factors controlling these traits. In the Arabidopsis flower, the final shape and size of sepals is largely determined by endoreduplication and the formation of giant cells (Roeder *et al.*, 2012). Petals, on the other hand, have a morphology that requires differential regulation of cell proliferation and expansion in the basal and distal parts. The final shape and size of petals is mainly determined by cell elongation in the basal part, whereas the rate and direction of cell division determine the shape and size of the distal region (the blade) of the petal, which contains small and round conical cells (Irish, 2008; Hase *et al.*, 2005).

Several key regulatory genes that ensure control of petal growth and development in Arabidopsis have been identified. *JAGGED* (*JAG*) for instance, is suggested to suppress premature cell-cycle arrest in the distal part of an Arabidopsis petal (Dinneny *et al.*, 2004; Schiessl *et al.*, 2014). *RABBIT EARS* (*RBE*) is expressed in petal primordia, where it ensures cell proliferation in petal precursor cells (Takeda *et al.*, 2004). *AINTEGUMENTA* (*ANT*) maintains cell proliferation in developing petals (Krizek *et al.*, 2000; Mizukami and Fischer, 2000) and *BIG PETAL* (*BPE*) affects cell size by interfering with post-mitotic cell expansion (Szecsi *et al.*, 2006). A number of downstream genes have been identified, including members of the TEOSYNTE BRANCHED/CYCLOIDEA/PROLIFERATING CELL FACTOR (*TCP*) TF family, which are thought to act downstream of *JAG* (Schiessl *et al.*, 2014) and *RBE* (Huang and Irish, 2015).

The *TCP* TF family (Martín-Trillo and Cubas, 2010) in Arabidopsis has 24 members, which can be divided into two classes based on a difference in the DNA-binding *TCP* domain (Cubas *et al.*, 1999). The class II *TCP*s are generally thought to act as repressors of cell division and inducers of cell differentiation (Efroni *et al.*, 2008), and can be further subdivided into CINCINNATA (*CIN*)-type and CYC/TB1-type *TCP*s (Cubas *et al.*, 1999). The roles of several of these class II *TCP*s in floral organ

development have been studied. In *Antirrhinum* for example, CYC is responsible for the asymmetric development of petals (Luo *et al.*, 1995), whereas CIN promotes growth and cell division in these organs (Crawford *et al.*, 2004).

The CIN-type TCPs are represented in Arabidopsis by the Jagged and Wavy (*JAW*) TCPs (*TCP2*, -3, -4, -10 and -24) and the *TCP5*-like genes (*TCP5*, -13 and -17). All five *JAW*-TCPs are targeted by the same micro RNA, *miR319*, which, upon overexpression in the *jaw-D* mutant, simultaneously downregulates the expression of *TCP2*, -3, -4, -10 and -24 (Palatnik *et al.*, 2003). This downregulation gives rise to a delay in the arrest of cell proliferation in the margin and distal end of organs, such as leaves and petals, resulting in overproduction of cells in these regions (Palatnik *et al.*, 2003; Nath *et al.*, 2003).

It has been suggested that the other CIN-genes, *TCP5*, *TCP13* and *TCP17*, although not targeted by *miR319*, are responsible for similar processes in a redundant manner (Efroni *et al.*, 2008). However, mutants in the *TCP5*-like genes show some phenotypic differences when compared with the *JAW*-TCP mutants and have larger leaves for example, but lack the *jaw-D* characteristic crinkled phenotype. The constitutive overexpression of *TCP5* results in a smaller petal area (Huang and Irish, 2015), whereas downregulating all three *TCP5*-like genes by ectopically expressing an artificial micro-RNA (also known as *miR:3TCP*) and a triple *tcp5 tcp13 tcp17* knockout results in larger petals and leaves (Huang and Irish, 2015; Efroni *et al.*, 2008). The single *tcp13* and *tcp17* mutants show no phenotypic alterations during petal development, whereas the single *tcp5* mutant grows a slightly wider petal claw (Huang and Irish, 2015). This suggests that of these three genes, *TCP5* is the major player in petal development. Further analyses revealed that the reduced petal size in *TCP5* overexpressing lines versus the increased size in *miR:3TCP* is attributed to the duration of growth and cell differentiation (Huang and Irish, 2015).

In this study, we aim to shed light on the molecular mode of action underlying the functioning of *TCP5* in flowers, with a special focus on its function in petals. We show that *TCP5* is expressed in petals of stage 9 flowers and onwards and hypothesize that it is involved in controlling cell expansion, which is initiated at this stage of petal development (Irish 2008).

Furthermore, we analysed gene expression by RNA-sequencing analysis in whole inflorescences and petals of *tcp5 tcp13 tcp17* knockout mutants and in constitutive- and inducible *TCP5* overexpression lines. This revealed a possible role for *TCP5* in ethylene biosynthesis and signalling. Ethylene is known to play a role in the growth and elongation of (petal) cells (Chen *et al.*, 2013; Ma *et al.*, 2008; reviewed by Pierik *et al.*, 2006). The involvement of *TCP5* in ethylene biosynthesis was confirmed by an altered rate of ethylene accumulation in the analysed mutants, and complementation experiments with an ethylene pathway inhibitor were able to recover the *tcp5 tcp13 tcp17* phenotype to wild type. Together with showing direct binding of *TCP5* at the *ACS2* promoter, these findings provide strong

evidence for a central role of *TCP5* in ethylene-mediated control of petal growth.

Results

***TCP5* is expressed during cell elongation stages of petal development, regulating the final shape and size of Arabidopsis petals**

To visualize the spatial expression pattern of *TCP5* in petals, a transgenic *gTCP5-GFP* line was generated. Expression of *TCP5* seems to be uniformly distributed in the petal and occurs from stage 9 onwards (Figure 1), which is slightly earlier than previously reported (Huang and Irish, 2015). However, expression in these early stages is very low in comparison with later developmental stages. Analysis of *TCP5* expression during later developmental stages was done by quantitative (q)RT-PCR and showed constant *TCP5* expression until stage 15/16, when petal senescence occurs (Figure 1D; stages according to Smyth *et al.* 1990). Furthermore, the qRT-PCR analyses revealed that the expression of *TCP13* increased during later petal development whereas hardly any *TCP17* expression was detected in any of the analysed stages.

To further understand the function of *TCP5*, we decided to study the effect of *TCP5* overexpression in the epidermal layer of petals, because growth appears to be controlled and regulated to a large part from this cell layer (Urbanus *et al.*, 2010; Savaldi-Goldstein *et al.*, 2007; Anastasiou *et al.*, 2007). For this purpose, the promoter of the Arabidopsis L1-specific gene *MERISTEM LAYER 1* (*AtML1*) was used; this drives expression in the epidermis of all above ground organs (Lu *et al.*, 1996). In this experiment, *TCP5* was tagged with GFP, enabling the protein inside tissues to be visualized and tracked (Figure 2A). Confocal analysis showed that the expression of *TCP5-GFP* in *ATML1_{pro}:TCP5-GFP* plants is limited to the epidermis, as expected, and that no migration to underlying layers occurs (most likely due to the nuclear entrapment of the *TCP5-GFP* fusion protein Figure 2B). Quantitative RT-PCR analysis showed upregulation of *TCP5* expression of approximately 3.5 times relative to Col-0 (Figure 2C). Phenotypical analysis of *ATML1_{pro}:TCP5-GFP* plants during the vegetative stage of development showed the development of long elongated leaves, from which the blade was curled downward at the periphery and had a smaller surface area (Figure 2D and 2E). This phenotype is completely opposite to the leaf phenotype of the triple *tcp5 tcp13 tcp17* knock-out mutant (Efroni *et al.*, 2008; Huang and Irish, 2015). In addition, we observed significantly smaller petals of *ATML1_{pro}:TCP5-GFP* flowers compared to wild type petals (Figure 3), which is opposite to the petal phenotype of the triple knockout line. Notably, the petal phenotype observed in the *ATML1_{pro}:TCP5-GFP* plants is similar to the *35Spro:TCP5* phenotype previously observed by Huang and Irish (2015), revealing that specific ectopic expression of *TCP5* in the epidermal layer is sufficient to trigger this developmental response.

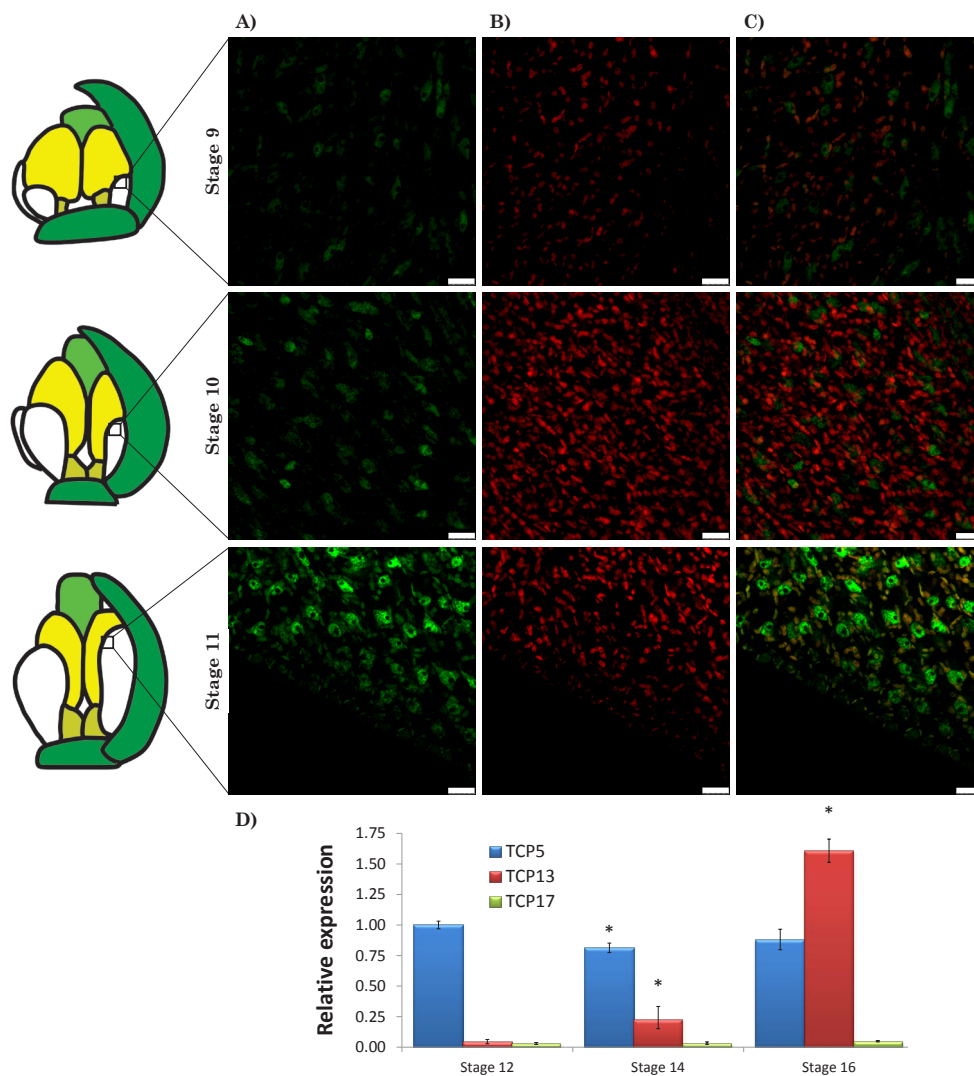


Figure 1. Expression pattern of *TCP5* in *Arabidopsis* petals during early and later stages of flower development.

(A-C) Confocal microscopy of GFP-tagged *TCP5* in the distal part of the petal. The GFP fluorescence can be seen as a green signal in (A), while the autofluorescence of chromo and/or chloroplasts is shown in red (B). The overlay is shown in (C), highlighting the nuclear localization of the GFP signal. (D) shows qRT-PCR analysis of cDNA of wild type petals from stage 12 (flowers close to anthesis), stage 14 (fully opened flowers) and stage 16 (senescing flower). The y-axis shows the relative expression with *TIP41* used as housekeeping gene for normalisation. The expression of *TCP13* and *TCP17* is scaled to the relative expression of *TCP5*. Asterisks indicate significantly different expression compared to expression at stage 12 using three biological replicates (Student's *t*-test, $P < 0.05$). The stages and graphic representation thereof are according to Smyth et al. (1990). Scale bars in (A-C) are 7.5 μm .

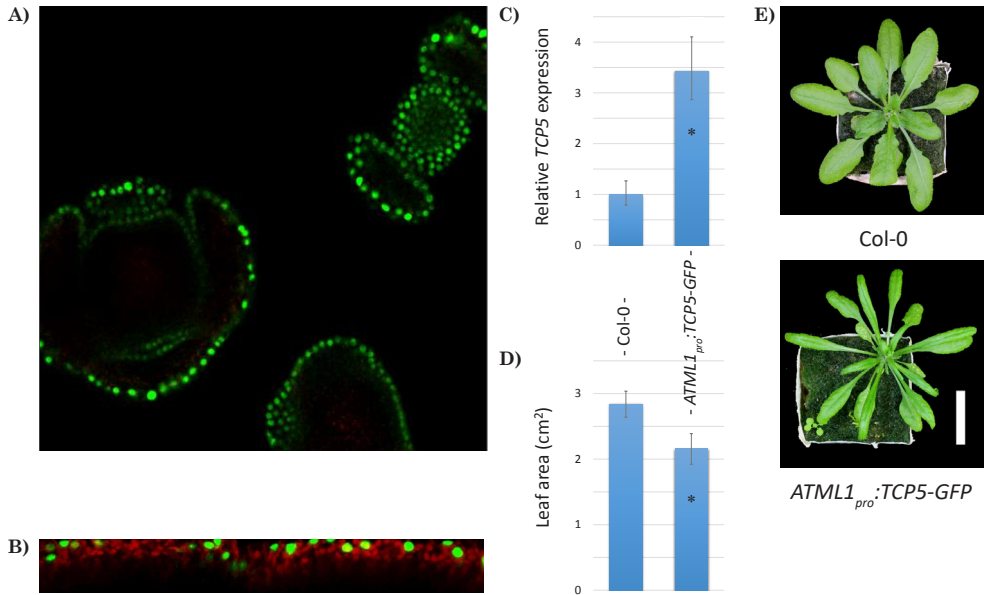


Figure 2. Construction, expression and leaf phenotype of *ATML1_{pro}::TCP5-GFP*.

(A) Confocal images showing the spatial expression pattern of *ATML1_{pro}::TCP5-GFP* in young buds and (B) the epidermal specificity due to nuclear entrapment in the abaxial leaf epidermis. (C) shows the relative overexpression of TCP5 in *ATML1_{pro}::TCP5-GFP* compared to wild type using three biological replicates. (D) quantification of leaf area (N=25), (E) overview of the leaf phenotype (bar = 1cm). An asterisk in figures (C) and (D) indicates a significant difference compared to wild type (Student's *t*-test, $P < 0.05$)

Next, we phenotyped a single *tcp5* mutant line and a *tcp5 tcp13 tcp17* triple mutant. Detailed phenotyping showed that petals of the *tcp5 tcp13 tcp17* mutant grow significantly longer and wider, (Figure 3), which is in line with previously published data (Huang and Irish, 2015). The single knockout of *tcp5* showed no differences from the wild type for these specific macroscopic characteristics (Figure 3).

***TCP5* and the *TCP5*-likes alter conical cell morphology**

To unravel the cellular causes of the observed petal phenotypes we took a closer look using Scanning Electron Microscopy (SEM). We focussed initially on the adaxial side of the distal part of the petal, where conical cells are located. In all three analysed lines (*tcp5*, *tcp5 tcp13 tcp17* and *ATML1_{pro}::TCP5-GFP*) the cells in the petal blade are bigger and more irregularly shaped than the round conical cells in wild type petals (Figure 4A and 4D). The shape of the conical cells was quantified by calculating the ratio of cell length to cell width, resulting in a measure of the cells roundness. Conical cells at the distal end of the petal are expected to be (close to) perfectly round (Szécsi *et al.*, 2014), which could be

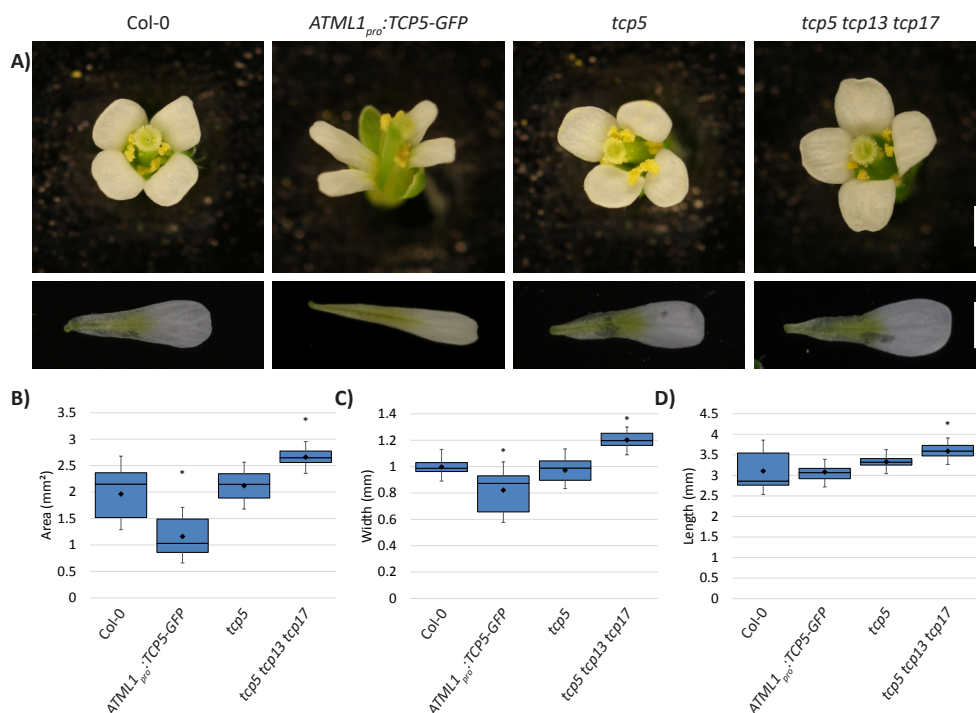


Figure 3. Floral phenotypes in *TCP5* overexpression and mutant lines.

(A) Overview of flower and petal phenotypes of Col-0, *ATML1_{pro}::TCP5-GFP*, *tcp5* and *tcp5 tcp13 tcp17* mutant plants. Scale bar is 1 mm. Detailed analysis of petal area (B), width (C) and length (D) represented by boxplots. The marker represents the average, an asterisk indicates a significant difference (Student's *t*-test, $P < 0.05$) compared to wild type Col-0 (N=36).

confirmed for Col-0 (Figure 4E). In contrast, the *ATML1_{pro}::TCP5-GFP* overexpressor plants and the T-DNA knockout lines showed a decrease of conical cell roundness.

Subsequently, we combined the cell shape and size measurements to infer the directionality of cell elongation in petal conical cells. We noted that in the wild type the vector (direction) of elongation of the conical cells is quite random, which is expected for the more or less round petal blade cells (Figure 4H and Supplemental Figure 1B and 1C). However, in *ATML1_{pro}::TCP5-GFP* the direction appeared to be more proximodistally (PD) oriented, which explains the narrower petals. In the case of the *tcp5 tcp13 tcp17* T-DNA knockout line this directionality seemed to be more medial-lateral (ML). This observation is in line with the observed wider petals in this mutant background (Figure 3A and 3C). The observation that the petal area is smaller in the *ATML1_{pro}::TCP5-GFP* mutant compared with the wild type, although the cells are larger, can be explained by the reduction in total cell number in this mutant (Figure 4F).

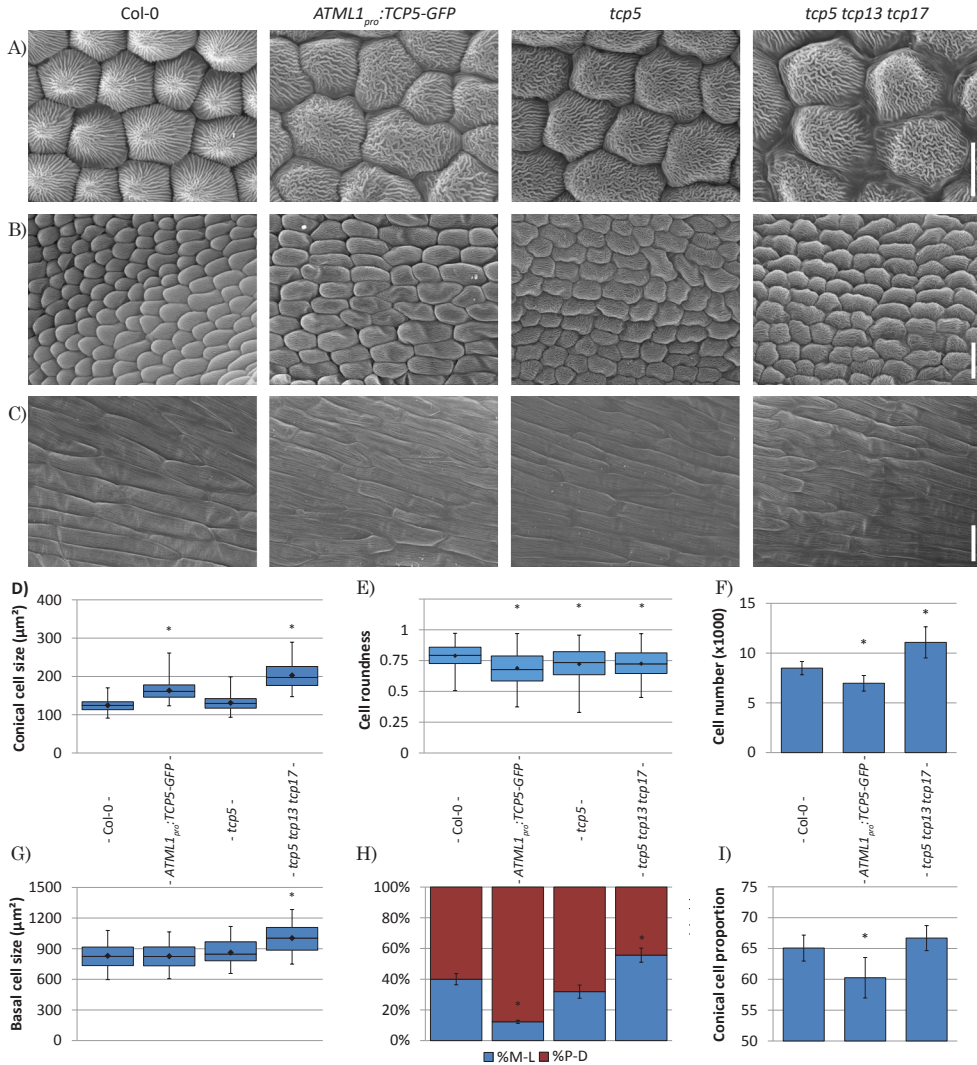


Figure 4. Overview of cellular phenotypes in petals of *Col-0*, *ATML1_{pro}::TCP5-GFP*, *tcp5* and *tcp5 tcp13 tcp17* mutant plants.

Scanning electron micrographs of the distal (A), central (B) and proximal (C) parts of the petal. Boxplots show the cell sizes of conical cells at the distal part of the petal in (D). (E) The roundness of the conical cells and (F) the total number of conical cells. (G) the size of basal cells. (H) The direction of cell-elongation, medial-lateral (blue) or proximo-distal (red). (I) The proportional area of conical cells in the petal. Scale bars (A) 10 μm ; (B), (C) 20 μm . Box plots (D, E and G) show mean (dot on horizontal line), median (middle horizontal line), second to third quartiles (box), and minimum and maximum ranges (vertical lines). The bars (F, H and I) indicate means and SDs. In both cases an asterisk indicates that the mean is significantly different from wild type ($P < 0.05$, Student's *t*-test). At least 50 cells from 12 petals were analysed.

Conical cells at the distal end of a petal possess a dome-shaped structure with cuticular ridges that run from the edges of the cell (where the cell touches its neighbouring cells) to the top of the conical cell (Panikashvili *et al.*, 2011) (Figure 4A). In the case of the single *tcp5* knockout, these ridges are oriented similarly to wild type cells towards the tip of the cone, despite the differences in cell size and shape; however, in the case of *ATML1_{pro}:TCP5-GFP* and the triple mutant, the ridges seem to be running more randomly and parallel to each other.

Finally, we investigated potential effects of *TCP5* alterations on cell elongation at the base of the adaxial side of the petal and found that these cells are significantly larger in the *tcp5 tcp13 tcp17* mutant (Figure 4C and 4G). Nonetheless, no significant differences were observed in either the single *tcp5* mutant or the *ATML1_{pro}:TCP5-GFP* overexpression line.

Molecular analysis of *tcp5*, *tcp5 tcp13 tcp17* and *ATML1_{pro}:TCP5-GFP*

To obtain insight into the potential molecular causes of the observed phenotypes, an RNA-seq analysis was performed on dissected petals of stage 12 flowers of Col-0 wild type, *tcp5*, *tcp5 tcp13 tcp17*, and *ATML1_{pro}:TCP5-GFP* lines. We found a total of 2682 genes differentially expressed in *ATML1_{pro}:TCP5-GFP* petals compared with the wild type, 1581 in *tcp5*, and 1519 in the *tcp5 tcp13 tcp17* triple knock-out. Of these, 345 differentially expressed genes (DEGs) were found in all three mutant backgrounds (Supplemental Figure 2C; Supplemental Table 1).

Subsequently, a Gene-Ontology (GO) enrichment analysis was done to identify the biological and molecular processes affected by *TCP5*. To produce a first overview, the GO Slim method was chosen, which gives broad insight into ontology. A summary of GO-terms found to be overrepresented in multiple samples is shown in Supplemental Figure 3 (full list in Supplemental Table 2). Previously, CIN-TCPs have been described as being involved in cell growth and differentiation (Efroni *et al.*, 2008), and the petal phenotypes of the *TCP5* overexpressor and *tcp5 tcp13 tcp17* mutants are in agreement with a function of *TCP5*-like genes in these cellular processes (present work; Huang and Irish, 2015). Enrichment was found for GO-terms such as cell wall (GO:0005618), anatomical structure morphogenesis (GO:0009653), membrane (GO:0016020) and the regulation of cell size (GO:0008361), cell differentiation (GO:0030154), cell growth (GO:0016049) and growth (GO:0040007). Nevertheless, steady-state differential expression in stable mutant backgrounds does not provide information about the direct targets of the *TCP5* TF. We therefore generated an inducible transgenic *35Spro:TCP5-GR* Arabidopsis line, which allowed us to use the glucocorticoid receptor to activate *TCP5* at specific moments during development by the application of dexamethasone (DEX) (Aoyama and Chua, 1997). Continuous DEX treatment resulted in phenotypes in line with those of the stable *ATML1_{pro}:TCP5-GFP* line (Supplemental Figure 4). To shed light on the molecular mode of action of *TCP5* in flower development, inflorescences were harvested after 2 and 8 hours of DEX treatment.

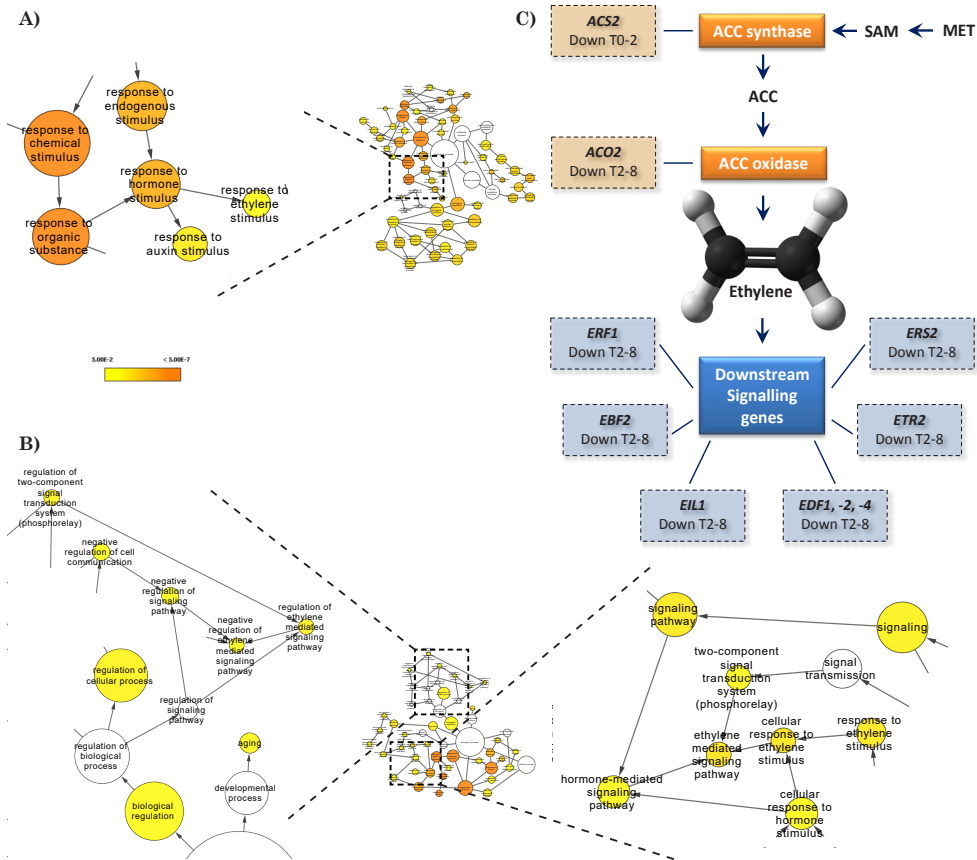


Figure 5. Overrepresentation of ethylene signalling genes among the differentially expressed genes.

(A), (B) Hormone related Gene Ontology (GO) terms for (A) differentially expressed genes after 2 hours induction (T0-2) and (B) after 8 hours induction (T2-8). The colour bar in (A) and (B) indicates significance levels for the GO categories (FDR<0.05). The circle size represents the number of genes present for a particular GO-term. In the case of, for example, response to ethylene biosynthesis, the size corresponds to 12 and 17 genes respectively. (C) Differentially expressed genes in the ethylene biosynthesis and signalling pathway in either the first time point (T0-2) or the second (T2-8); lines indicate that, for example, *ACS2* is a 1-amino-cyclopropane-1-carboxylate (ACC) synthase and link the different gene classes to individual genes in that class showing differential expression. SAM, S'-adenosyl-L-methionine; MET, methionine.

This two-step analysis allows us to distinguish between the direct and indirect effects of *TCP5* induction. We found 1057 genes differentially regulated after 2 hours of treatment, which after 8 hours had increased to 1350 genes. In these lists of significantly differential regulated genes upon induction of *TCP5*, we found more downregulated than upregulated genes (Supplemental Figure 2B; Supplemental Table 1).

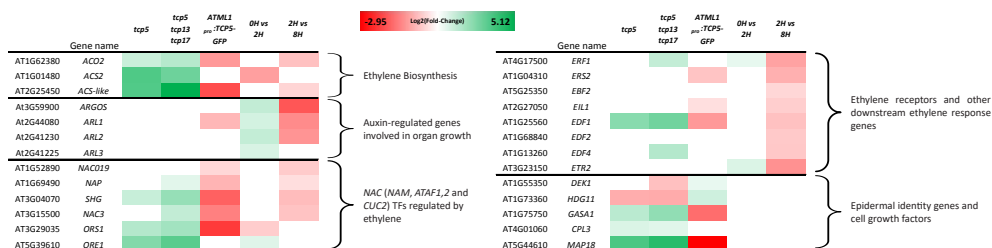


Figure 6. Differentially expressed genes.

Heatmap of differentially expressed genes categorised by function and/or process involved. The colour scale indicates the $\log_2(\text{fold-change})$, based on fragments per kilobase of transcript per million reads (FPKM) values, for upregulated genes (green) through genes that show no difference (white) towards downregulated genes in red.

For a detailed analysis of the differentially expressed genes, we performed a full GO-term analysis for genes differentially expressed at 2 hours after induction (T0-2) and genes differentially expressed between 2 and 8 hours after induction (T2-8). Analysis of both time points revealed a profile strikingly rich in terms related to plant defence and hormonal responses (Figure 5A and 5B; Supplemental Table 3).

Two hormones known to be growth regulators are found in our GO-term overrepresentation analysis. Response to auxin stimulus (GO:0009733) is found in all samples, and a striking finding in both the *35S_{pro}:TCP5-GR* induction as well as the stable *ATML1_{pro}:TCP5-GFP* was the presence of the GO-term response to ethylene stimulus (GO:0009723) (Figure 5 and Supplemental Table 3). Ethylene is known to influence cell expansion in petals (Pei *et al.*, 2013) and therefore we focussed our further experiments on this hormone. Mutual targets of both ethylene and auxin are the *ARGOS* and *ARGOS*-like (*ARL*) genes, which all appear to be upregulated immediately after *TCP5* induction (Figure 6). Additionally, in the list of differentially expressed genes we found the ethylene biosynthesis genes 1-AMINOCYCLOPROPANE-1-CARBOXYLIC ACID SYNTHASE 2 (*ACS2*), which catalyses the rate-limiting step in ethylene biosynthesis (Graaff *et al.*, 2006), and ACC-oxidase 2 (*ACO2*), which converts ACC into ethylene. Both *ACS2* and *ACO2* are upregulated in the *tcp5* and *tcp5 tcp13 tcp17* mutants and downregulated in the transgenic lines in which *TCP5* is overexpressed. Similarly, many ETHYLENE RESPONSE FACTORS (*ERFs*), which are downregulated in our overexpressing lines, are upregulated in the knockout lines (Figure 6).

***TCP5* inhibits ethylene biosynthesis**

The differential gene expression analysis led to the hypothesis that *TCP5* primarily inhibits ethylene biosynthesis and secondly ethylene response. We indeed observed a significant increase in accumulated ethylene in the inflorescences of the *tcp5* and *tcp5 tcp13 tcp17* knockout mutants versus

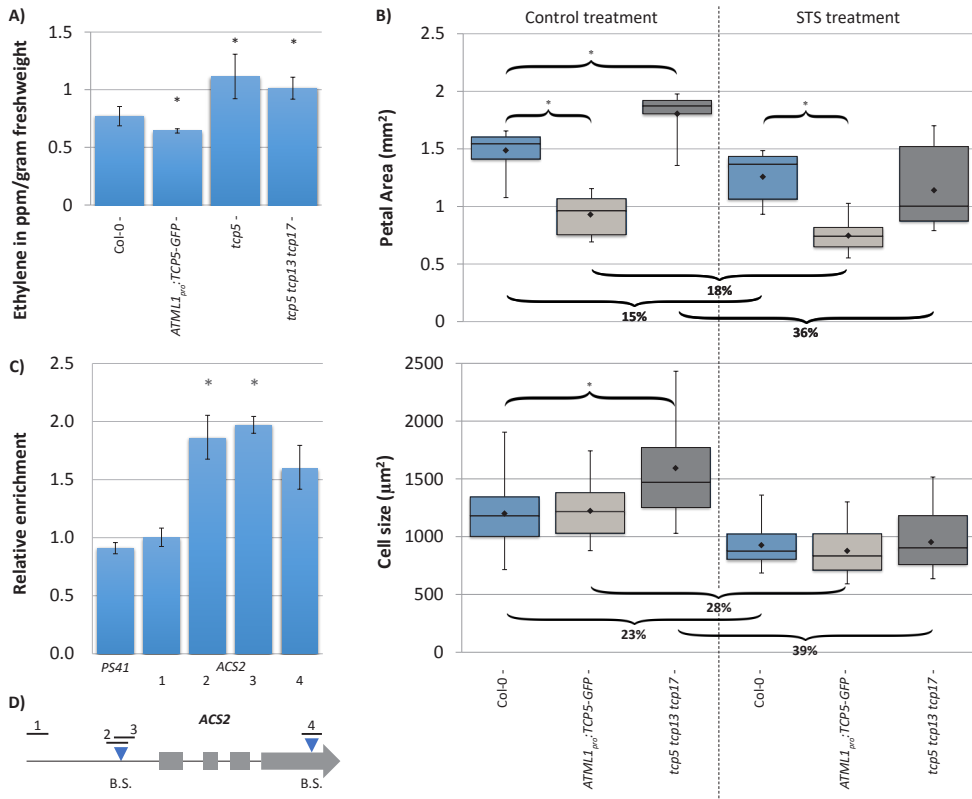


Figure 7. TCP5 inhibits ethylene biosynthesis.

(A), (B) Quantification of ethylene production of inflorescences (per hour per gram fresh weight) (A) and petal area and petal cell size analysis in control (left) and silver thiosulphate (STS) (right) treatment (B). Curly brackets with asterisks above indicate a significantly different area versus Col-0 wild type. Curly brackets below show the percentage of decline in petal area and cell size in STS treated samples compared with the control treatment. Treatment with STS had a significant effect for all plants tested. Bars in (A) show the mean of at least five biological replicates. The boxplot in (B) show mean (dot on horizontal line), median (middle horizontal line), second to third quartiles (box), minimum and maximum ranges (vertical lines). Twelve petals were analysed for petal area and at least 50 cells from these petals were analysed for size. In both cases an asterisk indicates a significantly different mean from the wild type ($P < 0.05$, Student's t -test). (C) Binding of TCP5-GFP to the *ACS2* locus confirmed by chromatin immunoprecipitation (ChIP)-qPCR. Binding of TCP5 is tested for the regions (1-4), of which regions 2, 3 and 4 cover a putative binding site, indicated in (D). *PS41* is the negative control. The data were normalized against *ACT2*. Means \pm SEM of three biological replicates are shown. The asterisks above the columns indicate significant difference between TCP5-GFP and input ($P < 0.05$, t -test). (D) Schematic diagram of the *ACS2* locus. Grey boxes indicate the exons, blue triangles indicate the positions of putative TCP-binding motifs (B.S.) and black lines show the amplified fragments in ChIP-qPCR.

a significant decrease in the *ATML1_{pro}::TCP5-GFP* overexpressor (Figure 7A).

If the disruption in ethylene biosynthesis/signalling is (at least partly) accountable for the observed phenotypes, exogenous alteration of the ethylene pathway should be able to restore mutant phenotypes. For that purpose, we conducted an experiment in which we added silver thiosulphate (STS), an inhibitor of the ethylene pathway (Beyer, 1979). After application of STS, which should block the enhanced ethylene response in the *tcp5 tcp13 tcp17* mutant, petal and cell sizes returned to wild type dimensions (Figure 7B).

Ethylene has a well-studied regulatory role in Arabidopsis leaf senescence (Kim *et al.*, 2015; Weaver *et al.*, 1998; Koyama, 2014), but a lot less is known about its role in petal senescence in Arabidopsis (Wagstaff *et al.*, 2009; Rogers, 2013). The RNA-seq data revealed a number of differentially expressed NAC TFs (Figure 6) known to act downstream of the ethylene signalling pathway and to be involved in senescence-related processes: *NAC019*, *NAP*, *SHG*, *NAC3*, *ORS1* and *ORE1* (Kim *et al.*, 2014). Their direction of differential regulation perfectly fits the increase or decrease in ethylene biosynthesis and signalling genes in our mutants, prompting us to take a closer look at petal senescence in our lines. However, Arabidopsis petals have been questioned as suitable organs for studying senescence since a clear progress of senescence is lacking (Jones 2009). Pollination triggers senescence in these organs after which they abscise without substantial wilting in a very short time, making differences hard to detect. Indeed, we could not observe any differences related to senescence in petals of the various mutant lines in comparison with the Col-0 wild type.

Finally, we tested the binding of TCP5 to putative TCP-binding motifs in the promoter and genic regions of *ACS2* (Figure 7D). We compared the immunoprecipitated DNA of inflorescences of *gTCP5-GFP* with input DNA by qPCR and found a significant enrichment for the putative TCP-binding site in the promoter (Figure 7C), showing direct binding of *ACS2* by TCP5 *in vivo*.

Discussion

In this study, the roles of *TCP5*-like genes in Arabidopsis petal development were studied with a special focus on the underlying molecular mechanisms. During organ development, cell differentiation is preceded by a period of rapid cell division. This holds true for most developing organs and tissues, but has been most extensively studied in leaves (Andriankaja *et al.*, 2012). Petal cell differentiation seems to be a more gradual process along the proximodistal (base to tip) axis (Sauret-Güeto *et al.*, 2013), in contrast to the prompt transition from proliferation to cell differentiation in leaves (Andriankaja *et al.*, 2012). This makes petals interesting organs in which to study growth and development. Petals grow from petal primordia that emerge from stage 5 flower buds (Smyth *et al.*, 1990). Initially, the petal primordia remain small, but the cells start to divide faster from stage 7 and

8 of flower development onwards and cell division rate reaches a plateau around stages 9-11, after which it rapidly declines. During petal development, stage 9 marks the onset of cell expansion (Irish, 2008), which is exactly the moment when *TCP5* expression becomes apparent.

A role for *TCP5* in later petal developmental stages

Based on our results from the detailed phenotyping of petal development and previously published data (Huang and Irish, 2015), *TCP5* seems to be involved in petal development from the onset of cell elongation (stage 9) and into the maturation phase until the later stages of flower development (stage 14-15). These observations led to the hypothesis that *TCP5* is mainly involved in cell elongation, which was confirmed by whole transcriptome analysis using RNA-seq and subsequent Gene Ontology analysis, in which we identified overrepresentation of the GO terms regulation of cell size (GO:0008361) and cell growth (GO:0016049). Hence, in line with the observed morphological changes in the mutants, the RNA-seq results also point to cell elongation-related processes, suggesting a major role for *TCP5* in the regulation of petal growth. Furthermore, these results show which growth-related genes are responsible for the observed altered phenotypes.

Previous research has shown that *TCP5* is repressed by *RBE* during the early stages of petal development, limiting the function of *TCP5* towards later stages of petal development (Huang and Irish, 2015). Interestingly, *TCP4*, a *JAW*-TCP, is also repressed by *RBE* during the early stages of petal development (Li *et al.*, 2016) and there is considerable overlap in the petal phenotypes of the different *TCP5*-like and *JAW*-TCP gene mutants. For example, a mutation in the *CIN* gene of *Antirrhinum*, which is orthologous to the *CIN*-TCPs in *Arabidopsis* (*TCP2*, -3, -4, -5, -10, -13, -17 and -24 Uberti Manassero *et al.*, 2013), results in flattening of the conical cells, as well as an increase in cell size in certain petal regions (Crawford *et al.*, 2004), which is in perfect agreement with our data on the *tcp5 tcp13 tcp17* knockout. Furthermore, in the loss-of-function mutant *miR319a129*, where the *JAW*-TCPs are overexpressed, petals are significantly smaller and narrower (Nag *et al.*, 2009), which is a phenocopy of the *TCP5* overexpression phenotype.

It might be expected that the conical cell phenotype of *jaw-D* plants resembles that of *tcp5 tcp13 tcp17*, which would further strengthen the hypothesis that the *JAW*-TCPs and the *TCP5*-like TCPs share regulatory functions during petal development (Efroni *et al.*, 2008; Koyama *et al.*, 2007). Additionally, the similarity in phenotypes might be explained by the fact that *TCP5*-like proteins preferentially interact with *jaw*-like TCP proteins to form heterodimers (Danisman *et al.*, 2013).

Another phenotype shared by the *cin* mutant in *Antirrhinum* and our *tcp5* mutant and overexpression lines is the clear difference in cuticle ridges on conical cells compared with that on conical cells of wild type petals. The precise mechanism that controls the patterning of the petal cuticle is still unknown but is thought to be linked to cell shape, because mutants defective in cutin biosynthesis

show impaired cell expansion (Noda *et al.*, 1994; Glover *et al.*, 2016; Cominelli *et al.*, 2008). This seems to be confirmed in our experiments, because we also observed effects on both cuticle ridge formation and conical cell sizes. Since the effect of altered *TCP5* expression is primarily on genes involved in cell elongation, this implies that the cuticle patterning defect is a consequence, not the cause, of the altered petal cell size in the different *tcp5* mutants.

Does the L1 layer have an important role in petal development related to TCP5 action?

The petal phenotypes observed in the *ATML1_{pro}:TCP5-GFP* lines are similar to the *35S_{pro}:TCP5* phenotypes published previously (Huang and Irish, 2015). Although *TCP5* is expressed normally throughout the different cell layers of the petal, the fact that it can act non-cell autonomously from the epidermal layer is in agreement with the hypothesis that control of organ growth is mediated to a large extent by the epidermal L1 cell layer (Savaldi-Goldstein *et al.*, 2007). Of note is the differential expression of several genes involved in epidermal specification in the *ATML1_{pro}:TCP5-GFP* overexpression line, as well as in the *tcp5* and *tcp5 tcp13 tcp17* mutants, including genes such as CAPRICE-LIKE MYB3 (*CPL3*) (Grebe, 2012), DEFECTIVE KERNEL1 (*DEK1*) and its downstream-acting HD-ZIP IV-encoding genes *HDG11* and *HDG12* (Galletti *et al.*, 2015) (Figure 6). Although the overexpression of *TCP5* in the epidermal L1 layer is ectopic and petals are derived solely from L1 and L2 layers of the floral meristem (Jenik and Irish, 2000), the fact that this differential expression is also seen in the loss-of-function mutants suggests a specific growth regulatory function for *TCP5* in, and coordinated from, the epidermis.

TCP5 controls petal growth and development via ethylene biosynthesis and signalling

Analysis of the genes differentially expressed after *TCP5* induction showed enrichment for processes related to stress, defence responses and hormone responses. This might not be surprisingly since TCPs have been described to act directly on hormonal pathways, that regulate both defence responses and plant growth (reviewed by Nicolas and Cubas, 2016; Li, 2015; and Danisman, 2016). Furthermore, it is well known that there is a trade-off between growth and defence (Todesco *et al.*, 2010). We therefore hypothesise that *TCP5* primarily targets and regulates certain hormonal pathways which ultimately lead to the growth phenotypes observed here.

Further analysis of the RNA-seq results pointed our attention towards ethylene signalling (GO:0009723), as it was overrepresented in the GO-term analysis upon DEX induction of the *35S_{pro}:TCP5-GR* plants. All samples showed a deregulation of ethylene biosynthesis genes, as well as numerous downstream signalling elements. Analysis of ethylene production in the headspace of inflorescences confirmed the differential gene expression. We found a reduction of ethylene levels in the *ATML1_{pro}:TCP5-GFP* overexpressor and an increase of ethylene in the headspace of both the

tcp5 and *tcp5 tcp13 tcp17* knockout mutants, suggesting a role for *TCP5* as an inhibitor of ethylene biosynthesis. Alternatively, these alterations can be caused by effects on the expression of ethylene biosynthesis and signalling genes, because the ethylene signalling pathway is known to have feedback regulatory loops (Rai *et al.*, 2015; Prescott *et al.*, 2016) and hence effects downstream of ethylene can ultimately result in differences in ethylene production.

Next to ethylene, the response to auxin (GO:0009733) was also overrepresented in our differential gene lists. Both auxin (Varaud *et al.*, 2011) and ethylene (Pei *et al.*, 2013; Ma *et al.*, 2008; Chen *et al.*, 2013) have been shown to function in cell proliferation and elongation during petal development. Analysis of the two time points upon *TCP5* activation revealed differential expression in ethylene biosynthesis in the first time point (T02), whereas only the second time point (T2-8) shows differential expression in downstream ethylene signalling genes (Figure 2C). This suggests that *TCP5* has a direct effect on the biosynthesis of ethylene, which is further confirmed by our finding that *TCP5* binds the promoter of *ACS2* *in vivo* (Figure 7C).

Previous research has shown that reduced ethylene signalling leads to an increase in petal size due to an increase in conical cell size (e.g. in the loss-of-function mutant *ein2*) (Pei *et al.*, 2013). This effect on petal development was confirmed by us by an analysis of petal size in *ein2* and two other mutant lines defective in the ethylene signalling and transcription cascade, *ein3* and *etr1* (Supplemental Figure 5). However, there is evidence to suggest that ethylene can both induce cell elongation (reviewed by Van de Poel *et al.*, 2015; Feng *et al.*, 2017) and repress cell growth, depending on the exact concentration and cellular context (Pierik *et al.*, 2006; Dugardeyn and Van Der Straeten, 2008). As a consequence, a low ethylene concentration can have the same effect on cell elongation as a high concentration (Abts *et al.*, 2014; Lv *et al.*, 2018).

The latter results seem to corroborate the data from our mutants that all show an increase in cell size, regardless of an increase or decrease in ethylene biosynthesis. We suggest that there is a tight balance between the ethylene concentration and its effect on cell size, as opposed to a linear relationship, linked to an 'on' or 'off' status for cell elongation. A deviation from 'normal' physiological ethylene concentrations then results in an enhanced cell elongation phenotype, as previously seen in root cells (Abts *et al.*, 2014; Lv *et al.*, 2018). This is further strengthened by the fact that we revert the phenotype of the *tcp5 tcp13 tcp17* line (which produces more ethylene but grows bigger petals with bigger cells) to a wild type phenotype by blocking the ethylene signalling pathway with STS, demonstrating that a large part of the mutant phenotype is caused by altered ethylene signalling. Moreover, blocking the ethylene pathway by STS also reduced petal growth in our Col-0 control plants, albeit to a much lesser extent than that of the *tcp5 tcp13 tcp17* mutant.

The perturbation in the ethylene balance might also lead to the observed differential direction of cell elongation, which is known to be influenced by the effect that ethylene has on microtubule

orientation (Le *et al.*, 2004; Plett *et al.*, 2009). In addition, genes involved in directional cell growth, such as MICROTUBULE ASSOCIATED PROTEIN 18 (*MAP18*) (Wang *et al.*, 2007) were found to be deregulated. This could in part also explain the defect in cuticle patterning, as the composition of cuticular ridges has been linked to differences in cell morphology (Shi *et al.*, 2011), and microtubule orientation was recently shown to control conical cell shape (Ren *et al.*, 2017).

Downstream of ethylene biosynthesis are numerous genes involved in cell elongation processes, which might account in part for the phenotypes observed in our mutants. For example, auxin is known to induce the production of ethylene (Pierik *et al.*, 2006; Tsuchisaka and Theologis, 2004). Interestingly, the ARGOS gene family is involved in a negative feedback loop in ethylene signalling, downstream of ethylene biosynthesis (Rai *et al.*, 2015). Upregulated by both ethylene and auxin, it inhibits a proper downstream ethylene signalling response. In our induction experiment, ARGOS and ARGOS LIKE 1, -2, and -3 (*ARL1*, -2 and -3) were upregulated after the first time point. In the second time point however, these genes were downregulated. This might point towards initial upregulation by TCP5 after which the ethylene biosynthesis is downregulated, possibly both through the activity of ARGOS and the ARLs and directly by TCP5. Consequently, downregulation of ethylene biosynthesis would then downregulate ARGOS and the ARLs.

In conclusion, we have demonstrated that TCP5 is an important regulator of growth and development of the Arabidopsis petal. However, in contrast to directly regulating growth regulatory genes, we show here that one of the functions of TCP5 is to act as a regulator of ethylene biosynthesis, after which the downstream targets of ethylene signalling are responsible for various of the observed developmental phenotypes. Several TCP TFs have been described to regulate hormone synthesis, transport and signal transduction for a number of key plant hormones (reviewed by Nicolas and Cubas (2016)). However, no TCP protein has yet been linked to ethylene yet and we provide proof in this study for a tight association between TCP5 and ethylene biosynthesis and signalling.

Experimental Procedures

Plant materials and growth conditions

The triple T-DNA insertion mutant *tcp5 tcp13 tcp17* contains the mutant alleles *tcp5-1* (SM_3_29639), *tcp13* (SM_3_23151) and *tcp17* (SALK_147288) all three of which have insertions in the coding regions. The *tcp5-1* single mutant was kindly provided by Dr. Koyama and the triple *tcp5 tcp13 tcp17* was a gift from Professor Eshed. All three lines defective in the ethylene signalling and transcription cascade (*etr1-1*, *ein2-5* and *ein3-2*) were obtained through the Nottingham Arabidopsis Stock Centre (NASC; <http://arabidopsis.info/>). Plants were grown under long-day conditions (16 h/8 h light/dark cycle) at 21°C on Rockwool and received 1 g l⁻¹ Hyponex plant food solution twice a week.

Constructs and transformation

The coding sequence (without a STOP-codon) of *TCP5* was amplified by PCR and recombined into the modified pK7FWG2 destination vector, containing the *AtML1* (AT4G21750) promoter in place of CaM35S (Urbanus *et al.*, 2010), resulting in *ATML1_{pro}:TCP5-GFP*. Simultaneously, the coding sequence was recombined in pARC146 (Danisman *et al.*, 2012), resulting in the destination vector *35S_{pro}:TCP5-GR*. Next, a 3 kb promoter region was cloned together with the *TCP5* coding sequence and recombined into pMDC204 (Curtis and Grossniklaus, 2003) resulting in the destination vector *TCP5_{pro}:TCP5-GFP*. All primer sequences can be found in supplemental table 4. All three constructs were transformed into *Agrobacterium tumefaciens* strain C58C1-PMP90. Arabidopsis transformation was conducted by the floral dip method (Clough and Bent, 1998). The T1 seeds were selected on germination medium containing 30 µg ml⁻¹ kanamycin for 2 weeks, after which rooting green T1 seedlings were transferred to Rockwool and grown until seed set. The following T2 generation was checked for expression of the transgene by reverse-transcription PCR. Col-0 was used as the wild type and reference in all experiments.

Petal and cell measurements and analyses

Petals were collected from fully grown flowers at stage 14-15 (Smyth *et al.*, 1990) and subjected to further analysis either by epidermal imprinting for cellular phenotype analysis or by overall shape and size phenotyping. We used three plants of which 12 petals were analysed from four or five flowers; 50 cells from each petal were subject to analysis.

Petals destined for SEM were fixed in paraformaldehyde (4% in 9 phosphate buffer) and dehydrated in absolute ethanol, critical 10 point dried (Balzers CPD 030), mounted onto metallic stubs and gold-sputtered (with 40-nm colloidal gold, Balzers SCD 004). Observation and documentation were performed in a LEO 435 VP 11 scanning electron microscope. Digital images were obtained with LEOUNIF software. Samples destined for optical microscopy were mounted in a drop of glycerol on a microscopy slide, covered with a cover slip, observed and documented under a Zeiss Axioskope optical microscope (<https://www.zeiss.com/>) equipped with a digital camera.

The microscopic drawings of the abaxial petal epidermis were scanned for digitisation. Conical cells from the most distal third of the petal were digitised, but the epidermal cells at the petal margin were not considered. At least 19 petals were imaged for each genotype. Data on cell area and cell roundness were collected from digital images, essentially following the protocol described by Andriankaja *et al.* (2012). Colour gradients according to cell area as well as vectors of maximum and minimum cell diameters were assessed from each cell image using the ImageJ macro language (<http://rsbweb.nih.gov/ij/>). At least 10 000 cells from each genotype were analysed. A two-sample t-test was used to distinguish between mutant and wild type.

Epidermal imprinting

An addition-reaction silicone elastomer Polyvinyl Siloxane (dental resin kit) was used to obtain imprints of petals epidermis. Equal amounts of the two types of paste from the kit were mixed together to make the working dental resin. The resin was placed onto a glass slide with the help of a toothpick, forming a layer of 1-2 mm thick. Using tweezers, petals were placed on the resin layer with the adaxial surface facing the resin for at least 5 minutes or until the resin solidified. After gently removing the petals from the resin the impression was left to fully set for 5 minutes. Then clear nail polish was applied to the surface of the resin impression and left to completely dry for approximately 20 minutes. The nail polish layer was carefully peeled off from the resin and placed onto a new glass slide with the imprinted surface face up. The imprints were observed and imaged using a differential interference contrast microscope for further image analysis by ImageJ.

Tissue sampling and RNA isolation for qRT-PCR and RNA-sequencing

Petals of stage 12 flowers (Smyth *et al.*, 1990) were harvested from 50 flowers per biological replicate. For induction of *35Spro::TCP5-GR*, inflorescences were treated with a DEX-induction solution (2 μ M dexamethasone, 0.01% (v/v) ethanol, and 0.01% Silwet L-77), or with an identical mock solution that lacked DEX. Whole inflorescences were harvested 0, 2 and 8 hours after induction and RNA was isolated using the InviTrap® Spin Plant RNA Mini Kit (Strattec Molecular, <https://www.molecular-strattec.com/>) according to the manufacturer's protocol. TURBO™ DNase (ThermoFisher Scientific, <https://www.thermofisher.com/>) was used to clean the RNA samples from DNA.

iScript reverse transcriptase was used for cDNA synthesis. The complementary DNA made this way was used for qRT-PCR using the SYBR Green mix from Bio-Rad (<http://www.bio-rad.com/>). The reference genes used for all expression analyses were a *SAND* family gene, At2G28390, and the *TIP41*-like gene At4G34270, both 'superior reference genes' (Czechowski *et al.*, 2005).

Library preparation for whole-genome RNA sequencing was done using the Illumina Truseq Library Preparation Kit. Library quality was evaluated using a Bioanalyzer and an RNA Nano 6000 kit (Agilent, <http://www.agilent.com/>). RNA concentrations were determined using the Xpose 'DSCVRY' (Trinean). The libraries were then sequenced with the Illumina system Hi-Seq 2500.

Gene expression and gene set enrichment analysis

Libraries of three biological replicates were sequenced and analysed using the Bowtie–Tophat–Cuffdiff (BTC) pipeline (Trapnell *et al.*, 2012). Differential gene expression was based on FPKM (fragments per kilobase per million mapped reads) values and determined for all samples using Col-0 as the control. The cut-off was set at a false-discovery rate (FDR) <0.05 in all analyses performed. The RNA-seq data are made available via NCBI and can be accessed through GEO accession number

GSE103762.

The BINGO 3.03 plug-in (Maere *et al.*, 2005), implemented in CYTO-SCAPE 2.81 (Shannon *et al.*, 2003), was used to determine and visualize the GO enrichment according to both GO Slim (Supplemental Table 2) and GO enrichment (Supplemental Table 3) categorization. A hypergeometric distribution statistical testing method was applied to determine the enriched genes and the Benjamini Hochberg correction was performed in order to limit the number of false positives (FDR<0.05).

Ethylene treatment and quantification

Flowering plants with an inflorescence of approximately 4 cm were treated every other day for 1 week with a 50µM STS solution by floral dipping. Petals were harvested from stage 14-15 flowers and subjected to further analysis, either by epidermal imprinting for cellular phenotype analysis or by overall shape and size phenotyping. We used three plants of which 12 petals were analysed from four to five flowers.

Ethylene production (*EP*) was measured by putting the top 1.5 cm of an Arabidopsis inflorescence in a 5ml headspace vial (one inflorescence per vial). To prevent wilting of the inflorescence, 1ml of MS10 (Murashige and Skoog, 1962) was poured into the vial into which the inflorescence was placed. Before being sealed, the headspace vials were kept open for 1 hour to allow the wound-induced ethylene burst to subside. After closure the vials were kept for 7 h at 21°C to accumulate sufficient endogenous ethylene. Then, to determine the ethylene content, 0.5ml of headspace gas was injected into a Thermo Focus Gas Chromatograph (Thermo Electron S.p.A, Rodano, Italy) fitted with a Valco sample valve and analysed using a Restek RT QPLOT column, (0.53mm ID x 15m Interscience B.V., Breda, NL) at a column temperature of 50°C and flame ionisation detection. Quantitative data were obtained by using a certified calibration gas, namely 1.01 p.p.m. ethylene in synthetic air (Linde Gas Benelux, Schiedam, NL).

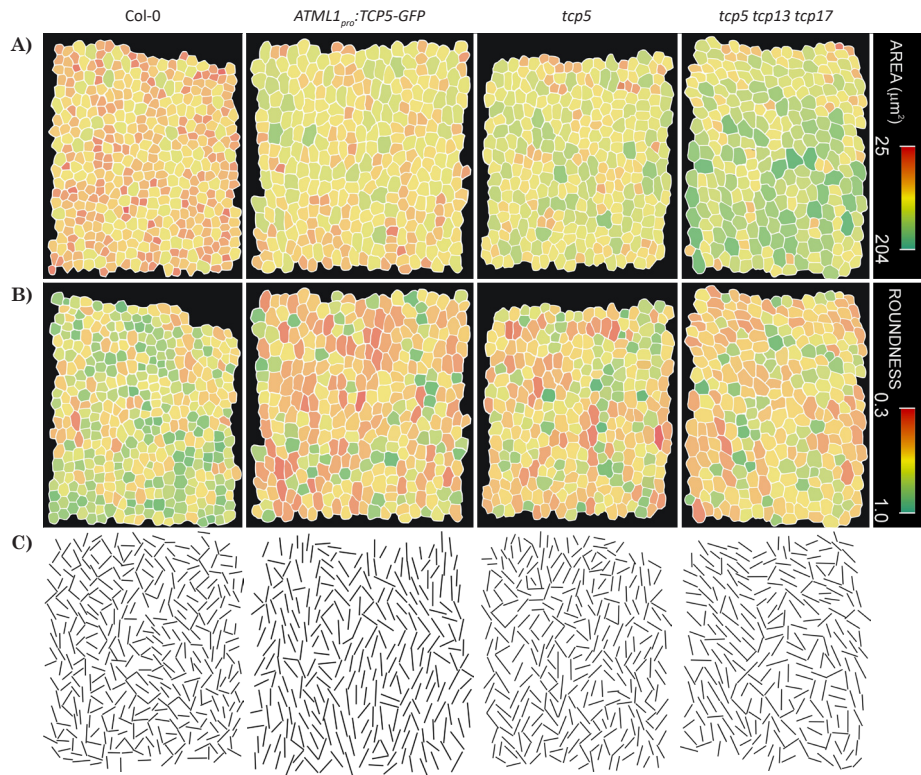
Chromatin Immunoprecipitation

Chromatin Immunoprecipitation (ChIP) was performed as described (Mourik *et al.*, 2015) on gTCP5-GFP inflorescences, using µMACS Anti-GFP (Miltenyi). Primers used for qPCR can be found in Supplemental Table 4. Regions of ACTIN 2 (*ACT2*, At3g18780), a peptidase S41 family protein (At4g17740) and *ACS2* (At1g01480) without a *TCP5*-binding site were used as negative controls. *ACT2* was used as a normalizer for DNA quantity and *PS41* as a background control for immunoprecipitated DNA. The same results were obtained when *PS41* was used as a normaliser and *ACT2* as a background control. Three biological replicates were used and a *t*-test ($P < 0.05$) was done to calculate significant enrichment in the ChIP-qPCR. Four primer combinations were designed in the promoter and genic regions of *ACS2* (Figure 4D). Primer combination 1 was used as a negative

control since no consensus TCP-binding site was present. Primer combinations 2 and 3 cover a single putative TCP-binding site in the promoter of *ACS2*, and primer combination 4 covers a putative TCP-binding region in the fourth exon of *ACS2*. We used the PlantPAN 2.0 website for promoter analysis to search for putative binding sites (Chow *et al.*, 2016).

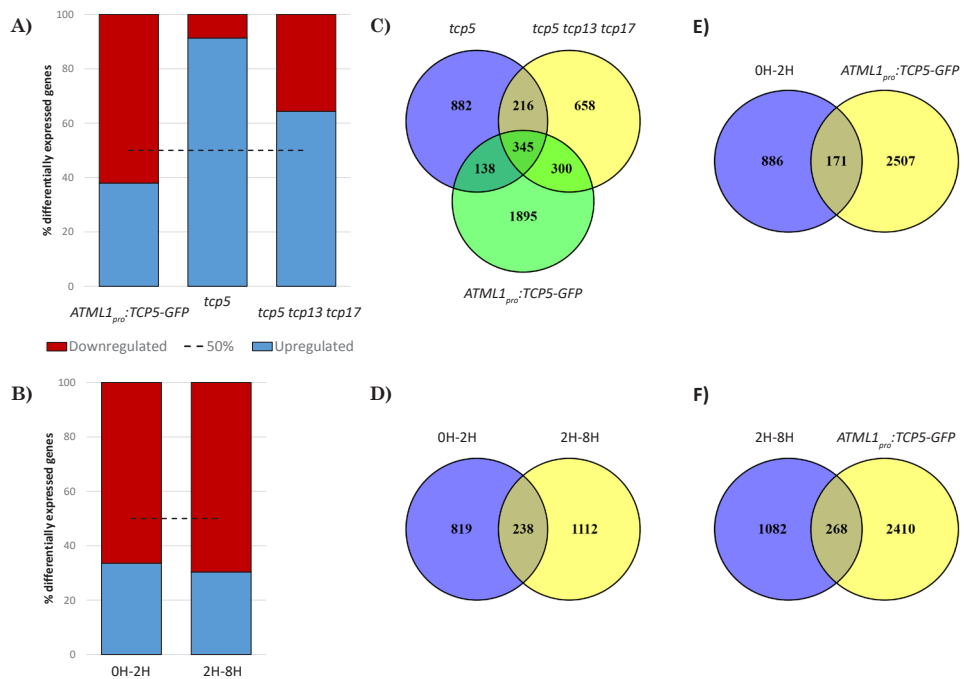
Acknowledgements

We thank Dr. Alice Pajoro for her help with establishing the ChIP protocol on gTCP5:GFP inflorescences, Dr. Koyama for providing the *tcp5-1* mutant and Professor Y. Eshed for sending us the triple *tcp5 tcp13 tcp17* T-DNA insertion line. We thank A.C. van de Peppel for help with the ethylene measurements. Our work is supported by grants from the Dutch Scientific Organization (NWO); (NWO-JSTP grant 833.13.008), CAPES/NUFFIC (no. 010/07) and CAPES/NUFFIC (no. 033/2012).



Supplemental Figure 1. Graphic representation accompanying the cell morphology phenotyping.

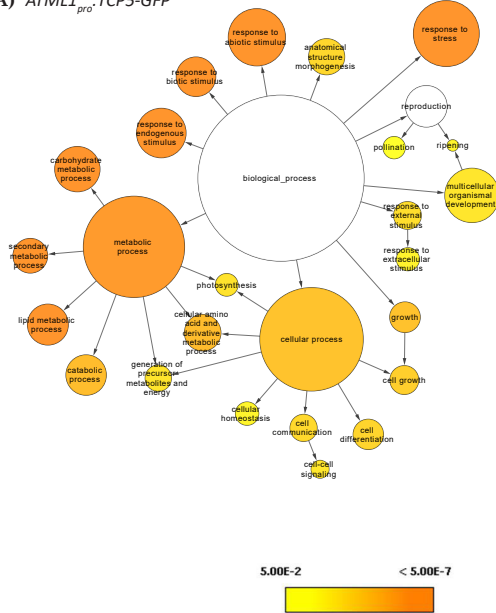
Cell area (A), roundness (B) and the direction of cell elongation by vector in (C).



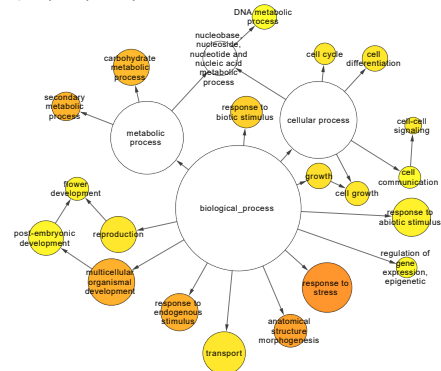
Supplemental Figure 2. Summary of RNA-seq results.

Percentage of DEGs that are either downregulated (in red) or upregulated (in blue) in the RNA-seq samples of the mutants (T-DNA and ATML1-promoter driven) in (A) versus the dexamethasone induction experiment (B). (C-F) Venn diagrams showing the overlap in DEGs.

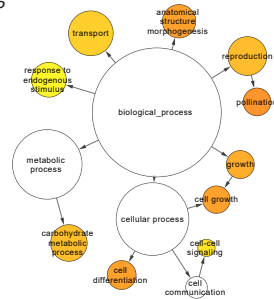
A) *ATML1_{pro}::TCP5-GFP*



B) *tcp5 tcp13 tcp17*

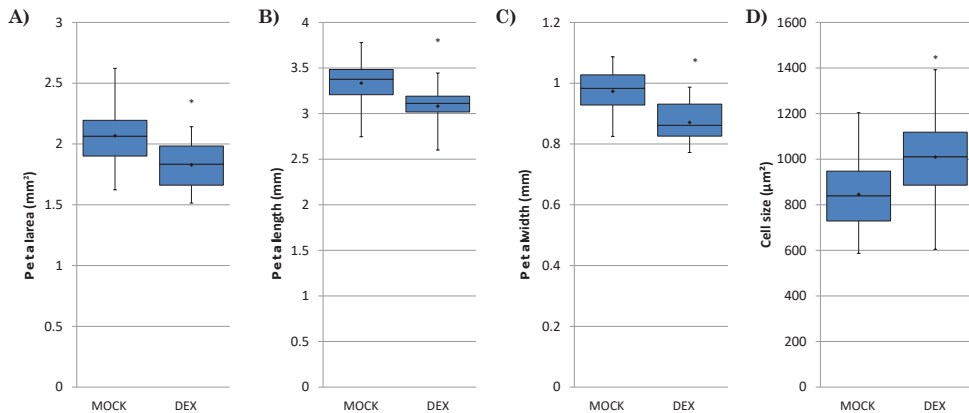


C) *tcp5*



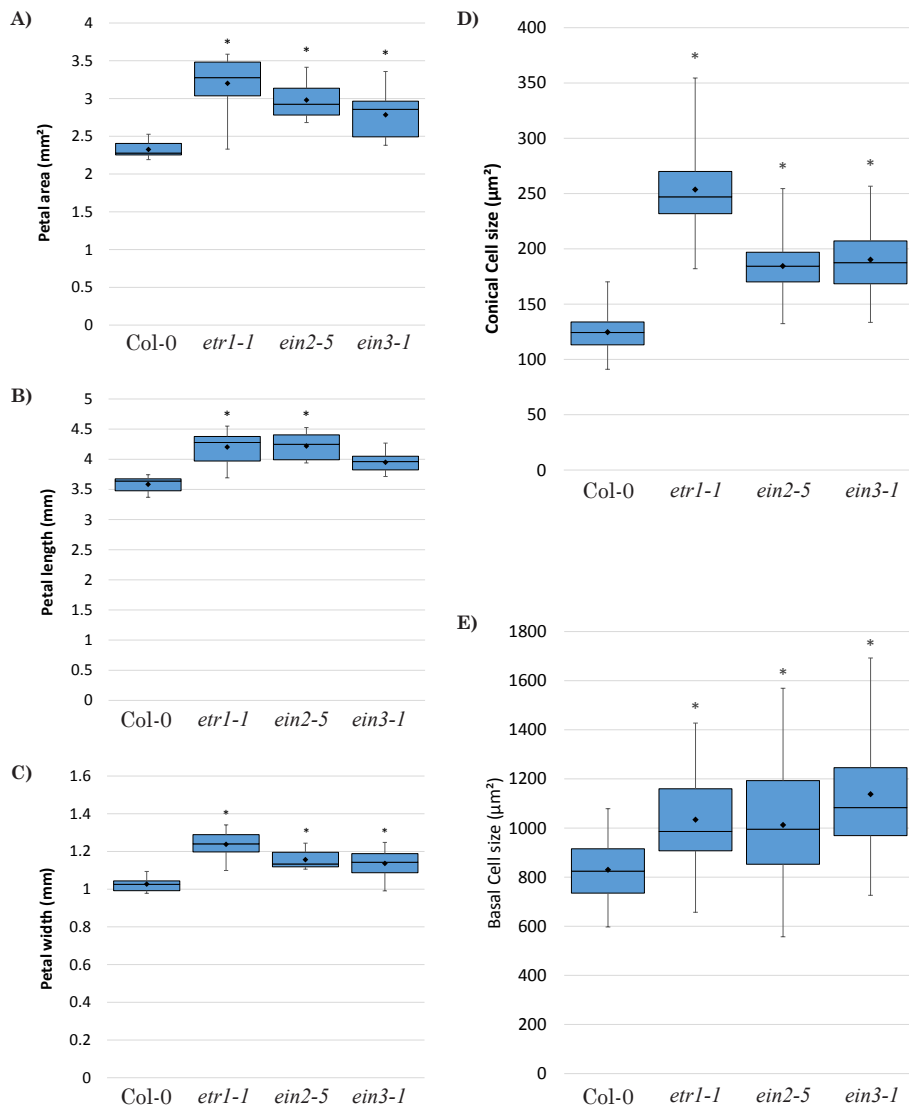
Supplemental Figure 3. GO term analysis.

Classification of DEGs by Gene Ontology (GO) slim term enrichment analysis for DEGs in the *TCP5* overexpressing line *ATML1_{pro}::TCP5-GFP* (A) triple mutant *tcp5 tcp13 tcp17* (B) and the single mutant *tcp5* in (C). The colour bar indicates significance levels for the GO categories (FDR < 0.05).



Supplemental Figure 4. Phenotypes of the *35Spro::TCP5-GR* mutant after dexamethasone treatment.

Petal area, length and width are shown in (A), (B) and (C) respectively. Cell area is shown in (D). An asterisk indicates a significant difference compared to Col-0 wild type.



Supplemental Figure 5. Phenotypal alterations in petals of mutants deficient in ethylene reception and signal transduction.

Quantification of petal area (A), length (B) and width (C). Quantification of cell size is shown for conical petal cells (D) and basal cells (E). Asterisks indicate a significant difference between Col-0 wild type and the respective mutants, *etr1-1*, *ein2-5* and *ein3-1* ($P < 0.05$, $N=36$).



Chapter 4:

The regulatory role of BRC1 in bud dormancy through various downstream signalling pathways

Sam W. van Es

Carlos Tarancón

Aalt D.J. van Dijk

Gerco C. Angenent

Pilar Cubas

Richard G.H. Immink

“Never saw off the branch you are on, unless
you are being hanged from it.”

Stanislaw Lec

Abstract

The *Arabidopsis* transcription factor *BRC1* plays an important role in the inhibition of axillary bud outgrowth and as such determines plant architecture. We used chromatin immunoprecipitation coupled to next generation sequencing (ChIP-seq) to determine direct genome-wide targets of *BRC1* and to elucidate the molecular mode of action of *BRC1* during axillary bud dormancy. The search for a putative consensus binding site that is centrally enriched in the *BRC1* ChIP-seq peaks, resulted in the identification of the cis-element 'GDCCCA', which is close to previously observed consensus TCP binding sites. Additionally, we identified enrichment of the 'G-box' either up- or downstream of the centrally enriched consensus TCP binding site. Subsequently, we linked the identified *BRC1* binding peaks to the nearest gene, revealing a potential role for *BRC1* in ABA biosynthesis. Several ABA biosynthesis genes, including *NCED3*, *NCED9* and *ABA2*, were bound by *BRC1* and showing differential expression upon induction of *BRC1*. Furthermore, we provide evidence for a regulatory role of *BRC1* in repressing cytokinin (CK) levels in dormant buds by activating two CK oxidases and repressing several CK signalling genes. These direct effects on ABA and CK pathways, together with the binding of several other gene loci, including genes involved in cell wall composition and genes with a potential role in symplastic intercellular connectivity, provide a molecular and potential mechanistic basis for the functioning of *BRC1* in the repression of axillary bud outgrowth.

Introduction

Plants are versatile in their appearance and are able to adapt their architecture in response to environmental changes. The main diversity in plant architecture can be attributed to branching patterns, which depend on the outgrowth of branch primordia in for example leaf axils. This process is highly flexible and depending on, among others, the amount and quality of light and availability of nutrients. Day-length has a profound effect on the initiation of axillary buds, which are initiated acropetally (from the base towards the apex) in the axils of leaves in short day conditions whereas long day results in basipetal initiation of axillary buds (Hempel and Feldman, 1994; Grbić and Bleecker, 2000; Long and Barton, 2000). Most axillary buds remain dormant until the appropriate environmental conditions or endogenous cues arise. The outgrowth of the main shoot and repression of axillary bud outgrowth imposed by a growing shoot apex is termed apical dominance (Cline, 1997) and has been instrumental in the domestication of a number of crop plants. In maize (*Zea mays*) for example, the inhibition of axillary bud outgrowth was pivotal to the domestication of this species from its highly branched ancestral species teosinte. The gene responsible for the repression of bud outgrowth, *TEOSINTE BRANCHED1* (*TB1*), was first characterized in this species (Doebley *et al.*, 1995; Doebley *et al.*, 1997). *TB1* is a member of the plant-specific TCP transcription factor (TF) family. In *Arabidopsis* this family consists of 24 members, three of which are closely related to *TB1* in maize. *AtTCP18*, also known as *BRANCHED1* (*BRC1*), seems to be most important in the repression of axillary bud outgrowth (Aguilar-Martínez *et al.*, 2007); *BRC1* expression is limited to axillary buds and its downregulation is tightly correlated with the development of branches. Transcriptional changes related to axillary bud outgrowth, through for instance the disruption of apical dominance by decapitation (Tatematsu, 2005) and changes in R:FR ratio (González-Grandío *et al.*, 2013; Reddy *et al.*, 2013), provide valuable insight into the precise function of *BRC1* during these processes. Genes of which the expression changed in low R:FR conditions in wild-type plants, but not in *brc1* mutant plants, were thought to require *BRC1* function for their regulation. As a result these genes were labelled *BRC1*-dependent genes (González-Grandío *et al.*, 2013). Comparing these data with that of decapitated plants (Tatematsu, 2005), the authors conclude that many of the *BRC1*-dependent genes are closely associated with bud activity, regardless of treatment or stimulus. A subsequent analysis of all three datasets mentioned above (Tatematsu, 2005; González-Grandío *et al.*, 2013; Reddy *et al.*, 2013) has led to the identification of two groups of genes potentially related to axillary bud outgrowth. These two groups have been termed 'bud activation' and 'bud dormancy' genes, respectively, depending on whether they are higher expressed in active buds and lower expressed in dormant buds (*bud activation genes*), or vice versa (*bud dormancy genes*) (González-Grandío and Cubas, 2014). The *bud activation* genes can be divided in three groups related to (1) DNA replication,

S phase and mitosis, (2) flavonoid synthesis, and (3) cytokinin signalling. The *bud dormancy* genes on the other hand can be sub-divided into four groups related to (1) ABA signalling, (2) ethylene and auxin signalling, (3) genes involved in autophagy and protein degradation and (4) a set of genes known to be dark-induced and sugar-repressed (González-Grandío and Cubas, 2014).

Strikingly, in all analysis performed in which active versus dormant buds were compared upon different stimuli, an ABA gene-regulatory network showed up. This drew the attention on a possible key regulatory role for ABA signalling directly downstream of *BRC1*. ABA has previously been implicated in the control of axillary bud outgrowth during exposure of plants to low R:FR conditions (Reddy *et al.*, 2013) and is described as negative regulator of bud outgrowth (Yao and Finlayson, 2015). Plants defective in ABA biosynthesis show an increased branching phenotype (Reddy *et al.*, 2013; Yao and Finlayson, 2015) and exogenous application of ABA inhibits branching (Chatfield *et al.*, 2000; Holalu and Finlayson, 2017). One of the proposed roles of ABA is the direct repression of the cell cycle machinery and thereby inhibiting outgrowth of branches. In line with this, it was found that *BRC1* directly activates three related homeobox genes, (*HOMEBOX PROTEIN 21*, -40 and -53). These three genes are sufficient to enhance the expression of *9-CIS-EPOXYCAROTENOID DIOXYGENASE 3 (NCED3)*, a key ABA biosynthesis gene (González-Grandío *et al.*, 2017). *BRC1* expression was not affected by exogenous ABA treatment, which suggests lack of a feedback mechanism and a function for *BRC1*, solely upstream of the ABA response.

Here we present a whole-genome transcriptomic analysis and a genome-wide target gene analysis of *BRC1* in Arabidopsis. An integrated analysis of the ChIP-seq dataset with an RNA-seq dataset, obtained on the same *BRC1*-inducible plant material, enabled determining which of the aforementioned *bud activation* and *bud dormancy* genes are directly activated or repressed by *BRC1*. We show that *BRC1* binds and regulates ABA biosynthesis genes, suggesting direct transcriptional regulation of the ABA response. Next to this, we show that *BRC1* might directly repress cytokinin signalling and enhance cytokinin degradation. Furthermore, we show that *BRC1* directly regulates several genes related to cell wall component biosynthesis and deposition, presenting an alternative mode of action for the *BRC1* inhibition of axillary bud outgrowth.

As this paper presents the first genome-wide binding analysis of a TCP protein, it contains a wealth of information regarding binding sites and possible consensus binding motifs of TCP proteins. We show that *BRC1* binds the TCP-like motif 'GDCCCA', which was preferentially found in the centre of the ChIP-seq peaks. This motif is often accompanied by a G-box motif, suggesting co-regulation of the identified targets by bZIP and/or bHLH TFs.

Results

BRC1 DNA binding analysis by ChIP-seq

To identify BRC1-bound loci in the *Arabidopsis* genome, we performed a Chromatin Immunoprecipitation assay for BRC1, followed by next-generation sequencing (ChIP-seq; Kaufmann *et al.*, 2010a). *BRC1* expression is limited to axillary buds (Aguilar-Martínez *et al.*, 2007), which complicates the study of protein-DNA binding events, as the main technique currently at hand (Chromatin Immunoprecipitation) is challenging for proteins present in low abundance (Kidder *et al.*, 2011). We therefore used an estradiol inducible line (*GFP:BRC1^{ind}*) for the experiments. The moment of plant material fixation for ChIP-seq was chosen in the afternoon, since at this moment expression of the native *BRC1* gene peaks (González-Grandío *et al.*, 2013). Seven-day-old seedlings were used, as this stage has proven effective in previously performed targeted ChIP-qPCR experiments (González-Grandío *et al.*, 2017).

ChIP-seq was performed five hours after BRC1 induction for three independent biological replicates and the obtained results are summarized in Figure 1A. To assess the reproducibility of the datasets, a pair-wise correlation analysis was done, revealing Pearson correlation co-efficiencies ranging from 0,77 to 0,83 (Fig. 1B) and hence, showing the reproducibility and quality of our experiments. Because of the lower number of peaks in sample 3 (Fig. 1A), we decided to perform most further analyses on the first two ChIP-seq datasets. We approached these datasets by creating a file representing their overlap, which was inferred by the distance between peaks in the individual samples. The average peak size was $\pm 300\text{bp}$, so if the centre of a peak in one sample is no more than 150bp apart from the centre of a peak in the other sample, the peaks are assumed to be in fact the same and were saved in a separate file for subsequent analyses. This criterion resulted in a file containing roughly 60-70% of the peaks of sample 1 and 2 (Figure 1A). Since this merging of peaks may result in a slight shift of the actual binding site, analyses looking specifically at the exact location of the binding site were done on the individual datasets. TFs may bind anywhere in a locus they control, including e.g. introns and 3'-regions, although plant TFs studied by ChIP-seq and DHS-Seq show the tendency of binding more frequent in promoter regions of target genes (Yu *et al.*, 2016). We confirmed this tendency for BRC1 and showed that the location of the peaks relative to the nearest gene are most often in promoters ($\pm 60\%$; Fig. 1D). Furthermore, these peaks are located, in the majority of these cases, on average within 300bp of the transcription start site (TSS in Figure 1C). A more detailed look at the BRC1 peak distribution showed that about 9% is positioned in introns, exons, or UTRs, and the remaining 10 and 20% in the downstream and intergenic regions, respectively. This distribution is comparable to that found for ChIP-seq performed on the MADS-domain protein SEP3 ((Kaufmann *et al.*, 2009), and Figure 1D) and for other TFs (e.g. REPLUMLESS (RPL), Bencivenga *et al.*, 2016).

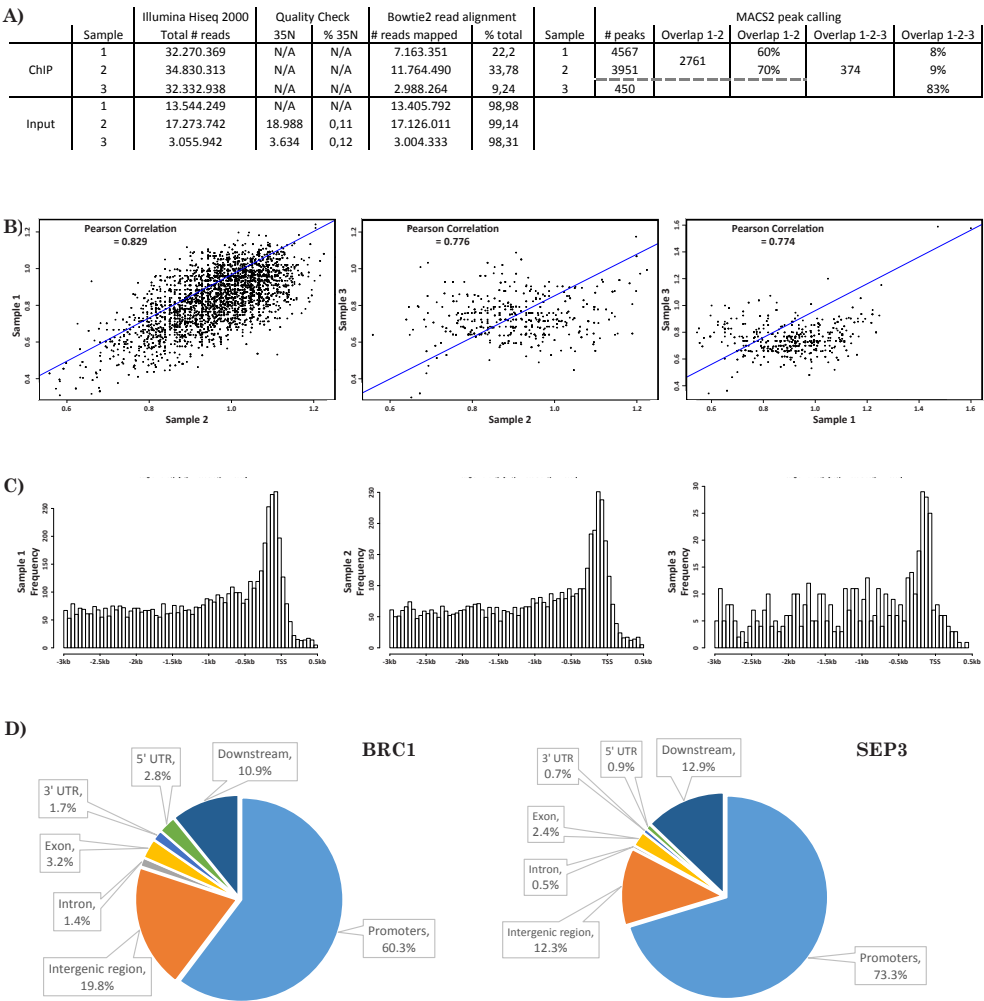


Figure 1. Overview of ChIP-seq data acquisition and analysis

Overview of sequencing information is shown in **(A)**. From left to right: total number of reads with the amount and percentage of failed reads (35N) and the number of reads mapping to the Arabidopsis genome, the number of peaks significantly enriched and the overlapping peaks between samples are shown. Percentage of overlap, as well as the number of overlapping peaks is shown between sample 1 and 2, and sample 1, 2 and 3. Briefly: 2761 peaks overlap between sample 1 and sample 2, which is 60% of total number of peaks in sample 1 and 70% of the peaks in sample 2. Pearson Correlation Coefficients between biological replicates are shown in **(B)**. In **(C)**, read distribution is shown 3kb up- to 500bp downstream of the transcription start site (TSS). Comparing read distributions between SEP3 ChIP-seq (Kaufmann *et al.*, 2009) and the BRC1 ChIP-seq samples in **(D)**.

BRC1 consensus binding motif

The ChIP-seq dataset provided us with an unprecedented amount of data to determine binding specificity of BRC1 and to identify its consensus binding motif. There have been several *in vitro* studies on binding site preferences of TCPs, most of them focussed on class I TCPs; TCP16 and TCP20 (Viola *et al.*, 2012) and TCP11 (Viola *et al.*, 2011). The main class II TCP TF studied in this respect is TCP4 (Viola *et al.*, 2012; Aggarwal *et al.*, 2010). The consensus binding sites that arose from these studies are GTGGGNCC for class I TCPs, whereas class II proteins showed a preference for the sequence GTGGNCCC (Kosugi and Ohashi, 2002; Schommer *et al.*, 2008; Viola *et al.*, 2011). A protein-binding microarray on BRC1 uncovered GGSVCCMM to be its consensus binding site (González-Grandío *et al.*, 2017). Though different, this resembles the earlier found (though not a clear class I or class II) putative TCP binding site.

Motif enrichment analysis on our dataset by MEME identified a motif closely resembling a TCP binding site: GDCCCA, in which D can be an A, G or T (Figure 2A). Recently, a database was published based on DNA affinity purification sequencing (DAP-seq) as a high-throughput TF binding site discovery method (O'Malley *et al.*, 2016). This database provides the opportunity to search among the binding sites of 529 Arabidopsis TFs, including 13 TCPs, both class I and class II. The site that was enriched in all samples in our study (GDCCCA) closely overlaps the binding sites for TCPs in that database. However, a detailed comparison shows that our motif is somewhat shorter than those found by DAP-seq and previously published studies, lacking the GTGG or GTG at the 3' end of the motif (Kosugi and Ohashi, 2002; Schommer *et al.*, 2008; Viola *et al.*, 2011; O'Malley *et al.*, 2016). Another observation is that the A identified at the end of the BRC1-binding site seems to be limited to class I TCPs for the motifs identified by O'Malley *et al.* (2016), whereas BRC1 is a class II TCP.

Motif enrichment

Next, we were interested whether other potential TF binding sites were overrepresented in the BRC1 ChIP-seq peaks. The detailed analysis of peak distribution was used to determine random promoter sequences as the appropriate control for motif enrichment analysis by MEME (Bailey *et al.*, 2009). The motif enrichment analysis was performed on a number of datasets, which were compiled of the extracted sequences under the peaks of sample 1, 2 and 3, respectively, the overlapping peaks in sample 1 and 2, and the restricted subset of overlapping peaks in samples 1, 2 and 3. The sequences under the peaks of the two samples with most peaks (1 and 2) show enrichment for several motifs, most notably BACGTGKC and GDCCCA (Figure 2B). We used the TOMTOM package (Gupta *et al.*, 2007) to compare motifs against a database of known motifs, in our case the O'Malley database (2016). The BACGTGKC closely resembles a G-box (CACGTG) recognized by bHLH and bZIP TFs (Menkens *et al.*, 1995). The latter (GDCCCA) is mainly recognized by TCP TFs, according to the

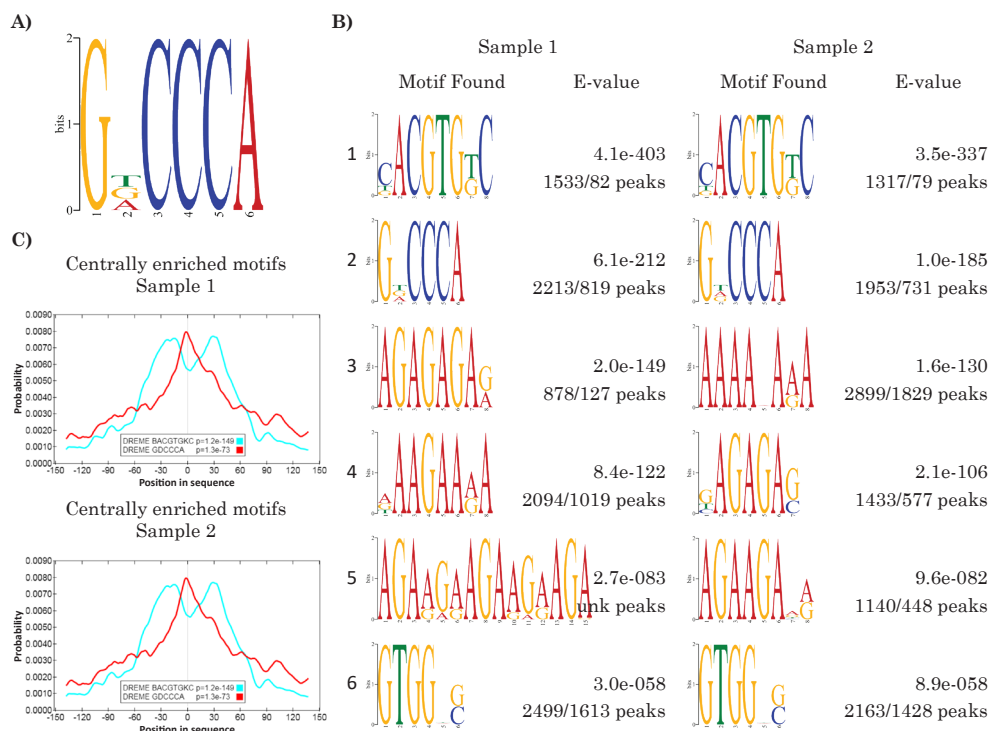


Figure 2. MEME motif enrichment analysis of sequences under peaks of sample 1 and sample 2.

The consensus BRC1 TCP-like binding motif is shown in (A). The top six motifs and their corresponding E-value are shown in (B), ranking from highest significance (peak 1) to the least significant (peak 6). A visualization of peak location relative to the center is shown for the peaks that are found to be centrally enriched in sample 1 and sample 2 (C). In both samples the CACGTG (motif 1; G-box) and GDCCCA (motif 2; TCP-binding motif) were centrally enriched.

O'Malley database (2016). Interestingly, in all samples, the TCP motif was highly centrally enriched, whereas the G-boxes seem to be positioned approximately 30bp to the left or right of the TCP binding site (Figure 2C). The same results were found in a dataset comprising peaks that overlap between sample 1 and sample 2 (Supplemental Figure 1A and 1B). We found that, in both samples, approximately 60% of all peaks contained a TCP-like binding motif versus 50% that contained a G-box (see Supplemental Figure 1C). Although the figure gives the impression that in these cases the TCP binding site is flanked on both sides by a G-box, the majority of the TCP binding sites were accompanied by a single G-box only (1273 instances in sample 1), whereas only incidentally the TCP site was flanked on both sides by a G-box (32 out of the 1305 instances in sample 1).

BRC1 target gene analysis

In order to identify those BRC1-bound loci that also show a direct transcriptional response, gene expression analysis by RNA-seq was done on the same type of material and under the same induction conditions as used for the ChIP-seq experiments. The plants received five hours of estradiol treatment and after sequencing and comparisons, 5529 genes were found to be differentially expressed, of which 1783 were upregulated and 3746 were downregulated. The cut-off for differential expression was determined using a false discovery rate (FDR) value of <0.05 . In addition, we looked at the more strongly differentially expressed genes (strong DEGs) with a $\text{Log}_2(\text{fold change})$ difference of >1 . Using this criterion, we found 1478 downregulated genes and 518 upregulated genes. Gene Ontology (GO)-term analysis on the set of ‘strong’ downregulated DEGs showed overrepresentation of various growth-related terms, including ‘cell wall modification’ (GO:0042545) and ‘cell wall organization’ (GO:0071555). Both processes were not enriched among the upregulated genes. Several hormone stimuli were enriched in both up- and downregulated genes such as the ‘response to jasmonic acid’, ‘auxin’ and ‘salicylic acid stimuli’ (GO:0009753, -0009733 and -0009751 respectively). Uniquely for the upregulated genes were the ‘responses to ABA’ and ‘gibberellin stimuli’ (GO:0009737 and -0009739). These two hormones had their ‘metabolic process’ (ABA, GO:0009687) and ‘signalling pathway’ (gibberellin, GO:0010476) enriched in the set of ‘strong’-upregulated genes. A full list of the observed GO-term enrichment can be found in Supplemental File 1.

Subsequently, we compared genes significantly enriched in the ChIP-seq dataset and differentially expressed in the RNA-seq dataset. Analysis of the overlap between the ChIP-seq and RNA-seq showed approximately 35% of genes enriched in the ChIP-seq dataset to be differentially expressed in the RNA-seq experiment (Supplemental Figure 2C). Initially, we used all differentially expressed genes ($\log(\text{fold}) < 1$ and > 1) for the analysis. Of the BRC1-bound loci in this set around 55-60% are upregulated, whereas 40-45% are downregulated. We labelled these upregulated genes ‘BRC1-activated’ and the downregulated genes ‘BRC1-repressed genes’, respectively (Supplemental File 2). Next, we examined the motif enrichment in the activated and repressed genes, respectively, and found a high overlap. Both the activated and the repressed genes are enriched for the TCP-motif, the G-box as well as the GAGA-repeat (Supplemental Figure 2A and 2B) and no significant activation or repression specific-consensus binding site(s) could be found.

Previous research has shown several gene-regulatory networks to be affected during bud dormancy or, oppositely, bud activation (González-Grandío and Cubas, 2014). We compared these networks with our datasets and noticed that 18% of the bud activation genes were bound by BRC1. Surprisingly, 46% of the bud dormancy genes were directly bound. This suggests a more direct role for BRC1 in the regulation of the bud dormancy genes, among which the aforementioned ABA signalling genes, than in the regulation of the bud activation genes.

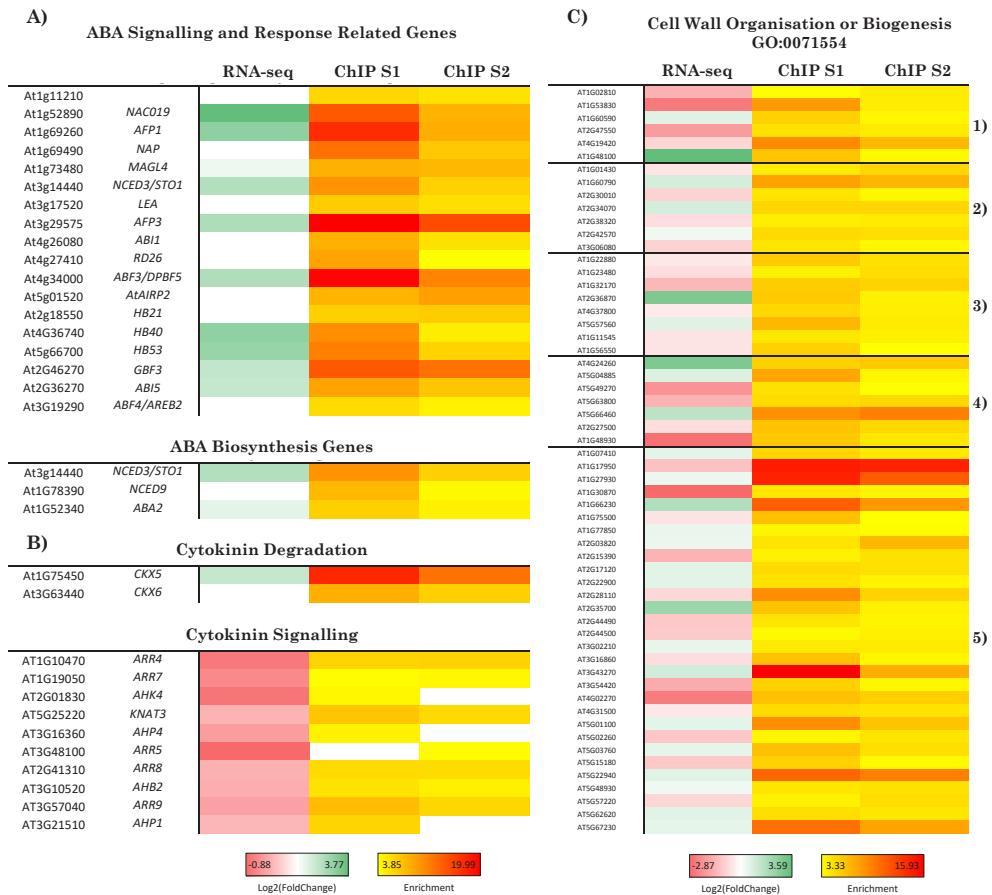


Figure 3. BRC1 regulated genes

ABA signalling and response related genes, some present in the ABA GRN (González-Grandío et al., 2014) and three ABA biosynthesis genes, *NCED3*, *NCED9* and *ABA2* are shown in **(A)**. Genes involved in the degradation and signalling of Cytokinins are shown in **(B)**. Genes differentially regulated upon *BRC1* induction and having the Gene Annotation term ‘Cell Wall Organisation or Biogenesis’ (GO:071554) are shown in **(C)**, subdivided in pectin related genes **(1)**, Trichome Birefringe (TBL) genes **(2)**, xyloglucan- **(3)** and cellulose-related genes **(4)**. Group **(5)** hosts the genes in the enriched GO-terms, which cannot easily be associated to a particular pathway or process. The scale bars show the Log2(FoldChange) for significantly differentially expressed genes in the RNA-seq dataset and the Enrichment relative to the Input sample for significantly enriched peaks in ChIP Sample 1 and Sample 2 (FDR in both cases <0.05).

A GO-term analysis showed that among the BRC1-activated genes, several classes related to abscisic acid (ABA) were enriched (ABA metabolism, cellular response, stimulus), whereas among the BRC1-repressed genes only the term ‘response to ABA stimulus’ was enriched (see Supplemental File 3). The enrichment for ABA-related terms herein is in line with the previously found set of ‘bud-

dormancy genes' in which an ABA gene-regulatory network (GRN) is present (González-Grandío and Cubas, 2014). Recently, BRC1 has been implicated as a regulator of ABA signalling through the regulation of three HD-ZIP-encoding genes (*HB21*, *-40* and *-53*) which, together with BRC1, enhance *NCED3* expression, leading to ABA accumulation (González-Grandío *et al.*, 2017). These genes (genes in the ABA GRN, and the HBs) seem to be directly activated by BRC1 (Figure 3A). Next to this, several other ABA related genes were regulated, such as *ABA INSENSITIVE 5 (ABI5)*, one of the master regulators in ABA signalling (Finkelstein, 2000) and *G-BOX BINDING FACTOR 3 (GBF3)*. Also two ABA biosynthesis genes are bound by BRC1: *ABA-DEFICIENT 2 (ABA2)* and *9-CIS-EPOXYCAROTENOID DIOXYGENASE 9 (NCED9)* (Figure 3A). The latter was also upregulated upon BRC1 induction, which, together with the direct binding and upregulation of *NCED3*, indicates a direct regulation of ABA biosynthesis by BRC1, besides the indirect regulation via the HD-ZIP TFs. A closer look at the BRC1-repressed genes revealed several GO-terms related to cytokinin ('cytokinin mediated signalling pathway', 'cellular response to cytokinin stimulus' and 'response to cytokinin stimulus'). This reduced cytokinin (CK) response is in line with the supposed growth-promoting role of this hormone in branching (Domagalska and Leyser, 2011), and several genes involved in CK signalling are found to be repressed upon BRC1 induction (Figure 3B).

Furthermore, the GO-term enrichment analysis revealed enrichment for Cell Wall Organisation and Biogenesis (GO:0071554) (Supplemental File 3). The data shows differential regulation of genes involved in the deposition and biosynthesis of secondary wall cellulose as well as cell wall modification enzymes and several cellulases and cellulose synthase genes (Figure 3C).

Discussion

BRC1 binds a class I-like consensus binding site, GDCCCA, *in vivo*

There have been a number of studies on TCPs and their preferred binding sites. These are all based on *in vitro* experiments and used either monomers or homodimers of TCP proteins. These studies revealed that the consensus-binding site of class I TCPs can be defined by the sequence GTGGGNCC, whereas class II proteins show a preference for the sequence GTGGNCCC (Kosugi and Ohashi, 2002; Schommer *et al.*, 2008; Viola *et al.*, 2011). This difference in binding preference was explained by the amino-acid residue present at position 11 of the basic region (Gly) of the class I TCP domain or the equivalent residue 15 (Asp) of the class II domain (Viola *et al.*, 2012). Intriguingly, class I TCPs can bind class II binding sites and vice versa, and some degree of flexibility for TCP4 (a class II TCP) to bind a class I motif *in vitro* was reported (Schommer *et al.*, 2008). The recently published database on DNA affinity purification sequencing (DAP-seq) provides information on 13 TCP consensus binding sites (O'Malley *et al.*, 2016). Three of these are class II TCPs (*TCP3*, *TCP13* and *TCP24*) that show a

consensus sequence of GTGGDCCC, while eight are class I TCPs and show more variation, however a consensus GGDCCCAC could be extracted. However, according to this database, TCP1, a class II TCP, seems to prefer a class I binding site, although previous EMSA experiments have shown that TCP1 binds a class II-like binding site GGNCCC (Gao *et al.*, 2015). TCP16 is a class I TCP that has previously been shown to bind Class II motifs (Viola *et al.*, 2012), which is supported by the aforementioned database.

In our comprehensive *in vivo* ChIP-seq experiments we found a strong enrichment for the motif GDCCCA for the class II TCP protein BRC1; in which D can be an A, G or T (Figure 2A). This motif, although similar to the motifs shown above, is yet another TCP-like consensus binding site, and slightly different from the previously identified BRC1 binding motif GGSVCCMM (González-Grandío *et al.*, 2017). Surprisingly though, the GDCCCA motif is more alike the definition of the above indicated class I *cis*-element, whereas BRC1 is a class II TCP protein. This result, in combination with the knowledge that the class II protein TCP1 can bind a class I binding site and that the class I protein TCP16 has the ability to bind a consensus class II binding site reveals that we have to rethink the definition of specific class I and class II TCP consensus binding sites. It has to be noted that in all *in vitro* binding assays as described above single TCP proteins were used. It is known from e.g. MADS-domain proteins that the composition of heterodimeric TF complexes affects the specificity of DNA binding (Smaczniak *et al.*, 2017). Also in the case of TCP TF complexes the presence of more TCP molecules, and other TFs, like bZIP or bHLH TFs, could influence the binding specificity by cooperativity or competition (reviewed in Bemer *et al.*, 2017). Therefore and also based on the contradicting examples, it seems that no strict division in classes of TCP binding sites can be made. This observation backs up the hypothesis that TCP from both classes can regulate the same process antagonistically by competing for the same or closely related binding sites, as TCP4 and TCP20 in their regulation of JA biosynthesis (Danisman *et al.*, 2012). Even more so, the antagonistic regulation might be irrespective of their classes, as TCPs from the same class can bind different binding sites.

BRC1 as downstream target of sugar signalling during bud dormancy

Combining the data from transcriptomic and binding site analysis enabled us to thoroughly investigate the targets of BRC1 and its functioning in bud dormancy. A number of studies on the transcriptional response in dormant buds show patterns resembling the Low Energy Syndrome (LES) (reviewed by Martín-Fontecha *et al.*, (2018)). The LES functions as retainer of carbon (C) to maintain essential processes by inhibiting growth (Tomé *et al.*, 2014). A well-known integrator of the LES is the SUCROSE-NON-FERMENTING-1-RELATED PORTEIN KINASE (SnRK1) and it was shown to physically interact with TCP3, TCP13 (both class II TCPs) and HB21 (Nietzsche *et al.*,

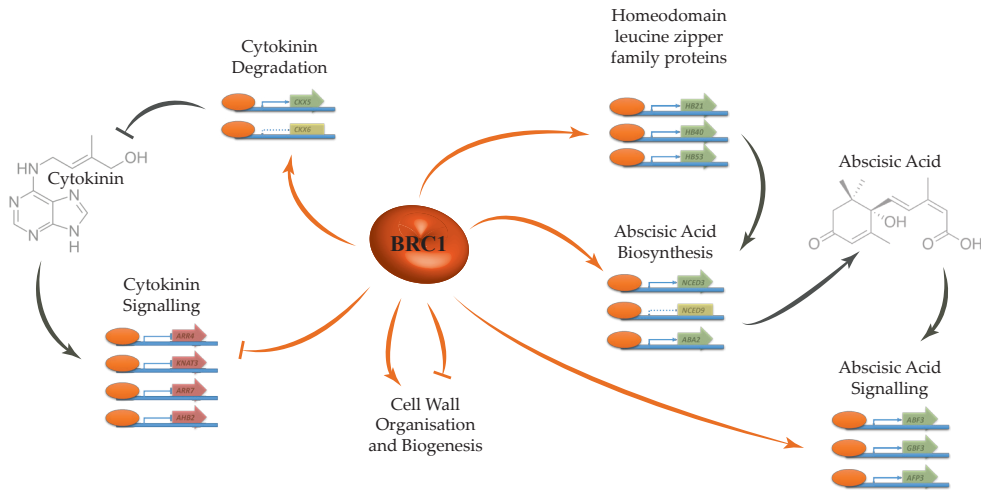


Figure 4. BRC1 regulatory processes, ensuring axillary bud dormancy

This model shows the direct regulation of genes by BRC1 (orange arrows). Regulatory processes as found in literature are shown by grey lines. Repression and activation are shown by bar and arrow, respectively. Amongst every process (e.g. Cytokinin Degradation) the individual genes are visualised, green arrows indicate activation, a yellow square means that on transcriptional level nothing happens, red arrows indicate a reduction in expression upon *BRC1* induction.

2016). This could indicate that that BRC1, possibly among other TCPs, can be regulated by SnRK1, although further research is required to investigate this. Next to this, sugar availability controls bud outgrowth in several species, such as pea (*Pisum sativum*; Mason *et al.*, 2014), rose (*Rosa hybrida*; Barbier *et al.*, 2015) and sorghum (*Sorghum bicolor*; Kebrom *et al.*, 2010). However, the lack of enriched Gene Ontology terms concerning glucose, sucrose or fructose, let alone their differentially regulated biosynthesis and signalling genes, seems to indicate that sugar availability isn't controlled directly by *BRC1*. This strengthens the hypothesis that sugars act upstream of *BRC1* via SnRK1 and other regulatory molecules (Jossier *et al.*, 2009).

An interesting feedback mechanism could take place as ABA is thought to enhance SnRK1 activity through antagonistic action on PP2CA phosphatases that interact with the SnRK1 catalytic subunit causing its inactivation (Rodrigues *et al.*, 2013). Next to this, the ABA signal transduction peptide ABI1 inhibits SnRK1 function (Rodrigues *et al.*, 2013) and is bound by BRC1 in our experiment. As previously suggested, BRC1 enhances ABA biosynthesis (González-Grandío *et al.*, 2017), closing the circle.

Co-regulation networks

A sequence motif recurring in all ChIP-seq enrichment analyses (Figure 2B) is a GAGA-repeat, which is the consensus binding site supposed to be bound by the plant specific TF family of BASIC PENTACYSTEINE proteins (Meister *et al.*, 2004). This group of TFs is thought to be involved in plant development (Monfared *et al.*, 2011), meristem control (Simonini *et al.*, 2012a), and recently, a link with ABA signalling was found (Mu *et al.*, 2017). Hence, this is a promising lead to decipher the regulatory mechanism of BRC1, in which this TCP protein acts in concert with BPC proteins. Interestingly, both sample 1 and 2 show binding of BRC1 in the promoter region of BPC2 which suggests a more intricate regulatory mechanism including a feedforward loop, though no differential expression was observed for *BPC2* upon BRC1 induction under our conditions.

The presence of CACGTG motifs accompanying the centrally enriched consensus TCP-like binding site suggests a form of co-regulation of these specific set of targets by BRC1 and bHLH or bZIP TFs. Both the bHLH and bZIP groups of TFs are rather large (162 and 111 members respectively, (Riechmann *et al.*, 2000; Feller *et al.*, 2011)) which complicates speculating on their regulatory role together with BRC1.

No interactions between BPCs, bZIPs and bHLH proteins have been reported yet. BPCs have been shown to interact with MADS-domain proteins to regulate their target genes by mediating DNA binding (Simonini *et al.*, 2012b). This could indicate more elaborate protein interaction complexes and would require a more detailed and comprehensive approach.

A function for BRC1 in cell cycle regulation?

Due to the profound effect of *BRC1* mutations on plant architecture, one of the presumed functions of BRC1 is direct inhibition of the cell cycle machinery. In this research however, we find no strong evidence to support this hypothesis. There are only two *CYCLIN-DEPENDENT KINASES* (*CDKs*) identified to be bound by BRC1, *CDKD1;1* and *CDKB1;2*, but they are both not differentially expressed upon BRC1 induction. This does not exclude the option that cell cycle is regulated via these few targets, but BRC1 seems to be at least not regulating this process ‘en masse’. However, we do find suggestions that BRC1 could directly regulate components of the cell wall. When looking at the Gene Ontology Enrichment analysis, Cell Wall Organisation and Biogenesis (GO:0071554) are enriched (Supplemental File 3). A closer look shows differential regulation of several members of the *TRICHOME BIREFRINGE-LIKE* (*TBL*) gene family, involved in the deposition and biosynthesis of secondary wall cellulose (Bischoff *et al.*, 2010) and Pectin Methylesterase (*PMEs*), which are important cell wall modification enzymes (Micheli, 2001), as well as several cellulases and cellulose synthase genes (Figure 3C). When investigating the differential expression, it is evident that both activated and repressed genes are among the aforementioned groups. This implies an intricate

network of growth regulation by BRC1.

Research in poplar has shown that axillary buds are separated from the rest of the plant by a physical ‘border’ that blocks cell-to-cell signalling (Rinne *et al.*, 2001). During the development of an axillary meristem, followed by axillary bud formation, cell-to-cell signalling networks are positioned to support pattern formation; plasmodesmata are the elements that connect the cells in the axillary meristem and that act to transfer signalling molecules. At later stages of axillary bud development, these networks are shut down by the formation of 1,3- β -D-glucan containing sphincters on all plasmodesmata, creating a physical border (Rinne *et al.*, 2016). As a result, cell-to-cell communication is blocked and the axillary bud enters a stage of dormancy, similar to that of the shoot apical meristem of woody species during winter (Paul *et al.*, 2014).

This border formation might require structural changes rather than an increase of cells in order to organize necessary components and change positioning of cell walls. This intricate regulation would explain the observation that is shown in figure 3C; genes involved in cell wall organisation or biogenesis are both activated and repressed. It would be worth a thorough look into possible border formation in developing axillary buds in Arabidopsis. Vice versa, our findings offer a potential explanation for this phenomena in poplar, suggesting that through the action and function of *BRC1* orthologues in this species the plasmodesmata sphincters are formed.

The tight grip of BRC1 on hormonal biosynthesis and signalling

We confirmed a role for BRC1 in ABA signalling through binding the promoter of three Homeodomain leucine zipper protein (HD-ZIP)-encoding genes: *HOMEODOMAIN PROTEIN 21* (*HB21*), *HB40* and *HB53*, as described by González-Grandío *et al.* (2017). In addition, we have uncovered a more elaborate and direct regulatory role of BRC1, as it directly regulates ABA biosynthesis by binding loci of several ABA biosynthesis genes. Next to binding the promoter of *NCED3*, *NCED9* and *ABA2*, these genes are also upregulated after BRC1 induction (Figure 3A), adding additional proof of direct regulation. ABA has long been implicated in the control of axillary bud outgrowth, during for example low R:FR conditions (Reddy *et al.*, 2013) and application of ABA was shown to inhibit branching (Chatfield *et al.*, 2000; Holalu and Finlayson, 2017). A proposed mode of action of ABA is the direct regulation of the cell cycle through for instance blocking the G1 to S transition in algae (Kobayashi *et al.*, 2016) and repression of cell cycle genes in dormant buds in grapevine (*Vitis vinifera*, Vergara *et al.*, 2017). Adding another layer of regulation to ensure bud dormancy, BRC1 seems to repress CK levels through the binding of two *CYTOKININ OXIDASE* (CK degrading) enzymes. No CK biosynthesis genes seem to be targeted, indicating a role for BRC1 more downstream in the CK pathway. This is confirmed by the downregulation of downstream CK signalling genes (Figure 3B) and is all in accordance with the role of CK as promoter of axillary bud outgrowth (Dun *et al.*, 2012). More research is however

required to confirm this, for example to see whether BRC1 induction leads to a reduction in CK levels.

The role for BRC1 in enhancing ABA levels, thereby ensuring bud dormancy, had been shown previously (González-Grandío *et al.*, 2017). However, in this study we have shown a more direct method of regulation by activating ABA biosynthesis directly, as well as a potential role for BRC1 in repressing CK levels. Furthermore, we show a possible role for BRC1 in ensuring structural changes in the dormant bud, as opposed to the direct regulation of numerous cell-cycle genes. Combining these functions for BRC1 into a model for its molecular mode of action (see figure 4) inevitably leads to a main function of BRC1 In the inhibition of bud outgrowth (Aguilar-Martínez *et al.*, 2007; Finlayson, 2007).

Materials and methods

Plant materials and growth condition

Wild-type *Arabidopsis thaliana* plants were of the Columbia-0 (Col-0) ecotype. The *brc1-2* mutant was described before (Aguilar-Martínez *et al.*, 2007) and the *GFP:BRC1^{ind}* lines have been generated previously (González-Grandío *et al.*, 2017). All lines were grown on 1/2MS medium 1% (w/v) agar plates under long day conditions (16/8 light/dark cycle) at 21°C.

RNA-seq and ChIP-seq material collection

For the RNA-seq experiment, plants of *brc1-2* (control) and *GFP:BRC1^{ind}* lines were grown on plate. Ten-day old seedlings were induced with 5mL of 10µM estradiol per plate. After an induction period of five hours, 1 g of tissue was harvested for each of the three biological replicates. Total RNA was isolated using the InviTrap® Spin Plant RNA Mini Kit according to the manufacturer's protocol. TURBO™ DNase was used to clean the RNA samples from DNA. Library preparation for whole genome RNA sequencing was done using the Illumina Truseq Library Preparation Kit. Library quality was evaluated using a Bioanalyzer and an RNA Nano 6000 kit (Agilent). RNA concentrations were determined using the Xpose 'DSCVRY' (Trinean). The libraries were then sequenced on the Illumina Hi-Seq 2500.

For the ChIP-seq experiment, plants of *GFP:BRC1^{ind}* lines were grown on plate. Ten-day old seedlings were induced with 5mL of 10µM estradiol per plate. After an induction period of five hours, 1.5g of tissue was collected per sample. ChIP was performed as described (Mourik *et al.*, 2015), using µMACS Anti-GFP beads (Miltenyi). Input DNA was used as control, which is isolated from the sonicated chromatin prior to immunoprecipitation.

Differential gene expression and gene ontology enrichment analyses

Libraries of three biological replicates were sequenced individually and analysed using the Bowtie–Tophat–Cuffdiff (BTC) pipeline (Trapnell *et al.*, 2012). Differential gene expression was determined for all estradiol induced *GFP:BRC1^{ind}* samples, using induced *brc1-2* samples as control. The cut-off was set at a false-discovery rate (FDR) <0.05 in all analyses performed. The RNA-seq data is made available via NCBI and can be accessed through GEO accession number GSE-XXXXX. The BINGO 3.03 plug-in (Maere *et al.*, 2005), implemented in CYTO-SCAPE 2.81 (Shannon *et al.*, 2003), was used to determine and visualize the Gene Ontology (GO)-enrichment categorization. A hypergeometric distribution statistical testing method was applied to determine the enriched genes and the Benjamini and Hochberg correction was performed in order to limit the number of false positives (FDR<0.05).

ChIP-seq data analysis

Libraries of three biological replicates of both the ChIP and Input samples were sequenced after which Bowtie2 was used to map the reads to the Arabidopsis genome (Langmead and Salzberg, 2012). MACS2 was used for peak calling (the statistical detection of protein binding sites in the DNA) (Zhang *et al.*, 2008) using the Input samples as control. The function Distance2Genes, part of the R-package ‘CSAR’, was used to determine the nearest gene (Muñoz *et al.*, 2011). These nearest genes are then presented in a list of candidate target genes (Mourik *et al.*, 2015) for further analysis. Reproducibility between two replicates was determined by Pearson correlation coefficients (PCC). The three replicates show Pearson correlation between 0.774 and 0.829 in the pairwise comparisons, which is relatively high (Bardet *et al.*, 2012).

The comparison of read distribution of our ChIP-seq dataset and that of SEP3 (Kaufmann *et al.*, 2009) was done by the R-package ChIPpeakAnno: ‘assignChromosomeRegion’. As a cutoff 1kb of promoter region with an immediate cutoff of 0.5kb was used.

All three biological replicates were initially analysed separately. To confirm the high rate of reproducibility the overlap between the two highest enriched samples and the overlap of all three samples was analysed.

Motif enrichment analysis

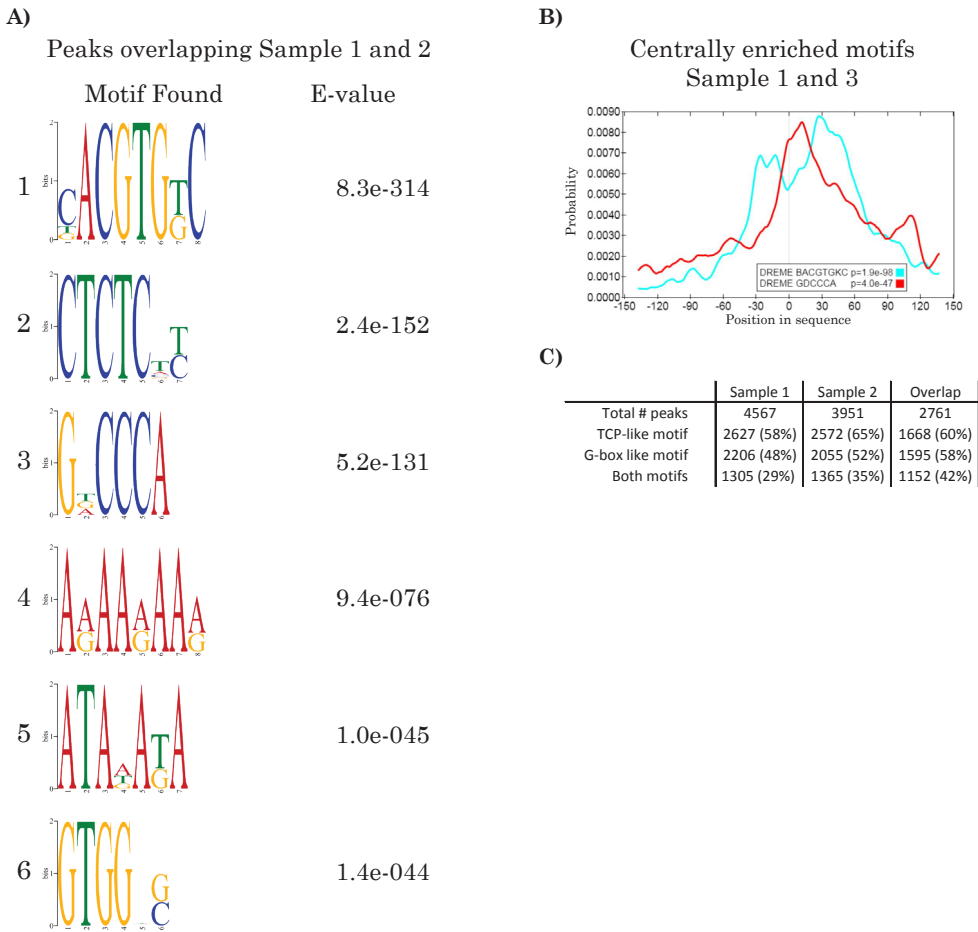
Motif discovery was carried out using MEME-ChIP (Machanick and Bailey, 2011). This program consists of several sub-programs that each perform a specific analysis. In the present study MEME and CentriMO were used. MEME (Bailey and Elkan, 1994) looks for overrepresented motifs in a set of sequences compared to a background model of nucleotide frequencies. The background model was generated using fasta-get-markov for the MEME suite, using a second order Markov model, and

a set of 207 randomly selected sequences from *Arabidopsis* promoters as input. CentriMO (Bailey and MacHanick, 2012) is used to test if the motifs found are centrally enriched. In the present study, motifs were investigated if they were in the top six motifs as defined by MEME-ChIP. Default settings for MEME were used, with the following exceptions: the setting `meme-mod-anr` was used, which assumes zero, one or multiple motif occurrences per sequence. Minimum and maximum width for the motifs were set to 4- and 15bp, respectively.

Motif comparison was done using TOMTOM (Gupta *et al.*, 2007), comparing the motifs found by MEME against a database of known motifs (O'Malley *et al.*, 2016). The calculated similarity is an indication that a particular motif is bound by a certain TF.

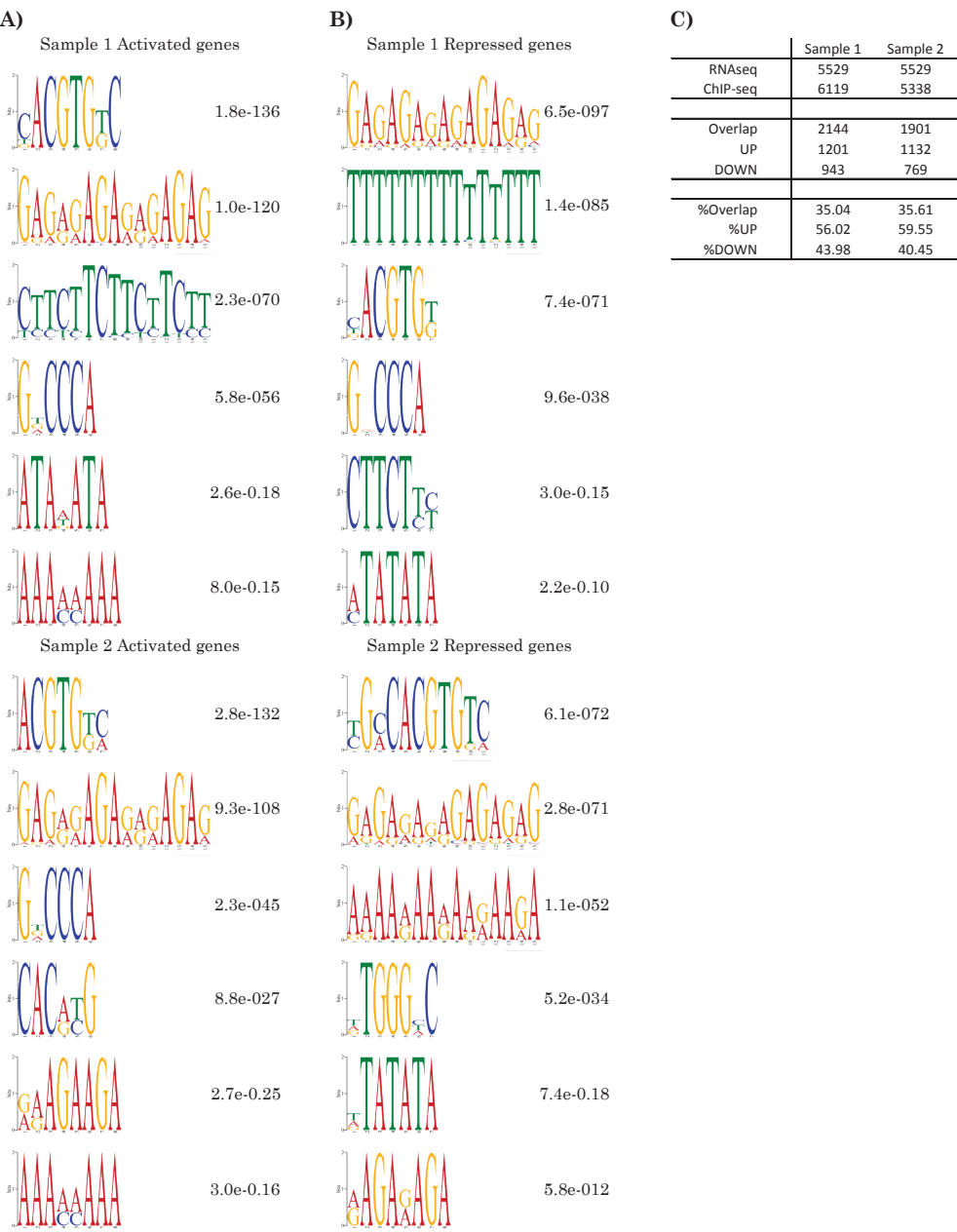
Acknowledgements

The research is supported by a grant from the Dutch Scientific Organization (NWO); (NWO-JSTP grant 833.13.008).



Supplemental Figure 1. MEME motif enrichment analysis of sequences under overlapping peaks in the two highest enriched samples, 1 and 2.

The top six motifs and their corresponding E-value are shown in **(A)**, ranking from highest significance (motif 1) to the least significant (motif 6). A visualization of motif location relative to the center is shown for the peaks that are found to be centrally enriched in **(B)**. In the overlapping peaks, both the CACGTG (G-box) and GCCCC (TCP-binding motif) were centrally enriched. An overview of G-box and TCP-motifs in sample 1, sample 2 and the overlapping peaks between them is shown in **(C)** which shows a relatively high co-occurrence of both motifs.



Supplemental Figure 2. MEME analysis on genes differentially expressed and enriched in ChIP-seq. Enriched motifs in upregulated genes (A) versus downregulated genes (B) in both sample 1 and sample 2. An overview of the number of overlapping genes is shown in (C).



Chapter 5:

Interactions between the organ identity specifying MADS domain proteins and growth regulatory TCP proteins in Arabidopsis flowers

Sam W. van Es
Garance Pontier
Sylvia R. Silveira
Froukje van der Wal
Sjef Boeren
Gerco C. Angenent
Richard G.H. Immink

“As far as playing jazz, no other art form, other
than conversation, can give the satisfaction of
spontaneous interaction.”

Stan Getz

Abstract

Floral organ identity specification and growth are two very distinct but intertwined processes. In this study we describe the physical interaction between the floral organ identity specifying MADS domain protein APETALA1 (AP1) and a member of the TCP transcription factor (TF) family, TCP5, previously described to be involved in petal growth. This interaction and other potentially interesting protein-interactions were identified by immunoprecipitation-based native protein complex isolation, using TCP5 as bait and followed by liquid chromatography-tandem MS (LC-MS/MS). Yeast two hybrid assays (Y2H) confirmed the identified AP1-TCP5 interaction. To determine the regions within the respective proteins and the exact amino acids vital for such an interaction, we created libraries of randomly mutagenized alleles for both *AP1* and *TCP5*, by error prone PCR. Subsequently, the Y2H assay was performed to find 'edgetic' alleles in which only the interaction of AP1-TCP5 was disturbed, while the well-known heterodimeric interactions of AP1 with other MADS domain proteins were maintained. We show by screening six mutated AP1 alleles the potential of this approach. Finally, we describe the possibilities of this technique and we provide suggestions for several strategies to scale-up this assay and to continue it by further functional characterisation *in planta*.

Introduction

One of the most quintessential characteristics of plants is their versatility in shape. Two genetically identical plants can show differences in leaf size and shape or can have different branching patterns, depending on growth conditions such as temperature (Hatfield and Prueger, 2015), light intensity (Shirley, 1929) and planting density (Casal *et al.*, 1986). Interestingly, it appears that flowers and their floral organs have instead a more predetermined shape and size, which are controlled by internal developmental cues, regardless of the environment (Weiss *et al.*, 2005).

The final appearance of a flower is determined by several processes, of which the specification of floral organ identity and the following growth regulation and cell differentiation contribute most. The basic body plan of a flower consists of concentric whorls of sepals, petals, stamens and carpels, whose identity is determined by the combinatorial action of organ-identity genes, following the ABCE-model of flower development (Coen and Meyerowitz, 1991; Krizek and Fletcher, 2005). The distinct organ identities are specified by a unique combination of homeotic 'A', 'B', 'C' and 'E' gene activities within each whorl (Causier *et al.*, 2010), where most ABCE genes encode members of the MADS domain class of transcription factors (TFs).

The characteristics and biological processes determining the final organ size and shape differ for every type of floral organ. In the case of sepals, shape and size are influenced by endoreduplication and the formation of giant cells scattered over this organ (Roeder *et al.*, 2012). Petal morphology is regulated differently; their length is determined by cell elongation in the basal part, whereas the rate and direction of cell division determine the shape and size of the distal region (the blade) of the petal, which contains in *Arabidopsis* small and round conical cells (Hase *et al.*, 2005; Irish, 2008).

Determining floral organ identity and the subsequent development and growth of the organ are two intertwined processes. It is known for instance that B-type floral organ identity mutants (e.g. the *pistillata* (*pi*) mutant, containing sepals instead of petals) have second whorl organs with the size and identity of a sepal (Bowman *et al.*, 1989). Another well-known example is the *agamous* (*ag*) mutant, which produces petals instead of stamens. Again, these petals maintain a 'normal' petal size despite the fact that they develop in a different flower whorl (Bowman *et al.*, 1989). These examples strengthen the hypothesis that floral organ size is tightly linked to organ identity. Furthermore, initial meristem size does not seem to affect the final organ size. An often used example in this case is the *clavata* (*clv*) mutant, which consists of a bigger floral meristem producing a higher carpel number, however the individual carpels maintain their 'original' size (Crone and Lord, 1993). Another example of a possible link between floral organ identity genes and growth comes from complementation experiments with epidermal driven expression of several MADS box genes.

Expression of the B-type MADS box gene *APETALA 3* (*AP3*) in *ap3* mutants under the control of the epidermal layer-specific *AtML1* promoter led to the complementation of organ size and shape, while organ identity was only partly reverted to wild type (Urbanus et al., 2010). Complementation of size and shape in this example may indicate a late function for MADS domain proteins in determining organ size and shape, besides their primary function as organ primordia identity specifying factors. In this light, an interesting observation is the fact that some of the organ identity genes continue to be expressed throughout flower development, even though their function as identity specifying proteins takes place very early after the formation of the flower meristem (Alvarez-Buylla et al., 2010). For example, expression of *API* is first observed in emerging floral primordia where it specifies the floral meristem itself (Ferrández et al., 2000). Hereafter *API* is involved in the specification of sepals and petals (Mandel et al., 1992). However, even at later stages of flower development, expression is maintained in the outer two whorls (Mandel et al., 1992; Gustafson-Brown et al., 1994). This has led to the hypothesis that the two processes, organ identity specification and growth regulation, is tightly linked by interactions between MADS domain proteins and proteins involved in flower organ growth and development (Dornelas et al., 2011).

The link between the two processes of growth and identity can be established through several processes. For example by transcriptional regulation of growth regulatory genes by MADS domain proteins, or e.g. through the combinatorial activity of MADS domain proteins and growth regulatory proteins in a complex, regulating downstream targets.

Some of the key regulatory genes that control petal growth and development in Arabidopsis have previously been identified and are of interest in relation to the previously raised hypothesis. One such organ growth regulator is *JAGGED* (*JAG*), which has been shown to suppress premature cell-cycle arrest in the distal part of an Arabidopsis petal (Dinneny et al., 2004; Schiessl et al., 2014). Furthermore, *RABBIT EARS* (*RBE*) is expressed in petal primordia, where it ensures cell proliferation in petal precursor cells (Takeda et al., 2004). Several other genes have been identified, including members of the *TEOSYNTE BRANCHED/CYCLOIDEA/PROLIFERATING CELL FACTOR* (*TCP*) transcription factor family, of which specific members have been shown to act downstream of *JAG* (Schiessl et al., 2014) and *RBE* (Huang and Irish, 2015). For one specific member of this family, *TCP5*, we have recently described a role of *TCP5* in petal development (van Es et al., 2018).

Previous research has shown a possible regulatory link between *TCPs* and ABC-class MADS domain proteins, and several *TCP* genes were identified as possible direct targets of *API* (Wellmer et al., 2006) and *SEP3* (Kaufmann et al., 2009). Furthermore, coexpression analyses revealed several *TCP* genes to be highly coexpressed with *API* (Wellmer et al., 2006). Perhaps the most compelling argument for a combinatorial role of MADS and *TCP* TFs *in vivo* was put forward by Kaufmann et al. (2009), who showed overrepresentation of a consensus *TCP* binding site next to the MADS-specific CArG-box in

a genome-wide SEP3 target gene analysis. The latter results indicate a possible regulatory role for a MADS-TCP complex, although independent regulation by TCPs or MADS domain proteins binding in close vicinity to each other in the regulatory regions of their target genes is still an alternative.

In this study, we describe the identification of a TCP5-AP1 protein interaction by immunoprecipitation-based native protein complex isolation from inflorescence and young floral buds, followed by liquid chromatography-tandem MS (LC-MS/MS) and confirmed by reciprocal Y2H assays. We investigated the molecular determinants essential for this interaction, and studied a possible biological function of the observed MADS-TCP complex.

Loss-of-function mutants of the floral organ identity genes result in identity changes at the beginning of organ development, masking a possible role of the identity genes at later developmental stages and therefore complicating functional analyses when *TCP* genes become active (Dornelas *et al.*, 2011). Consequently, genetic crosses of full knockout MADS and TCP mutants are ineffective in characterizing the possible biological function of such an interaction. We therefore intended to make use of so-called ‘edgetic’ alleles; alleles that lose interaction with a specific partner alone, rather than losing all or most of their interaction partners (Dreze *et al.*, 2009). By characterising the edgetic alleles for AP1 and TCP5, the potential function of their specific interaction could be evaluated *in vivo* by complementation of a full knockout mutant with such an edgetic allele.

We used a method in which a library of random mutations was produced, in the open reading frame (ORF) of both *AP1* and *TCP5*, by error-prone PCR (Gray *et al.*, 2007). The encoded proteins were eventually tested for interaction capacities by Y2H. The use of a Y2H assay enabled identification of edgetic alleles. When the library of mutated ORFs is big enough, it also allows for the identification of mutations causing a loss of interaction, as well as obtaining information on the regions and specific protein domains that are essential for the interaction with particular proteins. Due to time constraints we didn’t manage to perform the large-scale screen, but preliminary screenings showed that several point mutations in AP1 caused a loss of interaction with TCP5 and/or with other known-interactors.

Results

TCP5 in complex with floral organ identity MADS proteins

To test for interaction partners of TCP proteins in *Arabidopsis* inflorescences, we used plant lines expressing a TCP5 genomic construct including its native promoter linked to GFP as a C-terminal fusion (gTCP5-GFP) (van Es *et al.*, 2018). We used the native promoter of *TCP5*, transcriptionally fused to *GFP* (pTCP5:GFP), as negative control. Protein complexes were isolated by immunoprecipitation (IP) using anti-GFP antibodies and characterized by LC-MS/MS, followed by label-free protein

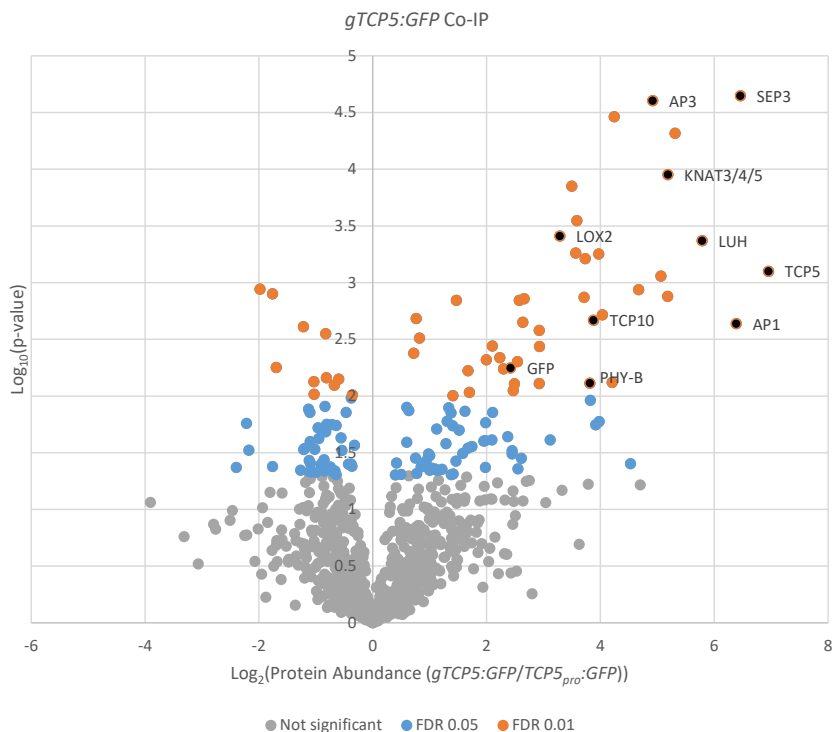


Figure 1. In planta TCP5 protein interaction profile in Arabidopsis inflorescences.

Graph represents the normalized protein abundance ratio between gTCP5:GFP ($TCP5_{pro}:TCP5:GFP$) and the TCP5pro:GFP control plotted against their significance. Significant protein abundance differences between sample and control at FDR < 0.01 (orange) or FDR < 0.05 (blue). Grey circles indicate non-significant hits. Several proteins are highlighted by label and a black dot. For a full list of potential TCP5 interaction partners, see Supplemental File 1.

quantification analysis (Smaczniak *et al.*, 2012a,b). The use of pTCP5:GFP as negative control enabled us to detect and remove false positives from the IP done on gTCP5:GFP. Comparing relative protein abundance between the control and TCP5 sample allowed us to identify enriched proteins, which represent potential direct TCP5 interactors and protein complex partners (Figure 1). Striking was the finding of several MADS domain proteins as putative interaction partners of TCP5. The floral MADS domain proteins APETALA1 (AP1), APETALA3 (AP3) and SEPALLATA3 (SEP3) were identified. Next to this, TCP5 seems to interact with TCP10, a member of the JAW-clade of TCP TFs, and LEUNIG-HOMOLOG (LUH), KNOTTED-LIKE 3 (KNAT3) and PHYTOCHROME B were highly abundant as possible interaction partners of TCP5.

Growth is thought to be regulated, at least partly, from the epidermal L1 layer (Savaldi-Goldstein *et al.*, 2007). We used a previously published construct (van Es *et al.*, 2018) where TCP5 was expressed



Figure 2. Yeast-two-Hybrid results of the AP1 vs TCP screen and TCP5 vs MADS screen.

Schematic overview of the interactions found in a targeted yeast-two-hybrid assay, in which 19 out of 24 Arabidopsis TCP proteins and 109 Arabidopsis MADS domain proteins were included. Interactions are indicated with grey lines, red indicates TCP proteins, green the MADS domain proteins. Note the presence of the full JAW-D clade of TCP TFs. Due to their high level of autoactivation, TCP8, -12, -14, -20, and -22 were not tested in this screen.

from the epidermis-specific *AtML1* promoter and fused to a GFP-tag for the identification of epidermal specific interaction partners. Confocal microscopy analyses showed that in these transgenic plants TCP5-GFP signal was uniquely present in the epidermal layer. We found a large overlap between proteins found with this specific immunoprecipitation assay and the proteins identified in the previous IP for gTCP5-GFP (Supplemental Figure 1). Despite the fact that no precise quantification was done (i.e. comparing exact protein abundance between experiments), the number of peptides identified in both lists appeared to be rather high (104 of the 143 significantly enriched proteins were overlapping). Especially when focussing on the proteins highest enriched in both samples the overlap is striking (Supplemental Figure 1A and 1B). Note for example the presence of AP1, AP3 and SEP3, similar to the IP on gTCP5-GFP, as well as LUH, LYPOXIGENASE2 (LOX2) and PHYTOCHROME B (PHY-B).

Based on the outcomes of these native TCP5 protein complex isolations, we decided to use a targeted yeast-two-hybrid (Y2H) assay to test the interaction of TCP5 with all 109 MADS domain proteins (Figure 2). In this experiment the floral MADS domain proteins AP1 and SEP4 were identified as TCP5 partners, as well as several others, for example AGL12/XAL1, a MADS domain protein preferentially expressed in roots but also implicated in flowering (Tapia-Lopez *et al.*, 2008). The interaction of AP1 with several TCP proteins, among which TCP5, was confirmed by a reciprocal Y2H experiment (Figure 2). Interesting to observe is the presence of all members of the JAW-D clade as interaction partners of AP1, which have previously also been found as specific interactors of TCP5 in a Y2H assay (Danisman *et al.*, 2013). TCP5 is known to be closely related to TCP13 and TCP17

(Efroni et al., 2008; Huang and Irish, 2015, van Es et al., 2018), but surprisingly, these are not found to interact with AP1 in the Y2H assays.

The reason for not retrieving all the IP-identified potential TCP5-MADS domain protein partners by Y2H might be that some of these interactions are indirect and bridged by other MADS domain proteins. AP3 and SEP3 for instance are found in the IP, which could potentially be due to the fact that these MADS domain proteins form a higher order complex with AP1 and PI (Theissen and Saedler, 2001).

Mutant allele library creation for AP1 and TCP5 full length alleles

We focussed on the AP1-TCP5 interaction and aimed to identify regions of specific importance for this interaction in both the *AP1* and *TCP5* coding regions. We would like to understand the role of this AP1-TCP5 interaction during floral organ development and particularly during petal development where both genes are highly expressed. As mentioned earlier, full knockout alleles of *AP1* have a rather strong phenotype (Mandel *et al.*, 1992), that has lost the petals in which the AP1-TCP5 interaction may occur and is functional in the wild type situation. Therefore, constructing a double *ap1tcp5* mutant to see its effect on flower organ growth will not be effective. Instead we started with an in vitro approach by which single nucleotide polymorphisms (SNPs) are introduced into the *AP1* and *TCP5* coding region by error-prone PCR. This method has proven useful in the identification of edgetic alleles (Dreze *et al.*, 2009). We aimed to identify alleles of AP1 that lost specifically their interaction with TCP5, while maintaining their interaction ability with the other floral organ identity specifying MADS domain proteins (Figure 3). As the mutant library of AP1, created by error-prone PCR, will firstly be screened for non-interaction with TCP5 (and vice versa) in a Y2H assay, it is expected that the majority of the mutations causing a frameshift or stop codon will be detected. This would make the identification of rare alleles with single missense mutations more difficult, as the library will then be highly overrepresented with loss of function alleles (See Figure 3). To avoid encountering those truncated alleles, we used a specific vector: pDONR-Express (Gray *et al.*, 2007). This vector has Gateway sites that allow cloning the insert in frame with a kanamycin resistance (Kanr) gene. Therefore, the bacteria transformed with this plasmid will be kanamycin resistant only if the insert has an ATG and no premature stop codon or frameshift, leading to the expression of an [insert-Kanr] fusion protein. The use of this Gateway compatible plasmid also enables the use of pDEST22 and -32 bait and prey vectors for future interaction analysis by Y2H. The expression of the insert in pDONR-Express is driven by an IPTG-inducible promoter and by inserting the product of the error-prone PCR into the pDONR-Express vector, we have enriched the library for full-length alleles. Next, we are able to proceed to specific AD and BD containing vectors for yeast transformation and screen for mutants that lose a specific interaction (Figure 3).

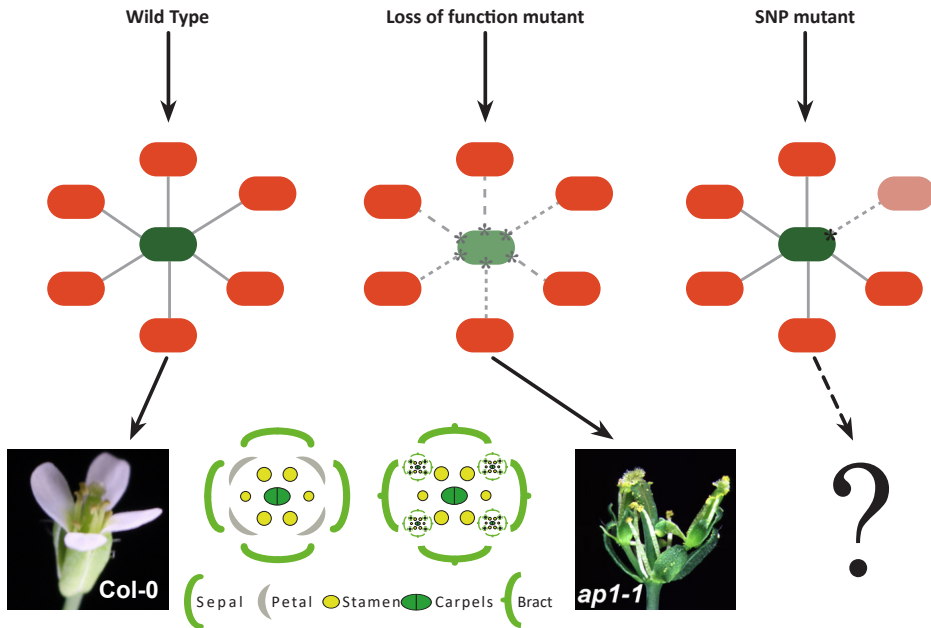


Figure 3. Three protein-protein interaction scenarios.

Shown are three possible interaction phenomena. In the case of a wild type protein (green ellipse) its interaction is shown with several proteins (red ellipse). In a full knock-out leading to a loss of function mutant all interactions are lost and the severity of the phenotype is exemplified by *ap1-1*. Our approach is shown on the right, where a SNP results in loss of only one interaction. The resulting phenotype is entirely dependent on the specific interaction loss. The figure is inspired by Dreze *et al.*, (2009), *ap1-1* mutant picture used from Nutt *et al.*, (2006).

For the creation of the library of mutagenized *AP1* and *TCP5* genes, we used the lack of proofreading capacity of the *Taq* DNA polymerase. Thus, by carrying out a normal PCR to amplify the coding sequence of *TCP5* and *AP1*, random mutations are introduced. Several methods have been described to increase the basal mutation rate of the *Taq* DNA polymerase, such as increasing the $MgCl_2$ concentration, increasing the extension time, varying the ratios of nucleotides in the reaction mixture or increasing the number of PCR cycles (Cadwell and Joyce, 1992). We found that varying the number of PCR cycles and using regular *Taq* polymerase was an effective method to introduce mutations in our genes. We determined the optimal number of PCR cycles for *TCP5* and *AP1*, and found that 25 cycles mainly introduced single mutations for *TCP5*, whereas the number of double and triple mutations was limited. As *AP1* is shorter than *TCP5*, we increased the number of cycles to 30 and found this to be a sufficient number to obtain (mainly) single mutations (using 25 cycles resulted in 90% of the sequenced PCR fragments to be wild type). Alleles with double or multiple mutations are not ideal for our approach as the causal SNP is harder to identify in the case of a loss of

Transition	Mutation		Occurrence
	T→C	A→G	
Trasversion	C→T	G→A	5
	T→G	A→C	3
	G→T	C→A	1
	T→A	A→T	2
	G→C	C→G	0
			0

Library		Total # Sequenced	Number of mutations				
			No	1	2	3	4
AP1	v1	9	3	5	1	0	0
	v2	15	10	3	2	0	0
TCP5	v1	17	9	4	3	0	1
	v2	13	5	6	2	0	0

Figure 4. The number and type of mutations resulting from error-prone PCR on *AP1* and *TCP5*. Shown are the type of mutations determined after sequencing random PCR fragments of the libraries resulting from error-prone PCR. Several individual clones from two independent libraries (v1 and v2) were sequenced.

interaction, and because a higher mutation frequency leads to a higher chance on premature STOP-codons. An overview of the number of mutations, as well as the type (transition or transversion) is shown in Figure 4. As guideline, Gray *et al.* (2007) suggested the amount of required clones for proper allele coverage to be 1000–2000 times the number of codons (i.e., 256.000-512.000 clones for AP1 and 360.000-720.000 for TCP5). We estimate to have reached, after transforming the pDONR-Express allele libraries in *E. coli*, 250.000 colonies for AP1, versus 260.000 colonies for TCP5, slightly fewer than suggested, though we believe sufficient variation will be obtained for a thorough analysis of the two alleles.

Proof of principle: losing specific, though not all, interactions in AP1 mutants

After sequencing several clones to check for the mutation rate, we chose six AP1 mutants, each having one missense mutation (Figure 5A). Unfortunately, AP1.6 contained one silent mutation next to the missense, though we believe that to be of no effect for the interaction capacity of this allele. No premature STOP-codons were observed in the six mutant clones, confirming the ability of pDONR-Express to screen against this (Dreze *et al.*, 2009). The mutations are situated in different domains of AP1 (Krizek and Meyerowitz, 1996; Riechmann, 1996), for several of which their role in MADS-MADS interactions have already been reported (Van Dijk *et al.*, 2010, reviewed by Immink *et al.*, 2010).

An overview of the mutations and their location in the respective MIKC-domains can be found in Figure 5C. This figure presents an initial version of an ‘atlas’ of *ap1* alleles and their effect on protein-protein interactions. The domains and their function during MADS-MADS protein interactions can be used as basis for MADS-TCP interaction characterization. For TCP5 a similar ‘atlas’ setup can be used though TCPs seem to have fewer conserved domains in their protein structure. All members of the TCP gene family share a 60 amino acid long conserved sequence, the TCP domain (Cubas *et al.*, 1999). Secondary structure prediction revealed that the TCP domain forms a basic region followed by two helices separated by a loop (Kosugi and Ohashi, 1997; Cubas, *et al.*, 1999). Differences in this domain has led to the distinction of two separate classes of TCP proteins. The second class of TCPs

contains a 4-amino-acid insertion in the TCP domain and have an R-domain which is predicted to form a coiled coil that may mediate protein-protein interactions (Lupas *et al.*, 1991).

In this study we identified several AP1 mutants which act as a showcase to demonstrate that the technique we used is suitable to determine specific regions and amino acids important for certain protein-protein interactions. The MADS domain (Figure 5C), where the AP1.1 mutation is situated, is crucial for DNA binding but is also involved in dimerization (Hayes *et al.*, 1988, Riechmann and Meyerowitz, 1997). The Intervening (I)-region, where the AP1.2 and AP1.3 mutations are situated, and the K-box, where only the silent AP1.6 mutation is situated, are involved in dimerization specificity (Krizek and Meyerowitz, 1996). The C-terminal region, where the AP1.4, AP1.5 and AP1.6 mutations are located has a role, together with the third α -helix of the K-box, in higher order complex formation (Egea-Cortines *et al.*, 1999).

To shed light on the effect of the SNPs on the interaction capabilities of the AP1 mutants, we performed a yeast-two-hybrid screen (Figure 5B). We used two MADS domain proteins known to interact with AP1 (SEP3 and SUPPRESSOR OF CONSTANS1 (SOC1)) and two known for their lack of interaction with AP1 ((SEEDSTICK (STK) and PI (de Folter *et al.*, 2005)). Three different TCP proteins were used: TCP2, TCP4, and TCP5 as known interaction partners (Y2H in Figure 2).

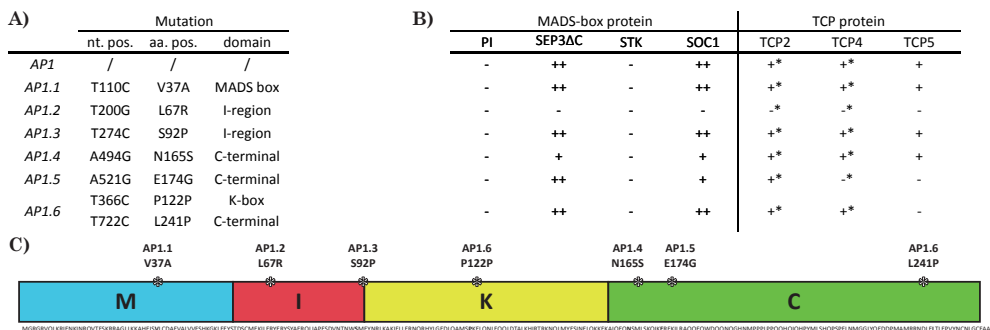


Figure 5. Small selection of six AP1 mutants.

Sequencing revealed the nucleotide position and amino acid change of the mutations introduced by error-prone PCR in (A). A Y2H screen was done on four MADS-box proteins and three TCP proteins to check for a possible change in interaction pattern (B). Interactions scored as: - no interaction, + interaction in only one direction, ++ interaction in both directions, * interactions tested in only one direction. (C) shows a graphic representation of the mutations and their position in the different domains of AP1.

Interactions were tested with the AP1 mutants as prey, fused to the activating domain of GAL4 (AD) and the other proteins as baits, fused to the DNA binding domain of GAL4 (DB) and vice versa. The MADS domain protein SEP3 is known to be auto-activating in the GAL4-Y2H assay, so we made use of a previously reported SEP3 protein with a truncated C-terminus (SEP3ΔC, (Immink *et al.*, 2009)).

The proteins TCP2 and TCP4 were only tested while fused to the AD domain as they are both known to have a certain level of auto-activation when used as baits (Danisman *et al.*, 2013).

In this screen (Figure 5B), the wild type AP1 protein behaved as previously found. We found interaction for AP1 with SEP3ΔC, SOC1, TCP2, TCP4, and TCP5, whereas no interaction was observed between AP1 and PI or STK. The three alleles AP1.1, AP1.3 and AP1.4 behaved exactly as wild type AP1, whereas the other ones showed deviations from the expected interaction patterns (Figure 5B). The interaction capacity of AP1.2 seems to have been lost completely. AP1.5 completely lost the interaction with TCP4 and TCP5 and lost interaction with SOC1 in one direction tested. AP1.6 only lost the interaction with TCP5. No gain of interaction was observed, although only two non-interacting transcription factors were tested.

Discussion

Flower development is made up of tightly regulated processes, starting with floral meristem initiation, followed by organ identity specification and finally the control of final shape and size of these organs. In this study, we have tried to connect the two latter processes. During flower development, TCP5 has a known role in cell growth and expansion during the development of petals (Van Es *et al.*, 2018). AP1 is known for its role as flower meristem determinant (Ferrándiz *et al.*, 2000), and is, as a MADS floral organ identity gene, involved in the specification of sepal and petal identity (Mandel *et al.*, 1992). Interestingly, *AP1* expression is maintained throughout later stages of petal development (Mandel *et al.*, 1992; Gustafson-Brown *et al.*, 1994). This has led to the hypothesis that organ identity specification by MADS domain proteins and growth regulation by TCP proteins might be linked by interactions between the proteins involved in these processes (Dornelas *et al.*, 2011). In Arabidopsis, the presence of an interaction and regulatory function of MADS domain proteins in combination with TCPs has been suggested by coexpression and ChIP-seq analysis on several MADS domain proteins (Wellmer *et al.*, 2006; Kaufmann *et al.*, 2009), though this in itself is no proof for a direct physical interaction. In rice, a functional MADS-TCP interaction has already been found in the form of an interaction between MADS domain protein OsMADS57 and the TCP protein OsTB1, a complex which is thought to modulate tillering in this species (Guo *et al.*, 2013).

Here we have confirmed that a MADS-TCP interaction can take place in Arabidopsis as well. We have shown, by IP followed by LC-MS/MS the ability of TCP5 to interact with AP1 *in planta*. The AP1-TCP5 interaction was confirmed by a Y2H assay.

TCP5 as epidermal regulator of growth and development

We identified several interesting potential interaction partners for TCP5, among them the floral

MADS domain proteins APETALA1 (AP1), APETALA3 (AP3) and SEPALLATA3 (SEP3) using IP-LC/MS on whole inflorescences. Next to this, TCP5 seems to interact with TCP10, a member of the JAW-clade of TCP TFs which confirms previous Y2H data (Danisman *et al.*, 2013). We also found LEUNIG-HOMOLOG (LUH) and KNOTTED-LIKE 3 (KNAT3) as putative TCP5 interaction partners. Interestingly, these proteins have previously been identified as complex partners of several MADS domain proteins, including AP1 (Smaczniak *et al.*, 2012), suggesting the presence of higher order TCP5-AP1-LUH/KNAT3 complexes. Furthermore, KNAT3 was found in Y3H as a direct interaction partner of the floral MADS dimers AP1/SEP4 and AP1/SEP3 (Smaczniak *et al.*, 2012), allowing for the presence of a TCP5-AP1-SEP3-KNAT/LUH complex.

We have recently shown that overexpressing *TCP5* in the epidermal layer results in growth-related phenotypes comparable to those of lines constitutively overexpressing *TCP5* (Van Es *et al.*, 2018). We expressed *TCP5-GFP* fusion driven by the epidermis-specific *ATML1* promoter (resulting in *ATML1_{pro}:TCP5-GFP*) for the identification of epidermal specific interaction partners and found petal phenotypes similar to the *35S_{pro}:TCP5* phenotypes published previously (Huang and Irish, 2015). We used the same epidermal overexpression mutant line for Co-IP and found a highly similar pattern of interaction partners when comparing the list with the natively expressed TCP5 (Supplemental Figure 1).

Control of organ growth is mediated to a large extent by the epidermal L1 cell layer (Savaldi-Goldstein *et al.*, 2007). In this respect, the presence of AP1, AP3 and SEP3 in the IP done on *ATML1_{pro}:TCP5-GFP*, as well as in the IP on *gTCP5:GFP*, suggests a role of these specific TCP5-MADS complex(es) in petal size determination. Even though petals derive from both L1 and L2 layers of the floral meristem (Jenik and Irish, 2000), the fact that the interacting proteins show such a high overlap suggests a specific growth regulatory function for TCP5, in, and coordinated from, the epidermis. This growth regulatory role could be executed in concert with AP1 and other MADS domain proteins.

Library creation and validation of edgetic alleles

This study aimed to identify edgetic alleles that have lost a specific interaction only, while retaining other interactions. We used an error-prone PCR to produce libraries of alleles with single nucleotide polymorphisms and found, quite surprisingly, that without changing anything to our usual PCR conditions but only the amount of cycles, the mutation rate seems high enough to create a library for mutant alleles of both *AP1* and *TCP5* composed of zero, one and two mutations per gene.

We performed an initial screen on six *AP1* mutants and by Y2H assay we found that the AP1.6 mutant loses interaction with TCP5 alone compared to the wild type AP1 protein. Although only six mutants were identified in this first screen, we believe it to be a proper strategy as ‘proof of principle’. We therefore recommend proceeding with a large-scale screen and further interaction analysis.

Ultimately, by characterising a whole library of ‘edgetic’ alleles, we hope to create an extensive map of both *AP1* and *TCP5* mutants in which regions can be identified specifically vital for the interaction between certain types of proteins.

Characterisation of vital domains for the MADS-TCP interaction

MADS domain proteins contain four domains (MIKC, reviewed by Immink *et al.*, 2010) and our approach enabled us to identify regions within these domains specific for the AP1-TCP5 interaction. Screening the allele libraries against other TF proteins enables us to pinpoint the exact amino acids vital for certain interactions. Our results show that, although preliminary, the complete loss of interactions in the AP1.2 mutant by the L67R mutation might have been caused by a misfolding of the AP1 protein, which abolishes AP1 interactions completely. This might illustrate the importance of the I-region for protein-protein interactions. Alternatively, the Y2H results with the L67R mutation could indicate that this amino acid is vital for the tested protein-protein interactions. The latter is supported by the prediction that this amino acid plays a role in interaction specificity between AP1 and other MADS domain proteins (Van Dijk *et al.*, 2010).

Next to the I-region, also the K-box is thought to be involved in MADS protein dimerization specificity. The K-box domain is named as such since it is structurally resembling the coiled-coil domain of keratin, and is supposed to fold into amphipathic α -helices with regularly spaced Leucine residues (Ma *et al.*, 1991). The presence of two consecutive helices has been confirmed by resolving the SEP3 K-domain crystal structure (Puranik *et al.*, 2014). Based on this combined knowledge, we would be able to predict the effect of our mutations on helix stability by analysing the coiled-coil probability and the Leucine repeat pattern. Unfortunately, the only mutation within the K-box of AP1 characterised so far is the silent P122P mutation in the AP1.6 allele. Next to the silent mutation this allele contained a mutation in the C-terminus (L241P) most likely to cause the observed loss of interaction with TCP5. Interestingly, it seems that the C-terminus is of special importance in the AP1-TCP5 interaction as both AP1.5 and AP1.6 mutants loose interaction with TCP5 alone. This could suggest that the TCP5 interaction domain is situated in the C-terminus of AP1. A higher density of SNPs in this region should allow us to pinpoint the exact region essential for the interaction. Finally, when a comprehensive edgetic mutant allele atlas is available, this approach of prediction and confirmation of interaction regions would be a useful tool in finding the underlying cause for a loss or gain of interaction.

Approach and speculations on the biological role of a MADS-TCP interaction

From an evolutionary perspective, the hypothesis that MADS-TCP protein-protein interaction serve as link between floral organ identity and growth is strengthened by the fact that the duplication

event of the *CYCLOIDEA*-like TCPs almost corresponded with duplication events of floral identity MADS box genes *AGAMOUS*, *SEPALLATA* and *APETALA3* (Howarth and Donoghue, 2006). This in itself is no proof for a shared function however, but, as nicely put by Danisman (2016), it does suggest that the genetic components important for floral organ identity diversified at a similar time as the components that are important for their growth regulation.

By complementing a full knockout mutant with an edgetic allele that complements all but one interaction we hope to show the function of this interaction *in planta*. It must be noted that TCPs are thought to be highly redundant and single *tcp* mutant phenotypes are usually very minor or absent (Danisman *et al.*, 2013). This would suggest that a specific loss of interaction would be very hard to characterize and suggests the use of an *ap1* mutant that has lost the interaction with a group of closely related TCPs. One can for example select an *ap1* mutant that is e.g. no longer able to interact with the whole clade of CIN-TCPs and choose this allele to complement the full knockout *ap1-1*. Alternatively, a mutation similar or identical to AP1.5 or AP1.6 that has lost the capacity to interact with TCP5 can be created by CRISPR-CAS9 mutagenesis *in planta*, preferably by base editing using dCAS9-cytidine deaminase (Zong *et al.*, 2017).

A major bottleneck of this method must be noted however, and is related to the limitations of the Y2H assay. From the preliminary screen of AP1 mutants described above we might conclude that AP1.5 or AP1.6 are the ideal candidates to complement the *ap1-1* full knockout or to mimic by a base editing approach as it loses interaction with TCP5 alone (Figure 5). The yeast screen however does not reveal possible changes of interaction capacities with other proteins which will inevitably complicate functional analysis *in planta*. The larger the initial screen, the more information on interaction partners is gained. One way to partially overcome this problem is to start with a screen that contains the most interesting and/or important interaction partners and use this screen for further studies. Next a large-scale TF-library screen can be performed on these candidates. It must be noted that Y2H as a screening method is limited and will not detect higher order complexes and therefore missing loss or gain of ternary interactions. More elaborate Y3H and Y4H systems are available and might prove useful in unravelling the complete picture, though one is recommended to start by testing all binary interactions between the proteins of interest by Y2H (de Folter and Immink, 2011).

Concluding remarks

This study has proven, by IP followed by LC-MS/MS, the ability of TCP5 to interact with AP1 *in planta*. This interaction was confirmed by a Y2H assay, supporting the postulated hypothesis that MADS domain and TCP proteins interact in petals (Dornelas *et al.*, 2011). We further present a method to unravel the precise mode of interaction and a strategy to unveil the potential biological function. Starting by the error-prone approach to create ‘edgetic’ alleles and testing the protein-

protein interaction capacities of these alleles, we might be able to identify regions in TCP5 and AP1 responsible for this particular interaction. This method promises to be an ideal method to investigate certain protein-protein interactions *in vitro* but also *in planta* by overexpressing or creating the same alleles *in vivo*.

Materials and methods

Yeast-two-Hybrid assays

Protein-protein interactions between MADS and TCP proteins were analysed in a pairwise yeast two-hybrid GAL4 assay (de Folter *et al.*, 2005). Bait vectors were transformed into yeast strain PJ69-4a, and the TCP5 or AP1 prey vector was transformed into yeast strain PJ69-4a (James *et al.*, 1996). The individual transformants were grown in liquid synthetic dropout (SD) medium lacking Leu and Trp, respectively. These overnight cultures were mated by spotting 5 mL of liquid culture of both colonies containing the bait and the prey vector on SD complete plates. After overnight incubation, yeast was transferred to freshly prepared SD plates lacking Leu and Trp, selecting for diploid yeast containing both plasmids. In the last step, the mated yeast strains were transferred on SD medium lacking Leu, Trp, and Ade or lacking Leu, Trp, and His, supplemented with 5 or 10 mM 3-amino-1,2,4-triazole (3-AT), respectively. Protein-protein interaction events were identified as growth of yeast, which was scored after 7 days of incubation at 20°C. Auto-activation capacity was determined beforehand for the baits by testing for growth of the single bait transformants on selective SD medium for the His and Ade -markers. All Y2H experiments were conducted in duplicate and interaction was only concluded when growth was found in both independent experiments.

Immunoprecipitation followed by LC-MS/MS

Seeds of the *TCP5_{pro}:TCP5:GFP*, *TCP5_{pro}:GFP*, *ATML1_{pro}:TCP5:GFP* and Col-0 wild type lines were sown on wet Rockwool® blocks and placed in a cold room (4°C) for stratification. After two days of stratification, trays were moved to a growth chamber where the plants were grown under long day conditions (16h light / 8h dark) at 22°C under a relative humidity of 70%. After induction of flowering, whole inflorescences were isolated from plants and subjected to immunoprecipitation (IP) as described previously (Smaczniak, Li, *et al.*, 2012; Jamge *et al.*, 2018) using 0.75g of plant tissue for three biological replicates. The protocol was optimised for TCP proteins and differed from the published protocols only in the use of Nonidet P-40 substitute (Roche) instead of using SDS as detergent (as suggested by Jamge *et al.*, 2018).

The LC-MS/MS data generated was analysed with the MaxQuant software package, a freely available tool for protein identification and quantification (Cox and Mann, 2008). Further analysis was done on

the Perseus software, part of MaxQuant, where missing LFQ values were imputed with a normalized artificial abundance background value (Hubner *et al.*, 2010).

Mutant allele library creation for AP1 and TCP5 full length alleles

The following protocol was identical for the construction of TCP5 and AP1 mutant libraries, unless otherwise stated. The coding sequences were isolated from cDNA and cloned separately into pGEM®-T Easy according to the manufacturer's instructions (Promega). The use of purified plasmid with either TCP5 or AP1, rather than cDNA, ensured an effective error-prone PCR. To check for correct starting material, vectors were sequenced with M13 forward and reverse primers. PAGE-purified, attB-flanked gene specific primers were used for the following error-prone PCR with Taq polymerase: 94°C for 4 min followed by 30 or 25 cycles (AP1 and TCP5 respectively) of 94°C for 30 sec, 64°C for 30 sec followed by 72°C (1 min for AP1 and 1.5 min for TCP5) ending with 7 min of 72°C. The products were then incubated at 12°C.

The library of PCR products were purified using the NucleoSpin PCR Clean-up Kit (Bioké) after which the library was cloned into fresh pDONR-Express by BP reaction. To obtain higher transformation efficiency, 7 BP reactions were pooled and transformed in *E. coli* DH5α after which they were plated on LB containing kanamycin as selection marker and 1 mM of IPTG as inducer of expression. The concentration of kanamycin was chosen as such that no background growth appears on plates independent of IPTG induction (Gray *et al.*, 2007). For AP1 the kanamycin concentration was found sufficient at 25 µg/ml whereas 7.5 µg/ml was sufficient for the TCP5 library.

The next step was isolating pDONR-Express that, after growth on kanamycin selection, contained only full-length alleles of either AP1 or TCP5. Colonies were scraped from LB plates after adding 3 mL of liquid LB and the suspension collected in buckets for Midiprep isolation according to the manufacturer's instructions (Qiagen®). Each bucket contained scraped colonies from 10 plates (as not to exceed 150.000 colonies per midiprep reaction) and after plasmid isolation the DNA was resuspended in Tris buffer and the samples were pooled per library.

Purified pDONR-Express plasmid with allele libraries of AP1 and TCP5 were then transformed in freshly prepared pDEST22 (Invitrogen) by LR reaction. Again, to obtain higher transformation efficiency, 7 LR reactions were pooled and transformed in *E. coli* DH5α after which they were plated on LB containing carbenicillin as selection marker.

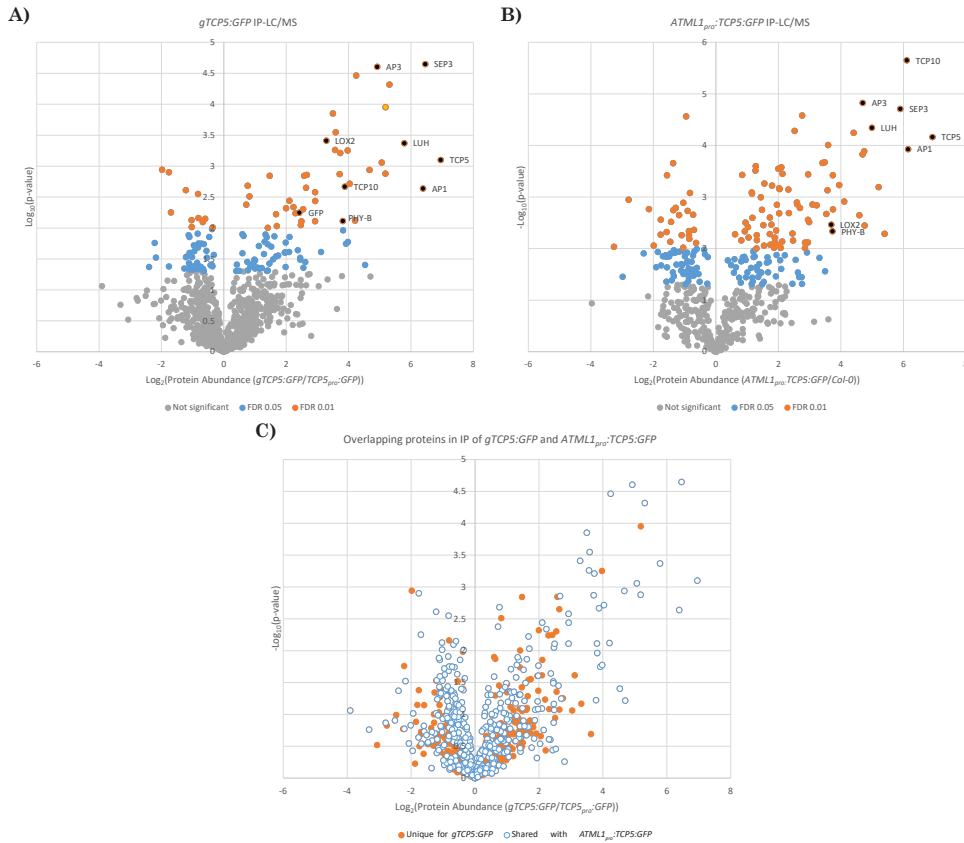
After overnight growth, 20 colonies of both pDEST22:AP1 and pDEST22:TCP5 were isolated and subject to sequencing to check for mutation rate (see following paragraph). All other plasmids were isolated using the midiprep protocol as described above to be used for further transformation in yeast for the Y2H screen.

Library check and proving the principle of edgetic alleles

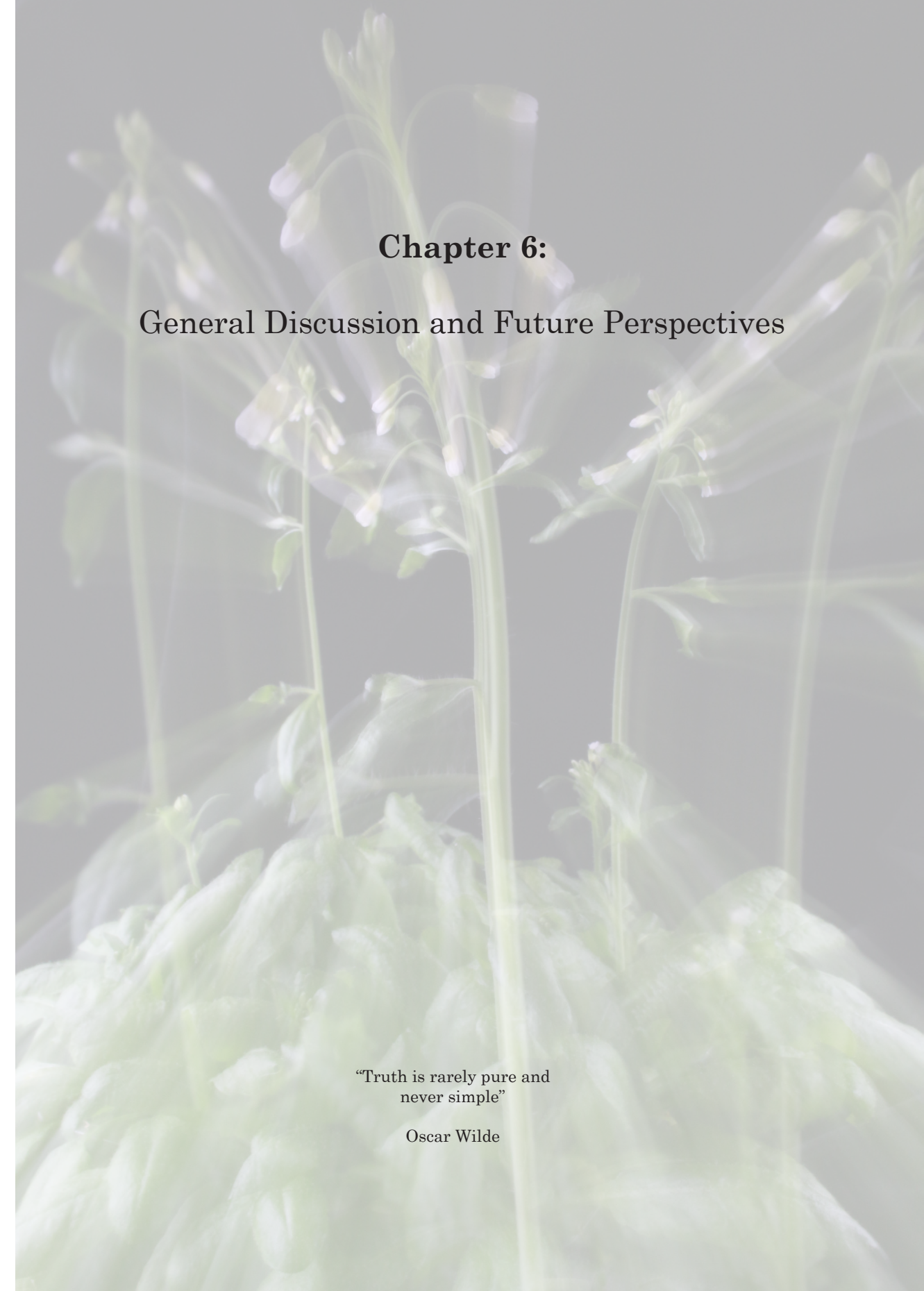
As mentioned above, plasmids of 20 single colonies of both the AP1 and TCP5 library were isolated and sequenced to get an idea on the mutation rate. Polymorphisms were identified by aligning the sequenced ORFs against that of wild type TCP5 and AP1 obtained through TAIR. Of the identified AP1 clones, seven, including an unaffected AP1 clone used as wild-type, were tested for interaction against several MADS and TCP proteins. The Y2H setup was done as described in the paragraph ‘Yeast-two-Hybrid assays’ above.

Acknowledgments

We would like to thank S. Jamge for helpful suggestions in the implementation of the Co-immunoprecipitation assay, C. Smaczniak for useful comments in the analysis of the obtained LC-MS/MS data using Perseus. We are grateful to B. Charlotiaux for providing the pDONR-Express vector. We thank Camila Maistro Patreze for some of the Y2H data. The research is supported by grants from the Dutch Scientific Organization (NWO); (NWO-JSTP grant 833.13.008), CAPES/NUFFIC (No 010/07) and CAPES/NUFFIC (No 033/2012).



Supplemental Figure 1. *In planta* TCP5 protein interaction profile in Arabidopsis inflorescences, the overlap. Graphs represent the normalized protein abundance ratio between *gTCP5:GFP* (*TCP5_{pro}:TCP5:GFP*) and the *TCP5pro:GFP* control in **(A)**, *ATML1_{pro}:TCP5:GFP* and the Col-0 control in **(B)** plotted against their significance. The overlapping proteins identified in the *ATML1_{pro}:TCP5:GFP* IP plotted on the graph of *gTCP5:GFP* is shown in **(C)** by blue circles with a white center. In **(A)** and **(B)**: significant protein abundance differences between sample and control at FDR < 0.01 (orange) or FDR < 0.05 (blue), grey circles indicate non-significant hits. Several proteins are highlighted by label and a black dot. See Supplemental File 1 for a full list of TCP5 interaction partners resulting from both *gTCP5:GFP* as well as *ATML1_{pro}:TCP5:GFP* protein complex identification.



Chapter 6:

General Discussion and Future Perspectives

“Truth is rarely pure and
never simple”

Oscar Wilde

TCPs, ‘Terribly Challenging Proteins’

The plant-specific family of TCP proteins has been first described in 1999 (Cubas *et al.*, 1999) and during the course of almost two decades, a wealth of knowledge has been gained in the precise role and function of some members of this transcription factor (TF) family in plant development and other processes (excellently reviewed by, among others, Martín-Trillo and Cubas, 2010; Uberti Manassero *et al.*, 2013; Nicolas and Cubas, 2015, 2016; Danisman, 2016). With this thesis I have tried to expand the available knowledge on TCP TFs, the processes in which they are involved and the unique properties of TCP proteins. In this final chapter I will put my findings in perspective and propose suggestions for future research.

The family of TCP TFs is very variable in their function, shown by the variety of phenotypes of different *tcp* mutants. For plant breeders, this family is also of great interest for application purposes as its members have key functions in agronomical important traits in crop species such as maize (Doebley *et al.*, 1995; Doebley *et al.*, 1997), rice (Takeda *et al.*, 2003), tomato (Ori *et al.*, 2007) and barley (Liller *et al.*, 2015), a fact I have elaborated upon in the introduction (Chapter 1). Besides the initially identified core functions in plant development, TCP genes appear to act in many more processes, ranging from pathogen susceptibility to nutrient and hormonal signalling, aspects that I will elaborate upon in this final chapter. Due to their multifaceted functionality and existing functional redundancy, revealing the exact roles and functions of individual TCP proteins in a plant's life cycle is incredibly complicated and challenging.

Two classes of TCPs, black and white or several shades of grey?

Historically, the TCP family of transcription factors has been divided into two classes based on sequence characteristics (Cubas *et al.*, 1999). TCP genes belonging to these two classes were hypothesized to act antagonistically, either by promoting cell growth and proliferation (class I) or through the repression of these processes (class II) (Martín-Trillo and Cubas, 2010). The division based on sequence characteristics is solid; however, the division into two classes with distinct and opposing functions deserves a closer look. Currently, only *TCP4* and *TCP20* have been described as having some antagonistic biological functions (Danisman *et al.*, 2012). Hence, the universality of this functional division of the plant TCP transcription factor family is questionable. To understand the function and phenotypic consequences of TCP mutants, I started this research with a comprehensive phenotyping analysis of a set of Arabidopsis TCP mutants during plant development. In this study I studied the effect on plant growth, architecture and seed yield characteristics of single and higher-order TCP mutants (Chapter 2). We created a mathematical equation that describes the growth curve of the analysed plants using four different parameters (β_1, β_4) and were able to reconstruct the growth pattern of the different mutants. This provided a unique dataset allowing a detailed look at

growth characteristics of the plants mutated in TCPs of the two proposed antagonistically operating classes. Interestingly, we have shown that during development, plants mutated for class I TCPs (e.g. *tcp8* and *tcp15*), as well as plants mutated for specific class II TCPs (e.g. *tcp5* and *brc1*), show a similarly altered growth pattern with a significantly increased β_1 and β_3 compared to wild type plants. Additionally, analysis of plant architecture revealed similar changes in branching irrespective of whether the mutation was in a class I or class II TCP gene, an increase in branching was observed in both the *tcp20tcp22* double mutant (class I) as well as the *brc1brc2* double mutant (class II). Interestingly, we also observed a reduction in the number of branches in *jaw-D* and *tcp14tcp15* mutants (class II and class I respectively). Furthermore, mutants of different TCPs belonging to either class showed similar effects on seed characteristics (seed number, and weight per plant): a reduction in these characteristics was observed irrespective of the class (see figure 3 in Chapter 2 for details).

The above discussed similarities in phenotypes suggest at least overlapping biological functions for proteins of both TCP classes and question the strict division in two antagonistically functioning classes. Nevertheless, it should be noted that the underlying cellular and molecular processes were not studied in this particular study. It is possible that a similar effect on whole plant level (an increase in e.g. leaf size) can be accomplished by different cellular processes such as an increase in cell size or in cell number. Therefore, coupling the cellular phenotypes and molecular responses to the plant growth parameters will be essential to provide full insight into the proposed antagonistic behaviour, or lack thereof, of class I and class II TCPs.

The expanding world of TCP functions and their involvement in hormonal pathways

Because of the observed phenotypes in *tcp* mutants in plant growth and development, TCPs have long been implicated in the direct regulation of cell proliferation. Next to this, the 'P' in the family name is derived from PCF1 and PCF2, two rice (*Oryza sativa*) genes known to bind the promoter of *PROLIFERATING CELL NUCLEAR ANTIGEN (PCNA)*, controlling cell cycle in meristems as well as DNA synthesis and repair (Kosugi and Ohashi, 1997), strengthening the hypothesised direct functioning in the regulation of cell proliferation. However, as of recent, more and more TCP proteins have been shown to primarily regulate genes involved in hormone biosynthesis and signalling (reviewed by (Nicolas and Cubas, 2016) and cell proliferation might be controlled indirectly as a downstream target of this hormonal regulation, leading to the observed phenotypes. In this thesis, I have both confirmed and strengthened this latter hypothesis by demonstrating that BRC1 is able to regulate abscisic acid (ABA) biosynthesis and signalling through direct binding of regulatory sequences of several ABA biosynthesis and signalling genes. Next to this, two Cytokinin (CK) oxidases and several CK signalling genes seem to be directly regulated by BRC1 (Chapter 4).

Furthermore, I have shown that TCP5 is able to bind the ethylene biosynthesis gene *ACS2* in its promoter, thereby providing an explanation for its observed repression upon TCP5 induction (Chapter 3 and van Es *et al.*, 2018). Overexpression of *ACS2* was observed in a *tcp5 tcp13 tcp17* loss-of-function mutant and its phenotype could be rescued by application of the ethylene inhibitor STS. The observed (de)regulation of the hormones ABA, CK and ethylene provide a neat explanation of the observed phenotypes in the *tcp* mutant plants studied. The regulatory role of BRC1 on ABA biosynthesis has been reported previously (González-Grandío *et al.*, 2017), but the comprehensive genome-wide ChIP experiment, coupled with transcriptome analysis by RNA-seq, revealed the number of ABA-related genes as direct targets of BRC1, and showed which ABA biosynthesis genes are bound by BRC1. ABA has been implicated in the direct control of cell cycle genes in algae by blocking the G1 to S transition (Kobayashi *et al.*, 2016) and by directly repressing cell cycle genes in dormant buds in grapevine (*Vitis vinifera*, Vergara *et al.*, 2017). Next to this, plants defective in ABA biosynthesis show an increased branching phenotype (Reddy *et al.*, 2013; Yao and Finlayson, 2015; González-Grandío *et al.*, 2017) and exogenous application of ABA inhibits branching (Chatfield *et al.*, 2000; Holalu and Finlayson, 2017). The newly found regulation of CK by BRC1 is in accordance with the role of CK as promoter of axillary bud outgrowth (Dun *et al.*, 2012), probably through direct regulation of cell proliferation and cell cycle progression (Werner *et al.*, 2003). Nevertheless, further research is necessary to unravel the exact role of BRC1 in this hormonal regulatory network. The arguments above beautifully explain the observed lack in axillary bud outgrowth through enhanced ABA biosynthesis and possible reduced CK accumulation by BRC1 activity (Chapter 4 of this thesis). Altogether the examples above provide evidence for indirect regulation of cell cycle genes by specific members of the TCP TF family via hormonal signalling, besides the few published examples of direct cell cycle gene targeting.

Ethylene has previously been shown to influence cell size and shapes in petals of rose (*Rosa hybrid*) and *Arabidopsis* (Pei *et al.*, 2013). The exact mode of action of ethylene on influencing cell size is not yet fully understood. Several NAC transcription factors are targeted by ethylene signal transduction proteins, and this has been shown to be a mechanism underlying cell elongation in waterlogged petioles (Rauf *et al.*, 2013). Our data showed deregulation of several NAC TFs upon *TCP5* induction mainly in the later time point (T2-8, Chapter 3), indicating that the deregulation of these NAC TFs is likely caused by the inhibition of ethylene biosynthesis by TCP5. A recent paper showed the interaction between two ethylene activated TFs and two genes involved in root hair elongation. That study showed that the transcriptional complex consisting of EIN3/EIL1 and RHD6/RSL1 control root hair initiation and elongation (Feng *et al.*, 2017). Yet another, very exciting mode of action of ethylene is its observed effect on microtubule orientation (Le *et al.*, 2004; Plett *et al.*, 2009; Ma *et al.*, 2018), thereby influencing cell elongation and elongation direction. Interestingly, microtubules have

recently been linked to the establishment of conical cell shape in the *Arabidopsis* petal (Ren *et al.*, 2017), a characteristic affected in our *TCP5* mutants as well (van Es *et al.*, 2018).

The cases presented in this thesis, *TCP5* directly controlling ethylene biosynthesis and *BRC1* as regulator of ABA biosynthesis and CK accumulation, perfectly corroborates the emerging view of TCPs as key hormonal regulators. It has been proposed that virtually every aspect of plant growth and development is controlled by one or more hormones (Gray, 2004) and it therefore might be not too much of a surprise that many members of a gene family known for their roles in plant development (Cubas *et al.*, 1999; Martín-Trillo and Cubas, 2010) are found to be linked to hormonal regulation. Next to our work on *TCP5*, a recent paper on the closely related *TCP17* protein showed its involvement in the biosynthesis of auxin (Zhou *et al.*, 2017) and auxin signalling related genes were also found overrepresented in our study on the functioning of *TCP5*. Because ethylene is known to be involved in a feedback mechanism with auxin (Rai *et al.*, 2015), the bigger and exact regulatory network will be a challenging endeavour to uncover. However, as is obvious from our recent addition of *TCP5* as direct regulator of ethylene to the list of TCPs involved in hormone biosynthesis, we are probably far from the complete picture. Hence, it will be an interesting line of research to characterise all possible links of TCPs with hormones.

Unravelling the cell type specific action of TCP proteins

The observed enrichment in the ChIP-qPCR of *TCP5* binding the *ACS2* promoter was rather limited, but it must be noted that the cellular phenotypes and the rescue of the knock out phenotype by STS application were observed in petal tissue only, whereas practical considerations forced us to perform the ChIP on whole inflorescences. The same restriction holds for *BRC1*, which was induced for the ChIP and expression studies in a constitutive manner, but which has its native expression in axillary buds only. Though, technically it is challenging and complicated to perform the various molecular analyses with specific tissue or cellular precision. Consequently, the magnitude of the observed enrichments in our experiments might be strongly reduced and other potential targets might have been missed due to these technical constraints. To overcome these issues, isolating specific cell types would allow us to look at certain processes more closely. Techniques such as INTACT (Deal and Henikoff, 2010), fluorescence-activated cell sorting (FACS) (Birnbaum *et al.*, 2005) and laser capture microdissection of specific tissues (LCM) (Kerk *et al.*, 2003) have been around for some time and might be of interest for future use. Their use will be of great value in unravelling cell specific functions of TCPs, in meristematic tissue, axillary buds or specific cell types in, for example, the *Arabidopsis* petal.

Binding site properties of TCP proteins

There have been a number of previous studies on preferred DNA binding sites of TCP TFs and based on these *in vitro* experiments the consensus-binding site of class I TCPs was defined by the sequence GTGGGNCC, whereas class II proteins showed a preference for the sequence GTGGNCCC (Kosugi and Ohashi, 2002; Schommer *et al.*, 2008; Viola *et al.*, 2011). In our comprehensive *in vivo* ChIP-seq experiment for the class II TCP protein BRC1 we found a strong overrepresentation of the motif GDCCCA, yet another putative binding site. Inspired by this observation, we rethought the definition of specific class I and class II TCP consensus binding sites. It seems that no strict division in classes can be made, as most likely every TCP has its own preferred binding sequence, independent of class. Interestingly though, the dichotomy in binding sites for both classes is rather strong in the *in vitro* analysis, whereas our *in vivo* ChIP-seq and the experiment described by O'Malley *et al.*, (2016) questions this strict division. It should be noted that TCP transcription factors are able to form dimers, even between class I and II, each with slightly different binding preferences (Danisman *et al.*, 2013). Interestingly, class II TCPs preferably interact with TCPs of the same class. Alternatively, TCPs could bind DNA together with other specific interaction partners, thereby regulating gene expression and gaining different binding specificities. Depending on the coexpression of a certain TCP and such an interaction partner, for instance a floral organ specific MADS domain protein (see Chapter 5), preferred binding specificity and hence target gene selection would be variable in time and place dependent on the overlap in expression. An interesting and worthwhile approach might be EMSA experiments in which putative interaction partners of TCPs can be combined to check for cooperative DNA binding and changes in binding site specificity. This will yield information about interaction capacities, as well as provide the opportunity to play around with different binding sites, possibly elucidating the conundrum of the role and function of the two classes of TCPs.

Another interesting and related hypothesis is that TCPs from both classes can regulate the same process antagonistically, by for instance competing for the same binding sites. However, competition between Class I and II TCP TFs for the same binding site has been described as a possible molecular mode of action for TCPs (Li *et al.*, 2005), but could not be confirmed in the *TCP4* and *TCP20* regulation of JA biosynthesis through binding the promoter of *LOX2*, a JA biosynthesis gene (Schommer *et al.*, 2008; Danisman *et al.*, 2012). In these studies, *TCP4* and *TCP20* were found to bind different regions in the *LOX2* promoter. However, physical hindrance of adjacent binding sites or effects on chromatin confirmation (Liu and Weigel, 2015) due to binding by a particular TCP cannot be ruled out and might be part of the underlying molecular mechanism.

Novel interaction partners of TCP5 during flower development

Flower development consists of processes determining organ identity followed by processes governing

cell growth and differentiation. Previous research has shown that these processes are tightly linked and that proteins involved in floral organ identity specification might be of vital importance during later processes as well. We have confirmed in Chapter 5 that MADS domain proteins, historically known for their role in organ identity, are able to interact with TCP proteins, regulators of cell growth and expansion, a hypothesis first postulated by Dornelas et al. (2011).

Several protein complex isolations on MADS domain proteins have been performed and published (for example Smaczniak et al., 2012a, 2012b), however in these complexes, TCPs have never been found. This might be due to the specific developmental stage in which the experiments were conducted. If, for example, the MADS-TCP interaction is of particular importance during later stages of floral organ development, then an immunoprecipitation aimed at identifying interaction partners of MADS domain proteins during the establishment of organ identity will fail to reveal interactions present at later stages. Immunoprecipitation assays during later stages of flower development, preferably with tissue in which an overlap in expression is expected, might lead to the identification of TCP interaction partners of MADS domain proteins. This might provide an explanation why at least at mRNA expression level, for example *API* is present during these late stages of development, as opposed to the early developmental stages where it exerts its well-known role as organ identity gene. An interesting follow up to investigate the possible biological role of the MADS-TCP interaction has been described in Chapter 5. Another *in vitro* approach would be to check for cooperative binding by electrophoretic mobility shift assays (EMSA). By EMSA we could try to unravel the function of closely located MADS and TCP binding sites in the genome, as observed for example by Kaufmann *et al.*, (2009). This would be a first step in studying the effects of MADS-TCP complexes on DNA binding. Binding sites preferentially bound by a combination of MADS domain proteins and TCPs could then be analysed on their genome-wide distribution and their vicinity to genes, allowing speculation on the functions of such specific complexes. A genetic approach to study the role of MADS-TCP interactions is described in Chapter 5, where I present a mutagenesis approach to manipulate the interaction between MADS and TCP proteins in order to specifically impair this interaction, but leaving the intra-family interactions intact. If such mutations can be created *in vivo* by e.g. CRISPR/CAS9 via base-editing, then we would be able to understand the role of MADS-TCP interaction in floral organ development.

Sticky proteins, omnipresent or simply imperative?

TCP proteins are notoriously sticky, i.e. they show-up regularly in for example yeast two-hybrid (Y2H) screens. Though it is debatable whether or not to use the term ‘sticky’. TCP TFs are expressed throughout the plant, mutants show a wide variety of phenotypes, and TCPs seem to be involved in a plethora of biological and molecular processes. A similar paradigm: drive anywhere in the

Netherlands and you will come across quite a number of Volkswagen cars, not because they are following you, but because they are among the most widely sold automobiles. The same might hold for TCPs, they pop-up in a large number of screens, probably just because they are widely expressed throughout the plant and involved in so many processes. A number of TCP proteins was for example identified as interactor of various pathogen effector proteins (Weßling *et al.*, 2014), among which TCP14 stands out and therefore is seen as network hub. I will elaborate further on the possible biological relevance of this observation in one of the next paragraphs. Furthermore, besides these interactions and the interactions with other type of TFs, association with proteins may modulate TCP's molecular functioning. A nice example is the proposed conjugation with Small Ubiquitin-like Modifier (SUMO), which can affect e.g. the localization and stability of nuclear proteins (Mazur *et al.*, 2017). However, to prevent that the abovementioned omnipresence in different large-scale Y2H assays reflects mainly false positives, one might be aided by several other *in vitro* and *in planta* experiments to confirm the wealth of identified possible TCP protein-protein interactions.

Plant development as yield determining factor

Increasing yield, in form of seeds, fruits, leaves or tubers, has been a driving force behind plant breeding since the dawn of agriculture. We tried, by phenotyping a large set of TCP mutants, to uncover possible correlations between developmental factors and final yield in the form of seed set (Chapter 2). A striking finding was that in most cases, no matter whether a plant developed more or fewer branches compared to wild type, this seemed to have a negative effect on yield from plants growing under our experimental conditions. A possible explanation could be that the plants have already acquired their optimal architecture for the highest yield. However, this does deserve a closer look, for instance by repeating the characterisation of traits as mentioned in Chapter 2 or studying other mutants known to be affected in branching. Plants defective in components of the strigolactone, ABA and auxin pathways show alterations in their branching patterns (reviewed by Leyser, 2009) and make for interesting candidates to look into the relation of branching and yield. In several crop species this relation has been a major subject of research. In cereals like wheat (*Triticum aestivum*) and barley (*Hordeum vulgare*) for example, yield is controlled by the shoot architecture and the number of side shoots (tillers) formed at the basal node of the plant (Sreenivasulu and Schnurbusch, 2012). Shoot architecture, or branching, was targeted during domestication of several cultivated cereals (Remigereau *et al.*, 2011), where mainly synchronous and low tillering was selected (Doust, 2007). Interestingly, in maize (Doebley *et al.*, 1995), rice (Goto *et al.*, 2005), barley (Ramsay *et al.*, 2011) and recently uncovered in wheat (Dixon *et al.*, 2018), the involved key genes in question are *BRC1* orthologues. Though, in tomato altered inflorescence branching related to yield optimization was linked to mutations in, and the balance in expression of, different members of the

phosphatidylethanolamine-binding protein (PEBP) gene family (Jiang *et al.*, 2013; Park *et al.*, 2014). Interestingly, previous research has shown that BRC1 interacts with the PEBP family member FLOWERING LOCUS T (FT) in Arabidopsis, also known as florigen. This complex is proposed to regulate plant architecture by inhibiting the floral transition in axillary meristems (Niwa *et al.*, 2013). Hence, there appears to be a close interaction between specific TCP and PEBP proteins and this regulatory mechanism might direct and fine tune the use of resources to the main inflorescence versus side branches, ensuring reproductive success for the plant and providing breeders with additional targets to optimize yield.

Nonetheless, targeting shoot architecture in breeding is limited by negative correlations between shoot branching and other major yield components such as seed number and weight. This trade-off has often be attributed to resource limitation and particular sink-source relationships. However, recent evidence suggests that the same genes or regulatory modules affect both seed number and weight as well as the tiller number (Ramsay *et al.*, 2011; Liller *et al.*, 2015). Therefore, understanding the regulation of both shoot and inflorescence branching is important to optimize shoot and inflorescence architecture and could be an effective and promising strategy to improve crop yield.

We have tried to couple the seed yield phenotypes to the growth parameters and found, though not exclusively, that mutants with an altered branching phenotype developed differently (i.e. had different β -parameters) compared with wild type plants. On the other hand, not all plants with an altered progression of their development showed differences in seed yield characteristics. This indicates that development and branching are not necessarily linked and provides a good starting point to uncouple these traits in the future aiming at maximal yield potential.

TCP proteins, so much more than growth regulators

TCPs have been shown to be involved in the plant defence response, next to the developmental and hormonal processes described in this thesis. This might not come as a huge surprise considering the different hormones to which TCPs are linked. Take the plant hormone JA and its biosynthesis for example, to which both *TCP4* and *TCP20* have been linked (Schommer *et al.*, 2008; Danisman *et al.*, 2012). JA has long been recognized as key regulator that plays a crucial role in plant defence responses to pathogens (reviewed by Pieterse *et al.*, 2012). An interesting study in rice showed that an infection of the *Rice ragged stunt virus* (RRSV) caused increased accumulation of miR319, thereby downregulating the miR319-regulated TCPs (Zhang *et al.*, 2016). This in turn led to decreased JA levels, which suppressed JA-mediated defence to facilitate further virus infection. Other pathogenic organisms that found their way into altering JA biosynthesis by targeting TCPs, are phytoplasmas; insect-transmitted phytopathogenic bacteria. The Aster Yellows phytoplasma strain Witches' Broom (AY-WB) secretes the effector protein SAP11, destabilising CIN-TCPs in Arabidopsis, leading to

the down-regulation of *LOX2* expression and thereby reducing JA biosynthesis (Sugio *et al.*, 2011). Interestingly, the same effector protein is targeting BRC1 for degradation, resulting in strongly increased outgrowth of axillary meristems, giving rise to the characteristic Witches' Broom phenotype. This altered plant architecture and downregulation of a plants' defence response results in an successful infection and a significant increase of progeny for the transmitting vector and second phytoplasmas host, *M. quadrilineatus* (leafhoppers).

Next to JA, the plant hormone SA plays a major role in disease resistance signalling (reviewed by Pieterse *et al.*, 2012). Several class I TCP proteins have been linked with SA biosynthesis; both TCP8 and TCP9 have been shown to promote *ICS1* (Wang *et al.*, 2015b), encoding for a key enzyme in SA biosynthesis. Double *tcp8tcp9* mutants have increased levels of susceptibility to infection with a *Pseudomonas syringae* strain (Wang *et al.*, 2015b). Next to this, a triple mutant consisting of *tcp8 tcp14* and *tcp15* allowed for increased growth of another *Pseudomonas syringae* strain (Kim *et al.*, 2014).

The abovementioned examples are probably just the tip of the iceberg. As shown in figure 1 of Chapter 1, many more TCPs have been linked, one way or the other, with hormones and many more hormones have been implicated in defence responses. Examples of cross talk between ethylene and JA and SA signalling have been reported, both ABA and CK signalling were shown to antagonize plant immunity by suppressing SA-dependent defences, and the ever present hormone auxin was shown to repress SA levels and signalling; lastly GA suppresses the response to JA and consequently shifts the balance between JA and SA signalling (reviewed by Pieterse *et al.*, 2012).

In conclusion, TCPs might have a far more elaborate regulatory role in plant defence responses through the regulation of hormone signalling or biosynthesis. The dichotomy in phenotypes, revealing a function for TCPs in defence responses and developmental processes, might present TCPs as the link between the two processes. It is well-known that a growth-defence trade-off exists in plants; thought to occur due to resource restrictions, demanding prioritization towards either growth or defence (reviewed by Huot *et al.*, 2014). The exact regulatory mechanisms behind have not been uncovered, though hormones have been shown to play vital roles (Denancé *et al.*, 2013). TCPs could be the missing link in this trade-off, regulating hormonal biosynthesis and signalling in such a way to promote growth and limit defences, or vice versa, depending on external and internal factors and conditions.

The odd ones out, organogenesis and evolution

Focussing this thesis on their involvement in plant development, touching upon hormonal regulation and, described above, venturing into plant defences, TCPs continue to amaze us. Adding to the growing list of functions that TCPs are involved in, recent observations provide evidence that specific

TCPs can even act as organ identity genes. A cucumber plant mutated for a TCP was shown to develop shoots instead of tendrils (Wang *et al.*, 2015a). A similar phenotype was found in melons where a single-nucleotide mutation in *CmTCP1* led to the Chiba tendril-less mutation. Also here, the tendrils were converted to shoot and leaf-like structures (Mizuno *et al.*, 2015). Interestingly, in both cases the TCP in question contained a highly conserved seven-amino-acid motif uniquely found in *Cucurbitaceae*, adding another layer to the diversity of the TCP TF family. This unique function of a TCP as organ identity gene in *Cucurbitaceae* specifically, questions the role of Arabidopsis as unique model system for TCP research. Arabidopsis is known to have 24 TCP genes (Riechmann *et al.*, 2000), whereas e.g. sorghum has 20 (Francis *et al.*, 2016), the orchid *Phalaenopsis equestris* has 23 (Lin *et al.*, 2016) tomato has 30 (Parapunova *et al.*, 2014), maize has 29 (Chai *et al.*, 2017) and cotton is believed to have even 36 different TCP genes (Ma *et al.*, 2016). This variation in number of TCP genes suggests species-specific duplication and probably also functions, as was shown in the *Cucurbitaceae*. Hence, TCPs might be involved in more elaborate processes still to be discovered. Looking into species with fewer, as well as species that have more and perhaps different types of TCPs, will greatly contribute to our understanding of the role and function of TCPs in plant development and beyond.

One of such species with fewer TCPs is the moss *Physcomitrella patens*, where only six TCPs have been reported, four class I and two class II TCPs. *PpTCP5*, a class II TCP, was shown to be involved in branching of the sporophyte in this species (Ortiz-Ramírez *et al.*, 2016). Sporophyte branching seems to have been instrumental in the evolutionary transition towards a complete sporophytic dominance over the gametophytic phase, together with other essential character changes such as the formation of a cuticle and lignified cells (Bennici, 2008). Loss of function of a class II TCP could have caused branching of the sporophyte, allowing it to gradually increase in size and complexity, eventually leading to sporophytic dominance in extant vascular land plants. Interestingly, the moment in evolution when branched sporophytes originated, occurred after the origin of mosses and before the origin of several extinct groups of primitive land plants (Kenrick and Crane, 1991). The oldest land plant fossil with a branched sporophyte is a *Cooksonia* species from the Middle Silurian (425 million years ago) (Edwards and Feehan, 1980; Gerrienne *et al.*, 2006). An interesting hypothesis that follows from this observation is the possibility that class II TCPs have been key in the evolution of vascular plants and that their function as growth repressor is ancient and conserved. In the moss *P. patens* *PpTCP5* represses the outgrowth of the sporophyte. In Angiosperms, many more class II TCPs are present though all seem to have maintained their function as repressors of proliferation. It is the location in which they are expressed or regulated that further specifies their function, BRC1 inhibits outgrowth of axillary meristems (Aguilar-Martínez *et al.*, 2007) and JAW-D TCPs inhibit cell proliferation in the margins of organs (Efroni *et al.*, 2008).

Past, present, future

Insights into the function of TCP transcription factors has changed tremendously since they were first described as an independent, plant specific family of genes (Cubas *et al.*, 1999). As a whole, the TCP gene family of transcription factors seems to be expressed throughout the plant lifecycle in almost every tissue and to fulfil a whole pallet of functions. Shifting from their initially proposed role as direct regulators of cell cycle genes, TCPs seem to be positioned ‘above’ this and instead, regulating hormone signalling, which on their turn regulate a plethora of downstream processes. To particularize TCPs as done above makes them sound like key regulators of vital processes. This might not be far from the truth, as studies constitutively overexpressing TCPs reveal that in a number of cases, this leads to meristem arrest (Koyama *et al.*, 2007). On the other hand, in most cases the observed phenotypes of knock-out mutants are rather minor under controlled laboratory conditions and higher order mutants are required to reveal the function of a group of TCPs, as exemplified for the CIN-like TCPs (Palatnik *et al.*, 2003; Schommer *et al.*, 2008). Finding the complete set of true functions of individual TCP genes in whatever process, tissue or cell type they might be involved in, remains a major challenge.



References

Summary

Samenvatting

Acknowledgements

About the author

EPS education statement

“Better get used to bein’
my used to be”

Rory Gallagher

– A –

- Abts, W., Van de Poel, B., Vandenbussche, B., and De Proft, M.P.** (2014). Ethylene is differentially regulated during sugar beet germination and affects early root growth in a dose-dependent manner. *Planta* **240**: 679–686.
- Aggarwal, P., Das Gupta, M., Joseph, A.P., Chatterjee, N., Srinivasan, N., and Nath, U.** (2010). Identification of Specific DNA Binding Residues in the TCP Family of Transcription Factors in Arabidopsis. *Plant Cell* **22**: 1174–1189.
- Aguilar-Martínez, J.A., Poza-Carrión, C., and Cubas, P.** (2007). Arabidopsis BRANCHED1 acts as an integrator of branching signals within axillary buds. *Plant Cell* **19**: 458–472.
- Aguilar-Martínez, J.A. and Sinha, N.** (2013). Analysis of the role of Arabidopsis class I TCP genes AtTCP7, AtTCP8, AtTCP22, and AtTCP23 in leaf development. *Front. Plant Sci.* **4**.
- Alvarez-Buylla, E.R., Benítez, M., Corvera-Poiré, A., Chaos Cador, Á., de Folter, S., Gamboa de Buen, A., Garay-Arroyo, A., García-Ponce, B., Jaimes-Miranda, F., Pérez-Ruiz, R. V., Piñeyro-Nelson, A., and Sánchez-Corrales, Y.E.** (2010). Flower Development. *Arab. B.*: e0127.
- Anastasiou, E., Kenz, S., Gerstung, M., MacLean, D., Timmer, J., Fleck, C., and Lenhard, M.** (2007). Control of Plant Organ Size by KLUH/CYP78A5-Dependent Intercellular Signaling. *Dev. Cell* **13**: 843–856.
- Andriankaja, M., Dhondt, S., De Bodt, S., Vanhaeren, H., Coppens, F., De Milde, L., Mühlenbock, P., Skirycz, A., Gonzalez, N., Beemster, G.T.S., and Inzé, D.** (2012). Exit from Proliferation during Leaf Development in Arabidopsis thaliana: A Not-So-Gradual Process. *Dev. Cell* **22**: 64–78.
- Aoyama, T. and Chua, N.H.** (1997). A glucocorticoid-mediated transcriptional induction system in transgenic plants. *Plant J.* **11**: 605–612.

– B –

- Bailey, T.L., Boden, M., Buske, F.A., Frith, M., Grant, C.E., Clementi, L., Ren, J., Li, W.W., and Noble, W.S.** (2009). MEME Suite: Tools for motif discovery and searching. *Nucleic Acids Res.* **37**: 202–208.
- Bailey, T.L. and Elkan, C.** (1994). Fitting a Mixture Model by Expectation Maximization to Discover Motifs in Bipolymers. *Proc. Second Int. Conf. Intell. Syst. Mol. Biol.*: 28–36.
- Bailey, T.L. and MacHanick, P.** (2012). Inferring direct DNA binding from ChIP-seq. *Nucleic Acids Res.* **40**: 1–10.
- Baker, N.R.** (2008). Chlorophyll fluorescence: a probe of photosynthesis in vivo. *Annu. Rev. Plant Biol.* **59**: 89–113.
- Balsemão-Pires, E., Andrade, L.R., and Sachetto-Martins, G.** (2013). Functional study of TCP23 in Arabidopsis thaliana during plant development. *Plant Physiol. Biochem.* **67**: 120–125.
- Barbier, F. et al.** (2015). Sucrose is an early modulator of the key hormonal mechanisms controlling bud outgrowth in *Rosa hybrida*. *J. Exp. Bot.* **66**: 2569–2582.
- Bardet, A.F., He, Q., Zeitlinger, J., and Stark, A.** (2012). A computational pipeline for comparative ChIP-seq analyses. *Nat. Protoc.* **7**: 45–61.
- Bemer, M., van Dijk, A.D.J., Immink, R.G.H., and Angenent, G.C.** (2017). Cross-Family Transcription Factor Interactions: An Additional Layer of Gene Regulation. *Trends Plant Sci.* **22**: 66–80.
- Bencivenga, S., Serrano-Mislata, A., Bush, M., Fox, S., and Sablowski, R.** (2016). Control of Oriented Tissue Growth through Repression of Organ Boundary Genes Promotes Stem Morphogenesis. *Dev. Cell* **39**: 198–208.

- Bennett, E., Roberts, J.A., and Wagstaff, C.** (2012). Manipulating resource allocation in plants. *J. Exp. Bot.* **63**: 3391–3400.
- Bennici, A.** (2008). Origin and early evolution of land plants: Problems and considerations. *Commun. Integr. Biol.* **1**: 212–8.
- Beyer, E.M.** (1979). Effect of silver ion, carbon-dioxide, and oxygen on ethylene action and metabolism. *Plant Physiol.* **63**: 169–173.
- Birnbaum, K., Jung, J.W., Wang, J.Y., Lambert, G.M., Hirst, J.A., Galbraith, D.W., and Benfey, P.N.** (2005). Cell type-specific expression profiling in plants via cell sorting of protoplasts from fluorescent reporter lines. *Nat. Methods* **2**: 615–619.
- Bischoff, V., Nita, S., Neumetzler, L., Schindelasch, D., Urbain, A., Eshed, R., Persson, S., Delmer, D., and Scheible, W.-R.** (2010). TRICHOME BIREFRINGENCE and Its Homolog AT5G01360 Encode Plant-Specific DUF231 Proteins Required for Cellulose Biosynthesis in Arabidopsis. *Plant Physiol.* **153**: 590–602.
- Blanke, M.M.** (2015). Ethylene levels along the food supply chain - a key to reducing food waste? *Sci. Food Agric.* **1091**: 101–106.
- Bowman, J.L., Smyth, D.R., and Meyerowitz, E.M.** (1989). Genes Directing Flower Development in Arabidopsis. *Plant Cell Online* **1**: 37–52.
- Boyes, D.C., Zayed, A.M., Ascenzi, R., McCaskill, A.J., Hoffman, N.E., Davis, K.R., and Görlach, J.** (2001). Growth stage-based phenotypic analysis of Arabidopsis: A model for high throughput functional genomics in plants. *Plant Cell* **13**: 1499–1510.
- Brant, A.N. and Chen, H.Y.H.** (2015). Patterns and Mechanisms of Nutrient Resorption in Plants. *CRC. Crit. Rev. Plant Sci.* **34**: 471–486.
- Busov, V.B., Brunner, A.M., and Strauss, S.H.** (2008). Genes for control of plant stature and form. *New Phytol.* **177**: 19.
- C —
- Cadwell, R.C. and Joyce, G.F.** (1992). Randomization of genes by PCR mutagenesis. *Genome Res.* **2**: 28–34.
- Cai, G., Yang, Q., Chen, H., Yang, Q., Zhang, C., Fan, C., and Zhou, Y.** (2016). Genetic dissection of plant architecture and yield-related traits in *Brassica napus*. *Sci. Rep.* **6**: 1–16.
- Casal, J.J., Sanchez, R.A., and Deregibus, V.A.** (1986). The effect of plant density on tillering: The involvement of R/FR ratio and the proportion of radiation intercepted per plant. *Environ. Exp. Bot.* **26**: 365–371.
- Causier, B., Schwarz-Sommer, Z., and Davies, B.** (2010). Floral organ identity: 20 years of ABCs. *Semin. Cell Dev. Biol.* **21**: 73–79.
- Chai, W., Jiang, P., Huang, G., Jiang, H., and Li, X.** (2017). Identification and expression profiling analysis of TCP family genes involved in growth and development in maize. *Physiol. Mol. Biol. Plants* **23**: 779–791.
- Chatfield, S.P., Stirnberg, P., Forde, B.G., and Leyser, O.** (2000). The hormonal regulation of axillary bud growth in Arabidopsis. *Plant J.* **24**: 159–169.
- Chen, W., Yin, X., Wang, L., Tian, J., Yang, R., Liu, D., Yu, Z., Ma, N., and Gao, J.** (2013). Involvement of rose aquaporin RhPIP1;1 in ethylene-regulated petal expansion through interaction with RhPIP2;1. *Plant Mol. Biol.* **83**: 219–233.
- Chow, C.N., Zheng, H.Q., Wu, N.Y., Chien, C.H., Huang, H. Da, Lee, T.Y., Chiang-Hsieh, Y.F., Hou, P.F., Yang, T.Y., and Chang, W.C.** (2016). PlantPAN 2.0: An update of Plant Promoter Analysis Navigator for

- reconstructing transcriptional regulatory networks in plants. *Nucleic Acids Res.* **44**: D1154–D1164.
- Cline, M.G.** (1997). Concepts and terminology of apical dominance. *Am. J. Bot.* **84**: 1064–1069.
- Clough, S.J. and Bent, A.F.** (1998). Floral dip: A simplified method for *Agrobacterium*-mediated transformation of *Arabidopsis thaliana*. *Plant J.* **16**: 735–743.
- Coen, E.S. and Meyerowitz, E.M.** (1991). The war of the whorls: genetic interactions controlling flower development. *Nature* **353**: 31–37.
- Cominelli, E., Sala, T., Calvi, D., Gusmaroli, G., and Tonelli, C.** (2008). Over-expression of the *Arabidopsis* AtMYB41 gene alters cell expansion and leaf surface permeability. *Plant J.* **53**: 53–64.
- Cox, J. and Mann, M.** (2008). MaxQuant enables high peptide identification rates, individualized p.p.b.-range mass accuracies and proteome-wide protein quantification. *Nat. Biotechnol.* **26**: 1367–1372.
- Crawford, B.C.W., Nath, U., Carpenter, R., and Coen, E.S.** (2004). *Cinnamata* controls both cell differentiation and growth in petal lobes and leaves of *antirrhinum*. *Plant Physiol.* **135**: 244–253.
- Crone, W. and Lord, E.M.** (1993). Flower development in the organ number mutant *clavata1-1* of *Arabidopsis thaliana* (Brassicaceae). *Am. J. Bot.* **80**: 1419–1426.
- Cubas, P., Coen, E., and Zapater, J.M.M.** (2001). Ancient asymmetries in the evolution of flowers. *Curr. Biol.* **11**: 1050–1052.
- Cubas, P., Lauter, N., Doebley, J., and Coen, E.** (1999). The TCP domain: a motif found in proteins regulating plant growth and development. *Plant J.* **18**: 215–222.
- Curtis, M. and Grossniklaus, U.** (2003). A gateway cloning vector set for high-throughput functional analysis of genes in planta. *Plant Physiol.* **133**: 462–469.
- Czechowski, T., Stitt, M., Altmann, T., Udvardi, M.K., and Scheible, W.-R.** (2005). Genome-Wide Identification and Testing of Superior Reference Genes for Transcript Normalization in *Arabidopsis*. *Plant Physiol.* **139**: 5–17.
- D –**
- Danisman, S.** (2016). TCP Transcription Factors at the Interface between Environmental Challenges and the Plant's Growth Responses. *Front. Plant Sci.* **7**: 1–13.
- Danisman, S., Van Dijk, A.D.J., Bimbo, A., Van Der Wal, F., Hennig, L., De Folter, S., Angenent, G.C., and Immink, R.G.H.** (2013). Analysis of functional redundancies within the *Arabidopsis* TCP transcription factor family. *J. Exp. Bot.* **64**: 5673–5685.
- Danisman, S., van der Wal, F., Dhondt, S., Waites, R., de Folter, S., Bimbo, A., van Dijk, A.D.J., Muino, J.M., Cutri, L., Dornelas, M.C., Angenent, G.C., and Immink, R.G.H.** (2012). *Arabidopsis* class I and class II TCP transcription factors regulate jasmonic acid metabolism and leaf development antagonistically. *Plant Physiol.* **159**: 1511–23.
- Davière, J.-M., Wild, M., Regnault, T., Baumberger, N., Eisler, H., Genschik, P., and Achard, P.** (2014). Class I TCP-DELLA interactions in inflorescence shoot apex determine plant height. *Curr. Biol.* **24**: 1923–8.
- Deal, R.B. and Henikoff, S.** (2010). A simple method for gene expression and chromatin profiling of individual cell types within a tissue. *Dev. Cell* **18**: 1030–1040.
- Denancé, N., Sánchez-Vallet, A., Goffner, D., and Molina, A.** (2013). Disease resistance or growth: the role of plant hormones in balancing immune responses and fitness costs. *Front. Plant Sci.* **4**: 1–12.
- Dennis, J.E., Gay, D.M., and Welsch, R.E.** (1977). An Adaptive Nonlinear Least Square Algorithm. *ACM Trans.*

- Math. Softw. **7**: 348–368.
- Van Dijk, A.D.J., Morabito, G., Fiers, M., Van Ham, R.C.H.J., Angenent, G.C., and Immink, R.G.H. (2010). Sequence motifs in MADS transcription factors responsible for specificity and diversification of protein-protein interaction. *PLoS Comput. Biol.* **6**.
- Dinneny, J.R., Yadegari, R., Fischer, R.L., Yanofsky, M.F., and Weigel, D. (2004). The role of JAGGED in shaping lateral organs. *Development* **131**: 1101–1110.
- Dixon, L.E., Greenwood, J.R., Bencivenga, S., Zhang, P., Cockram, J., Mellers, G., Ramm, K., Cavanagh, C., Swain, S.M., and Boden, S.A. (2018). *TEOSINTE BRANCHED1* Regulates Inflorescence Architecture and Development in Bread Wheat (*Triticum aestivum* L.). *Plant Cell*: tpc.00961.2017.
- Doebley, J., Stec, A., and Gustus, C. (1995). *teosinte branched1* and the origin of maize: Evidence for epistasis and the evolution of dominance. *Genetics* **141**: 333–346.
- Doebley, J., Stec, A., and Hubbard, L. (1997). The evolution of apical dominance in maize. *Nature* **386**: 485–488.
- Domagalska, M.A. and Leyser, O. (2011). Signal integration in the control of shoot branching. *Nat. Rev. Mol. Cell Biol.* **12**: 211–221.
- Dornelas, M.C., Patreze, C.M., Angenent, G.C., and Immink, R.G.H. (2011). MADS: The missing link between identity and growth? *Trends Plant Sci.* **16**: 89–97.
- Doust, A. (2007). Architectural evolution and its implications for domestication in grasses. *Ann. Bot.* **100**: 941–950.
- Dreze, M. et al. (2009). “Edgetic” perturbation of a *C. elegans* BCL2 ortholog. *Nat. Methods* **6**: 843–849.
- Dugardeyn, J. and Van Der Straeten, D. (2008). Ethylene: Fine-tuning plant growth and development by stimulation and inhibition of elongation. *Plant Sci.* **175**: 59–70.
- Dun, E.A., Germain, A. de Saint, Rameau, C., and Beveridge, C.A. (2012). Antagonistic Action of Strigolactone and Cytokinin in Bud Outgrowth Control. *Plant Physiol.* **158**: 487–498.
- E –
- Edwards, D. and Feehan, J. (1980). Records of Cooksonia-type sporangia from late Wenlock strata in Ireland. *Nature* **287**: 41–42.
- Efroni, I., Blum, E., Goldshmidt, A., and Eshed, Y. (2008). A protracted and dynamic maturation schedule underlies Arabidopsis leaf development. *Plant Cell* **20**: 2293–2306.
- Efroni, I., Han, S.K., Kim, H.J., Wu, M.F., Steiner, E., Birnbaum, K.D., Hong, J.C., Eshed, Y., and Wagner, D. (2013). Regulation of leaf maturation by chromatin-mediated modulation of cytokinin responses. *Dev. Cell* **24**: 438–445.
- Egea-Cortines, M., Saedler, H., and Sommer, H. (1999). Ternary complex formation between the MADS-box proteins SQUAMOSA, DEFICIENS and GLOBOSA is involved in the control of floral architecture in *Antirrhinum majus*. *EMBO J.* **18**: 5370–5379.
- Engelmann, W., Simon, K., and Phen, C.J. (1992). Leaf movement rhythm in *A.thaliana*. *Zeitschrift für Naturforsch.* **47**: 925–928.
- van Es, S.W., Silveira, S.R., Rocha, D.I., Bimbo, A., Martinelli, A.P., Dornelas, M.C., Angenent, G.C., and Immink, R.G.. (2018). Novel functions of the Arabidopsis transcription factor TCP5 in petal development and ethylene biosynthesis. *Plant J.*

– F –

- Feller, A., MacHemer, K., Braun, E.L., and Grotewold, E. (2011). Evolutionary and comparative analysis of

- MYB and bHLH plant transcription factors. *Plant J.* **66**: 94–116.
- Feng, Y., Xu, P., Li, B., Li, P., Wen, X., An, F., Gong, Y., Xin, Y., Zhu, Z., Wang, Y., and Guo, H.** (2017). Ethylene promotes root hair growth through coordinated EIN3/EIL1 and RHD6/RSL1 activity in *Arabidopsis*. *Proc. Natl. Acad. Sci.*: 201711723.
- Ferrándiz, C., Gu, Q., Martienssen, R., and Yanofsky, M.F.** (2000). Redundant regulation of meristem identity and plant architecture by FRUITFULL, APETALA1 and CAULIFLOWER. *Development* **127**: 725–734.
- Finkelstein, R.R.** (2000). The *Arabidopsis* Absciscic Acid Response Gene ABI5 Encodes a Basic Leucine Zipper Transcription Factor. *Plant Cell Online* **12**: 599–610.
- Finlayson, S.A.** (2007). *Arabidopsis* TEOSINTE BRANCHED1-LIKE 1 regulates axillary bud outgrowth and is homologous to monocot TEOSINTE BRANCHED1. *Plant Cell Physiol.* **48**: 667–677.
- Flood, P.J., Kruijer, W., Schnabel, S.K., van der Schoor, R., Jalink, H., Snel, J.F.H., Harbinson, J., and Aarts, M.G.M.** (2016). Phenomics for photosynthesis, growth and reflectance in *Arabidopsis thaliana* reveals circadian and long-term fluctuations in heritability. *Plant Methods* **12**: 14.
- de Folter, S. and Immink, R.G.H.** (2011). Yeast Protein–Protein Interaction Assays and Screens. In *Plant Transcription Factors*, pp. 1–8.
- de Folter, S., Immink, R.G.H., Kieffer, M., Parenicova, L., Henz, S.R., Weigel, D., Busscher, M., Kooiker, M., Colombo, L., Kater, M.M., Davies, B., and Angenent, G.C.** (2005). Comprehensive Interaction Map of the *Arabidopsis* MADS Box Transcription Factors. *Plant Cell Online* **17**: 1424–1433.
- Francis, A., Dhaka, N., Bakshi, M., Jung, K.H., Sharma, M.K., and Sharma, R.** (2016). Comparative phylogenomic analysis provides insights into TCP gene functions in *Sorghum*. *Sci. Rep.* **6**: 1–14.
- G —
- Galletti, R., Johnson, K.L., Scofield, S., San-Bento, R., Watt, A.M., Murray, J. a H., and Ingram, G.C.** (2015). DEFECTIVE KERNEL 1 promotes and maintains plant epidermal differentiation. *Development* **142**: 1978–83.
- Gao, Y., Zhang, D., and Li, J.** (2015). TCP1 Modulates DWF4 Expression via Directly Interacting with the GGNCCC Motifs in the Promoter Region of DWF4 in *Arabidopsis thaliana*. *J. Genet. Genomics* **42**: 383–392.
- Genty, B., Briantais, J.M., and Baker, N.R.** (1989). The relationship between the quantum yield of photosynthetic electron transport and quenching of chlorophyll fluorescence. *Biochim. Biophys. Acta - Gen. Subj.* **990**: 87–92.
- Gerrienne, P., Dilcher, D.L., Bergamaschi, S., Milagres, I., Pereira, E., and Rodrigues, M.A.C.** (2006). An exceptional specimen of the early land plant *Cooksonia paranensis*, and a hypothesis on the life cycle of the earliest eutracheophytes. *Rev. Palaeobot. Palynol.* **142**: 123–130.
- Giraud, E., Ng, S., Carrie, C., Duncan, O., Low, J., Lee, C.P., Van Aken, O., Millar, A.H., Murcha, M., and Whelan, J.** (2010). TCP Transcription Factors Link the Regulation of Genes Encoding Mitochondrial Proteins with the Circadian Clock in *Arabidopsis thaliana*. *Plant Cell* **22**: 3921–3934.
- Glover, B.J., Airoidi, C.A., Moyroud, E., Glover, B.J., Airoidi, C.A., and Moyroud, E.** (2016). Epidermis: Outer Cell Layer of the Plant. *eLS*: 1–7.
- Gnan, S., Priest, A., and Kover, P.X.** (2014). The genetic basis of natural variation in seed size and seed number and their trade-off using *Arabidopsis thaliana* magic lines. *Genetics* **198**: 1751–1758.
- Golyandina, N., Korobeynikov, A., Shlemov, A., and Usevich, K.** (2013). Multivariate and 2D Extensions of

- Singular Spectrum Analysis with the Rssa Package. *J. Stat. Softw.* **67**.
- González-Grandío, E. and Cubas, P.** (2014). Identification of gene functions associated to active and dormant buds in *Arabidopsis*. *Plant Signal. Behav.* **9**: 19–21.
- González-Grandío, E., Pajoro, A., Franco-Zorrilla, J.M., Tarancón, C., Immink, R.G.H., and Cubas, P.** (2017). Absciscic acid signaling is controlled by a *BRANCHED1/HD-ZIP I* cascade in *Arabidopsis* axillary buds. *Proc. Natl. Acad. Sci.* **114**: E245–E254.
- González-Grandío, E., Poza-Carrión, C., Sorzano, C.O.S., and Cubas, P.** (2013). *BRANCHED1* promotes axillary bud dormancy in response to shade in *Arabidopsis*. *Plant Cell* **25**: 834–50.
- Goto, Y., Tanabe, M., Ishibashi, T., Tsutsumi, N., Yoshimura, A., and Nemoto, K.** (2005). Tillering Behavior of the Rice *fine culm 1* Mutant. *Plant Prod. Sci.* **8**: 68–70.
- Graaff, E. Van Der, Schwacke, R., Schneider, A., Desimone, M., and Kunze, R.** (2006). Transcription Analysis of *Arabidopsis* Membrane Transporters and Hormone Pathways during Developmental and Induced Leaf Senescence. *Plant Physiol.* **141**: 776–792.
- Gray, P.N., Busser, K.J., and Chappell, T.G.** (2007). A novel approach for generating full-length, high coverage allele libraries for the analysis of protein interactions. *Mol. Cell. Proteomics* **6**: 514–526.
- Gray, W.M.** (2004). Hormonal regulation of plant growth and development. *PLoS Biol.* **2**.
- Grbić, V. and Bleecker, A.B.** (2000). Axillary meristem development in *Arabidopsis thaliana*. *Plant J.* **21**: 215–223.
- Grebe, M.** (2012). The patterning of epidermal hairs in *Arabidopsis*-updated. *Curr. Opin. Plant Biol.* **15**: 31–37.
- Guan, P., Wang, R., Nacry, P., Breton, G., Kay, S. a, Pruneda-Paz, J.L., Davani, A., and Crawford, N.M.** (2014). Nitrate foraging by *Arabidopsis* roots is mediated by the transcription factor TCP20 through the systemic signaling pathway. *Proc. Natl. Acad. Sci. U. S. A.* **111**: 15267–72.
- Guo, S., Xu, Y., Liu, H., Mao, Z., Zhang, C., Ma, Y., Zhang, Q., Meng, Z., and Chong, K.** (2013). The interaction between OsMADS57 and OsTB1 modulates rice tillering via DWARF14. *Nat. Commun.* **4**: 1512–1566.
- Guo, Z., Fujioka, S., Blancaflor, E.B., Miao, S., Gou, X., and Li, J.** (2010). TCP1 modulates brassinosteroid biosynthesis by regulating the expression of the key biosynthetic gene DWARF4 in *Arabidopsis thaliana*. *Plant Cell* **22**: 1161–73.
- Das Gupta, M., Aggarwal, P., and Nath, U.** (2014). CINCINNATA in *Antirrhinum majus* directly modulates genes involved in cytokinin and auxin signaling. *New Phytol.* **204**: 901–912.
- Gupta, S., Stamatoyannopoulos, J.A., Bailey, T.L., and Noble, W.S.** (2007). Quantifying similarity between motifs. *Genome Biol.* **8**.
- Gustafson-Brown, C., Savidge, B., and Yanofsky, M.F.** (1994). Regulation of the *Arabidopsis* floral homeotic gene APETALA1. *Cell* **76**: 131–143.
- H —
- Hase, Y., Fujioka, S., Yoshida, S., Sun, G., Umeda, M., and Tanaka, A.** (2005). Ectopic endoreduplication caused by sterol alteration results in serrated petals in *Arabidopsis*. *J. Exp. Bot.* **56**: 1263–1268.
- Hatfield, J.L. and Prueger, J.H.** (2015). Temperature extremes: Effect on plant growth and development. *Weather Clim. Extrem.* **10**: 4–10.
- Hayes, T.E., Sengupta, P., and Cochran, B.H.** (1988). The human c-fos serum response factor and the yeast factors GRM/PRTF have related DNA-binding specificities. *Genes Dev.* **2**: 1713–1722.

- Heim, M.A., Jakoby, M., Werber, M., Martin, C., Weisshaar, B., and Bailey, P.C.** (2003). The basic helix-loop-helix transcription factor family in plants: A genome-wide study of protein structure and functional diversity. *Mol. Biol. Evol.* **20**: 735–747.
- Hempel, F.D. and Feldman, L.J.** (1994). Bi-directional inflorescence development in *Arabidopsis thaliana*: Acropetal initiation of flowers and basipetal initiation of paraclades. *Planta* **192**: 276–286.
- Hervé, C., Dabos, P., Bardet, C., Jauneau, A., Auriac, M.C., Ramboer, A., Lacout, F., and Tremousaygue, D.** (2009). In vivo interference with attp20 function induces severe plant growth alterations and deregulates the expression of many genes important for development. *Plant Physiol.* **149**: 1462–1477.
- Holalu, S. V. and Finlayson, S.A.** (2017). The ratio of red light to far red light alters *Arabidopsis* axillary bud growth and abscisic acid signalling before stem auxin changes. *J. Exp. Bot.* **68**: 943–952.
- Howarth, D.G. and Donoghue, M.J.** (2006). Phylogenetic analysis of the “ECE” (CYC/TB1) clade reveals duplications predating the core eudicots. *Proc. Natl. Acad. Sci. U. S. A.* **103**: 9101–6.
- Huang, T. and Irish, V.F.** (2015). Temporal Control of Plant Organ Growth by TCP Transcription Factors. *Curr. Biol.* **25**: 1765–1770.
- Hubner, N.C., Bird, A.W., Cox, J., Splettstoesser, B., Bandilla, P., Poser, I., Hyman, A., and Mann, M.** (2010). Quantitative proteomics combined with BAC TransgeneOmics reveals in vivo protein interactions. *J. Cell Biol.* **189**: 739–754.
- Hughes, A.L.** (1994). The Evolution of Functionally Novel Proteins after Gene Duplication. *Proc. R. Soc. B Biol. Sci.* **256**: 119–124.
- Huot, B., Yao, J., Montgomery, B.L., and He, S.Y.** (2014). Growth-defense tradeoffs in plants: A balancing act to optimize fitness. *Mol. Plant* **7**: 1267–1287.
- I —
- Immink, R.G.H., Kaufmann, K., and Angenent, G.C.** (2010). The “ABC” of MADS domain protein behaviour and interactions. *Semin. Cell Dev. Biol.* **21**: 87–93.
- Immink, R.G.H., Tonaco, I.A.N., de Folter, S., Shchennikova, A., van Dijk, A.D.J., Busscher-Lange, J., Borst, J.W., and Angenent, G.C.** (2009). SEPALLATA3: The “glue” for MADS box transcription factor complex formation. *Genome Biol.* **10**.
- Irish, V.F.** (2008). The *Arabidopsis* petal: a model for plant organogenesis. *Trends Plant Sci.* **13**: 430–436.
- J —
- James, P., Halladay, J., and Craig, E. a** (1996). Genomic Libraries and a Host. *Genetics* **144**: 1425–1436.
- Jamge, S., Angenent, G.C., and Bemer, M.** (2018). Identification of in planta protein–protein interactions using IP-MS. *1675*: 315–329.
- Jenik, P.D. and Irish, V.F.** (2000). Regulation of cell proliferation patterns by homeotic genes during *Arabidopsis* floral development. *Development* **127**: 1267–1276.
- Jiang, K., Liberatore, K.L., Park, S.J., Alvarez, J.P., and Lippman, Z.B.** (2013). Tomato Yield Heterosis Is Triggered by a Dosage Sensitivity of the Florigen Pathway That Fine-Tunes Shoot Architecture. *PLoS Genet.* **9**.
- Joosen, R.V.L., Kodde, J., Willems, L.A.J., Ligterink, W., Van Der Plas, L.H.W., and Hilhorst, H.W.M.** (2010). Germinator: A software package for high-throughput scoring and curve fitting of *Arabidopsis* seed germination. *Plant J.* **62**: 148–159.

- Jossier, M., Bouly, J.P., Meimoun, P., Arjmand, A., Lessard, P., Hawley, S., Grahame Hardie, D., and Thomas, M.** (2009). SnRK1 (SNF1-related kinase 1) has a central role in sugar and ABA signalling in *Arabidopsis thaliana*. *Plant J.* **59**: 316–328.
- K –
- Kafri, R., Levy, M., and Pilpel, Y.** (2006). The regulatory utilization of genetic redundancy through responsive backup circuits. *Proc. Natl. Acad. Sci.* **103**: 11653–11658.
- Kaufmann, K., Muiño, J.M., Jauregui, R., Airoidi, C.A., Smaczniak, C., Krajewski, P., and Angenent, G.C.** (2009). Target genes of the MADS transcription factor SEPALLATA3: integration of developmental and hormonal pathways in the *Arabidopsis* flower. *PLoS Biol.* **7**.
- Kaufmann, K., Muiño, J.M., Østerås, M., Farinelli, L., Krajewski, P., and Angenent, G.C.** (2010a). Chromatin immunoprecipitation (ChIP) of plant transcription factors followed by sequencing (ChIP-SEQ) or hybridization to whole genome arrays (ChIP-CHIP). *Nat. Protoc.* **5**: 457–472.
- Kaufmann, K., Wellmer, F., Muiñ, J.M., Ferner, T., Wuest, S.E., Kumar, V., Serrano-Mislata, A., Madueño, F., Kraiewski, P., Meyerowitz, E.M., Angenent, G.C., and Riechmann, J.L.** (2010b). Orchestration of floral initiation by APETALA1. *Science* (80-.). **328**: 85–89.
- Kebrom, T.H., Brutnell, T.P., and Finlayson, S.A.** (2010). Suppression of sorghum axillary bud outgrowth by shade, phyB and defoliation signalling pathways. *Plant, Cell Environ.* **33**: 48–58.
- Kenrick, P. and Crane, P.R.** (1991). Water-Conducting Cells in Early Fossil Land Plants : Implications for the Early Evolution of Tracheophytes Author. *Bot. Gaz.* **152**: 335–356.
- Kerk, N.M., Ceserani, T., Tausta, L.S., Sussex, I.M., and Nelson, T.M.** (2003). Laser Capture Microdissection of Cells from Plant Tissues. *PLANT Physiol.* **132**: 27–35.
- Khan, M., Rozhon, W., and Poppenberger, B.** (2013). The role of hormones in the aging of plants - A mini-review. *Gerontology* **60**: 49–55.
- Kidder, B.L., Hu, G., and Zhao, K.** (2011). ChIP-Seq: Technical considerations for obtaining high-quality data. *Nat. Immunol.* **12**: 918–922.
- Kieffer, M., Master, V., Waites, R., and Davies, B.** (2011). TCP14 and TCP15 affect internode length and leaf shape in *Arabidopsis*. *Plant J.* **68**: 147–158.
- Killingbeck, K.T.** (1996). Nutrients in Senesced Leaves : Keys to the Search for Potential Resorption and Resorption Proficiency. *Ecology* **77**: 1716–1727.
- Kim, H.J. et al.** (2014a). Gene regulatory cascade of senescence-associated NAC transcription factors activated by ETHYLENE-INSENSITIVE2-mediated leaf senescence signalling in *Arabidopsis*. *J. Exp. Bot.* **65**: 4023–4036.
- Kim, J., Chang, C., and Tucker, M.L.** (2015). To grow old: regulatory role of ethylene and jasmonic acid in senescence. *Front. Plant Sci.* **6**: 1–7.
- Kim, S.H., Son, G.H., Bhattacharjee, S., Kim, H.J., Nam, J.C., Nguyen, P.D.T., Hong, J.C., and Gassmann, W.** (2014b). The *Arabidopsis* immune adaptor SRFR1 interacts with TCP transcription factors that redundantly contribute to effector-triggered immunity. *Plant J.* **78**: 978–989.
- Kobayashi, Y., Ando, H., Hanaoka, M., and Tanaka, K.** (2016). Absciscic Acid Participates in the Control of Cell Cycle Initiation Through Heme Homeostasis in the Unicellular Red Alga *Cyanidioschyzon merolae*. *Plant Cell Physiol.* **57**: 953–960.

- Kosugi, S. and Ohashi, Y.** (2002). DNA binding and dimerization specificity and potential targets for the TCP protein family. *Science* (80-.), **30**.
- Kosugi, S. and Ohashi, Y.** (1997). PCF1 and PCF2 specifically bind to cis elements in the rice proliferating cell nuclear antigen gene. *Plant Cell* **9**: 1607–1619.
- Koyama, T.** (2014). The roles of ethylene and transcription factors in the regulation of onset of leaf senescence. *Front. Plant Sci.* **5**: 650.
- Koyama, T., Furutani, M., Tasaka, M., and Ohme-Takagi, M.** (2007). TCP transcription factors control the morphology of shoot lateral organs via negative regulation of the expression of boundary-specific genes in *Arabidopsis*. *Plant Cell* **19**: 473–484.
- Krizek, B.A. and Fletcher, J.C.** (2005). Molecular mechanisms of flower development: An armchair guide. *Nat. Rev. Genet.* **6**: 688–698.
- Krizek, B.A. and Meyerowitz, E.M.** (1996a). The *Arabidopsis* homeotic genes *APETALA3* and *PISTILLATA* are sufficient to provide the B class organ identity function. *Development* **122**: 11–22.
- Krizek, B.A., Prost, V., and Macias, A.** (2000). *AINTEGUMENTA* promotes petal identity and acts as a negative regulator of *AGAMOUS*. *Plant Cell* **12**: 1357–66.
- Krizek, B. and Meyerowitz, E.M.** (1996b). Mapping the protein regions responsible for the functional specificities of the *Arabidopsis* MADS domain organ-identity proteins. *Proc. Natl. Acad. Sci. U. S. A.* **93**: 4063–4070.
- L —
- Langmead, B. and Salzberg, S.L.** (2012). Fast gapped-read alignment with Bowtie 2. *Nat. Methods* **9**: 357–359.
- Le, J., Vandenbussche, F., Van Der Straeten, D., and Verbelen, J.P.** (2004). Position and cell type-dependent microtubule reorientation characterizes the early response of the *Arabidopsis* root epidermis to ethylene. *Physiol. Plant.* **121**: 513–519.
- Leister, D., Varotto, C., Pesaresi, P., Niwergall, A., and Salamini, F.** (1999). Large-scale evaluation of plant growth in *Arabidopsis thaliana* by non-invasive image analysis. *Plant Physiol. Biochem.* **37**: 671–678.
- Leyser, O.** (2009). The control of shoot branching: An example of plant information processing. *Plant, Cell Environ.* **32**: 694–703.
- Li, C., Potuschak, T., Colón-Carmona, A., Gutiérrez, R.A., and Doerner, P.** (2005). *Arabidopsis* TCP20 links regulation of growth and cell division control pathways. *Proc. Natl. Acad. Sci. U. S. A.* **102**: 12978–12983.
- Li, J., Wang, Y., Zhang, Y., Wang, W., Irish, V.F., and Huang, T.** (2016). *RABBIT EARS* regulates the transcription of *TCP4* during petal development in *Arabidopsis*. *J. Exp. Bot.* **67**: 6473–6480.
- Li, S.** (2015). The *Arabidopsis thaliana* TCP transcription factors: A broadening horizon beyond development. *Plant Signal. Behav.* **10**: e1044192.
- Liller, C.B., Neuhaus, R., Von Korff, M., Koornneef, M., and Van Esse, W.** (2015). Mutations in barley row type genes have pleiotropic effects on shoot branching. *PLoS One* **10**: 1–20.
- Lin, Y.F., Chen, Y.Y., Hsiao, Y.Y., Shen, C.Y., Hsu, J.L., Yeh, C.M., Mitsuda, N., Ohme-Takagi, M., Liu, Z.J., and Tsai, W.C.** (2016). Genome-wide identification and characterization of TCP genes involved in ovule development of *Phalaenopsis equestris*. *J. Exp. Bot.* **67**: 5051–5066.
- Liu, C. and Weigel, D.** (2015). Chromatin in 3D: Progress and prospects for plants. *Genome Biol.* **16**: 1–6.
- Long, J. and Barton, M.K.** (2000). Initiation of axillary and floral meristems in *Arabidopsis*. *Dev. Biol.* **218**: 341–353.

- Lu, P., Porat, R., Nadeau, J.A., and O'Neill, S.D.** (1996). Identification of a meristem L1 layer-specific gene in *Arabidopsis* that is expressed during embryonic pattern formation and defines a new class of homeobox genes. *Plant Cell* **8**: 2155–68.
- Luo, D., Carpenter, R., Vincent, C., Copsey, L., and Coen, E.** (1995). Origin of floral asymmetry in *Antirrhinum*. *Nature* **383** IS-: 794-799 EP-.
- Lupas, A., Van Dyke, M., and Stock, J.** (1991). Predicting coiled coils from protein sequences. *Science* (80-.). **252**: 1162–1164.
- Lv, B., Tian, H., Zhang, F., Liu, J., Lu, S., Bai, M., Li, C., and Ding, Z.** (2018). Brassinosteroids regulate root growth by controlling reactive oxygen species homeostasis and dual effect on ethylene synthesis in *Arabidopsis*. *PLOS Genet.* **14**: e1007144.
- M –
- Ma, H., Yanofsky, M.F., and Meyerowitz, E.M.** (1991). AGL1-AGL6, an *Arabidopsis* gene family with similarity to floral homeotic and transcription factor genes. *Genes Dev.* **5**: 484–495.
- Ma, J., Liu, F., Wang, Q., Wang, K., Jones, D.C., and Zhang, B.** (2016). Comprehensive analysis of TCP transcription factors and their expression during cotton (*Gossypium arboreum*) fiber early development. *Sci. Rep.* **6**: 1–10.
- Ma, N., Xue, J., Li, Y., Liu, X., Dai, F., Jia, W., Luo, Y., and Gao, J.** (2008). Rh-PIP2;1, a Rose Aquaporin Gene, Is Involved in Ethylene-Regulated Petal Expansion. *Plant Physiol.* **148**: 894–907.
- Ma, Q., Wang, X., Sun, J., and Mao, T.** (2018). Coordinated Regulation of Hypocotyl Cell Elongation by Light and Ethylene through a microtubule destabilizing protein. *Plant Physiol.* **176**: pp.01109.2017.
- Machanick, P. and Bailey, T.L.** (2011). MEME-ChIP: Motif analysis of large DNA datasets. *Bioinformatics* **27**: 1696–1697.
- Maere, S., Heymans, K., and Kuiper, M.** (2005). BiNGO: A Cytoscape plugin to assess overrepresentation of Gene Ontology categories in Biological Networks. *Bioinformatics* **21**: 3448–3449.
- Mandel, A.M., Gustafson-Brown, C., Savidge, B., and Yanofsky, M.F.** (1992). Molecular characterization of the *Arabidopsis* floral homeotic gene APETALA1. *Nature* **360**: 273–277.
- Martín-Fontecha, E.S., Tarancón, C., and Cubas, P.** (2018). To grow or not to grow, a power-saving program induced in dormant buds. *Curr. Opin. Plant Biol.* **41**: 102–109.
- Martín-Trillo, M. and Cubas, P.** (2010). TCP genes: a family snapshot ten years later. *Trends Plant Sci.* **15**: 31–39.
- Mason, M.G., Ross, J.J., Babst, B.A., Wienclaw, B.N., and Beveridge, C.A.** (2014). Sugar demand, not auxin, is the initial regulator of apical dominance. *Proc. Natl. Acad. Sci.* **111**: 6092–6097.
- Mazur, M.J., Spears, B.J., Djajasaputra, A., van der Gragt, M., Vlachakis, G., Beerens, B., Gassmann, W., and van den Burg, H.A.** (2017). *Arabidopsis* TCP Transcription Factors Interact with the SUMO Conjugating Machinery in Nuclear Foci. *Front. Plant Sci.* **8**: 1–18.
- Meister, R.J., Williams, L.A., Monfared, M.M., Gallagher, T.L., Kraft, E.A., Nelson, C.G., and Gasser, C.S.** (2004). Definition and interactions of a positive regulatory element of the *Arabidopsis* Inner No Outer promoter. *Plant J.* **37**: 426–438.
- Menkens, A.E., Schindler, U., and Cashmore, A.R.** (1995). The G-box: a ubiquitous regulatory DNA element in plants bound by the GBF family of bZIP proteins. *Trends Biochem. Sci.* **20**: 506–510.

- Micheli, F.** (2001). Pectin methylesterases: Cell wall enzymes with important roles in plant physiology. *Trends Plant Sci.* **6**: 414–419.
- Mizukami, Y. and Fischer, R.L.** (2000). Plant organ size control: AINTEGUMENTA regulates growth and cell numbers during organogenesis. *Proc. Natl. Acad. Sci. U. S. A.* **97**: 942–947.
- Mizuno, S., Sonoda, M., Tamura, Y., Nishino, E., Suzuki, H., Sato, T., and Oizumi, T.** (2015). Chiba Tendril-Less locus determines tendril organ identity in melon (*Cucumis melo* L.) and potentially encodes a tendril-specific TCP homolog. *J. Plant Res.* **128**: 941–951.
- Monfared, M.M., Simon, M.K., Meister, R.J., Roig-Villanova, I., Kooiker, M., Colombo, L., Fletcher, J.C., and Gasser, C.S.** (2011). Overlapping and antagonistic activities of BASIC PENTACYSSTEINE genes affect a range of developmental processes in Arabidopsis. *Plant J.* **66**: 1020–1021.
- Mourik, H. Van, Muñio, J.M., Pajoro, A., Angenent, G.C., and Kaufmann, K.** (2015). Characterization of In Vivo DNA-Binding Events of Plant Transcription Factors by ChIP-seq: Experimental Protocol and Computational Analysis. In *Methods in Molecular Biology*, pp. 93–121.
- Mu, Y., Zou, M., Sun, X., He, B., Xu, X., Liu, Y., Zhang, L., and Chi, W.** (2017). BASIC PENTACYSSTEINE proteins repress Absciscic Acid INSENSITIVE 4 expression via direct recruitment of the polycomb-repressive complex 2 in arabidopsis root development. *Plant Cell Physiol.* **58**: 607–621.
- Muñio, J.M., Kaufmann, K., van Ham, R.C., Angenent, G.C., and Krajewski, P.** (2011). ChIP-seq Analysis in R (CSAR): An R package for the statistical detection of protein-bound genomic regions. *Plant Methods* **7**: 11.
- Murashige, F. and Skoog, T.** (1962). A revised medium for rapid growth and bioassays with tobacco tissue culture. *Physiol. Plant.* **15**: 473–497.
- N —
- Nag, A., King, S., and Jack, T.** (2009). miR319a targeting of TCP4 is critical for petal growth and development in Arabidopsis. *Proc. Natl. Acad. Sci. U. S. A.* **106**: 22534–22539.
- Nath, U., Crawford, B.C.W., Carpenter, R., and Coen, E.** (2003). Genetic Control of Surface Curvature. *Science* (80-.). **299**: 1404–1407.
- Navaud, O., Dabos, P., Carnus, E., Tremousaygue, D., and Hervé, C.** (2007). TCP transcription factors predate the emergence of land plants. *J. Mol. Evol.* **65**: 23–33.
- Nicolas, M. and Cubas, P.** (2016). TCP factors: new kids on the signaling block. *Curr. Opin. Plant Biol.* **33**: 33–41.
- Nicolas, M. and Cubas, P.** (2015). The Role of TCP Transcription Factors in Shaping Flower Structure, Leaf Morphology, and Plant Architecture (Elsevier Inc.).
- Nietzsche, M., Landgraf, R., Tohge, T., and Börnke, F.** (2016). A protein-protein interaction network linking the energy-sensor kinase SnRK1 to multiple signaling pathways in Arabidopsis thaliana. *Curr. Plant Biol.* **5**: 36–44.
- Niwa, M., Daimon, Y., Kurotani, K., Higo, A., Pruneda-Paz, J.L., Breton, G., Mitsuda, N., Kay, S.A., Ohme-Takagi, M., Endo, M., and Araki, T.** (2013). BRANCHED1 Interacts with FLOWERING LOCUS T to Repress the Floral Transition of the Axillary Meristems in Arabidopsis. *Plant Cell* **25**: 1228–42.
- Noda, K., Glover, B.J., Linstead, P., and Martin, C.** (1994). Flower colour intensity depends on specialized cell shape controlled by a Myb-related transcription factor. *Nature* **369**: 661–664.
- Nowak, M.A., Boerlijst, M.C., Cooke, J., and Smith, J.M.** (1997). Evolution of genetic redundancy. *Nature* **388**: 167–170.

Nutt, P., Ziermann, J., Hintz, M., Neuffer, B., and Theißen, G. (2006). Capsella as a model system to study the evolutionary relevance of floral homeotic mutants. *Plant Syst. Evol.* **259**: 217–235.

– O –

O'Malley, R.C., Huang, S. shan C., Song, L., Lewsey, M.G., Bartlett, A., Nery, J.R., Galli, M., Gallavotti, A., and Ecker, J.R. (2016). Cistrome and Epicistrome Features Shape the Regulatory DNA Landscape. *Cell* **166**: 1598.

Ori, N. et al. (2007). Regulation of LANCEOLATE by miR319 is required for compound-leaf development in tomato. *Nat. Genet.* **39**: 787–791.

Ortiz-Ramírez, C., Hernandez-Coronado, M., Thamm, A., Catarino, B., Wang, M., Dolan, L., Feijó, J.A.A., and Becker, J.D.D. (2016). A Transcriptome Atlas of *Physcomitrella patens* Provides Insights into the Evolution and Development of Land Plants. *Mol. Plant* **9**: 205–220.

– P –

Palatnik, J.F., Allen, E., Wu, X.L., Schommer, C., Schwab, R., Carrington, J.C., and Weigel, D. (2003). Control of leaf morphogenesis by microRNAs. *Nature* **425**: 257–263.

Panikashvili, D., Shi, J.X., Schreiber, L., and Aharoni, A. (2011). The Arabidopsis ABCG13 transporter is required for flower cuticle secretion and patterning of the petal epidermis. *New Phytol.* **190**: 113–124.

Parapunova, V., Busscher, M., Busscher-Lange, J., Lammers, M., Karlova, R., Bovy, A.G., Angenent, G.C., and De Maagd, R.A. (2014). Identification, cloning and characterization of the tomato TCP transcription factor family. *BMC Plant Biol.* **14**: 1–17.

Parenicova, L., De Folter, S., Kieffer, M., Horner, D.S., Favalli, C., Busscher, J., Cook, H.E., Ingram, R.M., Kater, M.M., Davies, B., Angenent, G.C., and Colombo, L. (2003). Molecular and Phylogenetic Analyses of the Complete MADS-Box Transcription Factor Family in Arabidopsis: New Openings to the MADS World. *Plant Cell Online* **15**: 1538–1551.

Park, S.J., Jiang, K., Tal, L., Yichie, Y., Gar, O., Zamir, D., Eshed, Y., and Lippman, Z.B. (2014). Optimization of crop productivity in tomato using induced mutations in the florigen pathway. *Nat. Genet.* **46**: 1337–1342.

Paul-Victor, C. and Turnbull, L.A. (2009). The effect of growth conditions on the seed size/number trade-off. *PLoS One* **4**.

Paul, L.K., Rinne, P.L.H., and Van der Schoot, C. (2014). Shoot meristems of deciduous woody perennials: Self-organization and morphogenetic transitions. *Curr. Opin. Plant Biol.* **17**: 86–95.

Pei, H., Ma, N., Tian, J., Luo, J., Chen, J., Li, J., Zheng, Y., Chen, X., Fei, Z., and Gao, J. (2013). An NAC transcription factor controls ethylene-regulated cell expansion in flower petals. *Plant Physiol.* **163**: 775–91.

Pierik, R., Tholen, D., Poorter, H., Visser, E.J.W., and Voesenek, L.A.C.J. (2006). The Janus face of ethylene: growth inhibition and stimulation. *Trends Plant Sci.* **11**: 176–183.

Pieterse, C.M.J., Van der Does, D., Zamioudis, C., Leon-Reyes, A., and Van Wees, S.C.M. (2012). Hormonal Modulation of Plant Immunity. *Annu. Rev. Cell Dev. Biol.* **28**: 489–521.

Plett, J.M., Mathur, J., and Regan, S. (2009). Ethylene receptor ETR2 controls trichome branching by regulating microtubule assembly in arabidopsis thaliana. *J. Exp. Bot.* **60**: 3923–3933.

Van de Poel, B., Smet, D., and Van Der Straeten, D. (2015). Ethylene and Hormonal Cross Talk in Vegetative Growth and Development. *Plant Physiol.* **169**: 61–72.

- Prescott, A.M., McCollough, F.W., Eldreth, B.L., Binder, B.M., and Abel, S.M.** (2016). Analysis of Network Topologies Underlying Ethylene Growth Response Kinetics. *Front. Plant Sci.* **7**.
- Pruneda-Paz, J.L., Breton, G., Para, A., and Kay, S.A.** (2009). A Functional Genomics Approach Reveals CHE as a Component of the Arabidopsis Circadian Clock. *Science* (80-.). **583**: 1481–1486.
- Puranik, S. et al.** (2014). Structural Basis for the Oligomerization of the MADS Domain Transcription Factor SEPALLATA3 in Arabidopsis. *Plant Cell* **26**: 3603–3615.
- R —
- Rai, M.I., Wang, X., Thibault, D.M., Kim, H.J., Bombyk, M.M., Binder, B.M., Shakeel, S.N., and Schaller, G.E.** (2015). The ARGOS gene family functions in a negative feedback loop to desensitize plants to ethylene. *BMC Plant Biol.* **15**: 157.
- Ramsay, L. et al.** (2011). INTERMEDIUM-C, a modifier of lateral spikelet fertility in barley, is an ortholog of the maize domestication gene TEOSINTE BRANCHED 1. *Nat. Genet.* **43**: 169–72.
- Rauf, M., Arif, M., Fisahn, J., Xue, G.-P., Balazadeh, S., and Mueller-Roeber, B.** (2013). NAC Transcription Factor SPEEDY HYPOPLASTIC GROWTH Regulates Flooding-Induced Leaf Movement in Arabidopsis. *Plant Cell* **25**: 4941–4955.
- Reddy, S.K., Holalu, S. V., Casal, J.J., and Finlayson, S.A.** (2013). Abscissic Acid Regulates Axillary Bud Outgrowth Responses to the Ratio of Red to Far-Red Light. *Plant Physiol.* **163**: 1047–1058.
- Remigereau, M.S., Lakis, G., Rekima, S., Leveugle, M., Fontaine, M.C., Langin, T., Sarr, A., and Robert, T.** (2011). Cereal domestication and evolution of branching: Evidence for soft selection in the TB1 orthologue of pearl millet (*Pennisetum glaucum* [L.] R. Br.). *PLoS One* **6**.
- Ren, H., Dang, X., Cai, X., Yu, P., Li, Y., Zhang, S., Liu, M., Chen, B., and Lin, D.** (2017). Spatio-temporal orientation of microtubules controls conical cell shape in Arabidopsis thaliana petals. *PLoS Genet.* **13**: 1–23.
- Riechmann, J.** (1996). DNA-binding properties of Arabidopsis MADS domain homeotic proteins APETALA1, APETALA3, PISTILLATA and AGAMOUS. *Proc. Natl. Acad. Sci. U. S. A.* **93**: 4793–4798.
- Riechmann, J.L. et al.** (2000). Arabidopsis transcription factors: Genome-wide comparative analysis among eukaryotes. *Science* (80-.). **290**: 2105–2110.
- Rinne, P.L.H., Kaikuranta, P.M., and Van Schoot, C. Der** (2001). The shoot apical meristem restores its symplasmic organization during chilling-induced release from dormancy. *Plant J.* **26**: 249–264.
- Rinne, P.L.H., Paul, L.K., Vahala, J., Kangasjärvi, J., and Van Der Schoot, C.** (2016). Axillary buds are dwarfed shoots that tightly regulate GA pathway and GA-inducible 1,3-β-glucanase genes during branching in hybrid aspen. *J. Exp. Bot.* **67**: 5975–5991.
- Rodrigues, A. et al.** (2013). ABI1 and PP2CA Phosphatases Are Negative Regulators of Snf1-Related Protein Kinase1 Signaling in Arabidopsis. *Plant Cell* **25**: 3871–3884.
- Rodríguez-Álvarez, M.X., Boer, M.P., van Eeuwijk, F.A., and Eilers, P.H.C.** (2016). Spatial Models for Field Trials.: 1–39.
- Roeder, A.H.K., Cunha, A., Ohno, C.K., and Meyerowitz, E.M.** (2012). Cell cycle regulates cell type in the Arabidopsis sepal. *Development* **139**: 4416–4427.
- Rogers, H.J.** (2013). From models to ornamentals: How is flower senescence regulated? *Plant Mol. Biol.* **82**: 563–574.
- van Rooijen, R., Aarts, M.G.M., and Harbinson, J.** (2015). Natural genetic variation for acclimation of

- photosynthetic light use efficiency to growth irradiance in *Arabidopsis thaliana*. *Plant Physiol.* **167**: pp.114.252239.
- Rubio-Somoza, I. and Weigel, D.** (2013). Coordination of Flower Maturation by a Regulatory Circuit of Three MicroRNAs. *PLoS Genet.* **9**.
- S –
- Sauret-Güeto, S., Schiessl, K., Bangham, A., Sablowski, R., and Coen, E.** (2013). JAGGED Controls *Arabidopsis* Petal Growth and Shape by Interacting with a Divergent Polarity Field. *PLoS Biol.* **11**.
- Savaldi-Goldstein, S., Peto, C., and Chory, J.** (2007). The epidermis both drives and restricts plant shoot growth. *Nature* **446**: 199–202.
- Schiessl, K., Muño, J.M., and Sablowski, R.** (2014). *Arabidopsis* JAGGED links floral organ patterning to tissue growth by repressing Kip-related cell cycle inhibitors. *Proc. Natl. Acad. Sci. U. S. A.* **111**: 2830–5.
- Schommer, C., Palatnik, J.F., Aggarwal, P., Chételat, A., Cubas, P., Farmer, E.E., Nath, U., and Weigel, D.** (2008). Control of jasmonate biosynthesis and senescence by miR319 targets. *PLoS Biol.* **6**: 1991–2001.
- Shannon, P., Markiel, A., Ozier, O., Baliga, N.S., Wang, J.T., Ramage, D., Amin, N., Schwikowski, B., and Ideker, T.** (2003). Cytoscape: a software environment for integrated models of biomolecular interaction networks. *Genome Res.*: 2498–2504.
- Shi, J.X., Malitsky, S., de Oliveira, S., Branigan, C., Franke, R.B., Schreiber, L., and Aharoni, A.** (2011). SHINE transcription factors act redundantly to pattern the archetypal surface of *arabidopsis* flower organs. *PLoS Genet.* **7**.
- Shirley, H.L.** (1929). The Influence of Light Intensity and Light Quality Upon the Growth of Plants. *Am. J. Bot.* **16**: 354.
- Simon, M., Bruex, A., Kainkaryam, R.M., Zheng, X., Huang, L., Woolf, P.J., and Schiefelbein, J.** (2013). Tissue-specific profiling reveals transcriptome alterations in *Arabidopsis* mutants lacking morphological phenotypes. *Plant Cell* **25**: 3175–3185.
- Simonini, S., Roig-Villanova, I., Gregis, V., Colombo, B., Colombo, L., and Kater, M.M.** (2012). BASIC PENTACYSSTEINE Proteins Mediate MADS Domain Complex Binding to the DNA for Tissue-Specific Expression of Target Genes in *Arabidopsis*. *Plant Cell* **24**: 4163–4172.
- Smaczniak, C., Immink, R.G.H., Muño, J.M., Blanvillain, R., Busscher, M., Busscher-Lange, J., Dinh, Q.D.P., Liu, S., Westphal, A.H., Boeren, S., and others** (2012a). Characterization of MADS-domain transcription factor complexes in *Arabidopsis* flower development. *Proc. Natl. Acad. Sci.* **109**: 1560–1565.
- Smaczniak, C., Li, N., Boeren, S., America, T., Van Dongen, W., Goerdal, S.S., De Vries, S., Angenent, G.C., and Kaufmann, K.** (2012b). Proteomics-based identification of low-abundance signaling and regulatory protein complexes in native plant tissues. *Nat. Protoc.* **7**: 2144–2158.
- Smaczniak, C., Muño, J.M., Chen, D., Angenent, G.C., and Kaufmann, K.** (2017). Differences in DNA-binding specificity of floral homeotic protein complexes predict organ-specific target genes. *Plant Cell*: tpc.00145.2017.
- Smyth, D.R., Bowman, J.L., and Meyerowitz, E.M.** (1990). Early flower development in *Arabidopsis*. *Plant Cell* **2**: 755–767.
- Sreenivasulu, N. and Schnurbusch, T.** (2012). A genetic playground for enhancing grain number in cereals. *Trends Plant Sci.* **17**: 91–101.

- Sugio, A., Kingdom, H.N., MacLean, A.M., Grieve, V.M., and Hogenhout, S.A.** (2011). Phytoplasma protein effector SAP11 enhances insect vector reproduction by manipulating plant development and defense hormone biosynthesis. *Proc. Natl. Acad. Sci.* **108**: E1254–E1263.
- Szecsí, J., Joly, C., Bordji, K., Varaud, E., Cock, J.M., Dumas, C., and Bendahmane, M.** (2006). BIGPETALp, a bHLH transcription factor is involved in the control of Arabidopsis petal size. *EMBO J.* **25**: 3912–3920.
- Szécsi, J., Wipperman, B., and Bendahmane, M.** (2014). Genetic and phenotypic analyses of petal development in Arabidopsis. In *Methods in Molecular Biology*, pp. 191–202.

– T –

- Takeda, S., Matsumoto, N., and Okada, K.** (2004). RABBIT EARS, encoding a SUPERMAN-like zinc finger protein, regulates petal development in Arabidopsis thaliana. *Development* **131**: 425–434.
- Takeda, T., Amano, K., Ohto, M.A., Nakamura, K., Sato, S., Kato, T., Tabata, S., and Ueguchi, C.** (2006). RNA interference of the Arabidopsis putative transcription factor TCP16 gene results in abortion of early pollen development. *Plant Mol. Biol.* **61**: 165–177.
- Takeda, T., Suwa, Y., Suzuki, M., Kitano, H., Ueguchi-Tanaka, M., Ashikari, M., Matsuoka, M., and Ueguchi, C.** (2003). The OsTB1 gene negatively regulates lateral branching in rice. *Plant J.* **33**: 513–520.
- Tapia-Lopez, R., Garcia-Ponce, B., Dubrovsky, J.G., Garay-Arroyo, A., Perez-Ruiz, R. V., Kim, S.-H., Acevedo, F., Pelaz, S., and Alvarez-Buylla, E.R.** (2008). An AGAMOUS-Related MADS-Box Gene, XAL1 (AGL12), Regulates Root Meristem Cell Proliferation and Flowering Transition in Arabidopsis. *Plant Physiol.* **146**: 1182–1192.
- Tatematsu, K.** (2005). Identification of cis-Elements That Regulate Gene Expression during Initiation of Axillary Bud Outgrowth in Arabidopsis. *Plant Physiol.* **138**: 757–766.
- Tatematsu, K., Nakabayashi, K., Kamiya, Y., and Nambara, E.** (2008). Transcription factor AtTCP14 regulates embryonic growth potential during seed germination in Arabidopsis thaliana. *Plant J.* **53**: 42–52.
- Theissen, G. and Saedler, H.** (2001). Floral Quartets. *Nature* **409**: 469–471.
- Thomas, J.H.** (1993). Thinking about genetic redundancy. *Trends Genet.* **9**: 395–399.
- Todesco, M. et al.** (2010). Natural allelic variation underlying a major fitness trade-off in Arabidopsis thaliana. *Nature* **465**: 632–636.
- Tomé, F., Nägele, T., Adamo, M., Garg, A., Marco-Ilorca, C., Nukarinen, E., Pedrotti, L., Peviani, A., Simeunovic, A., Tatkiewicz, A., Tomar, M., and Gamm, M.** (2014). The low energy signaling network. *Front. Plant Sci.* **5**: 1–12.
- Trapnell, C., Roberts, A., Goff, L., Pertea, G., Kim, D., Kelley, D.R., Pimentel, H., Salzberg, S.L., Rinn, J.L., and Pachter, L.** (2012). Differential gene and transcript expression analysis of RNA-seq experiments with TopHat and Cufflinks. *Nat. Protoc.* **7**: 562–78.
- Tsuchisaka, A. and Theologis, A.** (2004). Unique and Overlapping Expression Patterns among the Arabidopsis 1-Amino-Cyclopropane-1-Carboxylate Synthase Gene Family Members. *Plant Physiol.* **136**: 2982–3000.

– U –

- Uberti-Manassero, N.G., Lucero, L.E., Viola, I.L., Vegetti, A.C., and Gonzalez, D.H.** (2012). The class I protein AtTCP15 modulates plant development through a pathway that overlaps with the one affected by CIN-like TCP proteins. *J. Exp. Bot.* **63**: 809–823.
- Uberti Manassero, N.G., Viola, I.L., Welchen, E., and Gonzalez, D.H.** (2013). TCP transcription factors:

architectures of plant form. *Biomol. Concepts* **4**.

- Urbanus, S.L., Martinelli, A.P., Dinh, Q.D., Aizza, L.C.B., Dornelas, M.C., Angenent, G.C., and Immink, R.G.H. (2010). Intercellular transport of epidermis-expressed MADS domain transcription factors and their effect on plant morphology and floral transition. *Plant J.* **63**: 60–72.

– V –

- Varaud, E., Brioudes, F., Szécsi, J., Leroux, J., Brown, S., Perrot-Rechenmann, C., and Bendahmane, M. (2011). AUXIN RESPONSE FACTOR8 regulates Arabidopsis petal growth by interacting with the bHLH transcription factor BIGPETALp. *Plant Cell* **23**: 973–83.
- Velazco, J.G., Rodríguez-Álvarez, M.X., Boer, M.P., Jordan, D.R., Eilers, P.H.C., Malosetti, M., and van Eeuwijk, F.A. (2017). Modelling spatial trends in sorghum breeding field trials using a two-dimensional P-spline mixed model. *Theor. Appl. Genet.* **130**: 1375–1392.
- Vergara, R., Noriega, X., Aravena, K., Prieto, H., and Pérez, F.J. (2017). ABA Represses the Expression of Cell Cycle Genes and May Modulate the Development of Endodormancy in Grapevine Buds. *Front. Plant Sci.* **8**: 1–10.
- Viola, I.L., Reinheimers, R., Ripoll, R., Uberti Manassero, N.G., and Gonzalez, D.H. (2012). Determinants of the DNA binding specificity of class I and class II TCP transcription factors. *J. Biol. Chem.* **287**: 347–356.
- Viola, I.L., Uberti Manassero, N.G., Ripoll, R., and Gonzalez, D.H. (2011). The *Arabidopsis* class I TCP transcription factor AtTCP11 is a developmental regulator with distinct DNA-binding properties due to the presence of a threonine residue at position 15 of the TCP domain. *Biochem. J.* **435**: 143–155.

– W –

- Wagstaff, C., Yang, T.J.W., Stead, A.D., Buchanan-Wollaston, V., and Roberts, J.A. (2009). A molecular and structural characterization of senescing Arabidopsis siliques and comparison of transcriptional profiles with senescing petals and leaves. *Plant J.* **57**: 690–705.
- Wang, S., Yang, X., Xu, M., Lin, X., Lin, T., Qi, J., Shao, G., Tian, N., Yang, Q., Zhang, Z., and Huang, S. (2015a). A Rare SNP Identified a TCP Transcription Factor Essential for Tendril Development in Cucumber. *Mol. Plant* **8**: 1795–1808.
- Wang, X., Gao, J., Zhu, Z., Dong, X., Wang, X., Ren, G., Zhou, X., and Kuai, B. (2015b). TCP transcription factors are critical for the coordinated regulation of *ISOCHORISMATE SYNTHASE 1* expression in *Arabidopsis thaliana*. *Plant J.* **82**: 151–162.
- Wang, X., Zhu, L., Liu, B., Wang, C., Jin, L., Zhao, Q., and Yuan, M. (2007). Arabidopsis MICROTUBULE-ASSOCIATED PROTEIN18 Functions in Directional Cell Growth by Destabilizing Cortical Microtubules. *Plant Cell Online* **19**: 877–889.
- Weaver, L.M. and Amasino, R.M. (2001). Senescence is induced in individually darkened Arabidopsis leaves, but inhibited in whole darkened plants. *Plant Physiol.* **127**: 876–886.
- Weaver, L.M., Gan, S., Quirino, B., and Amasino, R.M. (1998). A comparison of the expression patterns of several senescence-associated genes in response to stress and hormone treatment. *Plant Mol. Biol.* **37**: 455–469.
- Weiss, J., Delgado-Benarroch, L., and Egea-Cortines, M. (2005). Genetic control of floral size and proportions. *Int. J. Dev. Biol.* **49**: 513–525.
- Wellmer, F., Alves-Ferreira, M., Dubois, A., Riechmann, J.L., and Meyerowitz, E.M. (2006). Genome-wide

- analysis of gene expression during early *Arabidopsis* flower development. *PLoS Genet.* **2**.
- Weraduwage, S.M., Chen, J., Anozie, F.C., Morales, A., Weise, S.E., and Sharkey, T.D.** (2015). The relationship between leaf area growth and biomass accumulation in *Arabidopsis thaliana*. *Front. Plant Sci.* **6**: 1–21.
- Werner, T., Motyka, V., Laucou, V., Smets, R., Onckelen, H. Van, and Schmuelling, T.** (2003). Cytokinin-Deficient Transgenic *Arabidopsis* Plants Show Functions of Cytokinins in the Regulation of Shoot and Root Meristem Activity. *Plant Cell* **15**: 2532–2550.
- Weßling, R. et al.** (2014). Convergent targeting of a common host protein-network by pathogen effectors from three kingdoms of life. *Cell Host Microbe* **16**: 364–375.
- Y –
- Yao, C. and Finlayson, S.A.** (2015). Absciscic Acid Is a General Negative Regulator of *Arabidopsis* Axillary Bud Growth. *Plant Physiol.* **169**: 611–626.
- Yu, C.-P., Lin, J.-J., and Li, W.-H.** (2016). Positional distribution of transcription factor binding sites in *Arabidopsis thaliana*. *Sci. Rep.* **6**: 25164.
- Z –
- Zhang, C. et al.** (2016). Suppression of Jasmonic Acid-Mediated Defense by Viral-Inducible MicroRNA319 Facilitates Virus Infection in Rice. *Mol. Plant* **9**: 1302–1314.
- Zhang, Y., Liu, T., Meyer, C.A., Eeckhoute, J., Johnson, D.S., Bernstein, B.E., Nussbaum, C., Myers, R.M., Brown, M., Li, W., and Shirley, X.S.** (2008). Model-based analysis of ChIP-Seq (MACS). *Genome Biol.* **9**.
- Zhou, M., Li, D., Li, Z., Hu, Q., Yang, C., Zhu, L., and Luo, H.** (2013). Constitutive Expression of a miR319 Gene Alters Plant Development and Enhances Salt and Drought Tolerance in Transgenic Creeping Bentgrass. *Plant Physiol.* **161**: 1375–1391.
- Zhou, Y., Zhang, D., An, J., Yin, H., Fang, S., Chu, J., Zhao, Y., and Li, J.** (2017). TCP transcription factors regulate shade avoidance via directly mediating the expression of both PHYTOCHROME INTERACTING FACTORS and auxin biosynthetic genes. *Plant Physiol.*: pp.01566.2017.
- Zong, Y., Wang, Y., Li, C., Zhang, R., Chen, K., Ran, Y., Qiu, J.L., Wang, D., and Gao, C.** (2017). Precise base editing in rice, wheat and maize with a Cas9-cytidine deaminase fusion. *Nat. Biotechnol.* **35**: 438–440.

Summary

Plant growth and the developmental program that orchestrates it appears to be strictly controlled. Cell division and expansion represent the major growth determinants and these growth parameters together with differentiation determine the size, shape and final appearance of a plant and its organs. It is the interplay between numerous genetic, hormonal and structural factors that makes the phenotype of a plant. Transcription factors (TFs) are major regulators of genes that are directly involved in these processes, such as cell cycle genes, or genes that are more indirectly involved in growth, e.g. genes coding for hormone biosynthesis or signalling proteins. Therefore, in this PhD-thesis research, I focussed on transcriptional regulation of growth. Members of the TCP family of TFs have long been known as regulators of plant growth, either by directly regulating cell cycle genes or indirectly through regulating the biosynthesis or signalling networks of different hormones, making them ideal candidates for our studies. Phenotypes of several members of this TF family have been characterised and molecular modes of action unravelled. This notwithstanding, our knowledge about this family is still very fragmented. The aim of my research was to contribute to our understanding of the TCP transcription factor family, starting in **chapter 1** with an overview of the existing knowledge and state-of-the art on TCP TF research. Experimentally, I used several approaches, from sophisticated quantitative phenotyping, TCP function analysis, to genome-wide DNA binding sites analysis.

The TCP TF family has long been known to affect plant growth and development at different moments during the life cycle of a plant. In **chapter 2** we implemented a phenotyping platform and created an algorithm that allowed us to analyse different aspects of rosette growth separately for a large collection of *tcp* mutants. We analysed growth speed, the time until plants reach this maximum growth, the final rosette size and circadian leaf movement for all plants individually and compared the *tcp* mutants to wild type controls for these aspects. Next to this, we analysed phenotypic effects of possible genetic interactions between single and multiple TCP mutants and investigated possible correlations between phenotypic characteristics, such as vegetative growth parameters versus several yield parameters, including total seed yield, seed number and seed weight.

These analyses showed the importance of comprehensive and comparative phenotyping of mutants and of detailed quantitative analyses in order to get a full understanding of the contribution of individual members of the TCP TF family to particular biological functions. It had for example previously been proposed that class I and class II TCP TFs fulfil opposite functions in plant growth and development, but interestingly, we revealed that this hypothesis needs revision, as mutation in members from both classes showed similar developmental effects.

Additionally, the supposed functional redundancy within particular sub-clades of the TCP TF family was analysed, revealing that stacking of mutations in several TCPs led in some cases to less severe phenotypes in comparison with single mutant phenotypes instead of the expected increased phenotypic effects. For some genes supposed to act redundantly, such as *BRANCHED1* (*BRC1*) and *BRC2*, contrasting phenotypes were found for particular traits in their respective single mutants. The *brc1* and *brc2* mutants are known to show altered axillary branch numbers, but we have shown that other members of the TCP TF family affect this trait as well and that this coincides with a reduction in seed yield under the applied environmental conditions. Additionally, we could confirm the link between several seed characteristics using correlation analysis. An increase in seed number for example appeared to be negatively correlated to both seed area and seed weight. This negative correlation has been found previously and is in line with an earlier proposed model describing a fixed amount of resources allocated to reproduction.

TCP TFs have historically been described as regulators of cell proliferation through directly acting upon cell cycle genes. As of recent, more and more studies suggest a role for TCPs as regulators of hormone biosynthesis and signalling, which then indirectly affects cell proliferation.

In this thesis, I have both confirmed and strengthened this hypothesis by showing in **chapter 3** that TCP5 is able to bind regulatory sequences of the ethylene biosynthesis gene *ACS2*, thereby providing an explanation for its observed repression upon TCP5 induction. Overexpression of *TCP5* in petal epidermal cells results in smaller petals, whereas *tcp5tcp13tcp17* triple knockout lines have wider petals with an increased surface area. We could show that mutants of *TCP5*-like TFs have effects on the expression of genes related to cell cycle, growth regulation, and organ growth. An experiment in which we induced *TCP5* expression revealed differential expression of the ethylene biosynthesis genes 1-amino-cyclopropane-1-carboxylate (ACC) synthase 2 (*ACS2*) and ACC oxidase 2 (*ACO2*) and several ETHYLENE RESPONSE FACTORS (*ERFs*). Chromatin immunoprecipitation–quantitative PCR showed direct binding of TCP5 to the *ACS2* locus *in vivo*. The petal phenotype of the *tcp5tcp13tcp17* mutant could be complemented by treatment of the plants with the ethylene pathway inhibitor STS.

Several ethylene biosynthesis and signalling mutants are known to show alterations in cell and organ size. A possible explanation for this is the effect ethylene has on microtubule orientation, a process known to affect the direction of cell elongation and to be involved in conical cell development.

Next to this, in **chapter 4** we used chromatin immunoprecipitation coupled to next generation sequencing (ChIP-seq), in concert with transcriptome sequencing by RNA-seq to determine direct genome-wide targets of BRC1, aiming to elucidate the molecular mode of action of BRC1 in axillary

bud dormancy. We showed that BRC1 is able to regulate abscisic acid biosynthesis and signalling through direct binding of regulatory sequences of several ABA biosynthesis and signalling genes, including *NCED3*, *NCED9* and *ABA2*. ABA is not the only hormone regulated by BRC1, because we found two CK oxidases and several CK signalling genes to be directly regulated by BRC1. These direct effects on ABA and CK pathways, together with the binding of several other gene loci, including genes involved in cell wall composition and genes with a potential role in symplastic intercellular connectivity, provide a molecular and potential mechanistic basis for the functioning of BRC1 in the repression of axillary bud outgrowth, a well-known conserved role for *BRC1*-like TFs in plant development.

We used the data on binding events to search for a putative consensus binding site that is centrally enriched in the BRC1 ChIP-seq peaks, resulting in the identification of the cis-element 'GDCCCA', which is close to previously observed consensus TCP binding sites. Additionally, we identified enrichment of the 'G-box' either up- or downstream of the centrally enriched consensus TCP binding site, which allows to speculate on coregulatory networks and interaction partners of BRC1.

Transcription factors commonly regulate genes and processes through the cooperation with other TFs. In **chapter 5** we describe the physical interaction between the floral organ identity specifying MADS domain protein APETALA1 (AP1) and a TCP known for its role in petal development, TCP5. This physical interaction could provide proof for a direct link between floral organ identity specification and growth. However, to confirm this we need a way to show the relevance of this interaction *in planta*. We describe a method by which this can be accomplished, using a library of randomly mutagenized alleles of both *AP1* and *TCP5*, created by error prone PCR. Subsequently, a Y2H assay was performed to find 'edgetic' alleles in which only the interaction of AP1-TCP5 was disturbed, while the well-known heterodimeric interactions of AP1 with other MADS domain proteins were maintained. We show by screening six mutated AP1 alleles the potential of this approach, using it for example to identify the regions within the respective proteins and the exact amino acids vital for such an interaction. Finally, we describe the possibilities of this technique and we provide suggestions for several strategies to scale-up this assay and to continue it by further functional characterisation *in planta*.

Besides the core functions identified in plant development, TCP genes appear to act in many more processes, ranging from pathogen susceptibility to nutrient and hormonal signalling, aspects that I have elaborated upon in **chapter 6**. Due to their multifaceted functionality and existing functional redundancy, revealing the exact roles and functions of individual TCP proteins in a plant's life cycle remains incredibly interesting but complicated and challenging.

Samenvatting

De manier waarop planten groeien en het ontwikkelingsprogramma dat dit dirigeert worden erg strak gecontroleerd. Of je nu kijkt naar de bladeren van een plant, de takken of specifieke bloemorganen; talloze genetische, hormonale en structurele factoren bepalen het bouwplan en uiteindelijke voorkomen en van een plant.

Celdeling en cel differentiatie zijn de belangrijkste factoren die groei bepalen. Met andere woorden: de uiteindelijke plant en zijn organen worden gecreëerd door de aantallen, grootte en vorm van cellen. Transcriptiefactoren (TF) reguleren genen die direct betrokken zijn bij bovengenoemde processen, zoals celcyclus genen. Een andere mogelijkheid is dat de expressie van genen gestuurd wordt die indirect betrokken zijn bij groei en ontwikkeling, zoals hormoon biosynthese en signalering. In dit PhD onderzoek heb ik mij toegelegd op de transcriptionele regulatie van groei. Leden van de TCP familie van TF staan al langer bekend als regulatoren van dit proces, ofwel direct middels regulatie van de cel cyclus ofwel indirect via het reguleren van hormoon biosynthese. Dit maakt ze ideale kandidaten voor studies naar de regulatie van groei en ontwikkeling. Er zijn al vrij veel fenotypes beschreven en moleculaire mechanismen ontrafeld voor leden van de familie. Niettemin is onze kennis nog vrij gefragmenteerd en het doel van mijn onderzoek was dan ook om het inzicht in de TCP TF familie te vergroten. In **hoofdstuk 1** begon ik met een overzicht van de beschikbare kennis en stand van zaken in het TCP onderzoek. Ik heb verscheidene experimentele methoden gebruikt, van kwantitatieve fenotypering en TCP functie analyse, tot analyses van TCP bindingsplaatsen op genoomwijde schaal.

De TCP familie staat bekend om hun effect op ontwikkeling en groei, tijdens verschillende momenten in de levenscyclus van een plant. In **hoofdstuk 2** combineren we een fenotyperings-platform met een algoritme dat we ontwikkelden om verschillende aspecten van rozet groei voor een grote collectie *tcp* mutanten te analyseren. Deze combinatie gaf ons de mogelijkheid om zowel groeisnelheid te meten, als de tijd die een plant nodig heeft om tot de maximale groei te komen, de uiteindelijke rozet grootte, en de bewegingen van het blad als resultaat van het dag-nacht ritme van een plant. Deze karakteristieken hebben we voor elke plant afzonderlijk bepaald en vergeleken met de wild type controle. Hiernaast hebben we enkele en dubbele *TCP* mutanten geanalyseerd om mogelijke fysieke interacties aan te tonen. Ook hebben we correlaties tussen verschillende karakteristieken in kaart gebracht, zoals de hierboven beschreven vegetatieve groei parameters en verscheidene opbrengst variabelen zoals totale zaad opbrengst, zaad aantallen en het gewicht.

Deze analyses hebben het belang laten zien van uitgebreide en vergelijkende fenotypering van mutanten. Hiernaast zijn ook kwantitatieve analyses van belang om een volledig beeld te

verkrijgen van de rol die de verschillende *TCP* genen hebben in de processen die we onderzochten. Zo werd voorheen voorgesteld dat de twee klassen TCP TF tegenovergestelde functies uitoefenden in de groei en ontwikkeling van een plant. Interessant genoeg hebben wij laten zien dat deze hypothese opnieuw bekeken dient te worden, aangezien leden van beide klassen dezelfde fenotypes lieten zien. Daarnaast hebben we ook onderzoek gedaan naar de veronderstelde functionele ‘overbodigheid’ van genen binnen groepen TCP TF. We lieten zien dat het stapelen van mutaties in verschillende TCP genen in sommige gevallen leidt tot minder ernstige fenotypes in vergelijking met de enkele mutant, in plaats van de verwachte versterking. Sommige genen waarvan we verwachtten dat een combinatie elkaar zou versterken, zoals *BRANCHED1 (BRC1)* en *BRC2*, lieten verrassend genoeg contrasterende fenotypes zien. De *brc1* en *brc2* mutanten staan al langer bekend om hun effect op het aantal scheuten dat vanuit de Arabidopsis rozet gevormd wordt. Hiernaast hebben wij een aantal andere TCP mutanten gekarakteriseerd. Ook vonden we een link tussen verscheidene zaadeigenschappen middels correlatie analyse. Een toename in bijvoorbeeld aantal zaden lijkt negatief gecorreleerd te zijn met zaadgrootte en zaadgewicht. Deze negatieve correlatie is eerder gevonden en sluit aan bij de hypothese dat er een vaste hoeveelheid grondstoffen zijn voor zaad productie.

Sinds de ontdekking van TCP TF als aparte groep genen zijn ze beschreven als directe regulatoren van celdeling middels het aansturen van cel cycli genen. Er verschijnt er meer en meer bewijs dat TCP genen de biosynthese van verschillende hormonen reguleren en daarmee wellicht indirect cel deling aansturen.

In dit proefschrift heb ik deze hypothese zowel bevestigd als versterkt in **hoofdstuk 3** en **hoofdstuk 4**. In **hoofdstuk 3** laat ik zien dat TCP5 regulatorie sequenties bindt van *ACS2*, en daarmee hoogstwaarschijnlijk ethyleen biosynthese reguleert. Overexpressie van *TCP5* in kroonbladen resulteert in kleinere, smallere kroonbladen, terwijl de drievoudige *tcp5tcp13tcp17* knock-out grotere en bredere kroonbladen vormt. We hebben laten zien dat *TCP5* effect heeft op de expressie van genen die gerelateerd zijn aan celcyclus, groeiregulatie en orgaangroei. Een experiment waarin we *TCP5* induceerden resulteerde in verandering in expressie van verschillende ethyleen biosynthese genen zoals *ACS2*, *ACO2* en verscheidene *ERFs*. Het fenotype van de triple *tcp5tcp13tcp17* mutant is op te heffen door de ethyleen signalering te blokkeren. Er zijn verscheidene voorbeelden van mutanten in ethyleenbiosynthese en -signalering die veranderingen in cel grootte tonen.

In **hoofdstuk 4** hebben we ChIP gekoppeld aan ‘next generation sequencing’ (ChIP-seq), tezamen met RNA-seq. Dit om directe doelen van BRC1 genoomwijd te identificeren en hiermee het moleculaire mechanisme waarmee BRC1 okselknoppen inactief houdt te ontrafelen. We hebben

laten zien dat BRC1 in staat is regulatoire sequenties van de ABA biosynthese genen *NCED3*, *NCED9* en *ABA2* te binden en hiermee de productie van abscisinezuur (ABA) te reguleren. Naast ABA wordt ook cytokine (CK) door BRC1 gereguleerd door directe binding van twee CK oxidasen en CK signaleringsmoleculen. De regulatie van deze twee hormonen, alsook genen die de celwand opbouwen wat de mogelijkheid biedt tot een fysieke barrière, bieden een verklaring voor de functie van BRC1 in het inactief houden van okselknoppen.

De data die hierboven gegenereerd is hebben we gebruikt om een consensus binding-motief te identificeren. Het motief dat hoogstwaarschijnlijk door BRC1 gebruikt wordt om zijn doel te herkennen is 'GDCCCA', erg gelijkend op eerder geobserveerde TCP binding-motieven. Hiernaast maken we melding van verrijking voor een G-box links of rechts van het TCP binding-motief. Dit biedt mogelijkheid tot speculatie over aanwezigheid van co-regulatiernetwerken en interactiepartners van BRC1.

Transcriptie factoren reguleren genen en processen over het algemeen in samenwerking met andere transcriptie factoren. In **hoofdstuk 5** beschrijf ik de fysieke interactie tussen APETALA1 (AP1), een MADS domein eiwit dat een rol speelt bij bloemorgaan identiteit, en een TCP bekend om zijn rol in kroonblad ontwikkeling, TCP5.

Deze fysieke interactie zou bewijs kunnen leveren voor een directe link tussen bloemorgaan identiteitsbepaling en groei. Om dit te bevestigen moet er een manier zijn om de relevantie van deze interactie *in planta* aan te tonen. Hier beschrijven we een methode om dit te bereiken, door het maken van een 'bank' van willekeurig gemutageniseerde allelen van zowel AP1 als TCP5, gemaakt middels foutgevoelige PCR reacties. Hierna hebben we een Y2H essay uitgevoerd om allelen te vinden waarvan de AP1-TCP5 interactie was verstoord maar waarvan de heterodimerische interacties van AP1 met andere MADS domein eiwitten nog wel plaatsvonden. We hebben de potentie van deze techniek laten zien door zes AP1 mutant allelen te screenen. Deze aanpak kan gebruikt worden om regio's en respectievelijke aminozuren te identificeren die van vitaal belang zijn voor zulk een interactie. Verder beschrijven we andere mogelijkheden van deze techniek en stellen we strategieën voor om deze op grotere schaal uit te voeren en de AP1-TCP interactie *in planta* te karakteriseren.

Naast de belangrijke functies die TCP genen uitoefenen in de regulatie van plantengroei en ontwikkeling zijn deze genen in veel meer processen van belang, zoals de verdediging van een plant tegen ziektekiemen en het waarnemen van voedingsstoffen in de bodem. Hier weid ik over uit in **hoofdstuk 6**. De TCP familie bekleedt een veelvoud aan functies en heeft leden waarvan de functie erg dicht bij elkaar ligt. Hierdoor blijft het karakteriseren van deze familie een bijzonder interessante uitdaging en doen TCP genen hun naam als 'bijzonder uitdagende eiwitten' eer aan.

A word of thanks

To start with the proverbial truism, I could not have gotten through four years of PhD research all by myself, it is with the help of quite a few people that the past four and a half years have been nothing but amazing! I will use this last part of my thesis to thank everyone that has played an important role and try my best not to forget anyone.

First and foremost, it is due to the amazing cluster of Plant Developmental Systems that the entire four and a half years of hard work have been fun! The PDS group is a special one, with great colleagues and an incredible team spirit in and outside the lab. I am convinced that a good working atmosphere is instrumental to the fun someone has at work and the latter is a great determinant for success.

There are two men whose evident enthusiasm and passion for research has been a great motivation and inspiration in the past years. Firstly, I believe I owe a lot to Richard, thank you for your support during the last four years! Combine a PhD project with TCPs and you have a challenge, a challenge in which you have been a great motivation in making it a success! Greatly appreciated is the always open door, no matter how busy you are. Going home, walking into your office for one last question and realizing that a short chat rarely happens, easily shifting from science to other subjects.

Then Gerco, the man around whom the world of 'Plant Developmental Systems' rotates. Thank you for creating the group, its amazing atmosphere and the awesome science we do within. It is hard to imagine you accomplish this with only one brain and two hands. Thank you for facilitating the cluster outings, barbeques and other excuses to drink some beers, I'm a great fan of your homebrews! Richard, Gerco, I have enjoyed the scientific discussions with the three of us and have learned a lot from you both, thanks!

Martijn, a.k.a. snuitefluitje and schattebout, thanks for being my paranymph! Your sense of humour and presence are sure to lift everyone their spirit, it certainly worked for me. Working with you in the lab, greasing up on Snack-Friday and enjoying beers afterwards, it has been fun! Sudden twinges in my back will be an everlasting memory of you, though I am not sure I am happy about that...

Hilda, my dear paranymph and neighbour in the open office, your attitude to life is one I admire greatly, keep it up! Thanks for recognizing my need for a quiet morning, leaving me be until lunch has helped me to get through many sleepy, grumpy mornings. In you I found a likeminded fan of 'De Dijk' and taking a detour in your orange wheels while singing along was totally worth it!

Froukje, the times you convinced me to stand on my head in the lab was a guaranteed way to wake up! I enjoyed our mutual ranting on commercials while working and we have engaged in quite some

interesting conversations in the lab. Grasnapsky was fun and your banana bread has helped me greatly in the final hours of writing!

Suraj! Sir, you have been a great friend over the past years and have been instrumental in many social activities of the group. Thank you for all the dinners, outings, game nights (games to which I still suspect you invented and/or changed most of the rules on the fly ;), never missing a photo opportunity (especially on the roof of the Duomo di Milano) and keeping an eye on everybody!

Someone without whom this thesis might never have finished, Sylvia! You arrived at the time I needed you most and it turned out to be a very fruitful cooperation. Together we managed to turn ‘TCP5’ into a very nice Plant Journal paper. Thank you for your everlasting patience, analysing petal cell sizes until you dreamt about them. You also took up the work from another great help, Garance, and the both of you have helped me greatly in actualising my last chapter on MADS-TCP interactions. Sylvia, if the both of us ever desire a switch in careers, I am still interested in starting the ‘S&S Buffers and Solutions Company’, I am sure we would be great at it!

Leonie, my neighbour in the lab, thanks for advice during work, talks during drinks and together with Anneke you were responsible for the musical atmosphere in the lab! It turned a lot quieter since you both have gone, though Martijn and I regularly turn up the radio volume to compensate. Leonie, thanks for inviting the band to play at your defence party, it was great fun and has been a great boost for the band!

Alice, your advice on many problems encountered during experiments has been of great help! Your sharpness of mind and tongue have been a great inspiration and are a pleasure to have witnessed. Going to Milano for your wedding with Luigi has been one of the highlights in the past years. Also, you were the Italian mama in the group, inducer of many social activities and organizer of many dinners at your place, thanks for your hospitality!

Each and every one in the PDS group, thank you for creating such a wonderful place to work. I enjoyed work, brakes and outings a lot, thanks to you all. To Cezary, Anneke, Suzanne and Romyana who have left the group but have been great teachers. To the senior staff, Ruud, Michiel, Marco, Jacqueline, Jan, Steven, Hana, Paul, Wilma, Kim, Mieke, Tjitske and Marian, in the lab and outside, thanks for numerous talks and discussions, on science and anything that occupied our minds. The coffee and tea breaks were a pleasant way to refresh the mind. Everyone at Bioscience, thank you for discussions during weekly meetings, and the fun we had during outings and Christmas dinners!

Wilma, it is great to know I am not the only nutjob enjoying TCPs. Ruud, your innate scepticism is a trait I greatly enjoy and admire. Marco, Michiel and Tjitske, the lab always runs smooth thanks to you! Jan and Steven, thanks for a different perspective. Mieke, thanks for being such an easy

victim for jokes, I am glad I could often return the favour. Kim, thanks for keeping everyone on their toes, scientifically and linguistically. Marian, I like your approach to life and have enjoyed our talks. Hana, the enthusiasm in anything you do really is contagious. Lastly Jacqueline and Paul, thanks for continuing the yeast work and lending a hand with my last experiments.

The PDS group in the open work space is a flexible one, with many people joining and leaving again. When I just started, the three musketeers made sure I felt at home in the group, Diego, Dennis and José, thanks! Several other Brazilians have visited us over the years, Greice, Fabia, Eveline, Haynna, Sylvia et al., thanks for the vibrant atmosphere and caipirinhas you brought into the group. Our group has been a temporary home for many BSc and MSc students and other guests, Han, Gian Luca, Francesca, Garance, Judit, Alice, Christine, Elwin, Patricia, Alba, Ellen, Charlotte, Stuart, William and many others, thank you for creating a nice environment to work in.

To all who started their PhD (relatively) recent, Lena, Vera, Charlotte, Ellen, Baojian, Xiaobing, Mengfan, Manjunath and Rufang, you will get there! Thanks for lunch-club (apologies for cooking far too seldom) and the barbeques and dinners outside work, you have truly been great colleagues and friends to be surrounded by! Ellen, thank you for critically reading the Dutch summary, I thought I was pretty capable of writing my mother tongue, you convinced me otherwise...

Then there are several people I hold responsible for the fun I had in doing science of the past four years and without whom this thesis would look completely different. Pilar, for our fruitful cooperation on BRC1. Marcelo and Adriana, for your help on phenotyping several characteristics of the *tcp5* mutants. Mark, Jeremy and Aina, you have been of great help setting up my experiments for the 'Phenovator' system. Aalt-Jan and Elwin in turning the 'Phenovator' data into biology and Aalt-Jan again in helping me on the analysis of the BRC1 ChIP-seq data. Elwin, I enjoyed our cooperation a lot, as it combined two people that knew very little of the others' field (me and maths... and you had never seen an Arabidopsis plant), in the end we taught each other a lot. I thank Elio and Bas for their help and service in sequencing several ChIP- and RNA-seq experiments and Sjef for the MS/MS runs. It has been great working with you, thank you all!

Even though they might not have noticed, several people have helped me a lot when writing my thesis. In the last months I had adopted a nomadic existence in Radix; Hana, Tjitske, Mieke, Wilma, Gerco, Ruud, Steven, Jacqueline and Froukje, thanks for allowing me to use your desks when you were not there! I would probably still be attempting to write, frustrated, in the open work space if it was not for your desks.

Acknowledgements

Léonie, Henk, Leo, Wilco, Juriaan, Mariana, Renaki, Elise, Mark, Jasper and the rest of the Seed and Plant Physiology group, thanks for keeping an eye on Gonda when I was at work! Thanks for adopting me on several parties and other occasions.

One of the things I have enjoyed most in the past four years outside the lab was making music, an excellent way to relax and enjoy the company of likeminded souls. Sloothaak, Thomas, Jasper, Ruben, Jaco, Marien, Thijs, Louis, Lennart and Paul, you have made the frequent travel to Utrecht worthwhile and Forsche Schapen has been the best outlet of PhD frustration. Thank you for being the best PhD party band ever! Gonda, Kris and Otto, thanks for adopting me and my saxophone into Mimosa, we have had fun playing gypsy jazz!

One of the most beautiful places in Wageningen, 'Rijnschans', has been the best home me and Gonda could have wished for, Erich and Jacqueline, thanks for having us and take care.

There are three hugely important people with whom I go way back. Mam, thanks for having my back for the past 30-something years! Bob, my oldest friend. Pap, you might be responsible for my love for biology, thanks for igniting this spark.

Saving the best for last, Gonda, I do not know where to start or what to say without getting horribly cheesy... you have become the most important person in my life, with you I share a love for many things; research, plants, music, travel, beers, food and together we make a pretty good team. You have been an enormous support during the past years, thank you for your patience and keeping me on track. You are making my life so much more fun, let us keep it up and together find out where it leads us.

Thank you all,

Sam

Publications

van Es, S.W., Silveira, S.R., Rocha, D.I., Bimbo, A., Martinelli, A.P., Dornelas, M.C., Angenent, G.C. and Immink, R.G.H. (2018), Novel functions of the *Arabidopsis* transcription factor *TCP5* in petal development and ethylene biosynthesis. *Plant Journal*, 94: 867-879. doi:10.1111/tpj.13904

van Es, S.W., van der Auweraert, E.B., Silveira, S.R., Angenent, G.C., van Dijk, A.D.J. and Immink, R.G.H. (In preparation), A spatio-temporal analysis of plant growth and development coupled to yield characteristics in several *Arabidopsis thaliana tcp*-mutant backgrounds.

van Es, S.W., Tarancón, C., van Dijk, A.D.J., Angenent, G.C., Cubas, P. and Immink, R.G.H. (In preparation) The regulatory role of BRC1 in bud dormancy through various downstream signalling pathways.

About the author

Sam van Es was born on the 25th of November, 1986 in a hospital in Eindhoven, The Netherlands. He lived his childhood in Best, a small village north of the city. Ever since he was still a little boy, going for walks with him proved a time-consuming business as every branch was picked up, flowers admired and birds looked at. Because of this fascination of anything that moves and grows, studying biology seemed like the obvious choice. Therefore, directly after obtaining his pre-university secondary education at the “Heerbeek

College” in Best in 2005 he moved to Wageningen to start his bachelor Biology at the Wageningen University. His bachelor focussed on the study of ecology and evolution, finished by a thesis on antibiotic resistance in *E. coli*.

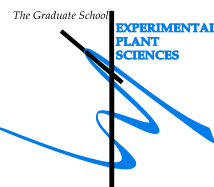
It was only during his master that he discovered a fascination for plant research and soon decided to specialize in ‘Plant Adaptation’. During this master he wrote his thesis at the Laboratory of Genetics on ‘Functional studies of *NcbZIP19* and *-23* in *Arabidopsis thaliana* and *Noccaea caerulea*’ in the group of Prof. Mark Aarts. After this he went on internship to the United Kingdom to work on ‘Genome-wide mutation analysis of *Arabidopsis thaliana* growing under stressful conditions’ in the group of Prof. Nick Harberd at the Department of Plant Sciences at the University of Oxford. Both the thesis and internship have laid the basis of a strong interest in research in general and molecular plant research in particular.

After obtaining his master degree, Sam started a PhD project at the Plant Developmental Systems group of Gerco Angenent under supervision of Richard Immink. The work performed during his time as a PhD student resulted in the publication of this thesis.



Education Statement of the Graduate School

Experimental Plant Sciences



Issued to: Sam W. van Es
Date: 18 September 2018
Group: Molecular Biology
University: Wageningen University & Research

1) Start-up phase	<u>date</u>
<ul style="list-style-type: none"> ► First presentation of your project Optimizing of yield potential by TCP transcription factors ► Writing or rewriting a project proposal ► Writing a review or book chapter ► MSc courses ► Laboratory use of isotopes 	21 Nov 2013
<i>Subtotal Start-up Phase</i>	<i>1.5 credits*</i>
2) Scientific Exposure	<u>date</u>
<ul style="list-style-type: none"> ► EPS PhD student days EPS PhD student day, Leiden, NL EPS PhD student day 'Get2Gether', Soest, NL EPS PhD student day 'Get2Gether', Soest, NL ► EPS theme symposia EPS theme 1 'Developmental Biology of Plants', Wageningen, NL EPS theme 1 'Developmental Biology of Plants', Wageningen, NL EPS theme 1 'Developmental Biology of Plants', Leiden, NL EPS theme 1 'Developmental Biology of Plants', Wageningen, NL ► National meetings (e.g. Lunteren days) and other National Platforms Annual meeting 'Experimental Plant Sciences', Lunteren, NL Annual meeting 'Experimental Plant Sciences', Lunteren, NL Annual meeting 'Experimental Plant Sciences', Lunteren, NL Annual meeting 'Experimental Plant Sciences', Lunteren, NL Annual meeting 'Experimental Plant Sciences', Lunteren, NL ► Seminars (series), workshops and symposia <i>Seminar Series:</i> Business Unit Bioscience Seminars <i>Seminar:</i> Jiayang Li - Understanding the molecular mechanisms underlying rice tillering <i>Seminar:</i> George Coupland - Seasonal flowering in annual and perennial plants <i>Seminar:</i> Marcelo C. Dornelas - Using the non-model species <i>Passiflora</i> to study plant reproductive development <i>Seminar:</i> Francois Parcy - An integrated structural biology approach to flower development <i>Seminar:</i> Martin Kater - Mining for floral meristem regulatory pathways in <i>Arabidopsis</i> and Rice <i>Seminar:</i> Claire Périlleux - Flowering time genes in roots <i>Seminar:</i> Teemu Teeri - Pelargonidin in flowers - why not? Gerbera and petunia flowers block pelargonidin biosynthesis in a different way <i>Symposium:</i> From Genotype to Phenotype: Modelling of Plant Adaptation seminar, Wageningen, NL ► Seminar plus ► International symposia and congresses Plant Organ Growth Symposium, Ghent, Belgium 9th International PhD School on Plant Development, Zellingen-Retzbach, Germany Plant Organ Growth Symposium, Elche, Spain Workshop on Molecular Mechanisms Controlling Flower Development, Padua, Italy ► Presentations <i>Talk:</i> Startsymposium 'Plant Developmental Biology' - Optimization of yield potential by TCP transcription factors <i>Talk:</i> 9th International PhD School on Plant Development - Novel functions of TCP5 during flower development <i>Talk:</i> Plant Organ Growth Symposium - How TCP5 keeps the <i>Arabidopsis</i> petal in good shape <i>Talk:</i> Workshop on Molecular Mechanisms Controlling Flower Development - How TCP5 keeps the <i>Arabidopsis</i> petal in good shape <i>Talk:</i> Annual meeting 'Experimental Plant Sciences' - How TCP5 keeps the <i>Arabidopsis</i> petal in good shape <i>Poster:</i> Annual meeting 'Experimental Plant Sciences' - How TCP5 keeps the <i>Arabidopsis</i> flower in good shape - awarded 2nd place in Best Poster Award <i>Poster:</i> Plant Organ Growth Symposium - How TCP5 keeps the <i>Arabidopsis</i> petal in good shape <i>Poster:</i> Annual meeting 'Experimental Plant Sciences' - How TCP5 keeps the <i>Arabidopsis</i> petal in good shape - awarded 2nd place in Best Poster Award ► IAB interview ► Excursions 	29 Nov 2013 29-30 Jan 2015 28-29 Jan 2016 24 Jan 2014 21 Jan 2016 28 Feb 2017 30 Jan 2018 14-15 Apr 2014 13-14 Apr 2015 11-12 Apr 2016 10-11 Apr 2017 09-10 Apr 2018 2013-2017 15 Nov 2013 19 Jan 2015 27 Jan 2015 15 Oct 2015 03 Nov 2015 09 Feb 2018 14 Mar 2018 16 Nov 2017 10-12 Mar 2015 05-07 Oct 2016 15-17 Mar 2017 03-07 Sep 2017 14 Oct 2013 05-07 Oct 2016 15-17 Mar 2017 05 Sep 2017 10 Apr 2018 11-12 Apr 2016 15-17 Mar 2017 10-11 Apr 2017
<i>Subtotal Scientific Exposure</i>	<i>19.5 credits*</i>

CONTINUED ON NEXT PAGE

3) In-Depth Studies ▶ EPS courses or other PhD courses <i>Postgraduate course:</i> Transcription Factors and Transcriptional Regulation, Wageningen, NL <i>Postgraduate course:</i> RNAseq course by Edouard Severin, Wageningen, NL <i>Postgraduate course:</i> Microscopy and Spectroscopy in Food and Plant Sciences, Wageningen, NL <i>Postgraduate course:</i> The Power of RNA-Seq, Wageningen, NL <i>Postgraduate course:</i> Transcription Factors and Transcriptional Regulation, Wageningen, NL <i>Workshop:</i> Basic R for researchers, Wageningen, NL ▶ Journal club Literature discussion group at Bioscience-Plant Developmental Systems ▶ Individual research training	<u>date</u> 17-19 Dec 2013 21-23 Jan 2014 06-09 May 2014 10-12 Feb 2016 12-14 Dec 2016 May 2017 2013-2017
<i>Subtotal In-Depth Studies</i>	<i>8.8 credits*</i>
4) Personal development ▶ Skill training courses <i>Course:</i> Scientific Writing, Wageningen, NL <i>Talk:</i> Career Discovery Day - Describing a PhD, Wageningen, NL <i>Course:</i> Presenting with Impact, Wageningen, NL <i>Career Day:</i> Wageningen UR Career Day, Wageningen, NL ▶ Organisation of PhD students day, course or conference ▶ Membership of Board, Committee or PhD council	<u>date</u> Jan-Mar 2015 28 Mar 2015 09 Mar, 04 & 11 Apr 2016 06 Feb 2018
<i>Subtotal Personal Development</i>	<i>4.1 credits*</i>
TOTAL NUMBER OF CREDIT POINTS*	33.9

Herewith the Graduate School declares that the PhD candidate has complied with the educational requirements set by the Educational Committee of EPS which comprises of a minimum total of 30 ECTS credits

* A credit represents a normative study load of 28 hours of study.

This research was supported by NWO JSTP grant number 833.13.008
“Optimization of yield potential by TCP transcription factors”

Financial support from Wageningen University for printing this thesis is
greatly acknowledged

Thesis layout by the author, cover design by the author and Dennis Hendriks

Printed by proefschriftmaken.nl | | DigiForce